

A genetic and functional analysis of novel chicken interleukin-1 gene family members

Mark Stephen Gibson

A thesis submitted for the degree of Doctor of Philosophy to
University College London

2012

Institute for Animal Health

Compton

Berkshire

RG20 7NN

Declaration

I, Mark Stephen Gibson, confirm that the work presented in this thesis is my own. Where information has been derived from other sources, I confirm that this has been indicated in the thesis.

Abstract

The interleukin-1 gene family in humans comprises eleven members (*IL-1F1-F11*) that act as either functional agonists or antagonists of inflammation. Prior to this project, only two members of the IL-1 family had been identified and characterized in the chicken. The aim of this project was to identify, clone and characterise novel IL-1 family members in this species.

EST sequences representing IL-1F5 (IL-36RN) and the secretory and intracellular structural variants of IL-1 receptor antagonist (IL-1RN) were identified by their similarity with chicken IL-1 β .

Chicken IL-1RN (chIL-1RN) cDNAs were isolated from LPS-stimulated HD11 cells. Two further putative splice variants (SVs) of both chIL-1RN structural variants were also isolated. Both full length variants of chIL-1RN exhibited biological activity resembling that of their mammalian orthologues. The four SVs, however, were not bioactive. ChIL-1RN was constitutively expressed in lymphoid and non-lymphoid tissues as well as several cell subsets. In response to bacterial and viral infection, chIL-1RN expression was inducible.

Chicken IL-36RN was cloned from a liver cDNA. In mammals, this cytokine is an IL-1R1L2 receptor antagonist and downregulates LPS-mediated inflammation. IL-1R1L2 agonist ligands have not been identified in the chicken; therefore, an alternative bioassay to establish its function was attempted. Using a macrophage cell line, chIL-36RN did not inhibit endotoxin-mediated inflammatory effects. Constitutive IL-36RN expression was found in all tissues and cell subsets examined. In response to viral infection, chIL-36RN expression was significantly downregulated.

The eleven human IL-1 genes are encoded at three separate loci. Nine of these genes, including IL-1 β , IL-1RN and IL-36RN, are present at a single locus. In the chicken genome, the equivalent locus contains only IL-1 β . Neither IL-1RN nor IL-36RN were identifiable anywhere in the chicken genome. Future work will seek to determine the true extent of the repertoire of chicken IL-1 family genes.

Table of Contents

Abstract	1
Table of Contents	2
Table of Figures.....	12
Table of Tables	17
Acknowledgements	18
Abbreviations	19
Chapter 1	22
Introduction & Aims	22
1.1 A general discussion on the difference between the human and chicken immune systems	24
1.1.1 The innate immune response	24
1.1.1.1 Humans	24
1.1.1.2 Chickens.....	29
1.1.2 The adaptive immune response.....	32
1.1.2.1 Humans	32
1.1.2.2 Chickens.....	36
1.1.3 Repertoires of cells and structural features.....	39
1.1.4 Cytokines	40
1.1.4.1 Humans	40
1.1.4.2 Chickens.....	41
1.2 The Interleukin-1 gene family	42
1.2.1 IL-1 ligands in mammals	44
1.2.1.1 IL-1F1 (IL-1 α) and IL-1F2 (IL-1 β).....	44
1.2.1.2 IL-1F3 (IL-1RN)	53
1.2.1.3 IL-1F4 (IL-18).....	56

1.2.1.4 IL-1F5 (IL-36RN)	57
1.2.1.5 IL-1F6 (IL-36 α).....	60
1.2.1.6 IL-1F7 (IL-37).....	62
1.2.1.7 IL-1F8 (IL-36 β).....	64
1.2.1.8 IL-1F9 (IL-36 γ).....	65
1.2.1.9 IL-1F10	67
1.2.1.10 IL-1F11 (IL-33).....	70
1.2.2 IL-1 receptors and signal transduction in mammals.....	73
1.2.2.1 IL-1RI (IL-1R1)	73
1.2.2.2 IL-1RII (IL-1R2).....	75
1.2.2.3 IL-1RAcP (IL-1R3).....	76
1.2.2.4 ST2 (IL-1R4/IL-33R α).....	77
1.2.2.5 IL-18R α (IL-1R5) and IL-18R β (IL-1R7/IL-1RAcP).....	77
1.2.2.6 IL-1RL2 (IL-1R6/IL-1Rrp2).....	78
1.2.2.7 TIGIRR-2 (IL-1R8/IL-1RAPL)	78
1.2.2.8 TIGIRR-1 (IL-1R9).....	79
1.2.2.9 SIGIRR (TIR8)	79
1.2.2.10 Signal transduction.....	79
1.2.3 Genomic organization and location	80
1.2.4 The chicken IL-1 family	82
1.2.4.1 Chicken IL-1 β	83
1.2.4.2 Chicken IL-18	85
1.2.4.3 Chicken IL-1RI	86
1.2.4.4 Chicken ST2.....	86
1.2.4.5 Chicken SIGIRR (TIR8)	87
1.2.4.6 Other chIL-1 receptors	87

1.3 The chicken genome.....	88
1.4 Aims of the project and experimental approach.....	90
Chapter 2	94
Materials and Methods	94
2.1 In silico materials	95
2.1.1 Genomic sequence resources	95
2.1.2 CodonCode aligner	95
2.1.3 ClustalX	96
2.1.4 SignalP	96
2.1.5 ProDom.....	96
2.1.6 PSIPRED	97
2.1.7 SoftBerry.....	97
2.2 In silico methods	97
2.2.1 Identification of the extent of the chicken IL-1 gene family using the ENSEMBL database	97
2.2.1.1 IL-1 ligand genes.....	97
2.2.1.2 IL-1 receptor genes	98
2.2.2 Identification of novel chicken IL-1 family members in the NCBI EST database.....	98
2.2.3 Establishing the identity of novel chIL-1 genes using BLAST	98
2.3 In vitro materials	99
2.3.1 Restriction enzymes	99
2.3.2 Oligonucleotide primers	99
2.3.3 Vectors	100
2.3.3.1 pCI-neo Mammalian Expression Vector (Promega E1841)	100
2.3.3.2 pGEM-T® Easy (Promega A1360)	100
2.3.3.3 pHLSec.....	102

2.3.3.4 pTarget TM Mammalian Expression Vector (Promega A1410)	103
2.3.4 Bacterial and viral strains	104
2.3.5 Cell lines	105
2.3.5.1 COS-7 cells	105
2.3.5.2 HD11 cells.....	105
2.3.5.3 HEK293T cells.....	105
2.3.6 Cell culture reagents	106
2.3.7 Recombinant protein.....	106
2.4 In vitro methods.....	106
2.4.1 Sources of chicken tissues and cells	106
2.4.1.1 Tissues and cells from specified-pathogen-free chickens.....	106
2.4.1.2 Tissues and cells from SPF chickens challenged with bacteria or virus	107
2.4.2 Purification of nucleic acids	108
2.4.2.1 Purifying total RNA from chicken tissues	108
2.4.2.2 Purifying total RNA from cell lines	109
2.4.2.3 Purifying genomic DNA from whole blood	109
2.4.2.4 Purifying genomic DNA from cell lines	110
2.4.3 Quantification of nucleic acids	110
2.4.4 DNA and RNA amplification	111
2.4.4.1 Oligonucleotide primer design.....	111
2.4.4.2 One-step reverse transcriptase-polymerase chain reaction (RT-PCR)...	111
2.4.4.3 Two step RT-PCR.....	112
2.4.4.4 DNA amplification by PCR	113
2.4.4.5 5' Rapid amplification of cDNA ends (RACE).....	114
2.4.4.5.1 First strand cDNA synthesis.....	115
2.4.4.5.2 5' RACE PCR.....	116

2.4.4.6 Real-time quantitative RT-PCR (TaqMan).....	117
2.4.5 Agarose gel electrophoresis of DNA.....	120
2.4.6 Purification of PCR products.....	121
2.4.6.1 PCR purification.....	121
2.4.6.2 PCR purification from agarose gel.....	121
2.4.7 Cloning and subcloning.....	122
2.4.7.1 Vector preparation.....	122
2.4.7.2 TA-cloning RT-PCR products.....	123
2.4.7.4 Directional sticky end cloning into an expression vector.....	123
2.4.7.5 Transformation and screening.....	124
2.4.8 Restriction digestion.....	124
2.4.9 Plasmid DNA purification.....	125
2.4.9.1 Small scale (mini) plasmid DNA preparation.....	125
2.4.9.2 Large scale (maxi) plasmid DNA preparation.....	126
2.4.9.3 Very large scale (mega) plasmid DNA preparation.....	127
2.4.9.4 Large scale BAC DNA preparation.....	128
2.4.10 Sequencing.....	129
2.4.10.1 Sequencing PCR.....	129
2.4.10.2 Ethanol precipitation of products.....	131
2.4.11 Chicken BAC library screening.....	131
2.4.11.1 Pre-hybridisation.....	132
2.4.11.2 Synthesising a radio-labelled DNA probe.....	132
2.4.11.3 Hybridisation and washing.....	133
2.4.11.4 Identification of positive clones.....	133
2.4.12 Cell culture.....	134
2.4.12.1 Resurrecting cryopreserved cell lines.....	134

2.4.12.2	Passaging cells	135
2.4.12.3	Transfecting cells with pure chicken DNA.....	135
2.4.12.3.1	Transient protein expression in COS-7 cells.....	135
2.4.12.3.2	HEK293T cells	137
2.4.13	Purification of HIS-tagged recombinant proteins.....	137
2.4.13.1	Under native conditions	137
2.4.13.2	Under denaturing conditions	138
2.4.14	Analysis of HIS-tagged recombinant proteins.....	138
2.4.14.1	SDS-polyacrylamide gel electrophoresis (SDS-PAGE)	138
2.4.14.2	Western blotting	139
2.4.15	HD11 bioassay	140
2.4.15.1	Pilot study	140
2.4.15.2	Quantifying the biological response.....	141
2.4.15.2.1	Griess assay	141
2.4.15.3	Optimised bioassay conditions.....	142
2.4.15.3.1	Optimising the [pure rIL-1 β].....	142
2.4.15.3.2	Final bioassay conditions	142
2.4.16	HD11 time course stimulation assay	143
2.4.17	Statistics	143
Chapter 3	144
Results 1: Analysis of the extent of the IL-1 family in chickens	144
3.1	Introduction	145
3.2	Methods	147
3.3	Results	148
3.3.1	IL-1 ligand genes in the chicken.....	148
3.3.2	IL-1 receptor genes in the chicken.....	149

3.4 Discussion	153
Chapter 4	158
Results 2: Identification, cloning and characterisation of chicken interleukin-1 receptor antagonist (IL-1RN)	158
4.1 Introduction	159
4.2 Methods	161
4.2.1 In silico techniques	161
4.2.2 In vitro techniques	162
4.3 Results	164
4.3.1 Identification and analysis of novel chIL-1 expressed sequence tag (EST) sequences	164
4.3.2 Signal peptide analysis of predicted chIL-1RN amino acid sequences	165
4.3.4 In silico analysis of chIL-1RN nucleotide and amino acid sequences	170
4.3.5 Structural determination of chIL-1RN by PCR amplification, sequencing and in silico analysis	176
4.3.6 Identification of the genomic location	190
4.3.7 Characterization of the 5' untranslated regions (5' UTRs) of icIL-1RN and sIL-1RN cDNA sequences	191
Chapter 5	202
Results 3: Characterisation of expression and bioactivity of chicken IL-1RN	202
5.1 Introduction	203
5.2 Methods	208
5.2.1 Sources of chicken tissues and cells	208
5.2.2 HD11 time course stimulation	208
5.2.3 Transfecting cells with pure chicken DNA	208
5.2.3.1 Transient protein expression in COS-7 cells	208
5.2.3.2 Transient protein expression in HEK293T cells	208
5.2.4 Purification and analysis of HIS-tagged recombinant proteins	209

5.2.5 HD11 bioassay	209
5.2.5.1 Pilot assay set up	209
5.2.5.2 Final bioassay conditions	210
5.2.5.3 Quantifying the biological response.....	210
5.2.6 Total RNA isolation and real-time qRT-PCR (TaqMan®) analysis of chicken mRNA expression.....	210
5.3 Results	212
5.3.1 Analysis of IL-1RN mRNA expression in unstimulated tissues by real-time qRT-PCR	212
5.3.2 Analysis of IL-1RN mRNA expression by real-time qRT-PCR in sorted lymphocyte subsets	212
5.3.3 Analysis of IL-1RN mRNA expression across a time course in three different populations of stimulated macrophages.....	213
5.3.4 Analysis of IL-1RN expression in vivo by qRT-PCR following bacterial or viral challenge.....	217
5.3.4.1 Infectious Bursal Disease Virus	219
5.3.4.2 Salmonella Typhimurium strain F98 NaI ^R	221
5.3.5 Characterization of the bioactivity of chIL-1RN.....	222
5.3.5.1 Pilot study	223
5.3.5.2 Characterization of the bioactivity of pure secretory and intracellular IL-1RN (purified recombinant proteins)	226
5.3.5.3 Characterization of the bioactivity of ex-COS secretory and intracellular IL-1RN splice variant proteins.....	228
Chapter 6	240
Results 4: Identification, cloning and characterisation of chicken interleukin-1F5 (IL-1F5)	240
6.1 Introduction	241
6.3.1 Identification and analysis of a novel chIL-1 EST sequence.....	245
6.3.2 Characterization of the putative processed form of chIL-1F5.....	249

6.3.3 Amplification and molecular cloning of the chIL-1F5 coding sequence cDNA	249
6.3.4 In silico analysis of the chIL-1F5 amino acid sequence	251
6.3.5 Structural determination by PCR amplification, sequencing and in silico analysis.....	252
6.3.6 Identification of the genomic location	256
Chapter 7	268
Results 5: Characterisation of expression and bioactivity of chicken IL-1F5	268
7.1 Introduction	269
7.2 Methods	274
7.2.1 Sources of chicken tissues and cells	274
7.2.2 HD11 time course stimulation	274
7.2.3 Transfecting cells with pure chicken DNA.....	274
7.2.4 Purification and analysis of HIS-tagged recombinant proteins	274
7.2.5 HD11 bioassay.....	275
7.2.5.1 LPS optimisation assay	275
7.2.5.2 Final bioassay conditions	275
7.2.5.3 Quantifying the biological response.....	275
7.2.6 Total RNA isolation and real-time qRT-PCR (TaqMan®) analysis of chicken mRNA expression.....	276
7.3 Results	277
7.3.1 Analysis of IL-1F5 mRNA expression in unstimulated tissues by real-time qRT-PCR	277
7.3.2 Analysis of IL-1F5 mRNA expression by real-time qRT-PCR in sorted cells which were either unstimulated or stimulated	277
7.3.3 Analysis of IL-1F5 mRNA expression across a time course by real-time qRT-PCR in three different populations of stimulated macrophages	278
7.3.4 Analysis of IL-1F5 expression in vivo by real-time qRT-PCR following bacterial or viral challenge.....	282

7.3.4.1 Infectious Bursal Disease Virus	282
7.3.4.2 <i>S. Typhimurium</i> strain F98 NaI ^R	283
7.3.5 Characterization of the bioactivity of IL-1F5	284
7.3.5.1 Characterization of the bioactivity of pure IL-1F5	284
7.4 Discussion	288
Chapter 8	292
Discussion	292
8.1 Discussion	293
8.2 Future work	300
8.3 Conclusion	304
References	306
Appendices	320

Table of Figures

Figure 1.1 Assembly of the NALP3 (NLRP3) inflammasome.	28
Figure 1.2 The general β-trefoil protein structure.	47
Figure 1.3 Non-caspase-1 processing of pro-IL-1β.	49
Figure 1.4 Potential mechanisms of mature IL-1β release.	51
Figure 1.5 Calpain-dependant processing and maturation of IL-1α.	52
Figure 1.6 The IL-1 ligand gene cluster on human chromosome 2.	68
Figure 1.7 Phylogenetic analysis of the human and mouse IL-1 amino acid sequences.	69
Figure 1.8 Independent IL-33 signalling pathways in mast cells.	71
Figure 1.9 Ribbon diagrams of IL-1β and IL-1Ra bound to IL-1RI.	76
Figure 1.10 IL-1 signal transduction.	81
Figure 2.1 Map of the pCI-neo mammalian expression vector.	101
Figure 2.2 Map of the pGEM-T® Easy vector.	102
Figure 2.3 Map of the pLEXm vector.	103
Figure 2.4 Map of the pTarget™ mammalian expression vector	104
Figure 2.5 Real-time quantitative RT-PCR (qRT-PCR).	119
Figure 3.1 Schematic depicting an IL-1 gene family locus conserved between humans and chickens.	149
Figure 3.2 Schematic depicting an IL-1 receptor gene family locus conserved between humans and chickens.	150
Figure 3.3 Schematic depicting the IL-18BP locus in humans and a region of the chicken genome with which it shares limited conserved synteny.	152
Figure 3.4 Schematic depicting the IL-33 locus in the human genome and a syntenic region of the chicken genome.	154
Figure 4.1 Nucleotide alignment between chIL-1RN EST BU214831.1 and Contig 81757.1.	166

Figure 4.2 Amino acid alignment between 2 chIL-1RN ESTs differing at their 5' ends.....	166
Figure 4.3 SignalP analysis of chIL-1RN amino acid sequences.	167
Figure 4.4 Agarose gel showing RT-PCR products from the amplification of the icIL-1RN CDS using ConA-stimulated splenocyte (S) and LPS-stimulated HD11 (H) macrophage cell line RNA as template.....	169
Figure 4.5 Agarose gel showing icIL-1RN splice variant clones released from pTargeT by restriction digestion..	170
Figure 4.6 Alignment between icIL-1RN (icFL), SV1 and SV2 CDS cDNA sequences using ClustalX.....	171
Figure 4.7 Agarose gel showing RT-PCR products from the amplification of the sIL-1RN CDS using LPS-stimulated HD11 (H) macrophage cell line RNA as template.....	172
Figure 4.8 Alignment between the six chIL-1RN CDS cDNA sequences in ClustalX.	174
Figure 4.9 Amino acid alignment of chicken sIL-1RN and icIL-1RN with human (secretory and intracellular variant 1), mouse, cow, and platypus IL-1RN sequences.....	175
Figure 4.10 Amino acid alignment between predicted icIL-1RN (icFL), SV1 & SV2 sequences.....	176
Figure 4.11 Phylogenetic analysis of chIL-1RN amino acid sequences using MEGA v5.0.....	177
Figure 4.12 The structures and identified protein coding transcripts of chicken and human IL-1RN genes.	180
Figure 4.13 Alignment of human and chicken transcript sequences created to predict the locations of the chicken gene introns.	182
Figure 4.14 Agarose gel of PCR products containing intron 2, exon 3 and intron 3 of chIL-1RN.....	182
Figure 4.15 Structure of exon/intron 1-3 of chIL-1RN.....	183
Figure 4.16 Structure of exon/intron 4 of chIL-1RN.....	186
Figure 4.17 Agarose gel of PCR products containing introns 1-4 of chIL-1RN....	188
Figure 4.18 The 5' end of the chIL-1RN gene.	189

Figure 4.19 Agarose gel electrophoresis of IL-1β and IL-1RN PCR products in lines 7₂, 15I & 0 genomic DNA and TAM32-21N6 BAC DNA.	192
Figure 4.20 Diagram of the locus on chicken chromosome 22 (v2.1) containing IL-1β and 4 adjacent sequence gaps.	192
Figure 4.21 Agarose gel electrophoresis of 5' RACE PCR products.	194
Figure 4.22 Agarose gel electrophoresis of sIL-1RN RT-PCR products.	195
Figure 5.1 IL-1RN_{fl} expression in lymphoid and non-lymphoid tissues as measured by real-time qRT-PCR.	213
Figure 5.2 IL-1RN_{fl} expression in sorted chicken lymphocyte subsets as measured by real-time qRT-PCR.	214
Figure 5.3 Expression of IL-1RN_{fl}, IL-1RN_{SV1} and IL-1β in the HD11 macrophage cell line following stimulation with LPS as measured by real-time qRT-PCR.	215
Figure 5.4 Expression of IL-1RN_{fl} in BM-M\emptyset stimulated with LPS or CD40L. ..	216
Figure 5.5 Expression of IL-1RN_{SV1} in BM-M\emptyset stimulated with LPS or CD40L.	217
Figure 5.6 Expression of IL-1RN_{fl} in Mo-M\emptyset stimulated with LPS or CD40L for 1-48 h.	218
Figure 5.7 Expression of IL-1RN_{SV1} in Mo-M\emptyset stimulated with LPS or CD40L for 1-48 h.	218
Figure 5.8 Expression of IL-1RN_{fl} mRNA in bursal cells from line 6₁ (resistant) and BrL (susceptible) chickens infected with IBDV.	220
Figure 5.9 Expression of IL-1RNSV1 mRNA in bursal cells from line 6₁ (resistant) and BrL (susceptible) chickens infected with IBDV.	220
Figure 5.10 Expression of IL-1RNSV2 mRNA in bursal cells from line 6₁ (resistant) and BrL (susceptible) chickens infected with IBDV.	221
Figure 5.11 IL-1RN expression in splenocytes from RIR chickens following infection with <i>Salmonella</i> Typhimurium strain F98 NaI^R.	222
Figure 5.12 IL-1β and iNOS expression in IL-1β-stimulated HD11 cells.	224
Figure 5.13 Establishing the optimal [rchIL-1β] required to stimulate HD11 cells.	225
Figure 5.14 IL-1β mRNA expression in IL-1β-stimulated HD11 cells.	226

Figure 5.15 Western blot of purified recombinant chIL-1RN proteins expressed in HEK293T cells.	227
Figure 5.16 Full length chIL-1RNs are bioactive as determined by TaqMan.	230
Figure 5.17 Full length chIL-1RNs are bioactive as determined by the Griess assay.	230
Figure 5.18 Chicken icIL-1RN splice variants do not antagonise IL-1β-mediated IL-1β expression.	231
Figure 5.19 Chicken icIL-1RN splice variants do not antagonise IL-1β-mediated iNOS expression.	232
Figure 5.20 Chicken sIL-1RN splice variants do not antagonise IL-1β-mediated IL-1β expression.	233
Figure 5.21 Chicken sIL-1RN splice variants do not antagonise IL-1β-mediated iNOS expression.	234
Figure 6.1 Amino acid alignment of truncated chicken IL-1F5 with the full length human, macaque, mouse, cow and platypus IL-1F5 sequences.	246
Figure 6.2 Nucleotide sequence alignment between the 3' end of the chIL-1F5 EST (BU247129.1) present in the NCBI database and the clone of the identical EST (ChEST734c4) after being fully sequenced in both directions.	247
Figure 6.3 Amino acid alignment of chicken IL-1F5 with the human, macaque, mouse, cow and platypus IL-1F5 sequences.	248
Figure 6.4 Agarose gel showing PCR products from the amplification of the IL-1F5 CDS using ChEST734c4 DNA as template.	250
Figure 6.5 Determination of the gene structure of chicken IL-1F5.	254
Figure 6.6 Agarose gel electrophoresis of IL-1β and IL-1F5 PCR products in lines 7₂, 15I, 0 (IL-1β) and line 6₁ (IL-1F5) genomic DNA and TAM32-21N6 BAC DNA.	258
Figure 6.7 Screening a BAC library to elucidate the genomic location of chIL-1F5.	258
Figure 6.8 Agarose gel showing PCR products from the amplification of IL-1F5 using BAC DNA and genomic DNA from line 6₁.	260
Figure 6.9 Agarose gel showing PCR products from the repeated amplification of IL-1F5 using BAC DNA and genomic DNA from line 6₁.	261

Figure 7.1 IL-1F5 expression in lymphoid and non-lymphoid tissues as measured by real-time qRT-PCR.	278
Figure 7.2 IL-1F5 expression in sorted chicken lymphocyte subsets as measured by real-time qRT-PCR.	279
Figure 7.3 Expression of IL-1F5 and IL-1β in the HD11 macrophage cell line following stimulation with LPS as measured by real-time qRT-PCR.	280
Figure 7.4 Expression of IL-1F5 in BM-M\emptyset stimulated with LPS or CD40L.	281
Figure 7.5 Expression of IL-1F5 in Mo-M\emptyset stimulated with LPS or CD40L.....	281
Figure 7.6 Expression of IL-1F5 mRNA in bursal cells from line 6₁ (resistant) and BrL (susceptible) chickens infected with IBDV.	283
Figure 7.7 IL-1F5 expression in splenocytes from RIR chickens following infection with <i>S. Typhimurium</i> strain F98 Nal^R.	284
Figure 7.8 Western blot of pure recombinant chIL-1F5 protein expressed in HEK293T cells.	285
Figure 7.9 Full length chIL-1F5 does not downregulate LPS-induced inflammation in HD11 cells.	287

Table of Tables

Table 1.1 The human and chicken Toll-like receptor families.....	31
Table 1.2 The IL-1 receptor family in humans.	74
Table 3.1 The IL-1 receptor gene family in humans and chickens.....	152

Acknowledgements

I would like to express my sincere thanks and immense appreciation to my IAH supervisors, Professor Pete Kaiser and Dr Mark Fife. They have both been hugely supportive, helpful and patient throughout my PhD. I would like to thank them for giving me the opportunity to be a part of the Avian Genomics group, for which I am extremely grateful. I would finally like to thank them for their humour which has made working with them a pleasure. I would also like to thank my UCL supervisor Professor Pat Woo, who has provided much helpful advice and has kindly continued to supervise me during her retirement.

I am also indebted to several other colleagues at the IAH for their various helpful contributions. In particular, I would like to give huge thanks to Lisa Rothwell, Nigel Salmon and James Birch who have offered me excellent advice and assistance. Thanks must also go to Zhiguang Wu, John Hammond and John Young for their help. Finally, my thanks to the (many) members of the Avian Genomics group who have made the lab such an enjoyable place to work.

I would also like to thank my parents, without whom I would not have got this far. They continue to be extremely supportive of everything I do and have encouraged me throughout my PhD.

Finally, I would like to thank my wonderful girlfriend Sarah who has always been willing to listen to my various problems, occasional successes and has been unfailingly supportive for the past four years.

Abbreviations

aa	Amino acid
Ab	Antibody
Ag	Antigen
AP-1	Activator protein 1
APC	Antigen presenting cell
ARTS	Aminopeptidase regulator of TNFR1 shedding
ASC	apoptosis-associated speck-like protein containing a C-terminal CARD domain
ATP	Adenosine triphosphate
BAC	Bacterial artificial chromosome
BALT	Bronchial associated lymphoid tissue
BCR	B cell receptor
BLAST	Basic local alignment search tool
BI-Mo/MΦ	blood-derived monocytes/macrophages
BM-DCs	Bone marrow-derived dendritic cells
BM-MΦ	Bone marrow-derived macrophages
bp	Base pair
BSA	Bovine serum albumin
C/EBPβ	CCAAT-enhancer binding proteins
CARD	Caspase-activating recruitment domain
CARDINAL	CARD inhibitor of NF-κB-activating ligands
CCAAT	Cytidine-cytidine-adenosine-adenosine-thymine
cDNA	Complementary DNA
CDS	Coding sequence
CEF	Chicken embryonic fibroblasts
ch	Chicken
CM	Conditioned medium
CMV	Cytomegalovirus
COX	cyclooxygenase
CRP	C-reactive protein
CSF	Colony-stimulating factors
Ct	Cycle threshold
DC	Dendritic cell
DEPC	Diethylpyrocarbonate
DMEM	Dulbecco's modified eagle medium
DNA	Deoxyribonucleic acid
dNTP	deoxynucleotide triphosphate
dpi	days post-infection
DTT	dithiothreitol
EDTA	Ethylenediaminetetraacetic acid
EID	embryonic incubation day
ERK	Extracellular signal related kinases
EST	Expressed sequence tag
ex-COS	Derived from COS-7 cells
FAM	5- or 6-carboxyfluorescein
FIIND	Function to find domain

FoxP3	Forkhead box P3
g	Gram
<i>g</i>	Gravity
GALT	Gut-associated lymphoid tissues
GI	Gastrointestinal
GM-CSF	Granulocyte-macrophage colony-stimulating factor
GndHCl	Guanidine hydrochloride
h	Hour
HAX-1	HS1-associated protein X-1
HEK	Human embryonic kidney
HLA	Human leukocyte antigen
HRP	Horseradish peroxidase
hu	Human
IBDV	Infectious bursal disease virus
IFN	Interferon
Ig	Immunoglobulin
IKK β	Inhibitor of nuclear factor- κ B kinase subunit β
IL	interleukin
iNOS	Inducible nitric oxide synthase
IPTG	Isopropyl β -D-1-thiogalactopyranoside
IRAK	Interleukin-1 receptor-associated kinase
iT _{reg}	inducible T _{reg} cells
JNK	c-Jun N-terminal kinase
l	Litre
LPS	Lipopolysaccharide
LRR	Leucine-rich repeat domain
M	Molar
MAPK	mitogen activated protein kinase
MBL	Mannose-binding lectin
MCR	Multiple cloning region
MHC	major histocompatibility complex
min	Minute
MMP	matrix metalloproteinases
MRC1	Macrophage mannose receptor
mRNA	Messenger ribonucleic acid
MyD88	Myeloid differentiation primary response gene 88
NACHT	NAIP, CIITA, HET-E, TP-1 domain
NAD	NACHT-associated domain
NALP3/NLRP3	NACHT, LRR and PYD domains-containing protein 3
NED	Naphthylethylenediamine
NF- κ B	Nuclear factor kappa-light-chain-enhancer of activated B cells
NK	Natural killer
NLR	NOD-like receptor
NO	Nitric oxide
nt	Nucleotide
nT _{reg}	natural T _{reg} cells
OD	Optical density
ORF	Open reading frame
oxLDL	Oxidised low density lipoprotein

PAGE	Polyacrylamide gel electrophoresis
PAMP	pathogen associated molecular pattern
PBMC	Peripheral blood mononuclear cell
PBS	Phosphate buffered saline
PEI	polyethylenimine
PGE ₂	Prostaglandin E2
PHA	Phytohaemagglutinin
PLA2	Phospholipase A2
PMA	Phorbol 12-myristate 13-acetate
poly(A)	Polyadenylation
PRR	pattern recognition receptor
PYR	Pyrin domain
qRT-PCR	quantitative real-time RT-PCR
R	Receptor
RACE	Rapid amplification of cDNA ends
RIG-I	Retinoic acid-inducible gene I
RLR	RIG-I-like receptor
ROR γ t	RAR-related orphan receptor gamma
RT	Reverse transcriptase
RV16	Rhinovirus type 16
s	Second
SCID	Severe combined immunodeficiency
SDS	Sodium dodecyl sulphate
SIGIRR	Single Ig IL-1 receptor-related protein
siRNA	Small interfering RNA
STAT	Signal transducer and activator of transcription
SV40	Simian virus 40
TAB	TAK-binding protein
TAK	TGF- β -activated kinase
TAMRA	tetramethylrhodamine
TBE	Tris-borate-EDTA
TCR	T cell receptor
TGF	Transforming growth factor
Th	Helper T cell
TIGIRR	three Ig domain-containing receptor-related proteins
TIR	Toll/IL-1 receptor
TLR	Toll-like receptor
T _m	Melting temperature
TNF	Tumour necrosis factor alpha
TNFSF	Tumour necrosis factor superfamily
Tollip	Toll interacting protein
T _R 1	Type 1 regulatory T cells
TRAF6	TNF receptor associated factor 6
T _{reg}	Regulatory T cells
UTR	Untranslated region
X-gal	5-bromo-4-chloro-3-indolyl-beta-D-galactopyranoside
μ	Micro

Chapter 1

Introduction & Aims

Understanding the immune response in the chicken is of fundamental importance for both human health and the economy. Worldwide consumption of chicken is on an immense scale with around 50 billion chickens reared for meat and eggs every year. Farming of poultry is carried out in an industrialised manner, with a significant proportion of birds farmed under intensive conditions. With so many chickens in such close proximity to one another, the potential for disease outbreak is huge and has serious implications for both poultry and human health. Although many birds carrying disease may not survive the rearing process, others can carry subclinical disease whilst healthy birds may come into contact with faecal matter containing pathogens. This can lead to contamination of the final product. Food poisoning from zoonotic diseases such as salmonellosis and campylobacteriosis is a well-recognised, persistent problem caused mainly by contaminated poultry products. Avian-specific disease also leads to significant economic losses, despite routine vaccination against many different pathogens. Although many common avian diseases can be efficiently countered with a good vaccine, pathogens have developed several ingenious strategies for evading the host immune response. Resistance to a vaccine can therefore develop, causing widespread loss of birds thought to be protected. One striking example of this is Marek's disease, where resistance to vaccination has driven the evolution of the virus to create novel strains with ever increasing virulence (Nair 2005).

Understanding the underlying immunological mechanisms subverted by pathogens to nullify the host response is therefore crucial. This requires a comprehensive understanding of the basic immunobiology of the chicken, in particular identification of the immune gene repertoire it possesses. Once this has been established, deciphering which genes may have a significant contribution to immunopathogenesis can then feed into strategies for combating disease. Although

vaccination is clearly useful, selective breeding to incorporate, for example, particular allelic variants of genes which confer disease resistance, would be highly desirable. Likewise, removing alleles that increase disease susceptibility would be advantageous. Breeding more robust chickens that are better equipped to fight disease is undoubtedly a long term goal of the poultry industry. Understanding the innate immune response in *Aves* is clearly a major stepping stone towards effective disease prevention. The interleukin-1 (IL-1) family of genes plays a pivotal role in this innate response and can critically determine disease outcome and severity. Establishing exactly which IL-1 genes are present in the chicken is therefore necessary.

1.1 A general discussion on the difference between the human and chicken immune systems

1.1.1 The innate immune response

1.1.1.1 Humans

The innate immune system acts as an initial barrier to prevent pathogens from invading a host and, in the event of physical defences being breached, to contain pathogens and limit the spread of infection. It is a collection of cells, proteins (receptors, cytokines, effector molecules) and anatomical barriers which provide the first line of defence. Innate responses are immediate and indiscriminate but do not confer inveterate protection to a host as the innate system has no capacity for immunological memory. Although generally considered as non-specific, innate recognition does differentiate between self and non-self and can also precisely identify different types of pathogen.

The innate response lasts up to around 96 hours post-infection after which time the adaptive system, if triggered, becomes more prominent.

Physical barriers provide an initial affront to pathogens in the form of the various surface epithelia. Outer surface and internal mucosal membranes are tightly sealed to restrict pathogen entry. Cilia covering many surfaces can expel pathogens trapped in mucus by aiding its flow. Epithelia also secrete various substances to directly attack pathogens whilst reducing the opportunity for adherence. These include mucins, antimicrobial peptides such as the β -defensins, and enzymes such as lysozyme in tears and saliva. The GI tract is considerably microbicidal, with many fatty acids and enzymes in its upper region and a low pH in the stomach. Commensal bacteria also occupy most epithelia, competing with pathogens for space and nutrients whilst secreting their own antibacterial peptides.

Should pathogenic organisms penetrate the epithelium, they become instantly recognised by macrophages which reside in many of the tissues that are close to epithelial surfaces. Further phagocytes, in the form of neutrophils, are attracted to areas of infection from the circulation. Neutrophils are a key component of the innate immune response as well as contributing significantly to the resolution of inflammation. Together, both cell types identify, engulf and eliminate a variety of pathogens. Several classes of preformed, germline-encoded receptors are expressed on the surface of phagocytes which directly recognise pathogens. The surfaces of bacteria and viruses consist of highly conserved repetitive structural motifs known as pathogen associated molecular patterns (PAMPs). The phagocyte receptors that detect PAMPs are collectively known as pattern recognition receptors (PRRs). The most extensively characterised group of PRRs are the Toll-like receptors (TLRs) which recognise a broad range of lipids, proteins, nucleic acids and sugars on the exterior of bacteria, viruses,

protozoa and fungi (Kawai and Akira 2010). Most TLRs are expressed on the surface of phagocytes; however, TLRs recognising viral (TLR3, 7, 8 and 13) and bacterial nucleic acids (TLR9) are found in intracellular endolysosomes. NOD-like receptors (NLRs) are another class of PRRs which sense bacterial, viral and protozoal PAMPs and also constitutive host molecules located in the cytoplasm of cells (Kumar, Kawai et al. 2011). Cytoplasmic recognition of RNA viruses is further carried out by the RIG-I-like receptors (RLRs) RIG-I, MDA5 and LGP2, as well as AIM2, DAI, and RNA polymerase III (O'Neill and Bowie 2010). Other PRRs include the macrophage mannose receptor (MRC1) and scavenger receptors. MRC1 is a macrophage-specific C-type lectin present on the cell surface that detects carbohydrates present on bacteria and viruses. Scavenger receptors, present on the surface of phagocytes, recognize low density lipoproteins modified by acetylation or oxidation. Not all PRRs, however, are expressed on phagocytes, with some present as soluble proteins in blood and on epithelia. Examples of these include mannose-binding lectin (MBL) and surfactant proteins.

Binding of pathogen by PRRs on macrophages initiates a sequence of immunological effects which can eventually lead to priming the adaptive immune response. Pathogens can initially become phagocytosed and destroyed in phagolysosomes by acids, proteins and enzymes. Antimicrobial peptides, nitric oxide, hydrogen peroxide and superoxide are also synthesised within phagocytes to destroy engulfed pathogens. Production of superoxide is facilitated by NADPH oxidase via a mechanism termed the respiratory burst. Pathogen recognition also activates macrophages to initiate inflammation by releasing cytokines and chemokines. The purpose of inflammation is to increase the numbers of phagocytes at sites of infection, to kill invading microbes, to induce clotting of the microvasculature to limit the spread

of infection, and to repair damaged tissues. Engagement of PRRs initiates intracellular signalling pathways which leads to NF- κ B-mediated pro-inflammatory cytokine production and IRF3/7-mediated production of type I interferons. Each different group of PRRs has its own specific intracellular signalling molecules, but this always culminates in activation of either NF- κ B or IRF, irrespective of how a cell is stimulated (Kumar, Kawai et al. 2011). Activation of several NLRs by PAMPs, toxins or danger signals leads to assembly of the inflammasomes (Martinon, Mayor et al. 2009). The most comprehensively studied of these, known as NLRP3 (NALP3), plays a key role in the generation of mature IL-1 β and IL-18 cytokines. NLRP3 is a complex of proteins which instigates the maturation of procaspase-1, leading to the activation of caspase-1. Mature caspase-1 then processes pro-IL-1 β into its mature, bioactive form which is then secreted by cells (Figure 1.1) (Martinon, Mayor et al. 2009).

Cytokines released by activated macrophages include the pro-inflammatory cytokines IL-1 β , IL-6, IL-12 and TNF- α , the chemokine CXCL8 and the interferons IFN- α and IFN- β which induce scores of stimulatory effects. One important effect is the induction of co-stimulatory molecule expression on the surface of macrophages and dendritic cells (DCs). These cells then prime the adaptive response by presenting antigen to T cells. Neutrophils are attracted to sites of infection following stimulation with CXCL8. They adhere to endothelial surfaces in blood vessels by binding to selectins, which are highly expressed on endothelial cells during an inflammatory response. Neutrophils roll along the endothelium under the influence of CXCL8 before extravasating the endothelial wall by diapedesis and migrating through tissues down a CXCL8 concentration gradient to the site of infection. Here, they phagocytose pathogens and participate in cellular crosstalk. They can also migrate to lymph nodes to affect the adaptive immune response

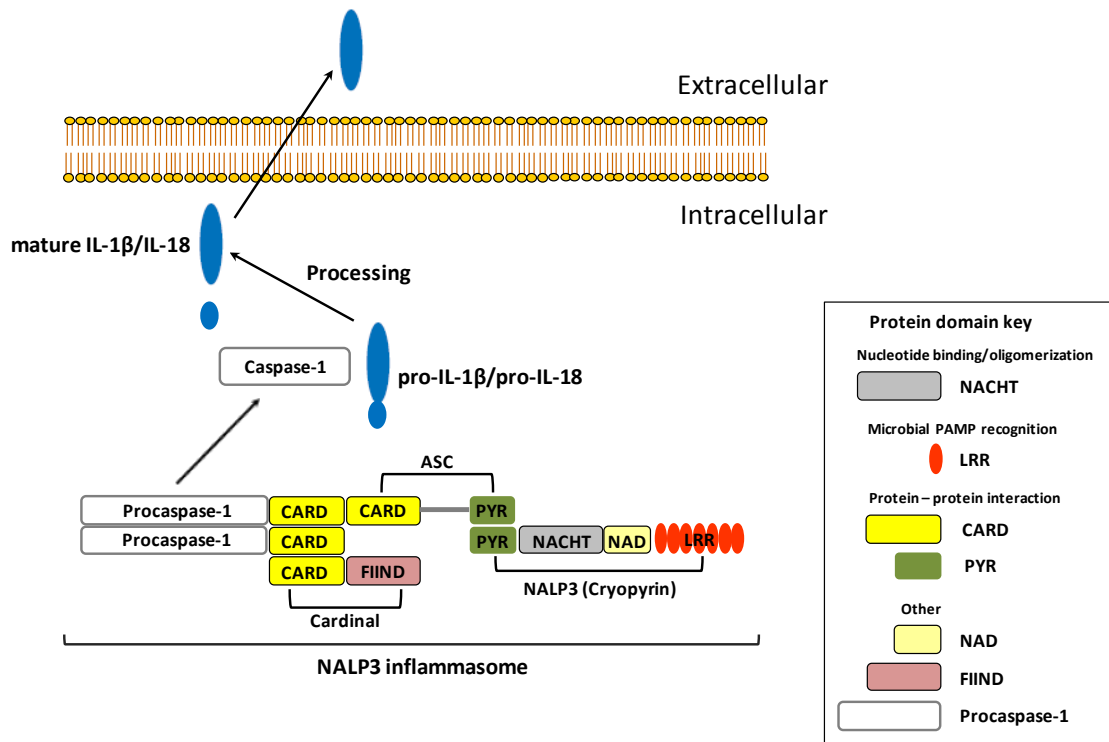


Figure 1.1 Assembly of the NALP3 (NLRP3) inflammasome. Activation of a cell leads to a fall in the intracellular concentration of K^+ which initiates assembly of the NALP3 inflammasome. This induces the processing of procaspase-1, which in turn promotes the maturation of bioactive caspase-1. Caspase-1 enzymatically cleaves pro-IL-1 β /pro-IL-18 at a conserved aspartic acid residue, which generates mature IL-1 β /IL-18. The bioactive cytokine then leaves the cell. ASC = apoptosis-associated speck-like protein containing a C-terminal CARD domain; CARD = Caspase-activating recruitment domain; CARDINAL = CARD inhibitor of NF- κ B-activating ligands; FIIND = function to find domain; LRR = leucine-rich repeat domain; NACHT = NAIP, CIITA, HET-E, TP-1 domain; NAD = NACHT-associated domain; PYR = pyrin domain. Figure adapted from Dinarello (2009).

(Mantovani, Cassatella et al. 2011). Many other pro-inflammatory effects are initiated by cytokines, and these are discussed in more detail in this Chapter, section 1.2.1.1.

Another important component of innate immunity is the complement system, a cohort of plasma proteins which, through a series of sequential interactions with each other, operate to remove pathogens. Three major pathways have been identified which initiate complement activation: the classical pathway, the lectin pathway and the alternative pathway (Zipfel and Skerka 2009).

An additional cellular contribution to the innate system comes from a small group of lymphocytes whose effector functions traverse both innate and adaptive immune responses. This group includes NK cells and the innate-like lymphocytes: B-1 cells, $\gamma\delta$ T cells and NKT cells. Finally, a novel innate effector cell population known as nuocytes have recently been described. They act as an early source of Th2 cytokines, priming the adaptive response against helminths (Neill, Wong et al. 2010).

1.1.1.2 Chickens

The innate immune response in the chicken could be accurately described as accommodating subtle differences amid general conformity with the system seen in humans. Both species have been separately evolving for over 300 million years, so this is perhaps to be expected. As with many areas of avian immunology, the availability of the chicken genome sequence has permitted the recent identification of a significant number of immune molecules previously “missing” in the chicken. Despite this, there are still many components of the human innate immune system for which an equivalent has yet to be recognised in the chicken.

Avian macrophages appear to be phenotypically similar to those in mammals

although they have not yet been characterised to the same extent. Mammalian macrophages colonise tissues after migrating from the circulation, and this also appears to be the case for chicken macrophages. Here, they actively recognise, phagocytose and eliminate pathogens, similar to mammals. They contain anti-microbial proteins and enzymes in phagolysosomes, demonstrate respiratory burst activity and produce nitric oxide.

Birds lack neutrophils and instead possess a functional equivalent known as the heterophil. These cells migrate to sites of infection more rapidly than other types and are the predominant subset in early innate responses. They phagocytose pathogens and eliminate them in phagolysosomes following degranulation. Unlike neutrophils, they do not contain myeloperoxidase and exhibit only modest respiratory burst activity. Similar to neutrophils, heterophils also have the ability to capture pathogens using extracellular traps (Chuammitri, Ostojic et al. 2009).

Avian macrophages and heterophils express a different repertoire of PRRs compared with mammalian phagocytes. Those most well characterised are the TLRs, where notable species-specific differences are apparent. For example, the region of the human genome containing the TLR1, 6 and 10 genes has conserved synteny with a locus in the chicken containing a pair of genes named TLR1LA and TLR1LB (Kaiser, 2010). In addition, the chicken genome contains two copies of TLR2 whereas only a single gene exists in humans. Bacterial PAMPs are recognised in humans by functional heterodimers of either TLR1 with TLR2, or TLR6 with TLR2 (Ozinsky, Underhill et al. 2000). This cooperation between TLRs facilitates recognition of a wide range of bacterial TLR agonists. An equivalent mechanism has also been described in chickens whereby heterodimers form between TLR1LA and TLR2B, as well as between TLR1LB and TLR2A (Keestra, de Zoete et al. 2007; Higuchi, Matsuo et al. 2008).

There are also “missing” TLRs in the chicken with no obvious orthologues of huTLR9 or huTLR11, whilst chTLR8 is a pseudogene (Philbin, Iqbal et al. 2005). Conversely, the chicken possesses genes for two TLRs (TLR15 and TLR21) which are absent in humans, although the latter is a direct functional equivalent of huTLR9 (Brownlie, Zhu et al. 2009). A comparison of the TLR repertoires of humans and chickens is provided in Table 1.1. Despite these striking differences between the species, there is no obvious loss of function in the chicken, which can deal with a comparable variety of PAMPs to those encountered by human TLRs.

	Human	Chicken	chTLR identification
Cell surface TLRs which recognise cell surface PAMPs	TLR1/6/10	TLR1LA and TLR1LB	(Iqbal, Philbin et al. 2005) _a , (Yilmaz, Shen et al. 2005)
	TLR2	TLR2A and TLR2B	(Fukui, Inoue et al. 2001)
	TLR4	TLR4	(Leveque, Forgetta et al. 2003)
	TLR5	TLR5	(Iqbal, Philbin et al. 2005) _b
	TLR11	Not present	
	Not present	TLR15	(Higgs, Cormican et al. 2006)
Intracellular TLRs which recognise nucleic acids	TLR3	TLR3	(Iqbal, Philbin et al. 2005) _a
	TLR7	TLR7	(Philbin, Iqbal et al. 2005)
	TLR8	Pseudogene	(Philbin, Iqbal et al. 2005)
	TLR9	TLR21 (functional equivalent)	(Roach, Glusman et al. 2005)

Table 1.1 The human and chicken Toll-like receptor families.

Mannose-binding lectin and scavenger receptors are conserved in the chicken. However, many of the NLRs and RLRs found in humans are not. Notably, none of the NALPs have been identified in chickens, and NOD2 is also missing (Kaiser 2010). Additionally, RIG-I has yet to be found in the chicken (Barber, Aldridge et al. 2010).

However, MDA5 has been cloned and is functionally analogous to the human orthologue (Karpala, Stewart et al. 2011). The partial gene sequence for LGP2 (DHX58) is apparent in the chicken genome (personal search), although it has missing exons at the N-terminal which are likely to be in the adjacent sequence gap.

Although both NK and $\gamma\delta$ T cells have been identified in the chicken, their contributions to the innate immune response have not been defined. A clear NKT cell population has yet to be described in the chicken (Rogers, Viertlboeck et al. 2008).

All three complement pathways are present in the chicken (Nonaka and Kimura 2006), although, fewer components of each have been isolated compared to mammals.

1.1.2 The adaptive immune response

1.1.2.1 Humans

The adaptive immune response is required when innate defences are insufficient to clear invading pathogens. It is based around the central dogma of the recognition of specific antigen by lymphocytes bearing a distinct antigen receptor. Although the initial response to antigen is slow by comparison to the innate system, it confers long lasting protection which is both specific and rapid upon re-exposure to the same antigen.

Two major types of lymphocytes are involved in adaptive immunity – T and B cells. Both express receptors that recognise a vast number of antigenic epitopes. This is the result of gene rearrangements which generate a hugely diverse repertoire of lymphocyte receptors. Both B and T cells originate from pluripotent haematopoietic stem cells in the bone marrow. B cells remain here and differentiate into immature B cells expressing immunoglobulin (Ig) on their surface. B cell precursors (pro-B cell) initially interact with stromal cells in the bone marrow leading to rearrangement of their

Ig genes. They then undergo negative selection where B cells which react strongly to self antigen are inactivated. Those that survive migrate to peripheral lymphoid organs, which, following activation by antigen and helper T cells, leads to their proliferation and differentiation into plasma or memory cells that secrete antibody (Ab).

Immunoglobulins from a single B cell, either surface-bound as the B cell receptor (BCR) or as secreted Abs, have the same antigen specificity. Every Ig has the same basic Y-shaped structure comprising of a constant (C) region and a pair of variable (V) regions. The Fc portion of the C region of secreted Abs engage with immune cells to initiate effector mechanisms, however, membrane-bound BCRs expressed on the surface of B cells lack such an interaction. The V region is highly diverse and binds native antigen which has not required processing. Antibody structure is also defined by two heavy and two light chains which are comprised of both C and V regions. The two heavy chains are disulphide bonded to one another, and both are also attached to a light chain. The five different classes of immunoglobulin, IgA, IgD, IgE, IgG and IgM, are characterised by their different heavy chains, or isotypes, which confer specific functionality. Secreted antibodies perform three main functions which are to bind pathogens to neutralise them, to opsonise pathogens to facilitate phagocytosis by cells that recognise antibody, and to activate complement.

T cells develop from lymphocyte progenitors in the bone marrow and then migrate to the thymus where they differentiate. Once in the thymus, their T cell receptor (TCR) genes become rearranged during a period of development and proliferation. Phases of thymocyte maturation can be distinguished by the presence of CD markers on the surface of developing cells. Thymocytes develop from double-negative ($CD3^-CD4^-CD8^-$) into one of two T cell lineages: either $\gamma\delta^+CD3^+CD4^-CD8^-$ T cells or double-positive $\alpha\beta^+CD3^+CD4^+CD8^+$ T cells which constitute the majority population

(Shortman and Wu 1996). Most thymocytes at the double positive stage then die after undergoing selection. Positive and negative selection determines whether T cells which recognise self MHC, but are not autoreactive to self antigen, survive. These cells are positively selected. Those which react too vigorously to self antigen are negatively selected and removed following apoptosis (Sebzda, Mariathasan et al. 1999). Positively selected cells mature into single-positive thymocytes ($CD3^+CD4^+CD8^-$ or $CD3^+CD4^-CD8^+$) which are then exported and migrate to peripheral lymphoid organs.

DCs are potent antigen presenting cells (APCs) that reside in tissues and peripheral blood. Functionally, they traverse innate and adaptive immune responses to coordinate efficient pathogen clearance. Two major DC subsets, myeloid (mDC) and plasmacytoid (pDC), have been extensively characterised in mammals. They differ from one another in the numerous cell surface proteins they express, the cytokines they secrete and crucially, in the types of immune response they elicit. Adaptive responses are initially mobilised by activated DCs that have taken up antigen in peripheral tissues. They then migrate to lymphoid organs to present the processed antigen to naive T cells. Antigen recognition takes place when the membrane-bound TCR of a naive T cell identifies its antigen presented by major histocompatibility (MHC) molecules on the surface of antigen presenting cells (APC) (Germain 1994). MHC molecules are highly polymorphic and classed as either type I or type II based on the antigens they process and present. MHC Class I molecules are expressed by all nucleated cells in the body and present antigen from intracellular pathogens. Class II MHC molecules are found exclusively on the surface of antigen-presenting cells (DCs, B cells, macrophages) and display antigen from extracellular pathogens.

Naive T cells which recognise their specific antigen undergo clonal expansion and differentiate into effector T cells. These can be divided into two major subsets –

CD8⁺ cytotoxic T cells which recognise antigen in the context of MHC I molecules, and CD4⁺ helper T cells that identify antigen presented by Class II MHC (Glimcher and Murphy 2000). Cytotoxic T cells drive a cell-mediated adaptive immune response where they secrete perforin and granzymes to directly kill infected cells, particularly those infected with virus. An ever-expanding group of CD4⁺ helper T cells, which carry out a broad range of functions, has been identified. They are defined by the cytokines they secrete and transcription factors they express in addition to their surface phenotype (Glimcher and Murphy 2000). The best characterised of these are the Th1 and Th2 subsets. Th1 cells secrete IFN- γ to activate macrophages which leads to the killing of cells infected with intracellular pathogens. Th2 cells secrete IL-4, IL-5 and IL-13 to promote antibody-mediated (humoral) responses against extracellular pathogens, but can also promote allergic immune responses (Glimcher and Murphy 2000). Other CD4⁺ helper T cell subsets include Th17, Th9, Th22 and T_{FH} (T follicular helper), which between them instigate a range of protective responses to clear pathogens. A further subset known as regulatory T cells (T_{reg}) mediate immunosuppression by dampening inflammatory responses. Two major types of T_{reg} cells have been identified in humans: natural T_{reg} cells (nT_{reg}), and inducible T_{reg} cells (iT_{reg}) of which there are two subsets, type 1 regulatory T cells (T_{R1}) and T helper 3 T cells (Th3) (Bettini and Vignali 2010). Both nT_{reg} and iT_{reg} cells secrete IL-10 in order to mediate immunosuppression and tolerance; however, there are a number of key differences between these populations. The nT_{reg} population is generated in the thymus, expresses the FoxP3 transcription factor and secretes IL-10 and TGF- β . By contrast, iT_{reg} cells are generated in the periphery. Th3 cells express FoxP3 but T_{R1} cells do not. Th3 cells primarily secrete TGF- β , whereas T_{R1} cells secrete many more cytokines, including IL-5 and IFN- γ (in addition to IL-10 and TGF- β) (Bettini and Vignali 2010).

Lymphocytes which persist after an infection has been cleared are called memory cells and provide long-term protective immunity against further exposure to the same pathogen. Upon re-encountering this pathogen, relevant memory cells are rapidly activated to produce a more robust and faster response. Memory B cells secrete antibodies which have a higher affinity for the antigen, following rearrangement of their BCR variable region genes by somatic hypermutation. This ensures further exposure will lead to an even more specific response. Memory T cells are present in much greater abundance than naive T cells specific for the same antigen. They are long-lived and can be identified by a distinct cohort of cell surface proteins, the types of responses upon activation and expression of cell survival genes. Two types of memory T cells, effector and central, exist. Effector memory T cells, upon activation, differentiate into an effector T cell which secretes multiple cytokines and migrates to tissues. Central memory T cells are more slow acting, do not rapidly secrete cytokines and stay in peripheral lymphoid tissues following activation.

1.1.2.2 Chickens

Despite a number of prominent differences between the human and chicken adaptive immune systems, they generate a broadly similar response to infection. The chicken possesses both B and T cell populations; however, their development is different compared to that of mammalian lymphocytes. Chicken B cell precursors develop from stem cells in the para-aortic foci, the allantois, and the bone marrow during embryonic development. Within these haematopoietic tissues, they undergo Ig gene rearrangement before migrating to a specialised gut-associated lymphoid organ known as the bursa of Fabricius. The bursa is colonised in a single period from embryonic incubation days (EID) 8-15, after which it rapidly increases in size due to

intense B cell proliferation. Once a chick has hatched, the bursa further increases in size as B cells continue to proliferate until ~3 months post-hatch. At this point, the bursa begins to involute and has disappeared after 6 months. Chicken BCR diversity emerges through a different mechanism to the one described in mammals. In mammals, Ig gene rearrangement generates Ab diversity. In birds, rearrangement of Ig genes also takes place; however, Ab diversity is created by somatic gene conversion. This is a one-off event which provides a bird with its BCR repertoire for life. This is in stark contrast to mammals, where Ab diversity is continuously generated (Ratcliffe 2006).

Compared with mammals, birds possess limited Ab isotype diversity, having only IgA, IgM and IgY. The latter is the functional equivalent of IgG in mammals but does not undergo subtype switching. Birds lack homologues of IgD and IgE (Ratcliffe 2006).

B cells emigrate from the bursa into the periphery; however, only ~5% of the total mature B cell population survives. Although the bursa has involuted fully after 6 months, peripheral blood maintains a steady supply of B cells. These are known as extra-bursal cells and it is thought they derive from the spleen; however, in bursectomized birds, levels of this population are reduced, indicating the earliest precursors of this B cell population originate in the bursa (Paramithiotis and Ratcliffe 1993). The activation of chicken B cells to stimulate antibody production is similar to mammals in that it requires both exposure to antigen and interaction with helper T cells (Vainio, Koch et al. 1984).

Chicken T cell precursors originate in the blood before migrating to the thymus. These cells populate the thymus in three separate stages during embryonic development at EID6, 12 and 18 (Coltey, Bucy et al. 1989). Both the development of avian T cells and the generation of TCR diversity in the thymus appear to resemble the mechanisms

in mammals. Variability in the chicken TCR is therefore created through somatic DNA recombination. Three distinct lineages of mature T cells, characterized by the monoclonal antibodies that recognise them, develop in the thymus. These cells then leave the thymus in three separate stages. TCR1⁺ cells comprise the $\gamma\delta$ T cell population which appear in the spleen at EID15. Notably, they constitute a much bigger proportion of total peripheral lymphocytes in birds than the respective population in humans (20-60% compared with 5-10%). The TCR2⁺ ($\alpha\beta$ V β 1 TCR) cells are the next to leave, and are localised in the spleen at EID19. Finally, the TCR3⁺ ($\alpha\beta$ V β 2 TCR) cells leave the thymus and appear in the spleen at 2 days post-hatch. As in mammals, the chicken $\alpha\beta$ populations are double-positive CD4⁺CD8⁺ cells which are positively selected, mature into single-positive thymocytes (CD3⁺CD4⁺CD8⁻ or CD3⁺CD4⁻CD8⁺) (Davidson and Boyd 1992) and are then exported.

A limited amount of evidence has shown that CD4⁺ helper T cells and CD8⁺ cytotoxic T cells, that are MHC restricted, are present in the chicken. Based on cytokine secretion, the Th1/Th2 paradigm appears to be conserved in *Aves* (Gobel, Schneider et al. 2003; Degen, Daal et al. 2005). In addition, a T_{reg} subset with immunosuppressive activity has recently been identified in the chicken (Shanmugasundaram and Selvaraj 2011).

As in humans, avian APCs process antigen and present it in the context of MHC molecules. The repertoire and genomic organization of MHC genes in the chicken, however, differs greatly from that in humans. Firstly, the chicken MHC (B locus) is around 20 times smaller than the human HLA locus, and is missing orthologues of many genes found in the human MHC (Kaufman, Milne et al. 1999). For example, most of the HLA Class III region is absent in the chicken. Of those genes found in the chicken, however, most have a direct orthologue in man. There are also some genes in

the avian MHC that lack human orthologues. The chicken contains only two class I and two class II β genes, with each class having a dominantly expressed, highly polymorphic major gene and a much less expressed, less polymorphic minor gene. The two class I genes flank the TAP1 and TAP2 genes in the chicken, whereas the TAP genes in humans are found in the class II region. The tapasin gene is situated between the two class II β genes in the chicken, but is separated from the class II genes by ~100 kb in mammals (Kaufman, Jacob et al. 1999). Finally, the class III region in humans separates the class I and II regions, but in the chicken, the class II and class III regions are separated by the class I region (Kaufman, Milne et al. 1999).

1.1.3 Repertoires of cells and structural features

Chickens possess the majority of the major populations of immune cells found in humans; however, several differences in the repertoires of the two species are apparent. Of the three types of granulocytes present in humans, chickens only possess basophils. They lack neutrophils; however, they possess a functional equivalent dubbed the heterophil which has demonstrated a prominent role in innate responses (Harmon 1998). Chickens also lack a direct functional equivalent of human eosinophils, which suggest birds may have developed a mechanism to compensate for the key functional roles that this subset performs in mammals in allergic and Th2 cell responses. Chickens do, however, possess mast cells which also play a central role in the progression of many allergic responses. The three major classes of lymphocyte are present in chickens, although NKT cells and several of the novel subsets of Th cells identified in mammals have yet to be described in birds.

There are a number of distinctive structural features of the avian lymphoid system. For example, chickens lack the classical lymph nodes found in man and instead

possess “dermal lymphoid nodules” (Igyarto, Lacko et al. 2006). These lymphoid aggregates bear very little resemblance to the human lymph node and, as such, it is not yet clear where antigen presentation takes place in the chicken.

The chicken also contains bronchial associated lymphoid tissue (BALT) and several gut-associated lymphoid tissues (GALT) which are not present in man. One example is the caecal tonsils which are lymphoid tissue aggregates containing both lymphocytes and phagocytes found at the proximal end of the caecum, a blind pouch at the junction of the ileum and the colon. Within the jejunum of the chicken is a lymphoid organ known as Meckel’s diverticulum. It contains germinal centres and is a source of antibody-secreting plasma cells. Chickens also possess a Harderian gland which is found behind the eye, contains externally sourced lymphocytes, and appears to be a site of B cell differentiation.

1.1.4 Cytokines

1.1.4.1 Humans

Cytokines are small signalling molecules that coordinate the functional properties of the cells involved in an immune response. They are typically produced in response to stimulation of a cell and can either be secreted by or retained within a cell to elicit their function. Secreted cytokines can affect cells in an autocrine, paracrine or endocrine manner. Collectively, cytokines have a diverse range of functions in both innate and adaptive immunity and have the capacity to either propagate or inhibit immune responses. Cytokines are classified according to their functional properties for which six major functional groups exist; interleukins (IL), colony-stimulating factors (CSF), interferons (IFN), transforming growth factors (TGF), tumour necrosis factors

(TNF) and chemokines. Interleukin, meaning “between leukocytes”, was originally coined to denote the fact they were produced by and acted upon white blood cells. This is now known to reflect only a small aspect of their biology as their synthesis is ubiquitous and they act on many different tissues. At present, around 40 interleukins have been identified in mammals, which are grouped into 6 major structural and functional subfamilies (IL-1, IL-10, IL-12, IL-17, T cell proliferative, and Th2) plus a small group of ILs which are sufficiently unique to remain unassigned. CSFs promote the differentiation of stem cells by directly activating them. IFNs stimulate macrophages and NK cells to elicit anti-viral immune responses. They can also increase the clearance of bacteria and viruses, as well as alerting the immune system to the existence of cancer. TGFs have several roles which include inhibiting cell growth, promoting cell survival and anti-inflammatory capability. The TNFs are pro-inflammatory cytokines that restrict tumour growth and induce apoptosis. Chemokines are critically important during inflammation, where they orchestrate the activation and migration of phagocytes to sites of infection, and homeostasis.

1.1.4.2 Chickens

Considerable progress has been made over the past decade to decipher the number of different cytokine genes in the chicken (Kaiser 2010). Progress was initially slow due to a paucity of reagents and low sequence identity with mammalian orthologues making identification challenging. The availability of the genome sequence (Wallis, Aerts et al. 2004), however, has hastened the rate at which new genes have been uncovered. Birds appear to possess fewer members of each distinct cytokine family; however, novel genes continue to be discovered so it is likely the true extent of the avian cytokine repertoire has yet to be realised. To date, genomic and EST analysis

has identified the genes for 27 interleukins, all three TGFs, 12 TNFSF members, all three CSFs, 10 type I IFNs, IFN- γ , a single IFN- λ , and 24 chemokines (Kaiser 2010). Of those identified so far in the chicken, effector functions appear to be conserved despite relatively low amino acid identities (18-40%) with human homologues. Although lacking certain direct orthologues from each family, birds appear to possess most Th1, Th2, Th17 and IL-10 family cytokines found in humans, emphasizing the probable conservation of their distinct T cell lineages in birds. Of the pro-inflammatory cytokines, IL-1 β and IL-6 are present but TNF- α , one of the major pro-inflammatory cytokines found in mammals, is notably absent. Strikingly, significantly fewer IL-1 family cytokines have been identified in the chicken compared with the number of these genes discovered in mammals. This is discussed in more detail in this Chapter, section 1.3.4.

1.2 The Interleukin-1 gene family

The interleukin-1 family consists of a large group of ligands and their receptors which have both pro- and anti-inflammatory activities. In humans, the family contains eleven ligand genes encoded at three separate loci. Nine of these, including IL-1 receptor antagonist (IL-1RN), are present at a single locus on chromosome 2, whereas IL-18 and IL-33 lie on chromosomes 11 and 9 respectively. Ligands are named IL-1F1-F11 (Sims, Nicklin et al. 2001), however, this nomenclature has recently been partially revised (Dinarello, Arend et al. 2010). Members IL-1F5-F9 are now named IL-36RN, IL-36 α , IL-37, IL-36 β , and IL-36 γ , respectively (Dinarello, Arend et al. 2010).

Ligand members have a broad and sometimes overlapping range of prominent roles in innate and adaptive immune responses. They have arisen following gene duplication which is reflected in their many shared characteristics. For instance, they are

structurally related to one another and encode three common exons which are at the C-terminus of every IL-1F gene. Within the final exon is a 63 bp sequence motif which is highly conserved in all eleven genes and is the defining signature of the IL-1 family (Nicklin, Barton et al. 2002). This section describes the specific bioactivities, expression, regulation and genomic organisation for each of the different ligands and receptors.

1.2.1 IL-1 ligands in mammals

1.2.1.1 IL-1F1 (IL-1 α) and IL-1F2 (IL-1 β)

Unless specified otherwise, the term “IL-1” is usually used to denote both IL-1 α and IL-1 β . This is due to the fact that these pleiotropic, pro-inflammatory cytokines have identical bioactivities. Although they share the same function, they do differ from one another in many ways. This section will firstly describe their general, shared effects, followed by a description of their major differences.

IL-1 affects multiple biological processes through its ability to act upon almost every tissue and cell type in the body. Its most prominent, well-characterised role is as a potent modulator of inflammation. It does this by increasing the transcription of a vast range of inducible genes (Dinarello 1996). IL-1 initiates the (intracellular) inflammatory cascade by upregulating transcription of the genes encoding the pro-inflammatory mediators cyclooxygenase-2 (COX-2), inducible nitric oxide synthase (iNOS) and type II phospholipase A2 (PLA2). The consequent increase in abundance of these enzymes leads to a surge in the production of leukotrienes, nitric oxide, platelet-activating factor and prostanoids. It is these mediator molecules that are responsible for fever, inflammation, vasodilation and increased vascular permeability, hypotension, a reduced pain threshold and ultimately, the destruction of tissues (Dinarello 2000; Dinarello 2009). Other important effects elicited by IL-1 include activation of JNK, p38, and members of the mitogen-activated protein kinase (MAPK) signalling pathway; increased transcription of pro-inflammatory genes via the transcription factors NF- κ B, AP-1 and C/EBP β ; increased expression of endothelial surface adhesion molecules; increased synthesis of numerous chemokines, many other cytokines (particularly IL-6, TNF- α and CSF1-3) and their receptors, matrix metalloproteinases, acute phase proteins

in the liver, growth factors, lipids, extracellular matrix components; and the activation and migration of neutrophils (Dinarello 1996; Dinarello 2000). Many of these effects are brought about when IL-1 acts synergistically with either bradykinin, TNF- α /IL-6/CSF or a growth factor (Dinarello 1996). The majority of these effects are instigated by the major target cell populations of IL-1 during the innate immune response, which are DCs, macrophages, monocytes, neutrophils, basophils and mast cells (Sims and Smith 2010).

In addition to its major pro-inflammatory role, IL-1 also has the capacity to co-stimulate T cells. For example, it influences the Th2-mediated immune response in asthma. In experimental mouse models, rodents that lack IL-1RI or have been injected with anti-IL-1 β antibodies exhibit an attenuated reaction when challenged with allergen (Johnson, Yucesoy et al. 2005). IL-1 is indispensable for IL-17 production from Th17 cells. Naive CD4⁺ T cells differentiate into Th17 cells following stimulation with either TGF- β plus IL-6 (Bettelli, Carrier et al. 2006) or IL-1 β / α plus IL-23 (Chung, Chang et al. 2009). These early Th17 cells show relatively high expression of IL-1RI (Chung, Chang et al. 2009) and, following further stimulation with IL-1 plus a STAT3-inducing cytokine (IL-6, IL-21 or IL-23), become fully committed Th17 cells (Guo, Wei et al. 2009). STAT3 induction with IL-1 stimulation induces ROR γ t in Th17 cells, leading to IL-17 production independently of TCR stimulation (Guo, Wei et al. 2009).

IL-1 is able to affect a broad range of fundamental, physiological effects, and as such it is no surprise that it is strongly associated with a large number of different diseases. To date, IL-1 has been recognised as contributing to the pathogenesis of several forms of arthritis, type-2 diabetes, several forms of cancer, atherosclerosis, heart disease and heart failure as well as a growing number of autoinflammatory diseases (Dinarello 1996; Dinarello 2011).

The number of agents capable of inducing IL-1 production is vast. These include many cytokines (including IL-1 itself), other inflammatory agents (e.g. C5a, CRP), clotting factors (e.g. thrombin), cell matrix-associated factors (e.g. collagen), stress factors (e.g. hypoxia), neuroactive agents (e.g. melatonin), lipids (e.g. oxLDL), and many drugs. Most known viruses, bacteria and many fungi are also able to increase its production (Dinarello 1996).

Both IL-1 β and IL-1 α signal through the IL-1RI. Upon receptor engagement, IL-1RAcP, a co-receptor essential for IL-1 signalling, is recruited on the cell surface leading to signal transduction and increased transcription of inducible genes. Both ligands also share the same three dimensional structure, the β -trefoil. This is comprised of a 6 β -strand “barrel”, at one end of which a further 6 β -strands are located (Murzin, Lesk et al. 1992). The β -trefoil structure (Figure 1.2) is separated into 3 distinct trefoils, each of which consists of a hairpin loop and a β -sheet (Chavez, Gosavi et al. 2006). The crystal structure of the first IL-1 family member, IL-1 β , was determined by (Priestle, Schar et al. 1989) at 2.0 Å resolution. Subsequent elucidation of the IL-1 α structure (Graves, Hatada et al. 1990) reported substantial similarity to that of IL-1 β , except for 3 important differences. In addition to the 12 β -strands (of IL-1 β), the IL-1 α molecule has 3 further secondary structure components: 2 extra β -strands (one close to the N-terminus), and, between residues 101-105, 2 “turns” of a 3_{10} helix. Having the extra β -strand adjacent to the N-terminus results in this end of the protein being situated in a different position within IL-1 α to where it is found in IL-1 β (Graves, Hatada et al. 1990). It has been proposed this may account for both precursor and mature forms of IL-1 α being biologically active.

IL-1 α has a number of distinctive properties which set it apart from IL-1 β . First, its synthesis and maturation is strikingly different from that of IL-1 β . IL-1 α is translated

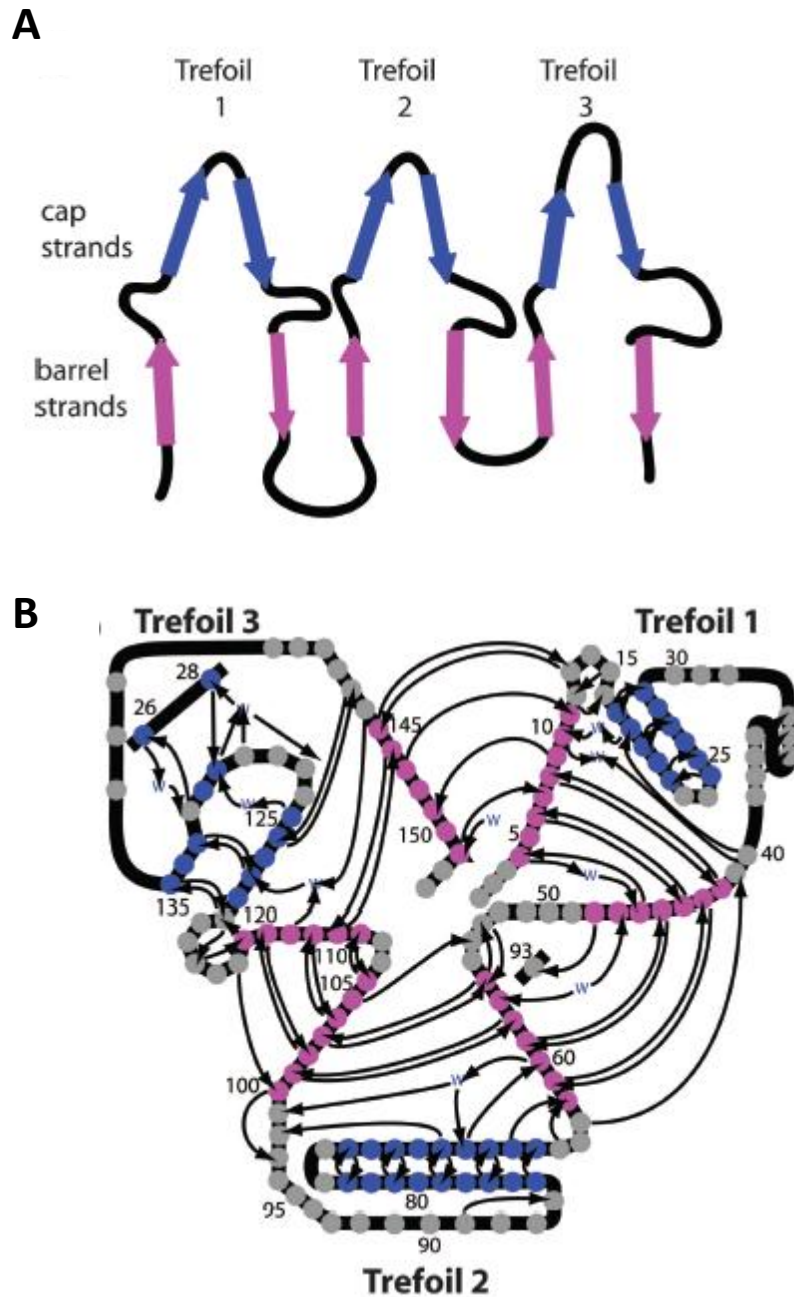


Figure 1.2 The general β -trefoil protein structure. **A.** The 12 β strands which form the cap and barrel are coloured in blue and pink, respectively. **B.** When the protein is folded, β strands form three distinct trefoils with “three-fold pseudo-symmetry”. Diagram reproduced from Chavez, Gosavi et al. (2006).

as a biologically active precursor (Mosley, Urdal et al. 1987) containing a pro-domain which is then processed in one of two potential ways. Either it is cleaved by the membrane-associated cysteine protease calpain (Kobayashi, Yamamoto et al. 1990) or it is myristoylated (Stevenson, Bursten et al. 1993), which localises it to the plasma membrane where it becomes inserted (Kurt-Jones, Beller et al. 1985). The majority of IL-1 α is retained intracellularly and is not secreted (Lonnemann, Endres et al. 1989). By contrast, IL-1 β is synthesised as a biologically inactive molecule containing a pro-domain (Jobling, Auron et al. 1988), which is cleaved by caspase-1 at a conserved aspartic acid residue (Black, Kronheim et al. 1988) facilitating secretion. The mechanisms underlying IL-1 β processing and secretion are complicated and not fully understood. What is clear, however, is that caspase-1 activation is dependent upon assembly of the NALP3 inflammasome (Agostini, Martinon et al. 2004). Several alternative proteases, such as proteinase-3, are also able to process IL-1 β (Figure 1.3) (Dinarello 2011). Secretion of the mature protein occurs thereafter via one of five possible mechanisms involving either vesicles, lysosomes, exosomes, membrane transporters or passive secretion upon lysis (Figure 1.4) (Qu, 2007), although exactly which process is correct is not known.

Calpain protease cleavage of IL-1 α yields the N-terminal propiece and the mature cytokine which are both bioactive. A recent study has elucidated the mechanism underlying secretion of IL-1 α (Fettelschoss, Kistowska et al. 2011). Mature IL-1 α is directly bound by IL-1 β which acts as a shuttle to transfer IL-1 α out of a cell. This process is dependent on activation of both the inflammasome and caspase-1, which are needed for IL-1 β maturation. The presence of IL-1 β is essential given that IL-1 β ^{-/-} mice do not secrete mature IL-1 α . The propiece along with full length pro-IL-1 α , however, translocate to the nucleus - one of the major recognised features of IL-1 α which

distinguishes it from IL-1 β (Figure 1.5). Both IL-1 α species possess a nuclear localisation sequence (KVLKKRR) which directs them across the nuclear membrane (Wessendorf, Garfinkel et al. 1993). Once intranuclear, IL-1 α elicits a range of functional effects which can be broadly categorised into three main types of effects: on cellular growth/proliferation/death, on gene expression and on the

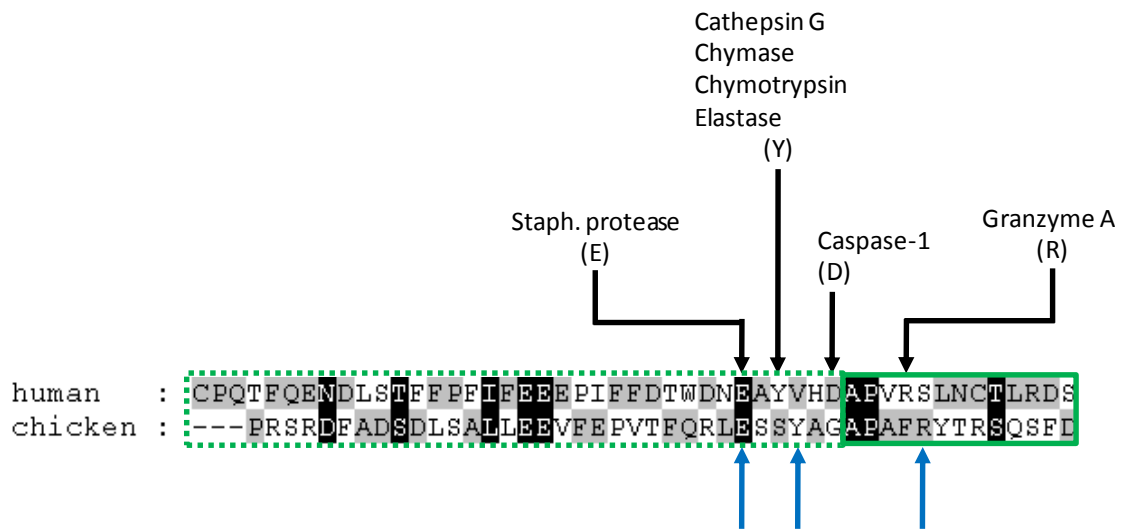


Figure 1.3 Non-caspase-1 processing of pro-IL-1 β . Neutrophil proteases process pro-IL-1 β at residues (E111, Y113, and R120) near the caspase-1 cleavage site (D) in the human sequence (indicated with black arrows). The chicken sequence lacks a conserved aspartic acid residue at the corresponding site. However, bioassays have indicated chIL-1 β is cleaved in this region (Gyorfy, Ohnemus et al. 2003). Although similar proteases to those found in neutrophils have yet to be identified in avian heterophils, their cut sites are conserved in the chIL-1 β amino acid sequence (indicated with blue arrows). The stippled green box indicates residues which belong to the pro-domain. The solid green box indicates the residues which belong to the mature protein. Figure adapted from Dinarello (2011).

migration of cells (Luheshi, Rothwell et al. 2009). The exact mechanisms underlying these reported effects have yet to be thoroughly characterised. However, IL-1 α directly binds to either RNA-binding proteins, histone acetyltransferases, IL-1RII, HS1-associated protein X-1 (HAX-1) or necdin (Luheshi, Rothwell et al. 2009). To date, the

intranuclear effects of IL-1 α have only been demonstrated *in vitro*. Some pro-IL-1 α is myristoylated then inserted into the plasma membrane.

IL-1 is produced by a range of different cells, including DCs, monocytes, macrophages, mast cells, neutrophils, B and T cells, endothelial cells, epithelial cells and cells undergoing lysis. IL-1 α is produced (although not secreted) by the entire range of cells; however, IL-1 β is predominantly secreted by monocytes and macrophages (Sims and Smith 2010). IL-1 α is also constitutively expressed, whereas basal expression of IL-1 β mRNA is very low (Dinarello 1996).

A distinguishing feature of IL-1 β is the discordance between transcription and translation. Several non-microbial ligands induce high levels of IL-1 β transcription in monocytes; however, only a fraction of this mRNA is translated, with the majority being degraded (Dinarello 1996). A conserved “instability element” in the IL-1 β coding region (functionally proven for IL-1F7b and inferred for IL-1 β by alignment) is responsible for the lack of translation (Bufler, Gamboni-Robertson et al. 2004). Translation is significantly increased when these monocytes are subsequently stimulated with LPS or IL-1 β (Schindler, Clark et al. 1990). It has been proposed that the 3' UTR of IL-1 β mRNA is stabilised by these ligands (Dinarello 1996).

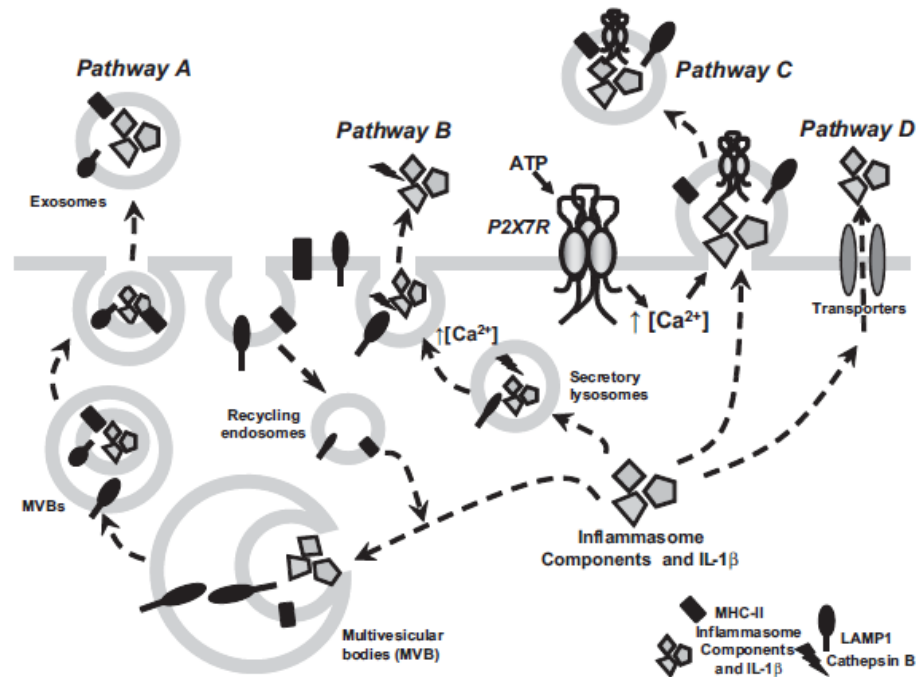


Figure 1.4 Potential mechanisms of mature IL-1 β release. Pathway A indicates the formation of multivesicular bodies to release IL-1 β in exosomes. Pathway B outlines the release of IL-1 β by exocytosis from secretory lysosomes which fuse with the plasma membrane. Pathway C suggests IL-1 β is released from cells in microvesicles which bud from the membrane. IL-1 β is subsequently released from vesicles. Pathway D describes IL-1 β release from a cell through ATP-activated membrane transporters. A fifth mechanism has suggested IL-1 β is passively released when cells are lysed. Figure reproduced from (Qu, Franchi et al. 2007). *Copyright 2007. The American Association of Immunologists, Inc.*

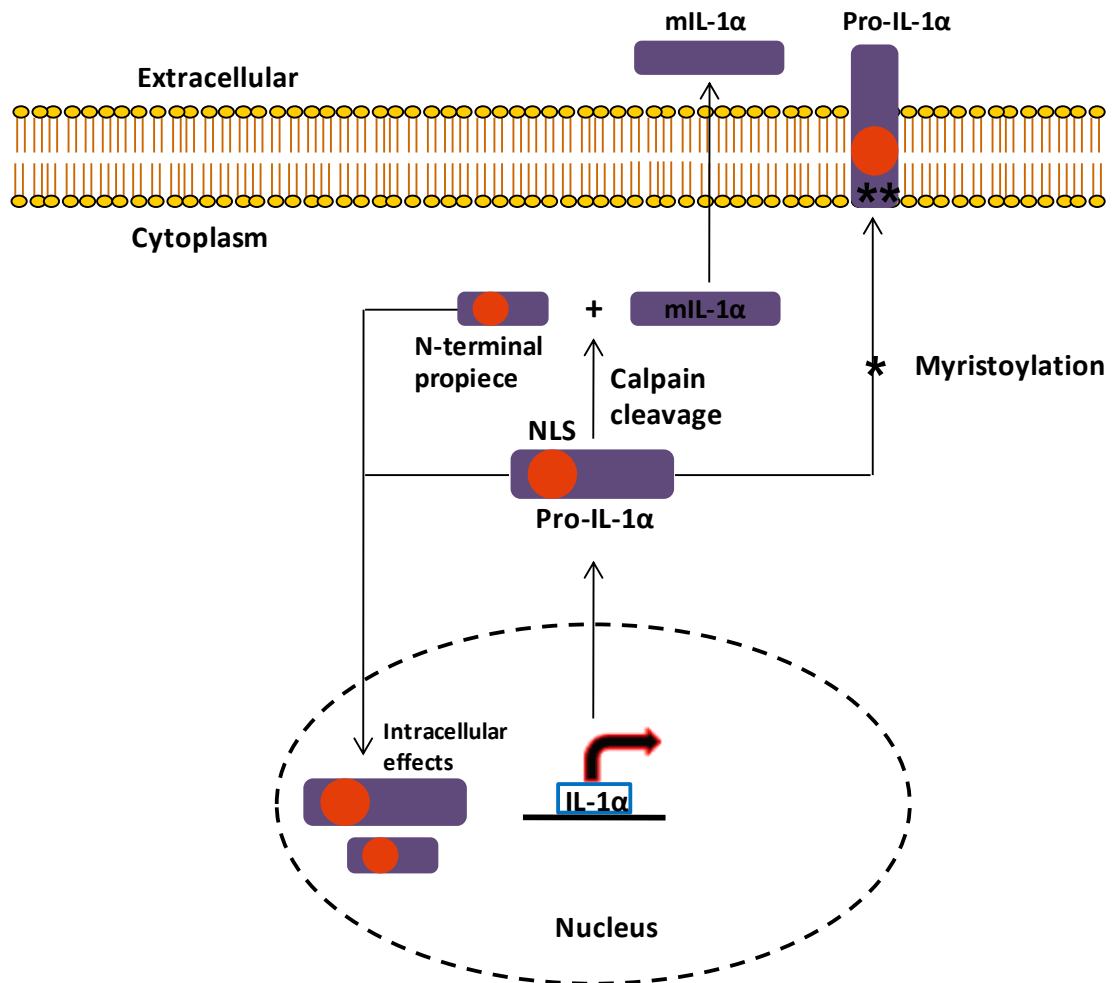


Figure 1.5 Calpain-dependant processing and maturation of IL-1 α .

Cleavage of pro-IL-1 α yields the N-terminal propeptide and the mature cytokine (mIL-1 α) both of which are bioactive. A very small amount of mIL-1 α is released in an IL-1 β , inflammasome and caspase-1-dependent manner. The NH₂-terminal propeptide translocates to the nucleus to mediate intracellular effects. Pro-IL-1 α enters the nucleus or becomes myristoylated which promotes localisation to the plasma membrane for insertion. Figure reproduced from Gabay, Lamacchia et al. (2010).

1.2.1.2 IL-1F3 (IL-1RN)

IL-1RN is an endogenous antagonist of inflammation. It physically blocks the IL-1RI preventing IL-1 α and IL-1 β from binding, which effectively limits inflammation. Target cells only require occupation of three to five IL-1RI with IL-1 to be fully stimulated. Such exceptional sensitivity combined with a relatively high abundance of IL-1RI on target cells means that a minimum of a 100-fold excess of IL-1RN (over IL-1) is required to inhibit cell activation (Arend and Guthridge 2000).

IL-1RN does not activate signal transduction (Dripps, Brandhuber et al. 1991), as it lacks the specific amino acids required to engage IL-1RAcP on the cell surface (Schreuder, Tardif et al. 1997; Wang, Zhang et al. 2010). Although IL-1RN binds to IL-1RI with near equal affinity to that of IL-1 α and IL-1 β (Dinarello 1996), it does not act as an agonist, as administering a million-fold excess (over IL-1 α and IL-1 β) of the cytokine in humans has no biological effect (Granowitz, Porat et al. 1992).

In mammals, there are two major structural variants of IL-1RN - secretory (sIL-1RN) and intracellular (icIL-1RN). The sIL-1RN variant contains a 25 aa signal sequence that is cleaved by a signal peptidase to permit post-translational modification and secretion of the protein via the secretory pathway (Eisenberg, Evans et al. 1990; Walter and Johnson 1994). Intracellular IL-1RN is retained within the cell as it lacks a signal peptide. In mammals, three alternatively spliced isoforms of icIL-1RN have been described. The first intracellular variant to be described, icIL-1RN1, is formed through alternative splicing of an upstream exon into the N-terminus of the sIL-1RN mRNA (Haskill, Martin et al. 1991). An additional upstream exon is spliced in between exons 1 and 2 of icIL-1RN1 to form icIL-1RN2 (Muzio, Polentarutti et al. 1995). The protein product of this variant has yet to be identified *in vivo*. The third intracellular variant,

icIL-1RN3, is created through use of an alternative translation initiation site located in exon 2 of the sIL-1RN transcript (Malyak, Guthridge et al. 1998). Although it has received no attention beyond the report describing its discovery, a fourth intracellular variant has been described (Holtkamp, de Vos et al. 1999), formed through yet another upstream exon which is spliced in between exons 1 and 2 of icIL-1RN2. Critically, this exon encodes an in-frame stop codon, which results in the predicted protein being significantly truncated to 27 amino acids in length. These variants are discussed in more detail in Chapter 5, section 5.1.

The biological role of sIL-1RN appears to be limited to blocking IL-1RI on the cell surface. By contrast, the icIL-1RN isoforms may function through any of three different mechanisms. Firstly, icIL-1RN may suppress intracellular signalling in a non-classical (non-IL-1R-dependent) manner (Banda, Guthridge et al. 2005). Secondly, icIL-1RN1 may compete with IL-1 α in the nucleus to inhibit the effects of the agonist (Merhi-Soussi, Berti et al. 2005). Thirdly, icIL-1RN isoforms may be released from cells and bind to membrane-bound IL-1RI to limit IL-1 activity, in a similar way to sIL-1RN (Corradi, Franzi et al. 1995; Levine, Wu et al. 1997; Yoon, Zhu et al. 1999; Evans, Dower et al. 2006). These three possible mechanisms are discussed in more detail in Chapter 5, section 5.1.

Global analysis of IL-1RN expression in tissues has been carried out in rabbits (Apostolopoulos, Ross et al. 1996; Matsukawa, Fukumoto et al. 1997), mice (Gabay, Porter et al. 1997), and rainbow trout (Wang, Bird et al. 2009), but not in humans. In rabbits, expression of the secretory transcript was constitutive in all of the tissues analysed. However, icIL-1RN expression was restricted to caecum, kidney, skin and thymus. In mice, sIL-1RN expression was undetectable and only skin contained constitutively expressed icIL-1RN. When LPS was used to stimulate mouse tissues,

intracellular transcripts were detected in the kidney, liver and spleen. Basal expression of IL-1RN in rainbow trout was ubiquitous.

The expression of IL-1RN in distinct cell populations has been extensively characterised in humans and mice. Secretory IL-1RN is expressed in all cells able to transcribe IL-1 α and IL-1 β , with particularly high levels of expression found in monocytes, macrophages, neutrophils and fibroblasts (Eisenberg, Evans et al. 1990; Arend, Smith et al. 1991; Janson, Hance et al. 1991; Malyak, Smith et al. 1998). By contrast, expression of icIL-1RN is highly restricted, being found in only a limited range of cell types. Expression of each of the different intracellular isoforms has been determined *in vivo*. The icIL-1RN1 protein is predominantly found in endothelial cells, epithelial cells, fibroblasts, keratinocytes and macrophages (Haskill, Martin et al. 1991; Andersson, Bjork et al. 1992; Bigler, Norris et al. 1992; Hammerberg, Arend et al. 1992). A single report has described icIL-1RN2 expression in fibroblasts, keratinocytes, monocytes and polymorphonuclear cells (Muzio, Polentarutti et al. 1995). However, the protein product of this variant has never been identified *in vivo* by any other groups. Neutrophils, PBMCs (Malyak, Smith et al. 1998) and hepatocytes (Gabay, Porter et al. 1999) are the major cell types that express icIL-1RN3.

A broad range of different agents induce IL-1RN expression, of which LPS, adherent IgG (Arend, Smith et al. 1991) and the cytokines GM-CSF (Roux-Lombard, Modoux et al. 1989; Shields, Bernasconi et al. 1990) and IL-4 (Fenton, Buras et al. 1992; Vannier, Miller et al. 1992) are the most effective substances *in vitro*. A similarly vast number of agents induce IL-1RN production *in vivo*. These include almost all known bacteria and viruses, many fungi, as well as multiple cytokines, enzymes and plasma proteins (Dinarello 1996). IL-1RN protein levels are also increased in all disease states in which IL-1 is raised (Arend, Malyak et al. 1998).

1.2.1.3 IL-1F4 (IL-18)

IL-18 induces scores of functional effects to regulate innate and adaptive immune responses. Most notably, it initiates both Th1-mediated and pro-inflammatory immune responses via its major target cell populations of Th1 cells, macrophages, DCs, basophils, NK cells and NKT cells (Smith 2011). IL-18 activates Th1 cells to proliferate and produce IFN- γ in the absence of TCR stimulation. In order to elicit the Th1 response, cells must be co-stimulated with IL-12 or IL-15. Without one of these cytokines, IL-18 induces a Th2 response characterised by IL-4 and IL-13 production (Nakanishi, Yoshimoto et al. 2001). IL-18 activates its target cells to effectively clear bacteria, fungi, viruses and protozoa. Neutrophils and macrophages kill bacteria and fungi following activation by IL-18-induced IFN- γ (van de Veerdonk, Netea et al. 2011). Anti-viral responses are coordinated following stimulation of antigen-specific CD8⁺ T cells, which leads to expansion of this population and downstream effector responses such as IFN- γ -mediated nitric oxide production (Gracie, Robertson et al. 2003). The cytolytic properties of NK cells are enhanced by IL-18 stimulation (Smith 2011), which can lead to effective antifungal activity (Gracie, Robertson et al. 2003). Bacteria and viruses can also be cleared, following increased innate responses, by NKT cells activated with IL-18. Multiple host-protective pro-inflammatory immune effects are modulated following stimulation of monocytes, macrophages, DCs and neutrophils by IL-18 (Smith 2011). IL-18 also has a pathological role in several autoimmune and inflammatory conditions (Nakanishi, Yoshimoto et al. 2001).

IL-18 binds to the IL-18R α , recruiting its co-receptor IL-18 β (IL-18RAcP) to facilitate signal transduction. Its activity is regulated by an endogenous inhibitor, IL-18 binding protein (IL-18BP) (Novick, Kim et al. 1999). It does not act as a receptor

antagonist but instead directly binds the cytokine to neutralise its activity. Several viral homologues of IL-18BP have been identified which act to restrict the host immune response in infected cells (Born, Morrison et al. 2000; Smith, Bryant et al. 2000; Calderara, Xiang et al. 2001; Xiang and Moss 2001).

As befits a cytokine with such a broad spectrum of effector functions, it is widely expressed. It has been detected in adrenal cortex cells, DCs, intestinal epithelial cells, keratinocytes, Kupffer cells, macrophages, microglial cells, monocytes, osteoblasts and synovial fibroblasts (Gracie, Robertson et al. 2003). In contrast to IL-1 β , it is also constitutively expressed, which may indicate a role in regulating homeostasis (Dinarello 2009).

The IL-18 gene has been identified in nearly 40 species of mammals, birds, reptiles and fish, underlining its fundamental importance in immunity. The human gene consists of six exons, which encode three different transcripts. IL-18 is closely related to IL-1 α and IL-33, with which it forms a distinct subgroup following phylogenetic analysis of the IL-1F ligand sequences (Smith 2011). Like IL-1 β , IL-18 is synthesised as an inactive precursor containing a pro-domain, which is cleaved by caspase-1 at a conserved aspartic acid to yield the bioactive mature form of the cytokine (Ghayur, Banerjee et al. 1997; Gu, Kuida et al. 1997).

1.2.1.4 IL-1F5 (IL-36RN)

IL-1F5 is an anti-inflammatory cytokine able to dampen the effects of a range of IL-1 agonist ligands as well as LPS. It acts as a receptor antagonist of IL-1RL2 (IL-1Rrp2), preventing the agonists IL-1F6 (IL-36 α), IL-1F8 (IL-36 β) (Towne, Garka et al. 2004) and IL-1F9 (IL-36 γ) (Debets, Timans et al. 2001) from binding this receptor to initiate gene transcription via NF- κ B and MAP kinases. Upon binding to this receptor,

IL-1F5 fails to recruit IL-1RAcP on the cell surface (Sims 2010), similar to the lack of an interaction when IL-1RN binds to IL-1RI.

IL-1F5 can also downregulate inflammation through activation of the orphan receptor single Ig domain-containing IL-1 receptor-related molecule (SIGIRR). It is not known, however, if IL-1F5 directly binds SIGIRR, as its activation of this receptor has only been described as via an “interaction”. In mice and rats, both IL-1 β - and LPS-induced inflammation is antagonized by IL-1F5 in the brain, leading to an anti-inflammatory response, characterised by increased IL-4 production. The ability of IL-1F5 to mediate this effect is abolished in either SIGIRR^{-/-} or IL-4^{-/-} knockout mice. This function of IL-1F5 appears to be restricted to the brain and is not elicited in mouse macrophages or DCs (Costelloe, Watson et al. 2008).

IL-1F5 is widely expressed in humans and mice, with transcripts detectable in all of the major organs investigated except for bone marrow, liver and the intestines (Mulero, Pace et al. 1999; Barton, Herbst et al. 2000; Busfield, Comrack et al. 2000; Smith, Renshaw et al. 2000). Many distinct populations of human cells also express IL-1F5. These include THP-1 (monocytic leukaemia cell) \pm PMA \pm LPS, PBMCs \pm PHA \pm LPS, LPS-stimulated monocytes, *in vitro* differentiated macrophages, B cells \pm stimulation, NK cells and LPS-stimulated DCs (Mulero, Pace et al. 1999; Barton, Herbst et al. 2000; Busfield, Comrack et al. 2000; Smith, Renshaw et al. 2000). IL-1F5 is constitutively expressed in cultured human bronchial epithelial cells. Stimulation of these cells with IL-4 or IFN- γ significantly decreases its expression (Chustz, Nagarkar et al. 2011).

Studies investigating the expression of IL-1F5 *in vivo* have been limited to inflammatory skin conditions. In several variants of human and mouse psoriasis, IL-1F5 expression is significantly increased compared to levels found in control skin (Debets,

Timans et al. 2001; Blumberg, Dinh et al. 2007; Johnston, Xing et al. 2011). Following the treatment of chronic plaque psoriasis with etanercept (a TNF- α scavenger), IL-1F5 expression is significantly decreased (Johnston, Xing et al. 2011). Inhibiting TNF- α leads to decreased activation of several genes and pathways controlling inflammation in psoriasis (Gottlieb, Chamian et al. 2005). This indicates IL-1F5 expression may be regulated by other pro-inflammatory cytokines. To date, there are no studies which have examined the expression of IL-1F5 following viral, fungal or parasitic infection. Expression in response to stimulation with bacterial agents (other than LPS) is also unknown.

The importance of IL-1F5 in regulating inflammation has recently been emphasised in a study reporting a deficiency of IL-36RN due to mutation. In the cohort of patients expressing this aberrant protein, unregulated inflammation and chronic pustular psoriasis, which can be fatal, were prevalent (Marrakchi, Guigue et al. 2011).

An IL-1F5 gene is present in almost all mammals with an available genome sequence (personal search). In humans, the IL-1F5 gene is comprised of six exons. Its first two exons (1a and 1b) are used alternatively to create two different five exon-containing transcripts which encode the same protein and only differ in their 5' UTRs. Compared to all of the IL-1 ligands, IL-1F5 is most similar to IL-1RN, with which it shares significant amino acid identity (47% and 52% with sIL-1RN and icIL-1RN, respectively) (Mulero, Nelken et al. 2000; Dinarello 2009). The positions of the exon-intron boundaries are also highly conserved between both genes. This led to suggestions that IL-1F5 emerged following gene duplication of IL-1RN (Mulero, Nelken et al. 2000). The crystal structure of mouse IL-1F5 adopts the same β -trefoil fold as IL-1 α , IL-1 β and IL-1RN, as well as containing two α -helices. These are situated in different positions and are of a different type to the two found in IL-1 β (Dunn, Gay et al. 2003).

The mechanism of IL-1F5 secretion has so far remained elusive. The lack of an obvious signal peptide indicates it is unlikely to be processed by signal peptidase. Similarly, the absence of a clear pro-domain containing a caspase-1 cut site suggests it will not be activated by the inflammasome. Recent unpublished observations indicate N-terminally truncated IL-1F5 is significantly more bioactive than the full length molecule (Sims and Smith 2010). This suggests enzymatic cleavage may take place to produce a mature form of the protein. Alternatively, an atypical mode of secretion may be utilised. For instance, IL-1F5 expression in cultured COS-7 and JEG-3 cells leads to significantly more protein in the supernatants than in cell lysates (Barton, Herbst et al. 2000). Importantly, analysis of both secreted and intracellular protein species revealed a product of equal size, suggesting a lack of enzymatic processing.

1.2.1.5 IL-1F6 (IL-36 α)

IL-1F6 is a pro-inflammatory cytokine which activates NF- κ B, ERK1/2, JNK and MAP kinases. After it binds to IL-1RL2 (IL-1Rrp2), IL-1RAcP is recruited, leading to signal transduction (Towne, Garka et al. 2004). This has been demonstrated with human and mouse IL-1F6 in, respectively, human (Jurkat and HepG2) and mouse (BA/F3) cell lines transfected with the receptor.

The expression of IL-1F6 *in vivo* has been studied in several inflammatory skin diseases. Overexpression of IL-1F6 leads to an inflammatory skin phenotype in newborn transgenic mice. Resolution of this condition occurs after 3 weeks, during which a significant reduction in IL-1F6 expression is observed (Blumberg, Dinh et al. 2007). High levels of IL-1F6 expression have been consistently found in the skin of humans and mice with psoriasis (Blumberg, Dinh et al. 2007; Johnston, Xing et al. 2011). Injecting anti-IL-1RL2 antibodies into human psoriatic skin transplanted onto

SCID (CB-17) mice led to disease resolution (Blumberg, Dinh et al. 2010). As IL-1F8 and IL-1F9 are also both elevated in psoriasis skin (Johnston, Xing et al. 2011) and signal through IL-1RL2 (Towne, Garka et al. 2004), reduced inflammation in this model cannot be solely attributed to inhibiting IL-1F6.

IL-1F6 is a pivotal member of the inflammatory cytokine network in psoriasis. Injecting the skin of mice with recombinant IL-1F6 led to statistically significant increases in the expression of IL-17A, IL-23, TNF- α and IFN- γ (Blumberg, Dinh et al. 2010). In addition to significantly increasing its own expression, substantial increases were also observed in further pro-inflammatory cytokines (IL-1 β , IL-1F9, IL-33 and IL-6), IL-10 family cytokines (IL-19, IL-22, IL-24), other important cytokines (IL-12p35, CSF2, CSF3, LT- β), several chemokines, chemokine receptors, iNOS and matrix metalloproteinases (MMP) (Blumberg, Dinh et al. 2010). Conversely, when many of these same cytokines were injected into mice, *il-1f6* expression increased significantly, suggesting a feedback mechanism may exist (Blumberg, Dinh et al. 2010). Synergistic increases in *il-1f6* expression were found following the injection of certain cytokine combinations, with TNF- α and IL-23 showing the biggest induction (Blumberg, Dinh et al. 2010).

IL-1F6 is evidently under the control of IL-17 and TNF- α . Normal human keratinocytes stimulated with IL-17A or IL-17A and IL-22 show significantly elevated IL-1F6 expression (Johnston, Xing et al. 2011). Bronchial epithelial cells cultured with IL-17A or TNF- α showed statistically significant increases in *IL-1F6* expression, which was synergistically increased with both cytokines (Chustz, Nagarkar et al. 2011). Treatment with etanercept leads to a significant reduction in IL-1F6 mRNA (Johnston, Xing et al. 2011). IL-1F6 induces decreased *PPAR γ* expression which inhibits the differentiation of adipocytes (van Asseldonk, Stienstra et al. 2010).

IL-1F6 has been identified in 22 mammals to date. The human gene consists of five exons, which are alternatively spliced to create two different transcripts. Compared with the rest of the IL-1 ligands, it is most closely related to IL-1F8 and IL-1F9, which is reflected in previous phylogenetic analyses of the family (Nicklin, Barton et al. 2002; Taylor, Renshaw et al. 2002).

IL-1F6 lacks both a signal peptide and a caspase-1 cleavage site and so its mode of secretion differs from IL-1RN and IL-1 β . Recent evidence indicates a truncated form of IL-1F6 (Arg8 as the first amino acid) exhibits ~10000-fold more bioactivity than the full length molecule (Blumberg, Dinh et al. 2010). This strongly suggests it is cleaved to yield a potent mature protein. An attempt to characterise a mechanism for its release was carried out in bone marrow-derived macrophages. Following overexpression, IL-1F6 was passively released from cells stimulated with LPS and/or ATP. The cytokine was externalised via the ATP-dependent P2X₇ receptor. IL-1F6 present in both conditioned medium and cell lysate was the same size (22 kDa) indicating it had not been proteolytically cleaved for export (Martin, Scholler et al. 2009).

1.2.1.6 IL-1F7 (IL-37)

The IL-1F7 gene has been found in twenty mammalian species to date. The human gene consists of six exons, which are alternatively spliced to create five different transcripts (Taylor, Renshaw et al. 2002). Of these, IL-1F7b is the longest, contains five of these exons, and has been the sole focus of functional studies on the gene. An IL-1F7-IL-1F9 chimera, expressed in testis and placenta, has also been found, although has never been examined beyond its initial identification (Taylor, Renshaw et al. 2002).

IL-1F7 is an anti-inflammatory cytokine that comprehensively inhibits the innate immune response. Its expression is increased in PBMCs stimulated with a range of TLR

ligands and pro-inflammatory cytokines, but suppressed by IL-4 and GM-CSF. In PBMCs transfected with either scrambled siRNA or siRNA against IL-1F7 (siIL-1F7), stimulation with LPS or Pam₃Csk₄ (a synthetic TLR1/2 agonist) led to a significant increase in the production of IL-1 β , IL-6 and TNF- α in siIL-1F7 cells. In RAW macrophages, THP-1 cells (monocytic cell line), and A549 cells (epithelial cell line), overexpression of human IL-1F7b (huIL-1F7b) led to highly significant decreases in pro-inflammatory cytokine production, compared to controls, following LPS or IL-1 β stimulation (Nold, Nold-Petry et al. 2010). These *in vitro* findings were replicated *in vivo* in mice transgenic for huIL-1F7b. Mice exhibited a marked reduction in the plasma concentration of 18 cytokines (significantly less IL-6, IL-17 and IL-1 β were found) after LPS-induced shock. These mice were protected from endotoxic shock, displaying far less physiological damage than control mice (Nold, Nold-Petry et al. 2010). IL-1F7 colocalises with Smad3 to facilitate anti-inflammatory activity in the nucleus of cells. Using either a specific Smad3 inhibitor (SIS3), shRNA coding for Smad3 or siRNA to silence Smad3, IL-1F7 activity was attenuated. For example, in RAW macrophages overexpressing IL-1F7, SIS3 treatment partially recovers the inflammatory phenotype (increased IL-1 α and IL-6 expression) usually found following LPS-stimulation (Nold, Nold-Petry et al. 2010). IL-1F7 also inhibits pro-inflammatory cytokine expression following nuclear localisation (Sharma, Kulk et al. 2008). Evidence of its ability to restrict cancer was shown in mice with experimentally-induced fibrosarcoma. Repeated injections with adenoviral vectors expressing IL-1F7 resulted in substantial tumour regression (Gao, Kumar et al. 2003).

IL-1F7 is ubiquitously expressed at very low levels except in the thymus, testis and uterus where expression is high. This experiment, however, did not differentiate between the five splice variant transcripts (Pan, Risser et al. 2001).

IL-1F7b binds to the IL-18 receptor (IL-18R α) (Pan, Risser et al. 2001; Kumar, Hanning et al. 2002), and IL-18 binding protein (IL-18BP) (Bufler, Azam et al. 2002), although the functional significance of these interactions is unclear.

IL-1F7 contains a caspase-1 cut site and is processed similarly to IL-1 β and IL-18 by the NALP3 inflammasome, yielding the mature form of the cytokine. It is also cleaved by caspase-4 (Kumar, Hanning et al. 2002). As indicated above, nuclear localisation of IL-1F7b led to a significant reduction in pro-inflammatory cytokine production (Sharma, Kulk et al. 2008). Nuclear localization of mature IL-1F7b is caspase-1 dependent, as introducing a specific inhibitor of this enzyme significantly decreases nuclear translocation of the cytokine (Sharma, Kulk et al. 2008).

1.2.1.7 IL-1F8 (IL-36 β)

IL-1F8 binds to IL-1RL2, recruiting its co-receptor IL-1RAcP to initiate a pro-inflammatory response. Signal transduction through the IL-1R heterodimer culminates in activation of NF- κ B, ERK1/2, JNK and MAP kinases (Towne, Garka et al. 2004).

Several cell types have increased IL-1F8 expression *in vivo*. Adipocytes express IL-1F8, although levels are not increased following LPS-stimulation. Stimulating primary human adipocytes with rIL-1F8 led to a significant rise in IL-6 and IL-8 expression (van Asseldonk, Stienstra et al. 2010). *IL-1F8* is expressed in glial cells in mice but stimulation of these same cells with recombinant IL-1F8 does not induce IL-6 production or PGE₂ release (Wang, Meinhardt et al. 2005). In contrast to these findings, human synovial fibroblasts and articular chondrocytes stimulated with rIL-1F8 secrete significantly higher amounts of IL-6, IL-8 and nitric oxide than untreated controls (Magne, Palmer et al. 2006). In human and mouse models of psoriasis, IL-1F8 expression is increased (Johnston, Xing et al. 2011). It is also significantly increased in

normal human keratinocytes stimulated with TNF- α or IL-1 α (Johnston, Xing et al. 2011). As with other IL-1F genes, its expression is markedly reduced with etanercept treatment, confirming it is regulated by TNF- α (Johnston, Xing et al. 2011).

Recent data revealed an additional function of IL-1F8 in psoriatic skin. Reconstituted human epidermal cultures stimulated with rIL-1F8 exhibited statistically significant increases in the expression of several antimicrobial peptides and MMPs. IL-1 α also induced this effect. However, IL-1F5, -F6 and -F9 did not (Johnston, Xing et al. 2011).

The ENSEMBL genome browser indicates a dozen mammalian species possess an IL-1F8 gene. The human orthologue consists of seven exons, which encode two transcripts of differing lengths, formed through the use of mutually exclusive exons. Its mechanism of secretion has not been described to date. NH₂-terminally cleaved IL-1F8 apparently exhibits increased bioactivity, although no data are available to show this (Sims and Smith 2010).

1.2.1.8 IL-1F9 (IL-36 γ)

IL-1F9 induces inflammation in the skin. After binding its receptor IL-1RL2 (Debets, Timans et al. 2001), IL-1RAcP is recruited, facilitating signal transduction (Towne, Garka et al. 2004).

IL-1F9 mRNA expression has been detected in several tissues, most notably in the skin, where constitutive levels are high (Debets, Timans et al. 2001). Expression has also been found in embryonic tissues (Debets, Timans et al. 2001), oesophageal squamous epithelium, and LPS-stimulated monocytes (Kumar, McDonnell et al. 2000).

IL-1F9 expression is regulated by other pro-inflammatory cytokines. TNF- α , IFN- γ (Kumar, McDonnell et al. 2000; Johnston, Xing et al. 2011), IL-1 β (Debets,

Timans et al. 2001), IL-1 α , and IL-17A (\pm IL-22) (Johnston, Xing et al. 2011) induce IL-1F9 expression in keratinocytes.

IL-1F9 is also highly expressed in psoriasis skin (Debets, Timans et al. 2001; Johnston, Xing et al. 2011). Its regulation in this condition is under the influence of TNF- α , as levels significantly decline in response to etanercept therapy (Johnston, Xing et al. 2011).

Its central role in regulating the cytokine network in bronchial epithelial cells has been comprehensively described (Chustz, Nagarkar et al. 2011). IL-1F9 expression was significantly increased following stimulation with TNF- α , IL-1 β , IL-17, dsRNA or FSL-1 (TLR2/6 agonist) (Chustz, Nagarkar et al. 2011). For IL-17 and dsRNA, increases in IL-1F9 expression were both dose-dependent and synergistic, increasing markedly by 24 hours post-stimulation (hps) before declining thereafter. IL-1F9 protein production correlates with mRNA expression in these cells, with protein detected in both lysate and supernatant. IL-1F9 also induces the production of other cytokines and chemokines in a dose-dependent manner. Following stimulation of lung fibroblasts, significantly elevated expression of IL-8, CSF3, CCL20 and CXCL3 was found (Chustz, Nagarkar et al. 2011).

Increased IL-1F9 expression was also observed following infection with the dsRNA virus, rhinovirus type 16 (RV16) (Chustz, Nagarkar et al. 2011). Re-stimulation of these cells with RV16 following siRNA knockdown of RELA (NF- κ B p65) led to significantly lower IL-1F9 expression compared with controls. IRF3 was also knocked down but this did not affect IL-1F9 levels. These results confirmed the dsRNA-induced increase in IL-1F9 expression is mediated via the NF- κ B, but not the IRF3/7 (TRAF-3 dependent), pathway (Chustz, Nagarkar et al. 2011). Infection with herpes simplex virus also increased IL-1F9 mRNA and protein expression (Kumar, McDonnell et al. 2000).

The mechanism of IL-1F9 secretion is unknown. Neither a signal peptide nor a pro-domain is present, similar to other IL-1F proteins, suggesting non-classical secretion. It may be cleaved at the N-terminus, however, as an IL-1F9 truncation mutant starting at Gly13 exhibits enhanced activity (Blumberg, Dinh et al. 2010). In ATP-treated human epidermal cultures, significantly more IL-1F9 protein was found in the supernatant than intracellularly following IL-1 α and TNF- α stimulation (Johnston, Xing et al. 2011). It is likely that protein export was due to passive diffusion through the ATP-dependent P2X₇ receptor.

The IL-1F9 gene has been located in 27 mammalian genomes. The human orthologue contains six exons which are alternatively spliced to produce three different transcripts. Following translation, three protein isoforms of differing lengths are formed.

1.2.1.9 IL-1F10

IL-1F10 was identified from screening a BAC clone (Bensen, Dawson et al. 2001) and a cDNA library (Lin, Ho et al. 2001). To date, there have been no reports that characterise its function. IL-1F10 expression was detected in the heart, placenta, foetal liver, spleen, thymus, and tonsil and foetal skin (Bensen, Dawson et al. 2001; Lin, Ho et al. 2001). Although recombinant human IL-1F10 binds to soluble IL-1RI, it had a much lower binding affinity for this receptor than IL-1RN and IL-1 β (Lin, Ho et al. 2001).

The protein does not contain a signal peptide or a prodomain. Following transfection into CHO cells, equally sized protein species were detected in both supernatant and cell lysates (Lin, Ho et al. 2001), indicating non-classical secretion may occur.

Despite a lack of functional evidence, IL-1F10 may act as a receptor antagonist as it is very similar to IL-1F5 and IL-1RN in a number of ways. The human gene is

situated between IL-1F5 (IL-36RN) and IL-1RN on chromosome 2 (Figure 1.6).

Phylogenetic analysis of the human and mouse IL-1 family amino acid sequences results in a separate clade containing only IL-1F5, IL-1F10 and IL-1RN (Figure 1.7).

IL-1F10 has much higher amino acid identity with IL-1F5 (41%) and IL-1RN (37%) than with the rest of the family (14-30%) (Lin, Ho et al. 2001).

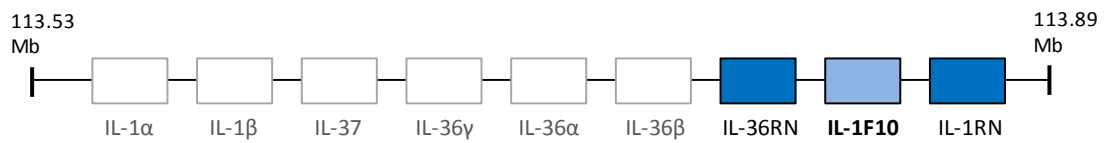


Figure 1.6 The IL-1 ligand gene cluster on human chromosome 2. Human IL-1F10 lies between IL-1RN and IL-1F5 (IL-36RN). Diagram not to scale.

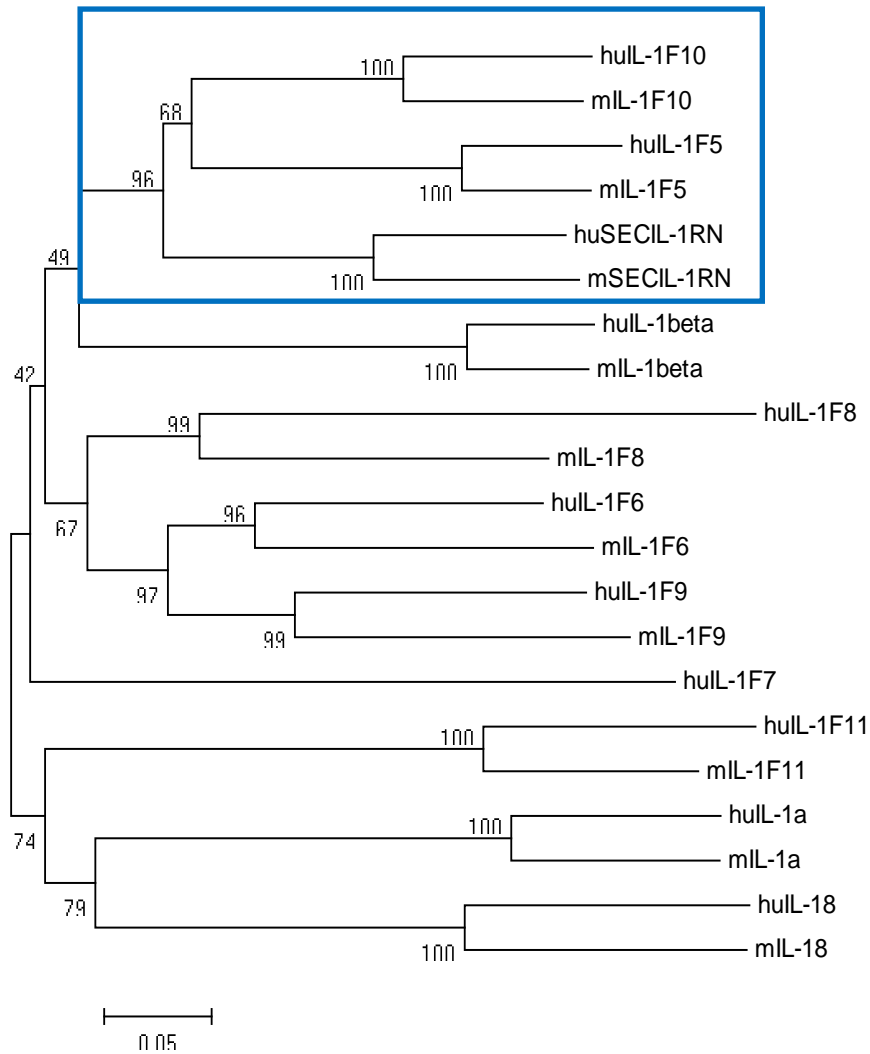


Figure 1.7 Phylogenetic analysis of the human and mouse IL-1 amino acid sequences. A separate “receptor antagonist” clade containing IL-1RN, IL-1F5 and IL-1F10 is indicated (blue box). Figure constructed using the Neighbour-Joining (N-J) method. hu = human, mu = mouse.

The gene structure of IL-1F10 is also similar to those of the two receptor antagonists. The positions of the exon-intron boundaries are highly conserved between all three genes (Lin, Ho et al. 2001). The coding region of IL-1F10 has four exons, which when translated, are very similar in size to those of IL-1F5 (11, 28, 43 and 70 amino acids compared to 10, 28, 43 and 74, respectively) (Bensen, Dawson et al. 2001).

1.2.1.10 IL-1F11 (IL-33)

The role of IL-33 has been described in a narrow range of disease states, each of which are characterised by a Th2 immune response. IL-33 initiates Th2-mediated immune responses via its major target cell populations, Th2 cells, mast cells, eosinophils, innate helper cells, macrophages, DCs, basophils, NK cells and NKT cells. It binds its receptor ST2, recruits IL-1RAcP, and facilitates signal transduction to activate Th2 cells in the absence of TCR stimulation (Smith 2011). IL-33 signalling has been partially defined in mast cells. Activation of ST2 facilitates intracellular recruitment of MyD88, IRAK1 and IRAK4 leading to mobilisation of two separate signalling pathways (Figure 1.8). In pathway 1, phospholipase D (PLD) and sphingosine kinase (SPHK) are activated, followed by an influx of Ca^{2+} . This activates NF- κ B causing mast cell degranulation and increased production of cytokines (IL-1 β , IL-3, IL-6, TNF- α), chemokines (CXCL2, CCL2 and CCL3), and lipids (prostaglandin D₂ and leukotriene B₄) (Allakhverdi, Smith et al. 2007; Moulin, Donze et al. 2007; Pushparaj, Tay et al. 2009). In pathway 2, mitogen-activated protein kinase kinases (MAPKKs) are stimulated leading to activation of ERK, p38 and JNK. This initiates IL-5, IL-13, CCL5, CCL17 and CCL24 production (Kurowska-Stolarska, Kewin et al. 2008). End products of these pathways contribute to the two major functional roles of

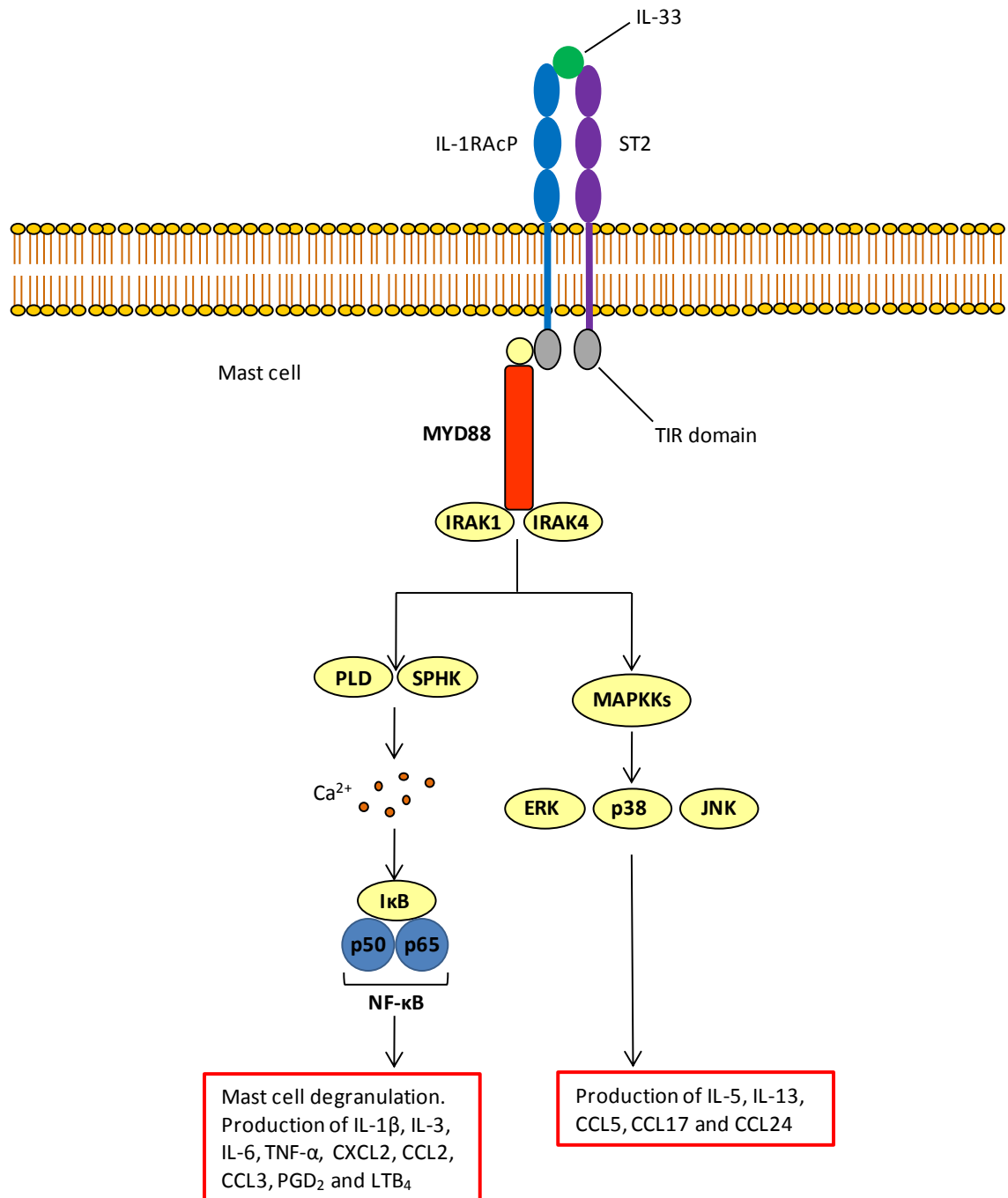


Figure 1.8 Independent IL-33 signalling pathways in mast cells. Activation of ST2 following IL-33 binding leads to recruitment of MyD88, IRAK1 and IRAK4. The MyD88 complex then activates two distinct signalling pathways by an unknown mechanism. Figure adapted from Liew, Pitman et al. (2010).

IL-33, in promoting host protection and aggravating allergic conditions.

IL-33 protects the host against infections from parasitic worms and also against cardiovascular disease by reducing atherosclerosis. The cytokine exacerbates the inflammatory milieu in asthma, atopic allergy and anaphylaxis by activating mast cells. IL-33 also has pathological, pro-inflammatory roles in central nervous system disease and arthritis (Liew, Pitman et al. 2010). In addition to being released from cells, IL-33 possesses intranuclear activity. Similar to IL-1 α , it contains a nuclear localisation sequence which directs its nuclear translocation (Carriere, Roussel et al. 2007).

IL-33 does not require co-stimulation with other cytokines to drive the Th2 response, although it can stimulate Th1 cytokine production (Smithgall, Comeau et al. 2008), in part due to activating target cells that are shared with IL-18 (Smith 2011). IL-33 is expressed in numerous organs and cell populations, with relatively low levels found in monocytes, macrophages and DCs, whilst high levels are found in the brain and spinal cord (Oboki, Ohno et al. 2010).

The IL-33 gene has been identified in 34 species of mammals. The human gene consists of eight exons, which encode three different predicted transcripts. An additional splice variant transcript has recently been identified (Hong, Bae et al. 2011). This transcript lacks the exon containing the putative caspase-1 cut site, yet retains functionality. There are conflicting findings regarding IL-33 processing. It was initially suggested that caspase-1 cleavage was required to yield a bioactive form of the cytokine (Schmitz, Owyang et al. 2005). Subsequent reports, however, have strongly disagreed with this (Ohno, Oboki et al. 2009; Talabot-Ayer, Lamacchia et al. 2009). One report has suggested caspase-1 cleavage actually inactivates IL-33 (Cayrol and Girard 2009). The splice variant that lacks the cleavage site but retains bioactivity supports the latter hypothesis.

1.2.2 IL-1 receptors and signal transduction in mammals

The biological effects of the IL-1 ligands are mediated by members of the IL-1 receptor (IL-1R) family which are expressed on the surface of target cells or secreted as soluble receptors. The family is comprised of eleven members (Table 1.2) that are characterised by an IgG-like extracellular domain and a cytoplasmic Toll/IL-1R (TIR) domain. The IL-1R family is part of a wider superfamily of TIR domain-containing receptors which includes the Toll-like receptors, intracellular molecules involved in signalling and recognising pathogens, and the Toll proteins of *Drosophila* (Boraschi and Tagliabue 2006).

1.2.2.1 IL-1RI (IL-1RI)

The type I IL-1 receptor (IL-1RI) contains three IgG domains in the extracellular portion and a cytoplasmic TIR domain (Sims, March et al. 1988). It binds the agonist ligands IL-1 β , IL-1 α and the antagonist IL-1RN. When IL-1 β or IL-1 α bind the receptor, its co-receptor IL-1RAcP is recruited on the cell surface forming a heterodimer. This ultimately leads to signal transduction and increased transcription of inducible genes. When IL-1RN binds IL-1RI, it physically occupies the receptor but does not initiate signal transduction. IL-1 β has two binding sites termed A (bsA) and B (bsB). It binds Ig-like domains I & II of IL-1RI with bsA. Upon binding, these domains become firmly fixed in place by sulphide bonds leading to a conformational change which allows bsB to bind domain III of IL-1RI. This conformational change permits IL-1RAcP to bind to IL-1RI, activating the intracellular signalling cascade. IL-1RN possesses bsA but lacks bsB. It therefore binds domains I and II of IL-1RI, blocking the receptor. The absence of bsB prevents any contact between IL-1RN and domain III of

Receptor	Protein name	Alternative names	Soluble/ membrane bound	Co-receptor	Ligand(s)
Interleukin-1 receptor 1	IL-1RI	IL-1R1, IL1R, CD121A, D2S1473, IL-1R- α , P80	Both	IL-1RAcP, TILRR	IL-1 β , IL-1 α , IL-1RN
Interleukin-1 receptor 2	IL-1RII	IL-1R2 IL-1RB, CD121b, MGC47725	Both	IL-1RAcP	IL-1 β
Interleukin-1 receptor accessory protein	IL-1RAcP	IL-1R3, C3orf13, FLJ37788	Both		
Interleukin-1 receptor-like 1	IL-1RL1/ ST2	IL-1R4, IL-33 α , T1, DER4, Fit-1, MGC32623	Both	IL-1RAcP	IL-33
Interleukin-1 receptor-like 2	IL-1RL2	IL-1R6, IL-1Rrp2	Membrane bound	IL-1RAcP	IL-36 α , - β , - γ , IL-36RN
Interleukin-18 receptor	IL-18R α	IL-1R5, IL-1Rrp1, CD218a	Both	IL-18R β	IL-18
Interleukin-18 receptor accessory protein	IL-18R β	IL-1R7, IL-18RAcP, IL18RAP, AcPL, CD218b, CDw218b, IL18RB, MGC120589, MGC120590	Both		
Three immunoglobulin domain-containing IL1 receptor-related-2	TIGIRR-2	IL-1RAPL1, IL-1R8, MRX10, MRX21, MRX34, OPHN4	Membrane bound	Unknown	Unknown
Three immunoglobulin domain-containing IL1 receptor-related-1	TIGIRR-1	IL-1RAPL2, IL-1R9	Membrane bound	Unknown	Unknown
Single immunoglobulin domain-containing IL-1-related receptor	SIGIRR	TIR8, MGC110992	Membrane bound	Unknown	Unknown

Table 1.2 The IL-1 receptor family in humans. The family is comprised of eight receptors, and three co-receptors which are required for signalling.

IL-1RI, thus IL-1RAcP cannot be recruited, and signalling cannot take place (Gosavi, Whitford et al. 2008) (Figure 1.9). An additional factor underlying the inability IL-1RN to activate IL-1RI was recently described. Upon binding, the absence of an interaction between bsB of IL-1RN and domain III of IL-1RI causes an angle to form between domains II and III of IL-1RI. The relative location of domain III is therefore different to its location when IL-1 β binds to IL-1RI. Thus, even if IL-1RAcP was able to be recruited following binding of IL-1RN, domain III of IL-1RI would be physically too far away from IL-1RAcP. The TIR domains of IL-1RI and IL-1RAcP would consequently not be close enough together to recruit MyD88, which is necessary for signal transduction (Sims 2010; Wang, Zhang et al. 2010). In mammals, a soluble form of IL-1RI has been identified. Its precise functional role is not clear, as conflicting reports have described both improved and worsening disease severity when it is administered (Subramaniam, Stansberg et al. 2004; Dinarello 2009).

1.2.2.2 IL-1RII (IL-1R2)

IL-1RII is a decoy receptor which acts to sequester excess IL-1 β and IL-1 α . It contains three Ig-like domains in the extracellular part of the receptor but crucially lacks a TIR domain; therefore signal transduction does not take place (Colotta, Dower et al. 1994). Upon ligand binding, IL-1RII can also recruit IL-1RAcP thereby competing with IL-1RI to effectively diminish the responsiveness of a cell to IL-1 (Lang, Knop et al. 1998). A soluble form of the receptor is generated following cleavage of the membrane-bound form to further regulate IL-1 activity. A specific protease, aminopeptidase regulator of TNFR1 shedding (ARTS), is necessary for IL-1RII release from the cell surface (Cui, Rouhani et al. 2003). Soluble IL-1RII forms a complex with soluble

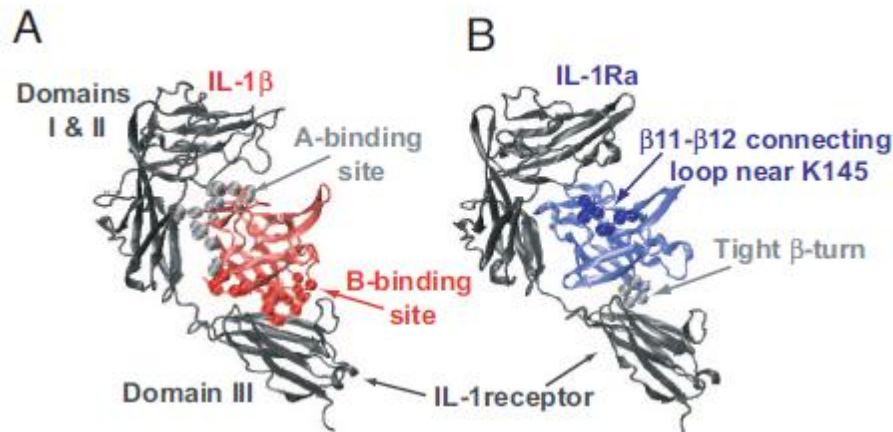


Figure 1.9 Ribbon diagrams of IL-1 β and IL-1Ra bound to IL-1RI. **A.** IL-1 β binds the Ig-like domains I and II of IL-1RI with bsA. Binding these domains leads to a conformational change allowing bsB to bind domain III of IL-1RI. This permits IL-1RAcP to bind to IL-1RI, activating the intracellular signalling cascade. **B.** IL-1RN possesses bsA but lacks bsB. It binds domains I and II of IL-1RI with bsA, blocking the receptor. The absence of bsB prevents any contact between IL-1RN and domain III of IL-1RI, IL-1RAcP is not recruited, and signalling cannot take place. Figure reproduced from Gosavi, Whitford et al. (2008).

IL-1RAcP which increases the affinity with which it binds IL-1 β and IL-1 α by ~100-fold (Smith, Hanna et al. 2003). This does not affect its affinity for IL-1RN, which remains weak.

1.2.2.3 IL-1RAcP (IL-1R3)

IL-1RAcP is an essential co-receptor for the IL-1RI (Cullinan, Kwee et al. 1998), ST2 (Ali, Huber et al. 2007; Chackerian, Oldham et al. 2007; Palmer, Lipsky et al. 2008) and IL-1RL2 (Towne, Garka et al. 2004) receptors. In order to modulate signalling through these receptors, recruitment of IL-1RAcP is fundamental. When IL-1 β or IL-1 α bind to IL-1RI, IL-1RAcP is recruited to form a functional receptor

complex. However, it does not physically interact with bound ligand (Subramaniam, Stansberg et al. 2004). Once the heterotrimeric receptor complex is active, the TIR domains of IL-1RI and IL-1RAcP are in close proximity which permits recruitment of MyD88 and Tollip in the cytoplasm (Dinarello 2009). This is the first step in the initiation of intracellular signalling.

A novel isoform, termed IL-1RAcPb, has recently been identified exclusively in the central nervous system. It alters the response to IL-1 in these cells by inhibiting the expression of some genes, whilst others remain unaffected (Smith, Lipsky et al. 2009). The soluble form of IL-1RAcP acts to regulate IL-1 activity by binding soluble IL-1RII which sequesters IL-1 β and IL-1 α (Smith, Hanna et al. 2003).

1.2.2.4 ST2 (IL-1R4/IL-33R α)

The ST2 receptor possesses a three Ig domain-containing extracellular portion and an intracellular TIR domain. It binds IL-33 (Schmitz, Owyang et al. 2005) which leads to IL-1RAcP recruitment (Ali, Huber et al. 2007; Chackerian, Oldham et al. 2007; Palmer, Lipsky et al. 2008) and formation of a heterotrimeric receptor complex. Three splice variants of ST2 have been identified – ST2L, sST2 and ST2V. ST2L and ST2V are membrane-bound forms of the receptor, whilst sST2 is a soluble variant consisting of the extracellular portion of ST2L (Boraschi and Tagliabue 2006). In addition to its role as the IL-33 receptor, the membrane-bound form of ST2 also inhibits IL-1RI and TLR4 signalling through sequestration of the intracellular adaptors MyD88 and Mal (Brint, Xu et al. 2004).

1.2.2.5 IL-18R α (IL-1R5) and IL-18R β (IL-1R7/IL-1RAcP)

IL-18R α and IL-18R β (IL-18RAcP) bind IL-18 in a functionally equivalent

manner to the IL-1RI complex binding to IL-1 β or IL-1 α . IL-18R α is a membrane-bound TIR domain-containing receptor with three Ig-like extracellular domains. Upon binding IL-18, IL-18R α forms a complex with its co-receptor, IL-18R β , on the cell surface. There is no physical interaction between IL-18 and IL-18R β ; however, the recruitment of this co-receptor significantly increases the affinity of IL-18 for IL-18R α . IL-18R β recruitment also leads to signal transduction, which cannot take place in its absence (Born, Thomassen et al. 1998; Debets, Timans et al. 2000). IL-1F7b also binds to the IL-18 receptor (IL-18R α) (Pan, Risser et al. 2001; Kumar, Hanning et al. 2002) but the purpose of this interaction is unclear.

1.2.2.6 IL-1RL2 (IL-1R6/IL-1Rrp2)

IL-1RL2 is structurally related to most other IL-1Rs, having three Ig-like domains in the extracellular portion of the receptor and an intracellular part consisting of a TIR domain. It binds the agonist ligands IL-1F6, IL-1F8 and IL-1F9, and is blocked by a specific receptor antagonist, IL-1F5. Upon binding agonist ligand, IL-1RAcP is recruited leading to signal transduction and gene transcription (Debets, Timans et al. 2001; Towne, Garka et al. 2004).

1.2.2.7 TIGIRR-2 (IL-1R8/IL-1RAPL)

Three Ig domain-containing receptor-related protein 2 (TIGIRR-2/IL-1RAPL) is an orphan receptor highly expressed in the brain (Carrie, Jun et al. 1999). Mutations in the IL-1RAPL gene are directly responsible for X-linked mental retardation (Carrie, Jun et al. 1999; Tabolacci, Pomponi et al. 2006). JNK activation by IL-1 β in mature neurons is mediated by IL-1RAPL (Pavlovsky, Zanchi et al. 2010).

1.2.2.8 TIGIRR-1 (IL-1R9)

TIGIRR-1 is an orphan receptor closely related to TIGIRR-2, and is highly expressed in foetal brain. Its extracellular domain does not bind IL-1 α , IL-1 β or IL-18 (Sana, Debets et al. 2000).

1.2.2.9 SIGIRR (TIR8)

Single Ig IL-1 receptor-related protein (SIGIRR) is an orphan receptor with a unique structure within the IL-1R family. As its name indicates, it contains only a single Ig domain in the extracellular portion. Its intracellular TIR domain is also unique, being 70 amino acids longer than those of the other IL-1Rs (Subramaniam, Stansberg et al. 2004). Although largely considered to be an orphan, it has a functional interaction with IL-1F5 which led to an anti-inflammatory response in murine glial cells (Costelloe, Watson et al. 2008). To date, there is no recognised co-receptor for SIGIRR. Functional studies have shown SIGIRR is in fact an extremely important inhibitory receptor able to regulate multiple signalling pathways to dampen inflammation and Th cell differentiation. Of note, it regulates the activity of IL-1 α , IL-1 β , IL-18, IL-33 and several TLR agonists by inhibiting signalling through their respective receptors (Garlanda, Anders et al. 2009).

1.2.2.10 Signal transduction

When IL-1 β or IL-1 α bind to IL-1RI, its co-receptor IL-1RAcP is recruited on the cell surface, forming a heterodimer (Figure 1.10). The intracellular TIR domains of both receptor components are then in close proximity which leads to the recruitment of the myeloid differentiation 88 (MyD88) and Toll interacting protein (Tollip) adapter

molecules. Binding of MyD88 to the TIR domains of both receptor chains induces phosphorylation of the IL-1 receptor-associated kinases (IRAK)-1, -2 and -4, which in turn recruits the TNF receptor-associated factor 6 (TRAF6) to the protein complex (Figure 1.10). Both TRAF-6 and phosphorylated IRAK-1 then translocate to the plasma membrane to associate with TGF- β -activated kinase 1 (TAK1) and its binding proteins TAB1 (TAK1-binding protein) and TAB2. A four-component protein complex, consisting of TAK1, TAB1, TAB2 and TRAF-6, translocates back to the cytosol (Figure 1.10). Once there, TRAF-6 becomes ubiquitinated, followed by TAK-1 phosphorylation. TAK1 then performs three functions - it activates the mitogen-activated protein kinases (MAPK) p38 and JNK, as well as activating inhibitor of nuclear factor- κ B kinase subunit β (IKK β). Activated IKK β phosphorylates I κ B, a protein complex which inhibits NF- κ B. Phosphorylation of I κ B facilitates its degradation, which liberates NF- κ B (Figure 1.10). This important transcription factor then moves into the nucleus to regulate gene expression (Dinarello 2009).

1.2.3 Genomic organization and location

Nine of the human IL-1 ligand genes are clustered in a region of ~360 kb on chromosome 2q13 (ENSEMBL coordinates; 2: 113,531,492-113,891,593). The gene order within the cluster, from centromere to telomere, is: *IL-1 α* , *IL-1 β* , *IL-1F7*, *IL-1F9*, *IL-1F6*, *IL-1F8*, *IL-1F5*, *IL-1F10* and *IL-1RN* (Figure 1.6). Phylogenetic analysis indicates the specific order reflects the sequential incidence of divergence events (Nicklin, Barton et al. 2002). For example, *IL-1F9*, *IL-1F6* and *IL-1F8* branch together, as do *IL-1F5*, *IL-1F10* and *IL-1RN* (Figure 1.7). The IL-1 gene order has been conserved through evolution except for the loss from the cluster of *IL-18*

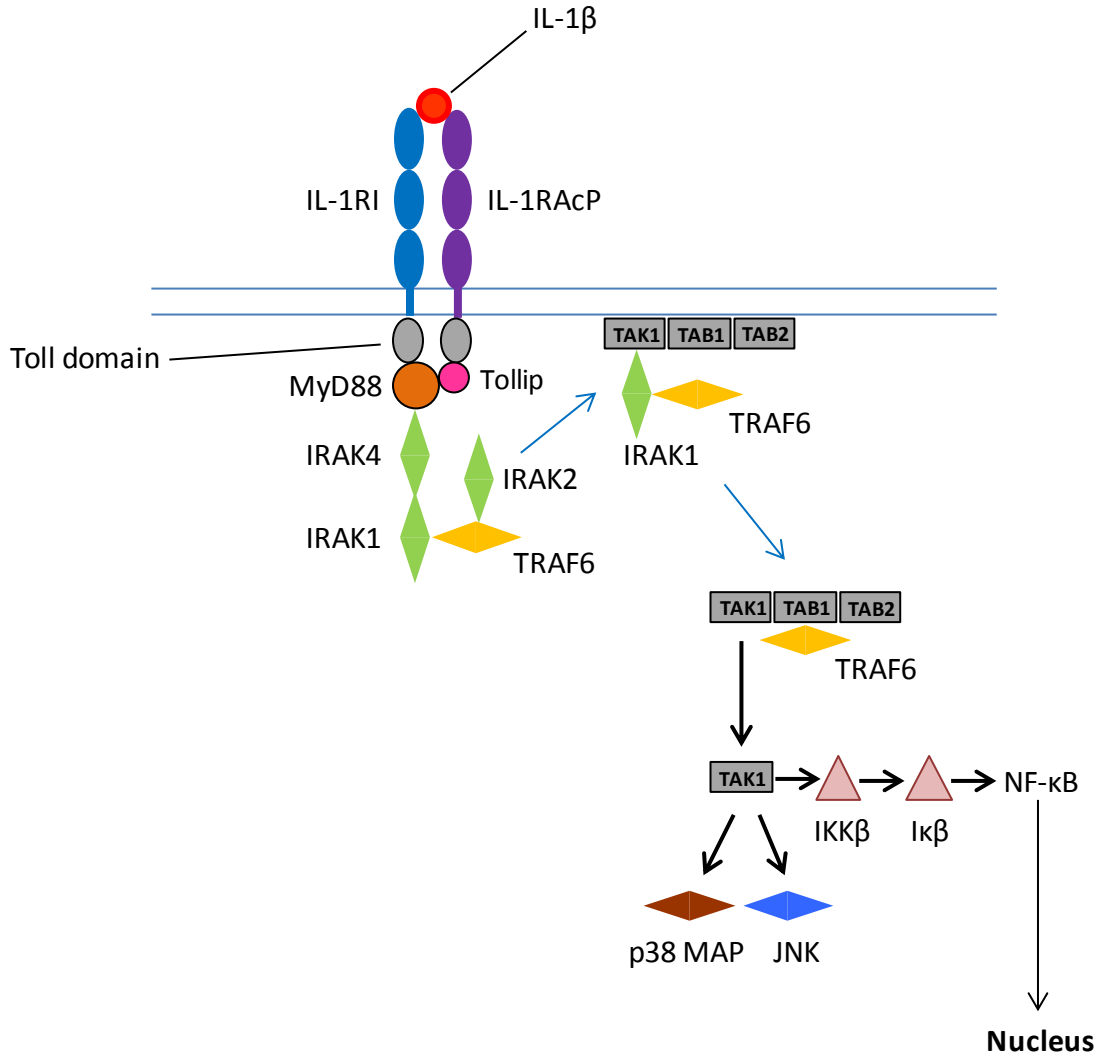


Figure 1.10 IL-1 signal transduction. Formation of the IL-1 receptor complex leads to approximation of the intracellular TIR domains of both IL-1RI and IL-1RAcP. This facilitates recruitment of MyD88 and Tollip adapter molecules. MyD88 binds to the TIR domains of both receptor chains inducing phosphorylation of IRAK-1, -2 and -4, which in turn recruits TRAF6 to the protein complex. Both TRAF-6 and phosphorylated IRAK-1 translocate to the plasma membrane and associate with TAK1 and its binding proteins TAB1 and TAB2. A protein complex consisting of TAK1, TAB1, TAB2 and TRAF-, translocates to the cytosol, whereby TRAF-6 becomes ubiquitinated, followed by TAK-1 phosphorylation. TAK1 then activates the MAPK p38 and JNK, as well as activating IKKβ. Activated IKKβ, phosphorylates IκB, a protein complex which inhibits NF-κB. IκB phosphorylation leads to its degradation, liberating NF-κB. Figure adapted from Dinarello (2009).

(Nicklin, Barton et al. 2002), which now resides on chromosome 11 (11: 112,013,974-112,034,840). *IL-33* is also not situated on chromosome 2, but is found at a discordant locus on chromosome 9 (9: 6,215,805-6,257,983) in the human genome.

The nine gene IL-1 cluster is largely conserved in most mammalian species, except for in the mouse, where *IL-1F7* is absent and *IL-1 β* and *IL-1 α* have become separated, by 105 Mb of sequence, from the rest of the cluster (*IL-1RN*, *IL-1F5*, *-F6*, *-F8*, *-F10*) following rearrangement of chromosome 2.

The majority of the human IL-1 receptor genes (*IL-1RII*, *IL-1RI*, *IL-1RL2*, *ST2*, *IL-18R*, and *IL-18RAcP*) span a 460 kb region of chromosome 2q11.2-12.1 (2: 102,608,306-103,069,025), with the remainder of the genes dispersed throughout the genome (Dale and Nicklin 1999). *IL-1RAcP* is on chromosome 3q28 (3: 190,231,840-190,375,843); both *TIGIRRs* are on the X-chromosome (*TIGIRR1*: X: 103,810,996-105,012,102; *TIGIRR2*: X: 28,605,516-29,974,840) whilst *SIGIRR* is on chromosome 11p15 (11: 405,716-417,455).

1.2.4 The chicken IL-1 family

Compared with mammals, far fewer members of the IL-1 family have been identified in the chicken. To date, the ligands *IL-1 β* and *IL-18* as well as the receptors *IL-1RI* and *ST2* are the only chicken orthologues that have been cloned. Expression analysis of *chSIGIRR* has been carried out but the cDNA has not been cloned. Chicken orthologues of *IL-18R α* , *IL-1RAcP* and *TIGIRR-1* have also been identified from EST libraries, but have not been fully characterised.

1.2.4.1 Chicken IL-1 β

The first chicken IL-1 (chIL-1) ligand to be cloned was IL-1 β (Weining, Sick et al. 1998). Prior to this, a small number of reports were published describing characteristic IL-1-like activity in avian macrophages. This was originally described in culture supernatants from avian macrophages stimulated with endotoxin (Hayari, Schauenstein et al. 1982). IL-1 was also released from four different sources of *E. coli*- or *S. aureus*-stimulated macrophages, partially purified, and stimulated thymocyte co-mitogenesis (Klasing and Peng 1987). Partial characterisation of signal transduction underlying IL-1 release from LPS-stimulated HD11 cells, a chicken macrophage cell line, was also carried out (Bombara and Taylor 1991), with findings similar to those reported in mice. Furthermore, the chicken orthologue of caspase-1 was cloned (Johnson, Bridgham et al. 1998), suggesting a mechanism of chIL-1 (and IL-18) maturation similar to that in mammals may exist.

The chIL-1 β cDNA was cloned from LPS-stimulated HD11 cells (Weining, Sick et al. 1998). It encodes a predicted protein of 267 amino acids which has 25% identity with the human orthologue and contains an NH₂-terminal pro-domain. Unlike mammalian IL-1 β proteins, it lacks a conserved aspartic acid at the predicted caspase-1 cut site. Purified recombinant mature chIL-1 β (lacking the pro-domain) exhibited biological activity which resembles that of its mammalian orthologues. In CEC-32 cells (a quail fibroblast cell line) stimulated with rchIL-1 β , a dose-dependent increase in CXC chemokine expression was detected. Similar to mammalian IL-1 β , an instability element was identified in the chIL-1 β coding region (Weining, Sick et al. 1998). Compared with full length chIL-1 β and three alternatively truncated forms, an N-terminal truncation mutant of chIL-1 β starting at Ala106 (the first residue after the

predicted caspase-1 cleavage site) exhibited significantly enhanced (100-fold) bioactivity (Gyorfy, Ohnemus et al. 2003). This suggests processing is required for maximal IL-1 β activity, possibly mediated by caspase-1. In mammals, caspase-1-independent processing of IL-1 β is carried out by several neutrophil proteases. Adjacent to the caspase-1 site, single tyrosine and alanine residues have been recognised as the protease cut sites in mammals (Figure 1.3) (Dinarello 2011). Although avian equivalents of the neutrophil proteases have yet to be identified in heterophils, their putative cut sites are both conserved in chIL-1 β .

Expression of chIL-1 β is increased in response to bacterial, viral and parasite challenge, consistent with its role as a rapidly induced pro-inflammatory mediator. In IFN- γ primed heterophils, stimulation with *Salmonella* Enteritidis led to statistically significant increases in IL-1 β expression (Kogut, Rothwell et al. 2005). Similarly, in chicken embryonic fibroblasts (CEF), kidney cells and HD11 cells, stimulation with *Salmonella*-derived flagellin induced significant increases in IL-1 β expression in all three cell types (Iqbal, Philbin et al. 2005). IL-1 β expression is also increased in bursal cells from IBDV-infected chickens (Eldaghayes, Rothwell et al. 2006) as well as in HD11 cells stimulated with TLR7 agonists (Philbin, Iqbal et al. 2005). Intraepithelial lymphocytes removed from the jejunum of *Eimeria maxima*-infected chickens contain high levels of IL-1 β mRNA compared with uninfected controls (Hong, Lillehoj et al. 2006).

The structure and genomic location of chIL-1 β have been elucidated (Kaiser, Rothwell et al. 2004). The exon-intron structure of mammalian IL-1 β is conserved in the chicken; however, the overall size of the chicken gene is substantially smaller than the human orthologue due to much shorter introns throughout. The genomic location of chIL-1 β was determined using single-stranded conformational polymorphism, which

identified a telomeric region of chromosome 2 (Kaiser, Rothwell et al. 2004). In the 2006 release (v2.0) of the chicken genome sequence, the genomic location was reassigned to chromosome 4 (Kaiser 2007).

The crystal structure of chIL-1 β has recently been resolved, which revealed the β -trefoil conformation of the human cytokine is conserved in the chicken. Significant differences were found between the chicken and human structures in the regions involved in receptor binding, providing a molecular explanation for the inability of these cytokines to cross-react (Cheng, Chen et al. 2011).

1.2.4.2 Chicken IL-18

A full length chicken IL-18 open reading frame (ORF) was identified in a bursal EST library and subsequently cloned from LPS-stimulated HD11 cells (Schneider, Puehler et al. 2000). The full length predicted protein contains 199 amino acids, has 30% identity with mammalian chIL-18 sequences and includes a pro-domain at the N-terminal. When aligned with mammalian sequences, a conserved aspartic acid is apparent at the predicted caspase-1 cleavage site, suggesting it may be processed by the enzyme. Purified recombinant mature chIL-18 (lacking the pro-domain) exhibited biological activity similar to that of mammalian IL-18. In primary chicken splenocytes stimulated with rchIL-18, a dose-dependent increase in IFN- γ production was detected (Schneider, Puehler et al. 2000). A conserved Th1 cell lineage similar to the one in mammals was subsequently proposed in the chicken. In chicken CD4⁺ T cells stimulated with chIL-18, cell proliferation, IFN- γ production and MHC class II expression were all increased (Gobel, Schneider et al. 2003). This was dependent upon the presence of macrophages in culture (Gobel, Schneider et al. 2003).

Elevated levels of IL-18 mRNA have been detected in the spleen of birds

infected with Marek's disease virus (Kaiser, Underwood et al. 2003), characteristic of a pro-inflammatory response to viral infection. IL-18 expression was also increased in the spleen of birds injected with *Salmonella* Typhimurium LPS (Sijben, Klasing et al. 2003) and the heterophils of chickens treated with corticosterone (Shini, Shini et al. 2010) reflecting the typical pro-inflammatory role of this cytokine.

Neither the genomic location nor the structure of the chIL-18 gene has been published.

1.2.4.3 Chicken IL-1RI

The type I chicken IL-1 receptor (chIL-1RI) was cloned from a primary chicken fibroblast cDNA library. When compared with its human and mouse orthologues, amino acid identity of the five major protein domains varied from 19-61%, with the cytoplasmic domain the most highly conserved region (Guida, Heguy et al. 1992). A bioactive form of soluble chIL-1RI (sIL-1RI) has also been cloned (Klasing and Peng 2001). Conditioned medium (CM) from LPS-stimulated HD11 cells contains chIL-1 β that induces thymocyte co-stimulation. To establish biological activity, this CM was pre-incubated with partially purified sIL-1RI and then tested for its ability to co-stimulate mitogenesis. Compared with controls, its capacity to stimulate thymocytes was significantly attenuated (Klasing and Peng 2001).

The genomic location of the chIL-1RI gene has not been elucidated.

1.2.4.4 Chicken ST2

The chicken orthologue of the ST2 receptor was cloned from cDNA isolated from chicken embryos (Iwahana, Hayakawa et al. 2004). Three different cDNAs were

identified, designated ST2, ST2L and ST2 LV. ST2 is the secreted, soluble form of the receptor of which an equivalent has also been identified in humans. ST2L is a longer, membrane-bound isoform which contains a transmembrane domain, whilst ST2LV is a novel splice variant of the ST2L transcript. ST2LV lacks the transmembrane domain present in ST2L and as such is a secreted protein. To date, this novel splice variant has not been found in any mammalian species. ST2L has 39.3% and 38.3% identity with its respective human and mouse orthologues. In all three species, ST2L contains a signal peptide of similar length and all six cysteine residues are conserved in the Ig-like domain region. The structures of the human and chicken ST2 genes are very similar in composition (Iwahana, Hayakawa et al. 2004). The genomic location of the chST2 gene has not been determined. The ligand for this receptor, IL-33, has yet to be identified in the chicken.

1.2.4.5 Chicken SIGIRR (TIR8)

A full length chicken SIGIRR transcript which has 86% identity with human SIGIRR was identified in the NCBI nucleotide database (Riva, Polentarutti et al. 2009). Northern blotting analysis of twenty-one different chicken tissues revealed expression was ubiquitous with relatively high levels in the kidney, small and large intestine, caecum, liver, glandular stomach and cloaca (Riva, Polentarutti et al. 2009). A splice variant was identified exclusively in the adrenal gland. No further analyses of this gene were carried out.

1.2.4.6 Other chIL-1 receptors

Partial cDNAs for apparent chicken orthologues of IL-18R α , IL-1RAcP and TIGIRR-1 receptors have been identified in the NCBI EST database (Huisin, Stet et al.

2004). Comprehensive phylogenetic analysis of the IL-1 receptor family showed all three chicken sequences grouped with their mammalian orthologues (Huisin, Stet et al. 2004).

1.3 The chicken genome

When attempting to discover the avian orthologues of genes present in the human genome, it is crucial to fully appreciate the genetic differences between the human and the chicken. Therefore, the extent to which the evolution of these two species has changed the composition of their genomes needs to be carefully considered. As both species are eukaryotes, they will possess conserved molecular mechanisms for common functions which are likely to be controlled by the same set of orthologous genes. Despite this, chickens and humans have evolved separately for ~310 million years (Hedges, Parker et al. 1996) and this has led to the emergence of many differences. One major difference between the two is the organisation of species karyotype. The avian karyotype is made up of macro- and micro-chromosomes whose length differ substantially from one another. In total, the chicken has 38 autosomes and one pair of sex chromosomes, thus $2n = 78$. In contrast to mammals, the male is homogametic (ZZ) whilst the female is heterogametic (ZW) (Griffin, Robertson et al. 2007).

Sequencing of the chicken genome (ICGSC 2004) has now allowed an even more detailed analysis of its genetic microarchitecture and how this compares to the human. For instance, the chicken and human genomes appear to contain roughly the same number of genes (~20-25,000), yet the chicken genome is ~3 times smaller than

the human. The chicken genome is composed, predominantly, of lengthy contiguous blocks of sequence that retain a lot of the ancient duplications. In both human and chicken genomes there is a relatively low incidence of chromosomal translocations; however, intrachromosomal rearrangements appear to be far more frequent in both species. When protein-coding gene sequences shared by the two species are aligned, exons show the highest conservation of sequence with very little homology between introns. The comparative analyses also showed ~60% of protein coding genes in the chicken have a sole orthologue in humans and that of these orthologous pairs, only ~75.3% of amino acids are similar. Orthologous genes responsible for immune function are relatively less well conserved in the chicken compared with other essential functional sequences. Around 5-10% of all genes found in humans are either missing in the chicken or significantly truncated. There also appears to be a lot of genes that were present in the common ancestor, which are broadly conserved amongst many mammalian species, but are missing in the chicken. Of the vertebrates currently sequenced, the chicken appears to have lost more genes than it has gained, although the large number of sequence gaps in the chicken genome may contain some of these.

Conservation of synteny is the term used to describe the conserved order of a defined cluster of genes on a single chromosome in different species. Many higher order eukaryotes have evolved from a common ancestor and this is reflected in the degree of similarity between their genomes. Although chromosomal rearrangements take place within a species through evolution, it is still common to observe large groups of orthologous gene clusters in different species. The degree of conserved synteny increases with the degree of relatedness between species. Despite the presence of a substantial number of regions of conserved synteny between the chicken and human genomes, the genetic composition of the two species differs markedly.

Since completion of the first draft of the chicken genome sequence in 2004 (ICGSC 2004), comparative genomics have been widely used to define functional elements in the chicken, using the more extensively annotated human genome for comparison. Whilst a degree of genetic divergence is to be expected, e.g. in the genes that encode observable phenotypic differences such as the presence of feathers, sufficient genome sequence identity exists between the two species to be able to uncover novel orthologues in the chicken. It needs to be emphasized, however, that even after three separate genome builds; the quality of the chicken genome sequence is poor by comparison to that of the human genome. There are a significant number of regions on many of the chicken chromosomes which contain large sequence gaps. In some cases, such as with at least six of the micro-chromosomes, there is no sequence information for entire chromosomes. As such, it is difficult to know how many of the genes found in humans, which are presumed missing in the chicken, are genuinely absent.

1.4 Aims of the project and experimental approach

The ever expanding array of functional roles exhibited by IL-1 family cytokines in mammals emphasizes their importance in both innate and adaptive immunity. A group of eleven genes which encode the ligand members of the family are responsible for eliciting these biological functions. Determining whether an equivalent set of functional orthologues is conserved in the chicken is crucial for understanding the immune response in this species. Analysis of the first draft of the chicken genome sequence, however, provided no evidence of additional IL-1 ligand genes beyond the already described IL-1 β and IL-18 (Kaiser, Poh et al. 2005). It was therefore not known

if the chicken possessed direct orthologues of the nine additional genes identified in man. Hence, the major aim of this project was to establish how many of these “missing” nine genes are present in the chicken. Once this was known, the aim was to characterise them fully at the genomic, mRNA and protein levels. Of these nine absent genes, six were discovered in man as recently as 2000 with a further gene found in 2005.

Intriguingly, despite much active research into many non-mammalian species (of which several have a published genome sequence), these seven most recently discovered IL-1F genes have only been identified in mammals. Scientists have therefore speculated that these genes must have originated following duplication in the mammalian lineage (Mulero, Nelken et al. 2000). Birds and mammals have been evolving separately for ~310 million years and have developed significant differences in the architecture of their genomes and specific gene content. Birds contain extra copies of certain immune function genes, e.g. TLR1, TLR2 and CXCL13, but are apparently missing others, such as TLR8, TLR9, NALP1 and IL-35. Discovery of direct orthologues of novel IL-1F genes in the chicken would thus not only suggest they have indispensable functions, it would also force a reappraisal of the evolution of this cytokine family.

The starting point for this project was two EST sequences mined by a collaborator from the NCBI database. Both sequences had homology with chicken IL-1 β . From amino acid alignments they were clearly different members of the IL-1 family yet neither were identifiable in the chicken genome. The initial approach to the project involved screening every available eukaryotic genome sequence with BLAST to determine the exact identity of these two ESTs. Once this had been done, their predicted amino acid sequences and that of chIL-1 β were used to screen build v2.1 of the chicken genome with BLAST. This was done for several reasons. Firstly, it was a different build to the previous two, and they had reported different genomic locations for IL-1 β

(unplaced in v1.0, and chromosome 4 in v2.0). The genomic location had also been reported as chromosome 2 (Kaiser, Rothwell et al. 2004). It was thus necessary to establish if the most recent location, chromosome 4, was maintained in this new build. This was important because of the possible implications for finding further IL-1 genes in the chicken. In mammals, IL-1 β is found at a locus containing a further eight IL-1 genes. We therefore sought to establish if the human IL-1 locus shared conserved synteny with the chicken. The degree of conserved synteny for the IL-1 locus is high between different mammals. Except for in the mouse, where the locus has become divided into two, most mammals have retained the IL-1 locus as found in the human genome. Examining conserved synteny between the human and chicken genomes had previously been successfully used to isolate several chicken cytokines. For example, the Th2 cytokines (Avery, Rothwell et al. 2004) and CSF3 (Gibson, Kaiser et al. 2009) loci are largely conserved between mammals and the chicken. The two IL-10 family loci, despite a discrepancy in the exact gene content, are also conserved in synteny between the human and chicken genomes. A genome-wide analysis of conserved synteny between the chicken and humans has identified many conserved regions (Bourque, Zdobnov et al. 2005).

Chicken IL-1 β was found in the genome at a locus on chromosome 22, although no other chIL-1 genes were apparent. This locus did, however, contain the chicken orthologues of two non-IL-1 genes which flank the human IL-1 cluster suggesting a minimal degree of conserved synteny. As this locus did not contain further chIL-1 genes, synteny was examined between the novel IL-1F genes in the human IL-1 cluster and other regions of the chicken genome. The chicken genome and the NCBI EST library were also screened with the amino acid sequences of all the novel IL-1F genes in humans. Despite a low degree of homology between chicken and human cytokine

genes, the IL-1 family contains a 21 amino acid signature motif which is unique to this family and highly conserved in all species (mammals, birds, and fish). It is therefore possible to identify IL-1 orthologues between species at this evolutionary distance, using this approach.

The first main experimental aim of the project was to clone the full length CDS of each of the novel chicken IL-1 genes. The second aim was to thoroughly characterise their expression in the chicken at the basal level and in response to infection using quantitative real-time RT-PCR (TaqMan®). This would allow us to gain an insight into their roles in the avian immune response and whether these roles were similar to those of their functional orthologues in man and mouse. A third aim was to determine their genomic structures and location(s) in the chicken. This would provide a greater understanding of the evolution of this cytokine family and may also identify further IL-1 genes at novel loci. A fourth aim was to express recombinant proteins for each novel IL-1 and to use cellular bioassays to characterise their precise function, to establish if these novel chicken cytokines are functionally analogous to their mammalian orthologues.

Chapter 2

Materials and Methods

2.1 In silico materials

2.1.1 Genomic sequence resources

Nucleotide and amino acid sequences from eukaryotic species (listed in the Appendix) were accessed from a range of internet-based genome browsers and sequence databases. Chicken expressed sequence tag (EST) sequences were acquired from the National Center for Biotechnology Information (NCBI) chicken genome resources database (<http://www.ncbi.nlm.nih.gov/projects/genome/guide/chicken/index.html>). The sequences and genomic locations of individual genes or clusters of genes were accessed using the Ensembl genome browser (<http://www.ensembl.org/index.html>), the NCBI map viewer (<http://www.ncbi.nlm.nih.gov/mapview/>), and the University of California Santa Cruz (UCSC) genome browser (<http://genome.ucsc.edu/>). Chicken genomic sequences were accessed from the public database of The Genome Institute at Washington University in St.Louis (WUSTL) (<http://genome.wustl.edu/>).

2.1.2 CodonCode aligner

Codoncode aligner (CodonCode Corporation, MA, USA) is a software program that uses ClustalW to assemble nucleotide sequences into contigs. Base calling uses the Phred-Phrap algorithm to ensure that only high quality sequences become aligned. All sequencing results were analysed using Codoncode aligner.

2.1.3 ClustalX

ClustalX is a software program that creates alignments of multiple nucleotide or amino acid sequences. Nucleotide or amino acid sequences from different species containing homologous genes or from variants of a gene within the same species were aligned using this software.

2.1.4 SignalP

SignalP3.0 (Center for Biological Sequence Analysis, Technical University of Denmark DTU; <http://www.cbs.dtu.dk/services/SignalP/>) is an online server that predicts the existence and position of signal peptides and the exact residues in an amino acid sequence where cleavage occurs. The analysis uses both artificial neural network and hidden Markov model algorithms to make a prediction. Information on the software can be found in (Bendtsen, Nielsen et al. 2004; Emanuelsson, Brunak et al. 2007).

2.1.5 ProDom

ProDom (<http://prodom.prabi.fr/prodom/current/html/form.php>) is a database containing protein domain families created following a large scale analysis of all available amino acid sequences. Protein sequences are derived from UniProt and organised into individual domain family records. BLASTP is used to search against this collection of domain families to indicate structural similarity of a protein to a pre-existing characterized protein domain. Further information can be found in (Bru, Courcelle et al. 2005).

2.1.6 PSIPRED

PSIPRED (Department of Computer Science, University College London; <http://bioinf.cs.ucl.ac.uk/psipred/>) is an online server that predicts the secondary structure of a protein. The analysis uses two “feed-forward neural networks” which analyse the results of an initial PSI-BLAST search to make the prediction.

2.1.7 SoftBerry

SoftBerry (<http://linux1.softberry.com/berry.phtml>) is an online server that compares submitted sequences with a database of 8458 transcription factor binding site consensus motifs. The exact programme used was NSITE.

2.2 In silico methods

2.2.1 Identification of the extent of the chicken IL-1 gene family using the ENSEMBL database

2.2.1.1 IL-1 ligand genes

To establish the extent of the chicken IL-1 ligand gene family, a search of the ENSEMBL chicken genome browser using the terms “IL-1” and “IL-18” was carried out. For all members of the human IL-1 family not identified in the chicken using this method, the full gene sequence, full amino acid sequence and the amino acid signature motif were analysed with BLAST against the chicken genome sequence using the ENSEMBL genome browser.

2.2.1.2 IL-1 receptor genes

The extent of the chicken IL-1 receptor family at a conserved locus was identified by first searching for the known chIL-1 receptor, IL-1RI (Guida, Heguy et al. 1992) in the ENSEMBL genome browser. Next, conserved synteny between the genomic location of chIL-1RI and its orthologue in the human genome was examined. This identified further chicken IL-1 receptor genes in a conserved locus in the chicken. For all members of the human IL-1 receptor gene family not identified in the chicken using this method, a search of their genomic locations in the human was carried out. Conserved synteny was then used to identify if/where chicken orthologues of these genes are located in the chicken genome.

2.2.2 Identification of novel chicken IL-1 family members in the NCBI EST database

A search of the NCBI Chicken Genome Resources expressed sequence tag (EST) database was performed in order to identify EST sequences for novel chicken IL-1 genes using TBLASTN.

2.2.3 Establishing the identity of novel chIL-1 genes using BLAST

A sequence similarity search using BLAST was carried out to confirm the gene identities of novel chIL-1 EST sequences mined from NCBI. Nucleotide sequences were first translated followed by a TBLASTN search against all 39 eukaryotic animal genomes present in ENSEMBL release 50 (July 2008). For the full list of species queried, see Appendix I.

2.3 *In vitro* materials

2.3.1 Restriction enzymes

All restriction enzymes and buffers from Invitrogen unless stated otherwise.

Buffer details are provided in Appendix III.

Restriction enzyme	Recognition site (5'→3')	Buffer
<i>Age</i> I (NEB)	A [↓] CCGGT	NEBuffer1
<i>Bam</i> HI	G [↓] GATCC	REact®3
<i>Dde</i> I	C [↓] TNAG	REact®3
<i>Eco</i> RI	G [↓] AATTC	REact®3
<i>Hind</i> III	A [↓] AGCTT	REact®2
<i>Hinf</i> I	G [↓] ANTC	REact®2
<i>Kpn</i> I	GGTAC [↓] C	REact®4
<i>Mlu</i> I (Roche)	A [↓] CGCGT	SuRE/Cut Buffer H
<i>Not</i> I	GC [↓] GGCCGC	REact®3
<i>Sal</i> I	G [↓] TCGAC	REact®2 (75% activity) REact®10 (100%)
<i>Xba</i> I	T [↓] CTAGA	REact®2
<i>Xho</i> I	C [↓] TCGAG	REact®2

2.3.2 Oligonucleotide primers

All oligonucleotides were ordered from Sigma-Genosys. Primer sequences are provided in Tables I-III in Appendix II.

2.3.3 Vectors

2.3.3.1 pCI-neo Mammalian Expression Vector (Promega E1841)

pCI-neo is a 5.47 kb mammalian expression vector used for cloning cDNA fragments. Plasmid DNA clones can be either transiently or stably transfected into mammalian cells to produce high levels of constitutive expression. The vector contains a number of components that confer this functionality. A cytomegalovirus (CMV) immediate-early enhancer/promoter region acts to promote its expression in cells. A simian virus 40 (SV40) enhancer/early promoter region containing the SV40 origin of replication is also present, allowing any cell type expressing an SV40 large T antigen, e.g. COS-7 cells, to permit transient replication of pCI-Neo. A chimeric intron, located adjacent to the multiple cloning region, is used to augment expression of the cDNA insert. Inserts are directionally cloned with restriction sites into the multiple cloning region (MCR) which is flanked by T7 and T3 RNA polymerase promoters that facilitate sequencing of the insert. Downstream of the MCR is an SV40 late polyadenylation signal that promotes effective processing and increased amounts of RNA copies of the insert. Two selectable markers, the neomycin phosphotransferase and β -lactamase coding regions, confer resistance to G-418 and ampicillin antibiotics, respectively.

2.3.3.2 pGEM-T® Easy (Promega A1360)

pGEM-T® Easy is a linear 3.015 kb vector used to clone DNA fragments. This vector has single deoxythymidine bases located at both 3' ends. Taking advantage of the single 3' deoxyadenosine overhangs added to PCR products by *Taq* polymerase,

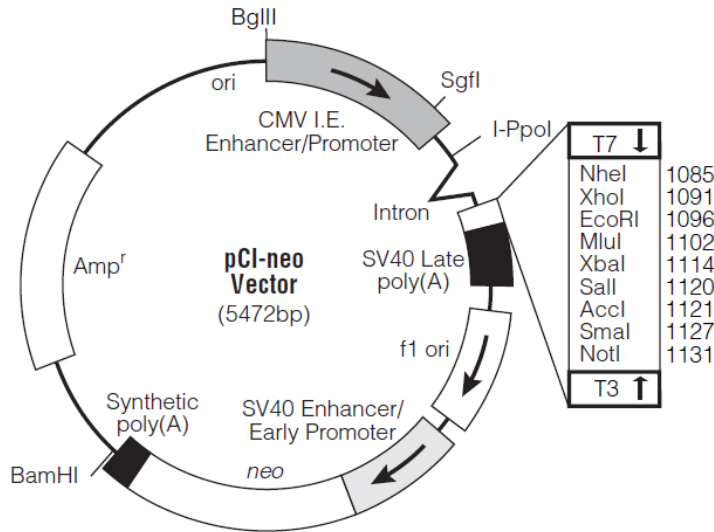


Figure 2.1 Map of the pCI-neo mammalian expression vector.

complimentary TA base pairing permits efficient ligation of DNA inserts into this vector. Following transformation, positive recombinant clones can be identified by selection of white colonies on an agar plate. Colour screening is possible due to the location of the MCR within a *lacZ* gene. This gene encodes the α subunit of *lacZ* protein, which forms part of the enzyme β -galactosidase. Agar plates are spread with X-gal, a sugar that becomes metabolised by β -galactosidase to form blue coloured bacterial colonies. DNA correctly inserted in the MCR inactivates *lacZ*, preventing functional β -galactosidase being produced so only white colonies are present. Blue colonies indicate no insert is present. The MCR contains T7 and SP6 RNA polymerase promoters facilitating RNA synthesis and sites for insert sequencing. An ampicillin resistance gene (*amp^r*) permits selection of only the bacteria containing positive clones.

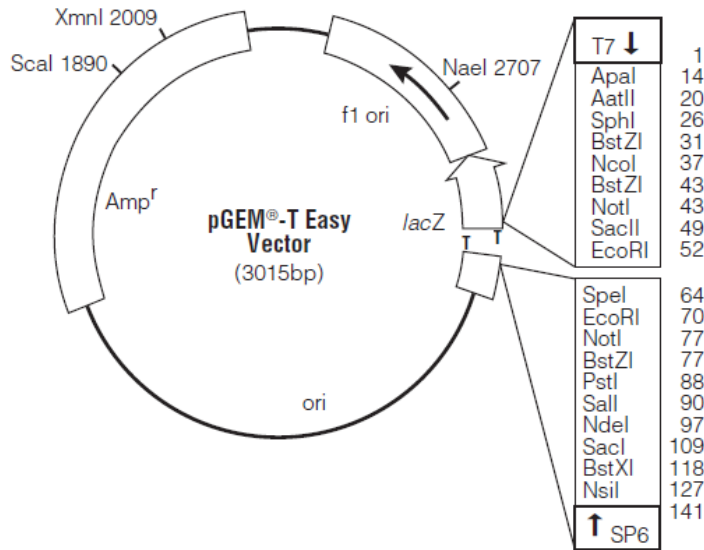
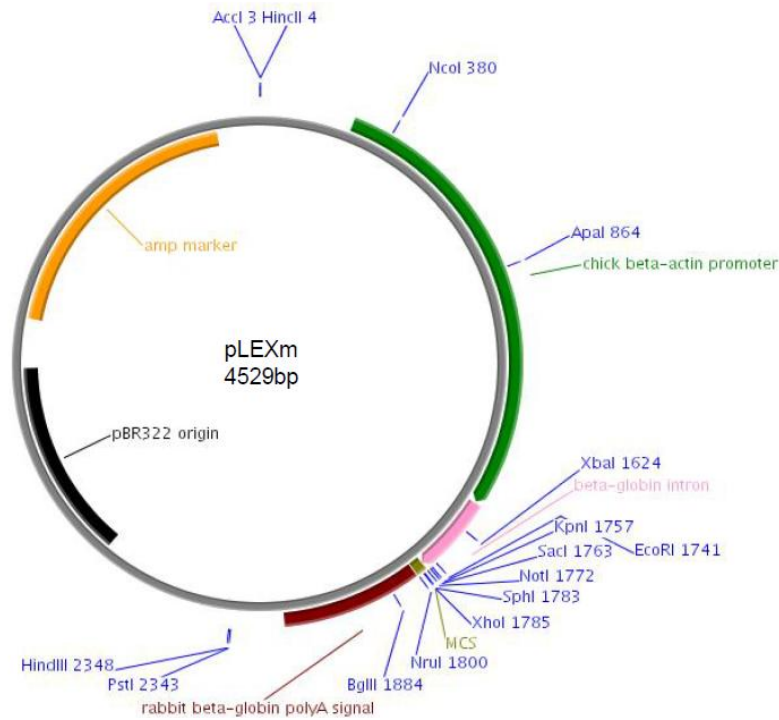


Figure 2.2 Map of the pGEM-T® Easy vector.

2.3.3.3 *pHLSec*

pHLSec is a 4.53 kb expression vector created following multiple modifications of the pCAGGS vector (Aricescu, Lu et al. 2006). Mammalian cells can be transiently transfected with pHLSec-cDNA clones to provide high level expression of constructs that become secreted. It contains a number of components that confer this functionality. It is comprised of a pLEXm backbone consisting of an origin of replication taken from the pBR322 vector. A CMV enhancer/chick β -actin promoter and a rabbit β -globin intron, adjacent to an MCR, enhance its expression in cells. A rabbit β -globin poly(A) signal adds a poly(A) tail to RNA transcripts of the insert, whilst an amp^r gene selectable marker allows visualisation of only positive clones following transformation. Several modifications were made to the MCR to permit the secretion of constructs from transfected cells. These include introducing a Kozak sequence (GCCACCATGG), a secretion signal sequence and a C-terminal K_His tag to facilitate protein purification.



EcoRI HindIII Kozak M G I L P S P G M P A L L S
 GAATTCAAGCTT G C C A C C A T G G G G A T C C T T C C C A G C C C T G G G A T G C C T G C G C T G C T C T C C

L V S L L S V L L M G C V A E T G
 CTCGTGAGCCTTCTCTCCGTGCTGCTGATGGGTTGCGTAGCTGAA A C C G G T ...insert...

G T K H H H H H * * XhoI
 GGTACC AAGCACCACCATCACCATCACTAATGATCACTCGAG

Figure 2.3 Map of the pLEXm vector. pHLSec is comprised of the pLEXm backbone (top) with a modified MCR which was reduced to incorporate the signal sequence and HIS-tag (bottom).

2.3.3.4 pTarget™ Mammalian Expression Vector (Promega A1410)

pTarget™ is a 5.67 kb mammalian expression vector for TA cloning cDNA fragments which can be transiently or stably transfected into mammalian cells. This

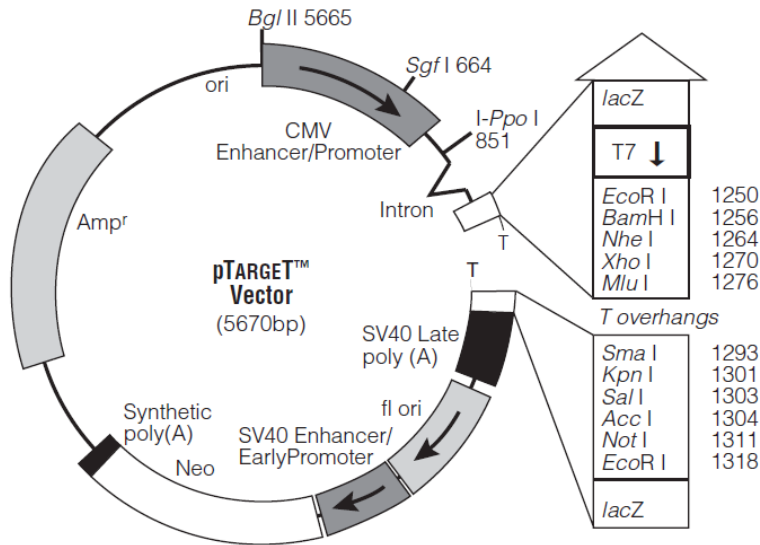


Figure 2.4 Map of the pTarget™ mammalian expression vector

vector is, in effect, a chimera of the pCI-neo and pGEM-T® Easy vectors. It consists of a pCI-neo backbone combined with the pGEM-T® Easy feature of the MCR being located within a *lacZ* gene to allow blue/white screening of recombinants. A solitary T7 RNA polymerase promoter facilitates RNA synthesis and a site for insert sequencing.

2.3.4 Bacterial and viral strains

Escherichia coli competent cells, JM109 strain (Promega L2001), were used to clone plasmid DNA. Chromosomal genotype: *endA1*, *recA1*, *gyrA96*, *thi*, *hsdR17* (rk–, mk+), *relA1*, *supE44*, D(*lac-proAB*), [F ϕ , *traD36*, *proAB*, *laqIqZDM15*].

Salmonella enterica subsp. *enterica* ser. Typhimurium strain F98 NaI^R.

Infectious Bursal Disease Virus strain 52/70.

2.3.5 Cell lines

2.3.5.1 COS-7 cells

COS-7 cells are an adherent cell line that can be transiently transfected for high level expression of recombinant proteins (Aruffo 2002). To create the COS-7 cell line, a CV-1 cell line derived from African green monkey kidney cells was transformed by a mutant of SV40 encoding a wild type T antigen. SV40 origin-containing plasmids, such as pTargetT, experience high copy number replication at 48-72 h after transfection into COS-7 cells.

2.3.5.2 HD11 cells

HD11 cells are an adherent myelomonocytic cell line used widely as a means of investigating immune responses in chicken macrophages. To create the HD11 cell line, bone marrow-derived chick macrophages were transformed with the replication-defective avian retrovirus, myelocytomatosis 29 (MC29) virus (Beug, von Kirchbach et al. 1979).

2.3.5.3 HEK293T cells

HEK293T cells are an adherent cell line with a wide range of experimental uses, mainly due to the ease with which they can be transfected, particularly to express recombinant proteins. The original 293 cell line was created by transforming human embryonic kidney (HEK) cell cultures with sheared adenovirus type 5 (strain Ad75) DNA (Graham, Smiley et al. 1977). HEK293T cells were created by expressing the

SV40 large T antigen to permit high copy number replication of SV40 origin-containing plasmids transfected into this line.

2.3.6 Cell culture reagents

All acquired from Sigma-Aldrich Ltd (Dorset, UK) unless otherwise stated.

Reagent details are provided in Appendix IV.

2.3.7 Recombinant protein

Recombinant mature chIL-1 β protein was purchased from AMS Biotechnology, Abingdon, UK. Full length chIL-1 β (pro-chIL-1 β) is a 267 amino acid precursor form of the cytokine which requires enzymatic cleavage to be converted into its mature, biologically active form. A previous study by Weining, Sick et al. (1998) identified the alanine at position 106 as the first residue of the mature form. We therefore amplified a cDNA encoding amino acids 106-267. AMSBio cloned the cDNA into the pET21a vector and HIS-tagged recombinant protein was expressed in *E. coli*.

2.4 In vitro methods

2.4.1 Sources of chicken tissues and cells

2.4.1.1 Tissues and cells from specified-pathogen-free chickens

Tissues were removed from a nine-week-old specified-pathogen-free (SPF) inbred line 7₂ chicken using a sterile scalpel and were immediately stabilised in RNAlater. Tissues taken were the thymus, spleen, bursa of Fabricius, Harderian gland, caecum, caecal tonsil, Meckel's diverticulum, bone marrow, brain, muscle, heart, liver,

kidney, lung and skin.

Further tissues (spleen, thymus and bursa of Fabricius) were removed from a six-week-old SPF inbred line 7₂ chicken. Splenocytes were divided equally into two groups. The first group of splenocytes, as well as all bursal cells and thymocytes, were stimulated as follows: splenocytes with 1 µg/ml Concanavalin A (ConA), bursal cells with 500 ng/ml phorbol myristate acetate (PMA), and thymocytes with 25 µg/ml phytohaemagglutinin (PHA). All stimulations were performed for 18 h as described (Wu, Hu et al. 2010). With the second group of splenocytes, specific lymphocyte subsets (CD4⁺, CD8α⁺, CD8β, TCR1⁺, TCR2⁺, TCR3⁺, Bu-1⁺ and KUL01⁺ cells) were isolated as previously described (Wu, Hu et al. 2010). All tissues and sorted cell subsets were kindly supplied by Dr Zhiguang Wu (The Roslin Institute, University of Edinburgh, UK).

Bone marrow-derived dendritic cells (BM-DCs), macrophages (BM-MΦ) and blood-derived monocytes/macrophages (Bl-Mo/MΦ) were isolated from 4-8-week-old SPF inbred line 7₂ chickens and stimulated with LPS or CD40L for 1, 2, 4, 8, 12, 24 or 48 h as described (Wu, Hu et al. 2010). All cell populations were kindly supplied by Dr Zhiguang Wu. Unstimulated and LPS-stimulated heterophils were a gift from Dr Mike Kogut (USDA College Station, Texas, USA).

2.4.1.2 Tissues and cells from SPF chickens challenged with bacteria or virus

Six-week-old outbred SPF Rhode Island Red (RIR) chickens were orally challenged with 2.8 x 10⁸ cfu/ml *S. Typhimurium* strain F98 NaI^R or LB medium (control). Birds were killed at 3, 7, 14, 21 and 27 dpi, and whole spleens were removed and immediately stabilised in RNAlater. The experiment was carried out and tissues kindly supplied by Dr Claire Powers (IAH, Compton, UK).

Three-week-old resistant (line 6₁) and susceptible (Brown Leghorn) groups of inbred SPF chickens were challenged intra-nasally with either 10^{1.3} embryonic infectious dose (EID₅₀) per 100 µl PBS of infectious bursal disease virus (IBDV) strain 52/70, or PBS (control). Birds were killed at 2, 3, and 4 dpi, and whole spleens and bursas of Fabricius were removed. The experiment was carried out and tissues kindly supplied by Dr Jean-Remy Sadeyen (IAH, Compton, UK).

2.4.2 Purification of nucleic acids

2.4.2.1 Purifying total RNA from chicken tissues

Total RNA was purified from chicken tissues using the RNeasy mini kit following the manufacturers' protocol for purification of total RNA from animal tissues. Following dissection, fresh tissues were stabilised in *RNAlater* and frozen at -80°C. After thawing, tissues were lysed and homogenised using buffer RLT and a TissueLyser. Buffer RLT contains β-mercaptoethanol and guanidine thiocyanate which lyses the cells and protects the RNA by inactivating RNases. To homogenise a single sample, <30 mg tissue, 600 µl buffer RLT and a 5 mm stainless steel bead were placed in a 2 ml safe-lock tube. All sample tubes were then agitated for 4 min at 20 Hz using the TissueLyser bead mill. Homogenisation releases cellular RNA whilst shearing genomic DNA to decrease lysate viscosity. Further homogenization was achieved by passing tissue lysates through QIAshredder columns according to the manufacturers' protocol. Ethanol was added to lysates to provide suitable binding conditions before samples were bound to RNeasy silica membranes (spin columns) by centrifugation at 1300 x g for 15 s. A single buffer RW1 and two buffer RPE washes were carried out to remove contaminants. The final RPE wash had a 2 min centrifugation step to dry the

spin column by removing residual ethanol. Spin columns were transferred to clean collection tubes and centrifuged at 1690 x g for 1 min to eliminate all traces of ethanol. RNA was eluted into clean 1.5 ml tubes, using 30-50 µl RNase-free water, by centrifugation at 1300 x g for 15 s. Buffer contents are given in Appendix III.

2.4.2.2 Purifying total RNA from cell lines

Total RNA was purified from cell lines using the RNeasy mini kit following the manufacturers' protocol for purification of total RNA from animal cells using spin technology. Cell lines were washed twice with PBS then directly lysed using 600 µl buffer RLT per 2×10^6 cells. RNA was extracted from cell lysates using the same method as described in section 2.4.2.1.

2.4.2.3 Purifying genomic DNA from whole blood

Genomic DNA was purified from whole blood using the DNeasy blood and tissue kit following the manufacturers' protocol for purification of total DNA from animal blood or cells (spin-column). To lyse the cells, 20 µl of proteinase K were mixed with 10 µl anticoagulated chicken blood, and the volume adjusted to 220 µl with PBS. Proteinase K also digests contaminating proteins as well as degrading nucleases that could damage the DNA. Next, 200 µl of buffer AL were added to the reaction, mixed thoroughly by vortexing, then incubated for 10 min at 56 °C. The guanidine hydrochloride (GndHCl) in buffer AL helps to lyse cells. To this, 200 µl of 100% ethanol were added and mixed by vortexing. The combination of ethanol with the GndHCl adjusts the buffer conditions for optimal DNA adsorption to a silica membrane. The mixture was then applied to a DNeasy mini spin column, in a 2 ml collection tube, and centrifuged at 1040 x g for 1 min. The column was transferred to a fresh collection

tube and washed with 500 μ l of buffer AW1, followed by centrifugation at 1040 x g for 1 min. The column was transferred to a fresh collection tube and washed with 500 μ l of buffer AW2 then centrifuged at 1820 x g for 3 min. This long centrifugation step eliminated all traces of ethanol. The column was transferred to a clean microcentrifuge tube and 200 μ l of buffer AE were added. After allowing 1 min for adsorption, DNA was eluted by centrifugation at 1040 x g for 1 min.

2.4.2.4 Purifying genomic DNA from cell lines

This protocol was identical to the purification from whole blood in section 2.4.2.3 except for the first steps. When extracting DNA from cells, $<5 \times 10^6$ cells were pelleted by centrifugation at 300 x g for 5 min. The pellet was resuspended in 200 μ l PBS then mixed with 20 μ l proteinase K. The remainder of the protocol, beginning with the addition of 200 μ l of buffer AL, was as described in section 2.4.2.3.

2.4.3 Quantification of nucleic acids

The concentration of pure RNA was determined using a NanoDrop ND1000 spectrophotometer. Concentration is calculated as the absorbance of a 1 μ l sample at 260 nm which equates to 1 optical density (O.D.) unit = 44 μ g/ml RNA. RNA concentration is automatically calculated in ng/ μ l, based on the Beer Lambert equation. RNA purity is also calculated as the ratio of absorbance at 260 nm and 280 nm (A_{260}/A_{280}). For pure RNA, this value should be in the range = 1.9-2.1.

The concentration of DNA was calculated using the same method; however, with this template 1 O.D. = 50 μ g/ml double-stranded DNA. DNA purity is also calculated using the A_{260}/A_{280} ratio and, if pure, should \approx 1.8.

2.4.4 DNA and RNA amplification

2.4.4.1 Oligonucleotide primer design

Oligonucleotide primers used to amplify genomic DNA or cDNA templates were designed using Primer3, an open access online design tool (Rozen and Skaletsky 2000).

2.4.4.2 One-step reverse transcriptase-polymerase chain reaction (RT-PCR)

PCR products were generated from RNA templates in a single step using Illustra Ready-To-Go™ RT-PCR beads. Following first-strand cDNA synthesis, the RNA:cDNA heteroduplex is denatured to permit PCR amplification of the cDNA template. Beads are supplied containing most of the reagents required for both of these stages. The user is required to add first-strand primer, a pair of gene-specific PCR primers, the RNA template and DEPC-H₂O, to a final volume of 50 µl. Reaction tubes were incubated on ice and beads were dissolved using 39 µl DEPC-H₂O. Twenty pmol of both forward and reverse gene-specific primers (in DEPC-H₂O) along with 1 µl RNA template were added to each tube to complete the reaction. Reverse strand gene-specific primers were always used as the first strand cDNA synthesis primer. The final 50 µl reaction contained 2 U Taq DNA polymerase, 10 mM Tris-HCl, 60 mM KCl, 1.5 mM MgCl₂, 200 µM dNTPs, Moloney murine leukaemia virus reverse transcriptase (RT) and RNAGuard ribonuclease inhibitor. Thermal cycling conditions were:

42°C / 30 min	x1 cycle	first strand synthesis
95°C / 5 min	x1 cycle	inactivates the RT and denatures the template
95°C / 1 min	} x40 cycles	
*55°C / 1 min		
72°C / 2 min		

* Annealing temperature is dependent on the T_m of the primers. The range of temperatures used was 55-70°C.

Thermal cycling was carried out using a Mastercycler (Eppendorf). Products were electrophoresed on a 1% agarose gel.

2.4.4.3 Two step RT-PCR

PCR products were generated from RNA templates in two separate reaction steps. In the first, cDNA was created from mRNA using Superscript II reverse transcriptase (RT). To a 0.2 ml nuclease-free centrifuge tube, the following reaction components were added: 1 μ l 500 μ g/ml oligo(dT)₂₀, 1 ng – 5 μ g total RNA, 1 μ l 10 mM dNTPs and sterile water to a total volume of 12 μ l. The oligo(dT) primer hybridizes to the poly(A) tail of mRNA molecules to facilitate first strand cDNA synthesis using reverse transcriptase. The reaction mixture was heated to 65°C for 5 min to enable the oligo(dT) to anneal to the mRNA template, then incubated on ice for 20 s. Next, the following components were added to the reaction: 4 μ l 5X first-strand buffer and 2 μ l 0.1 M DTT, followed by gentle agitation to mix. The first strand buffer contains MgCl₂ which stabilizes ATP and supports transfer of the phosphate group during the extension step. DTT (dithiothreitol) is a reducing agent added to break

disulphide bonds in any RNases present. The tube was briefly incubated at 42°C for 2 min to bring the reaction to the required temperature. Next, 1 µl Superscript II RT was added and gently mixed by pipetting followed by incubation at 42°C for 50 min to allow cDNA synthesis to take place. Finally, the RT was inactivated by heating the reaction at 70°C for 15 min.

PCR was performed in a standard 25 µl reaction containing 2 µl of cDNA template, 0.4 mM dNTPs, 1 x final volume PCR buffer, 1.5 mM MgCl₂, 0.625 U Go *Taq*® DNA polymerase and 0.2 µM of each primer. Thermal cycling conditions were:

95°C / 5 min	x1 cycle	denatures the template
95°C / 20 s	} x5 cycles touchdown i.e. annealing temperature decreases by 1°C per cycle	
*x°C / 20 s		
72°C / 1 min		
95°C / 20 s	} x25 cycles	
*x-5°C / 20 s		
72°C / 1 min		

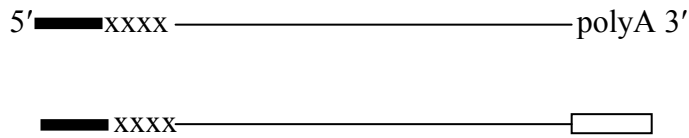
* Annealing temperature is dependent on the T_m of the primers. The range of temperatures used was 55-70°C.

Thermal cycling was carried out using an iCycler (Bio-Rad). Products were electrophoresed on a 1% agarose gel.

2.4.4.4 DNA amplification by PCR

Genomic DNA and cDNA were amplified by PCR in standard 25 µl reactions. Each reaction consisted of 50 ng DNA template, 0.4 mM dNTPs, 1 x final volume PCR buffer, 1.5 mM MgCl₂, 1.25 U of *Taq* polymerase and 0.2 µM of each primer. Thermal cycling conditions were the same as the PCR in section 2.4.4.3. Thermal cycling was

added by the RT enzyme, causing it to anneal to the cDNA tail. This permits the oligo to act as template for the RT. The RT jumps from the RNA to the oligo and copies the oligo sequence into the end of the cDNA.



The final product is a single-stranded full length cDNA with the SMARTer II A sequence (universal primer binding site) at the 5' end. PCR was performed using the universal primer (whose sequence is complementary to SMARTer II A) and a gene-specific reverse primer (GSP).



2.4.4.5.1 First strand cDNA synthesis

Buffer mix was made in multiples of 4 μ l (depending on the number of reactions being set up) containing 2 μ l 5X first strand buffer, 1 μ l DTT (20 mM) and 1 μ l dNTP (10 mM). Next, 5' RACE cDNA was made by combining 1-2.75 μ l RNA and 1 μ l 5' CDS Primer A (modified oligo (dT)), made up to 3.75 μ l with sterile water. This reaction was incubated for 3 min at 72°C, then 2 min at 42°C. It was allowed to cool briefly before centrifugation at 1690 x g for 10 s to collect the tube contents. Next, 1 μ l SMARTer II A oligo was added to each separate 5' RACE reaction.

Master mix was made consisting of 4 μ l buffer mix (see above), 0.25 μ l RNase inhibitor (40 U/ μ l) and 1 μ l SMARTscribe RT (100 U/ μ l). This was added to the 4.75

μl RNA (from above) for a total volume of 10 μl . After gently mixing with a pipette, reactions were incubated for 90 min at 42°C to facilitate cDNA synthesis followed by 10 min at 70°C to inactivate the RT. Reactions were diluted with 20-250 μl Tricine-EDTA buffer and stored at -20°C.

2.4.4.5.2 5' RACE PCR

PCR mastermix was made in multiples of 41.5 μl containing 34.5 μl sterile water, 5 μl 10X Advantage 2 PCR buffer (1X final volume), 1 μl dNTP (10 mM) and 1 μl 50X Advantage 2 polymerase mix (1X final volume). 5' RACE PCR amplification was carried out in 50 μl reactions consisting of 2.5 μl 5' RACE cDNA, 5 μl 10X universal primer mix (UPM) (1X final volume), 1 μl reverse GSP (10 μM) and 41.5 μl PCR mastermix. For each separate 5' RACE PCR, 3 control reactions were also set up. A positive control PCR was the same as the 5' RACE PCR except 4 μl sterile water and 1 μl forward GSP (10 μM) were substituted for the UPM. This reaction ensured the cDNA of interest was contained within the template. Two negative controls were set up: a UPM control substituting 1 μl of sterile water for the reverse GSP; and a GSP control whereby 5 μl of sterile water was substituted for the UPM. Thermal cycling conditions were:

If GSP $T_m > 70^\circ\text{C}$

95°C / 30 secs	}	x5 cycles
72°C / 3 mins		
94°C / 30 secs	}	x5 cycles
70°C / 30 secs		
72°C / 3 mins		

94°C / 30 secs
68°C / 30 secs
72°C / 3 mins

} x20 cycles (polyA RNA) or 25 cycles (total RNA)

If GSP T_m = 60-70°C

94°C / 30 secs
68°C / 30 secs
72°C / 3 mins

} x20 cycles (polyA RNA) or 25 cycles (total RNA)

2.4.4.6 Real-time quantitative RT-PCR (TaqMan)

Real-time quantitative RT-PCR (qRT-PCR) was used to measure the level of cytokine mRNA expression in a range of chicken cells and tissues. Expression levels of gene-specific transcripts were quantified alongside a house-keeping gene, 28S, for every sample that was assayed. The 28S ribosomal RNA gene encodes the RNA component of the large subunit found within ribosomes, so it is constitutively and relatively constantly expressed in all eukaryotic cells, and so is a suitable candidate to be used to normalize the expression levels of target genes. Standardization of the target gene quantity to the amount of RNA in a sample allows valid comparisons to be made between different samples.

For each different gene that was analysed, a pair of primers and a probe were designed against the target template using the Primer Express software package (Applied Biosystems). Primers were acquired from Sigma, whilst probes were acquired from Eurogentec, Sigma and Applied Biosystems. Standard probes were labelled at the

5' end with 5- or 6-carboxyfluorescein (FAM) fluorophore, and at the 3' end with tetramethylrhodamine (TAMRA) quencher dye. MGB probes were also labelled with FAM at the 5' end; however, the 3' end was labelled with dihydrocyclopyrroloindole tripeptide minor groove binder ligand (MGB). These probes have higher melting temperatures and increased specificity. Primers and probe sets were designed according to seven strict criteria to enable optimal reaction efficiency. The melting temperature of the primers was 58-60°C, with the probe T_m 10°C higher than this. Primers and probes were 15-30 nucleotides in length, with the GC content in the range of 30-80%. To reduce non-specific priming, no more than 2 G or C bases were present in the final 5 nucleotides at the 3' end of a primer. Amplicons should ideally be 50-150 bp long and were never more than 400 bp. Probes did not contain consecutive identical nucleotides, in particular ≥ 4 guanines, as this can lead to mispriming. Probes also contained more C's than G's, and did not have a G at the 5' end as this would have quenched the fluorophore. Finally, primer and probe sets were designed so that at least one of the oligonucleotides spanned a boundary between different exons. This ensured false-positive results from the amplification of contaminating genomic DNA would not be obtained.

The theory behind this assay is as follows: qRT-PCR probes are labelled at their 5' end with a reporter fluorophore and at their 3' end with a quencher. The close proximity of these moieties allows the quencher to inhibit the fluorescence of the reporter dye, although not completely so some background fluorescence can be observed. During the PCR, the probe anneals to the template between forward and reverse primers. Upon primer extension, facilitated by *Taq* polymerase, template replication takes place. Upon reaching the bound probe, the 5'-3' exonuclease activity of *Taq* degrades the probe releasing the reporter away from the close proximity of the

quencher. This leads to an increase in fluorescence intensity (see Figure 2.5). As this technique measures the number of copies of PCR product that have accumulated, the greater the fluorescence, the more transcripts are present in a sample. Results are presented as a cycle threshold (Ct) value, which represent the number of PCR cycles at which fluorescence emission of the reporter minus any background passes the threshold.

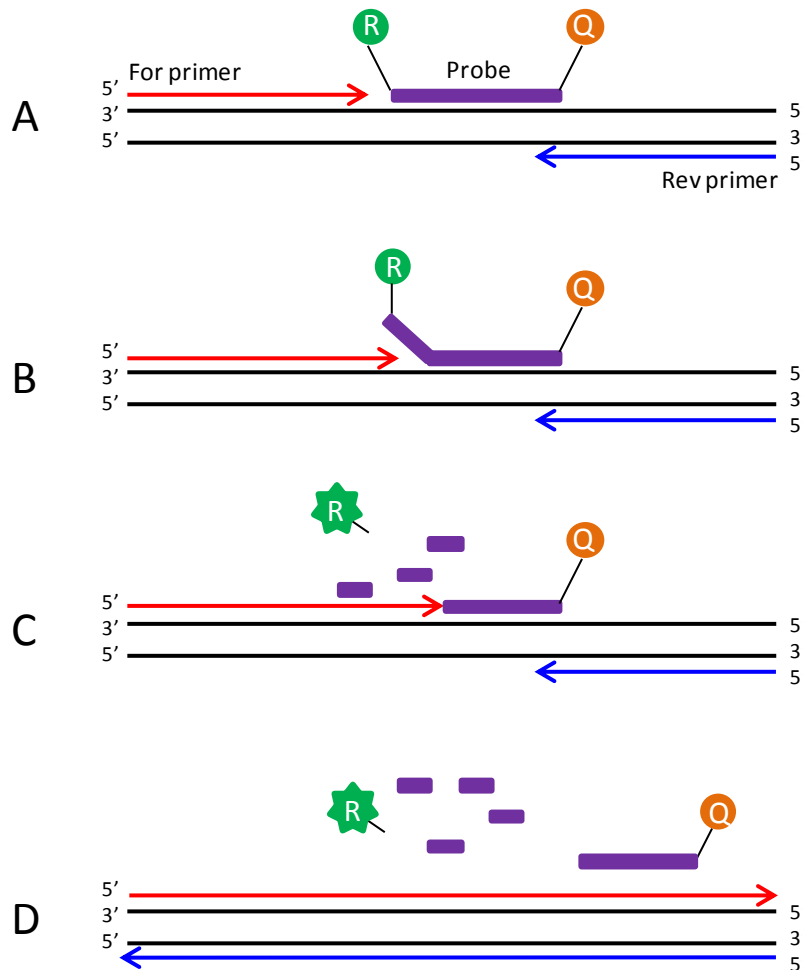


Figure 2.5 Real-time quantitative RT-PCR (qRT-PCR). **A.** Polymerization. A fluorescently labelled TaqMan probe hybridises to the target template between forward and reverse primers. Upon primer extension, template replication takes place, facilitated by *Taq* polymerase. **B.** Probe displacement. The elongated forward strand being synthesised, displaces the probe from the template. **C.** Probe degradation. The 5'-3' exonuclease activity of *Taq* polymerase degrades the probe, releasing the fluorescent reporter dye. **D.** Fluorescence. Probe degradation allows the reporter to move away from its close proximity to the quencher. This leads to an increase in fluorescence intensity.

Before working with test samples, it was necessary to determine the optimal concentration of primer to be used in a reaction. Primer concentrations for IL-1 β and 28S were optimised prior to this study (Kaiser, Rothwell et al. 2000). For iNOS, primer concentrations were optimised prior to this study by Dr Bas Baaten (IAH, Compton, UK). For IL-1RN and IL-1F5, COS-7 cells were transfected with full length pTarget cDNA clones of both. RNA from these cells was diluted in the range 10^{-2} - 10^{-7} and analysed with a range of primer concentrations from 0.25-2.5 μ M. RT-PCR was performed using the Taqman FAST Universal PCR Master Mix (kit 1) and TaqMan One-step RT-PCR mastermix (kit 2) reagent kits (Applied Biosystems). Samples were assayed in 10 μ l reactions consisting of: 5 μ l 2x FAST Master mix (kit 1), 0.5 μ l primer mix, 125 nM probe, 0.25 μ l 40X Multiscribe enzyme (kit 2), 1.5 μ l DEPC-H₂O and 2.5 μ l RNA. For the test sample RNA, 1:5 dilutions were made for the analysis of cytokine expression, and 1:500 dilutions for 28S analysis. All were assayed in triplicate. For IL-1RN and IL-1F5, standard curves were created with serial dilutions of ex-COS RNA in the range 10^{-2} - 10^{-6} . For 28S positive standard RNA, HD11 cells were stimulated with 200 ng/ μ l LPS for 6 h, then total RNA extracted and diluted in the range 10^{-3} - 10^{-7} . Amplification and quantification of products was carried out using the 7500FAST TaqMan machine (Applied Biosystems). Thermal cycling conditions were: one cycle of 48°C for 30 min, 95°C for 20 s, then 40 cycles of 95°C for 3 s, 60°C for 30 s. Optimised primer concentrations for all assays are in Table II in Appendix II.

2.4.5 Agarose gel electrophoresis of DNA

DNA products from RT-PCR, standard PCR, RACE and restriction digestion reactions were visualised following electrophoresis. Five μ l PCR or 10 μ l restriction digest products were added to 6X Orange G loading buffer (1X final volume) and

electrophoresed on 1% agarose gels at 100 V for 3 h. Agarose gels were made by dissolving 1% w/v pure agarose in 50 ml 0.5X Tris-borate-EDTA (TBE) buffer to which 5 µl 10000X GelRed™ (1X final volume) was added. GelRed intercalates with DNA which enabled visualisation of all products using a UV transilluminator. 100 bp and 1 kb DNA size markers (Invitrogen) were used to estimate product sizes.

2.4.6 Purification of PCR products

2.4.6.1 PCR purification

PCR products in solution were purified using the QIAquick PCR purification kit. Briefly, 5 volumes of buffer PB were added to 1 volume PCR product, mixed, applied to a spin column (in a 2 ml collection tube) and centrifuged at 1690 x *g* for 1 minute. Spin columns contain a silica membrane to which DNA adsorbs at the optimal pH and salt concentrations provided by buffer PB. Contaminants were removed by adding 750 µl buffer PE and centrifuging at 1690 x *g* for 1 min. After discarding the flow through, the spin column was centrifuged at 1690 x *g* for an additional minute to eliminate all traces of ethanol. The column was transferred to a clean microcentrifuge tube and 35 µl of sterile water was added. After allowing 1 min for adsorption, DNA was eluted by centrifugation at 1690 x *g* for 1 min.

2.4.6.2 PCR purification from agarose gel

Multiple PCR products from a single reaction required separation by gel electrophoresis on a 0.8% agarose gel. Using a clean scalpel, individual DNA fragments were excised from the gel under UV transillumination and purified using the QIAquick gel extraction kit following the manufacturer's protocol. Buffer QG was added at 3X

volume of the weight of the gel slice followed by incubation at 50°C for 10 min. This incubation allows buffer QG to solubilise the gel whilst providing the optimal pH (≤ 7.5) and salt concentration (high) for DNA adsorption to the silica membrane. Optimal pH is determined by the pH indicator present in buffer QG. Where a high pH (> 7.5) was found, 10 μl 3 M sodium acetate (pH 5.0) was added to adjust it for optimal DNA adsorption. Isopropanol was added to the sample at 1X gel volume, mixed, and applied to a QIAquick spin column (in a 2 ml collection tube). The sample was centrifuged at 1690 x g for 1 min to facilitate DNA adsorption. After discarding the flow through, 500 μl buffer QG were added to the spin column and centrifuged at 1690 x g for 1 min to remove any residual agarose. Next, the column was washed with 750 μl buffer PE and centrifuged at 1690 x g for 1 min to remove contaminants. After discarding the flow through, the column was centrifuged at 1690 x g for an additional minute to eliminate all traces of ethanol. The column was transferred to a clean 1.5 ml microcentrifuge tube to which 35 μl of sterile water was added. After incubating for 1 min to allow adsorption, DNA was eluted by centrifugation at 1690 x g for 1 min.

2.4.7 Cloning and subcloning

2.4.7.1 Vector preparation

In order to directionally clone or subclone genes of interest into the pCI-neo mammalian expression vector, it first needed to be linearised by restriction digestion. Using *EcoRI* and *MluI* restriction enzymes, pCI-neo was digested at 37°C for 2 h followed by electrophoresis of the products on a 0.8% agarose gel. Vector DNA was purified using the QIAquick gel extraction kit.

2.4.7.2 TA-cloning RT-PCR products

Purified RT-PCR products were ligated into the pTarget™ mammalian expression vector. The ligation reaction contained 60 ng of pTarget™ vector, x ng DNA insert, 1 µl of T4 DNA ligase and 1 x T4 DNA ligase buffer in a total volume of 10 µl. The concentration of insert was calculated using the following formula:

$$\frac{60 \text{ ng vector} \times y \text{ kb insert}}{5.67 \text{ kb vector}} \times 1.4 = x \text{ ng insert}$$

Ligations were incubated overnight at 4°C.

TA cloned RT-PCR products inserted into pTarget™ in the incorrect orientation were directionally subcloned into pCI-Neo following release from pTarget using *EcoRI* and *MluI* restriction enzymes. Ligation reactions were carried out exactly as for pTarget™ except 60 ng of linearised pCI-neo and x ng DNA insert with *EcoRI* and *MluI* restriction sites were used. The concentration of insert was calculated using the following formula:

$$\frac{60 \text{ ng vector} \times y \text{ kb insert}}{5.47 \text{ kb vector}} \times 1.4 = x \text{ ng insert}$$

Ligations were incubated overnight at 4 °C

2.4.7.4 Directional sticky end cloning into an expression vector

Purified PCR products with *AgeI* and *KpnI* restriction site overhangs were

directionally cloned into the linear pHLSec mammalian expression vector, kindly supplied by James Birch (IAH, Compton, UK). The ligation reaction contained 40 ng pHLSec, 40-200 ng DNA insert, 1 μ l of T4 DNA ligase and 1x T4 DNA ligase buffer in a total volume of 10 μ l. Ligations were incubated for 1 h at room temperature.

2.4.7.5 Transformation and screening

JM109 competent cells were thawed on ice for 5 min. To a chilled 1.5 ml eppendorf tube containing 2 μ l ligation mix, a 50 μ l aliquot of the cells was added and gently mixed by stirring with a pipette tip. The DNA/cells were incubated for 20 min on ice then heat shocked at 42°C for 50 s. This creates small holes in the bacterial cell membrane allowing the DNA to be taken up. Cells were then returned to ice for a further 2 min. A 950 μ l aliquot of room temperature SOC medium was added to the cells and gently mixed by inversion. Cells were incubated at 37°C with shaking at 170 rpm for 90 min. Next, cells were pelleted by centrifugation at 863 x *g* for 10 min. The supernatant was discarded and cells were resuspended in 200 μ l room temperature SOC medium. The transformed cells were plated out in 100 μ l aliquots onto LB agar plates containing 100 μ g/ml ampicillin, 80 μ g/ml Xgal and 0.5 mM IPTG. Plates were inverted and incubated overnight at 37°C. Positive recombinant clones in all vectors were indicated by white colonies, whilst blue colonies denoted an empty vector for pGEM-T® Easy or pTargeT clones.

2.4.8 Restriction digestion

Restriction digestions were carried out using the restriction enzymes and buffers

(buffer components in Appendix) listed in section 2.3.1 to release DNA inserts from cloning vectors, to linearise and create sticky ends in cloning vectors, and to digest BAC DNA. Digestions were carried out in 10 µl reactions containing 1 µg DNA, 1 µl 10X buffer (1X final volume), 1 µl restriction enzyme and made up to the final volume with sterile water. Reactions were incubated at 37°C for 90 min. Large scale digestions containing several enzymes were incubated at 37°C overnight (16 h) to ensure complete digestion.

2.4.9 Plasmid DNA purification

2.4.9.1 Small scale (mini) plasmid DNA preparation

Mini preps use an alkaline lysis method to purify DNA and were carried out following the manufacturer's protocol. In order to screen plasmid DNA clones, bacterial cells were picked and used to inoculate 5 ml LB medium supplemented with 100 µg/ml of ampicillin (LB/Amp₁₀₀). Cultures were grown overnight at 37°C with shaking at 170 rpm. The next day, cells were pelleted by centrifugation at 1942 x g for 10 min at 4°C. Cell supernatants were discarded and the cells resuspended in 250 µl of cold buffer P1 containing RNase A and LyseBlue reagent. Next, the cells were lysed by adding 250 µl of buffer P2 and mixing by inversion. The addition of buffer P2 to buffer P1 in the presence of LyseBlue causes the cell suspension to turn blue. Buffer P2 contains SDS and NaOH that encourage lysis as follows: SDS solubilises the protein and phospholipid bilayer of the cytoplasmic membrane releasing cell contents. NaOH provides high alkaline conditions that denature chromosomal DNA, plasmid DNA and proteins. Next, 350 µl buffer N3 were added and mixed by inversion. The blue appearance of the lysate disappeared indicating the SDS from buffer P2 had been precipitated. Buffer N3

neutralised the reaction whilst adjusting it to high salt conditions that led to precipitation of chromosomal DNA, denatured proteins and cellular debris. Plasmid DNA which is smaller by comparison, becomes renatured and remains in solution. The reaction was centrifuged at 1690 x g for 10 min to pellet precipitants. Supernatant containing plasmid DNA was applied to a spin column (in a 2 ml collection tube) and centrifuged at 1690 x g for 1 min. The column contains a silica membrane to which DNA adsorbs at the optimal high salt concentration. The column was washed with 500 µl buffer PB and centrifuged at 1690 x g for 1 min to remove contaminants and residual endonucleases. A further wash with 750 µl buffer PE was carried out. After discarding the flow through, the spin column was centrifuged at 1690 x g for an additional minute to eliminate all traces of wash buffer. The column was transferred to a clean 1.5 ml tube and DNA was eluted in 50 µl sterile water by centrifugation at 1690 x g for 1 min. Kit components are listed in the Appendix.

2.4.9.2 Large scale (maxi) plasmid DNA preparation

Maxi preps also use an alkaline lysis method to purify DNA and were carried out following the manufacturer's protocol. To synthesise a sufficient quantity of plasmid DNA for transfection, a 5 ml LB/Amp₁₀₀ seeder culture was set up as described in section 2.4.9.1 and incubated for 8 h at 37°C with shaking at 170 rpm. Next, a 100 ml aliquot of LB/Amp₁₀₀ was inoculated with 200 µl of the seeder culture and cultured overnight at 37°C with shaking at 170 rpm. The next day, cells were pelleted at 6000 x g for 15 min at 4°C. Cell resuspension, lysis and neutralisation steps followed the same method as for mini preps, using 10 ml of each of buffers P1, P2 and P3, respectively. After this, however, the maxi prep method differs. Cell lysates were added to a QIAfilter maxi cartridge and incubated at room temperature for 10 min to allow the

precipitated genomic DNA, proteins and detergent to float to the surface. Lysates were then filtered into a clean, endotoxin-free 50 ml tube to which 2.5 ml endotoxin removal buffer ER was added followed by incubation on ice for 30 min. During this incubation, a QIAgen tip 500 was equilibrated with 10 ml buffer QBT. This tip contains an anion exchange resin that binds plasmid DNA under optimal low pH and salt conditions. The filtered lysate was applied to the tip and passed through by gravity flow facilitating DNA binding. Contaminants and impurities were removed with 2 x 30 ml washes of medium salt buffer QC. DNA was eluted with 15 ml high salt buffer QN into a 30 ml endotoxin-free tube. Concentration, desalting and precipitation of the DNA was carried out by adding 0.7 volumes room temperature isopropanol. DNA was pelleted by centrifugation at 15000 x g for 30 min at 4°C. After discarding the supernatant, the pellet was washed with 5 ml 70% ethanol, centrifuged at 15000 x g for 10 minutes and dried. Finally, the pellet was resuspended in 500 µl endotoxin-free buffer TE.

2.4.9.3 Very large scale (mega) plasmid DNA preparation

Mega preps also use an alkaline lysis method to purify DNA and were carried out following the manufacturer's protocol, identical to the maxiprep protocol in section 2.4.9.2 except for the following differences. Volumes of buffers used were: 50 ml of buffer P1 containing RNase A and LyseBlue reagent, 50 ml of buffer P2, 50 ml of buffer P3, 50 ml of buffer FWB2, 12.5 ml of buffer ER, 35 ml of buffer QBT, 200 ml of buffer QC and 35 ml of buffer QN. Bacterial culture was carried out on a larger scale: a 500 ml aliquot of LB/Amp₁₀₀ was inoculated with 1 ml of a 5 ml LB/Amp₁₀₀ seeder culture set up as described in section 2.4.9.1. Cell lysates were added to a QIAfilter mega-giga cartridge and incubated at room temperature for 10 min to allow contaminants to float to the surface. Lysates were then filtered into a collection vessel

beneath the mega-giga cartridge using a vacuum pump. Once all the liquid had passed through, the vacuum was switched off and 50 ml of buffer FWB2 were added.

Precipitates were stirred after restarting the vacuum pump to aid the flow of liquid through the filter. A QIAgen tip 2500 was subsequently used to bind the DNA.

Volumes of isopropanol for DNA precipitation and 70% ethanol to wash the pellet were scaled up accordingly. Finally, DNA pellets were resuspended in 1 ml endotoxin-free buffer TE.

2.4.9.4 Large scale BAC DNA preparation

BAC clones were acquired as bacterial cells and re-streaked onto solid LB medium supplemented with 12.5 µg/ml of chloramphenicol (ChP_{12.5}) then incubated overnight at 37°C. From this LB plate, a single colony of cells was picked and used to inoculate 5 ml LB/ChP_{12.5} as described in section 2.4.9.1, then incubated for 8 h at 37°C with shaking at 170 rpm. The culture was used to seed a 500 ml aliquot of LB/ChP_{12.5} and this large culture was incubated at 37°C overnight. Bacterial cells were pelleted by centrifugation at 5000 x g for 10 min at 4°C. BAC DNA was purified from the pelleted bacteria using the NucleoBond® BAC 100 kit (Macherey-Nagel) following the manufacturer's instructions. This kit also uses a modified alkaline/SDS lysis method to purify BAC DNA. Cell supernatants were discarded and the cells resuspended in 24 ml of buffer S1 containing RNase A. Next, the cells were lysed by adding 24 ml of buffer S2 and mixing by inversion. Buffer S2 contains SDS and NaOH that encourage lysis whilst providing high alkaline conditions that denature chromosomal and plasmid DNA. The reaction was then neutralised by the addition of 24 ml of buffer S3. Buffer S3 contains 2.8 M potassium acetate that precipitates the denatured chromosomal DNA whilst plasmid DNA becomes renatured and remains in solution. During 5 min

incubation on ice, a NucleoBond filter was folded and placed in a funnel. The lysate was then clarified by loading onto the filter to remove SDS and cellular debris. This step is an alternative to centrifugation which can lead to large constructs such as BACs becoming sheared. During filtration, a BAC 100 column was equilibrated with 5 ml of buffer N2. The clarified lysate was loaded onto the column and passed through by gravity flow, facilitating DNA binding. Contaminants and impurities were then removed with 3 x 12 ml washes of buffer N3. DNA was eluted from the column with 6 ml of buffer N5 which had been pre-heated to 50°C. Purified BAC DNA was precipitated with 0.7 volumes of isopropanol and centrifuged at 15000 x *g* for 30 min at 4°C. After discarding the supernatant, the DNA pellet was washed with 0.35 volumes of cold 70 % ethanol and centrifuged at 15000 x *g* for 10 min at 4°C. Finally, the pellet was air dried for 30 min and resuspended in 200 µl buffer EB (Qiagen).

2.4.10 Sequencing

Sequencing was carried out using the Beckman Coulter CEQ™ 8000 Genetic Analysis System (Beckman Coulter, Bucks, UK). Samples were analysed by capillary electrophoresis sequencing using dye terminator cycle sequencing chemistry (GenomeLab DTCS with quick start kit, Beckman Coulter). This chemistry is based on classical chain termination by dideoxynucleotide triphosphates (ddNTPs), each of which is labelled with a fluorescent dye that emits light at different wavelengths.

2.4.10.1 Sequencing PCR

One quarter standard sequencing reactions were set up containing 2 µl quickstart master mix, 1.5 µl sequencing reaction buffer, 4 pmol primer, 10-400 ng DNA and sterile water to 20 µl. Difficult, GC-rich templates were pre-heat treated at 96°C for 2

min to destabilise DNA secondary structure, then sequenced using the methods development kit (Beckman Coulter). One quarter GC-rich sequencing reactions were set up containing 10-100 ng DNA, 4 pmol primer, 2 μ l 10X reaction buffer, 1 μ l dNTP(G) mix, 2 μ l ddUTP dye terminator, 3 μ l ddGTP dye terminator, 2 μ l ddCTP dye terminator, 2 μ l ddATP dye terminator, 1 μ l DNA polymerase and sterile water to 20 μ l. This kit contains all of the reagents found in the standard sequencing kit with the exception of the dNTP solution. In a standard sequencing reaction, dNTP(I) mix is used, whereas dNTP(G) mix is used to sequence through difficult GC-rich regions. Thermal cycle sequencing conditions were:

96°C / 20 secs	}	x 30 cycles (dITP standard sequencing)
50°C / 20 secs		
60°C / 4 mins		

96°C / 20 secs	}	x 30 cycles (dGTP difficult sequencing)
50-68°C / 20 secs		
68-72°C / 2 mins		

Custom primers were used to sequence PCR products, with vector primers used to sequence clones (sequences in the Appendix).

2.4.10.2 Ethanol precipitation of products

Reactions were terminated using 5 µl stop solution consisting of 2 µl of 100 mM EDTA, 2 µl of 3 M sodium acetate (pH 5.2), and 1 µl glycogen. To each reaction, 60 µl of ice-cold 95% ethanol was then added and vortexed thoroughly. Precipitated DNA was pelleted by centrifugation at 1690 x g for 15 min at 4°C. After decanting the supernatant, pellets were washed twice with 200 µl ice cold 70% ethanol and centrifuged after each wash at 1690 x g for 5 min 4°C. Pellets were air-dried for 30 min and resuspended in 40 µl sample loading solution (SLS). After waiting 1 min to allow the SLS to become absorbed, samples were vortexed thoroughly. Finally, reactions were overlaid with a drop of mineral oil. Analysis was carried out immediately using a CEQ8000 sequencer or samples were frozen at -20°C and analysed later.

2.4.11 Chicken BAC library screening

In order to uncover the genomic location of novel chIL-1 genes, four high-density BAC filters representing the Red Jungle Fowl genome sequence (CHORI-261 chicken BAC library) were acquired from the Children's Hospital Oakland Research Institute (CHORI), California, USA. The library was constructed from Red Jungle Fowl genomic DNA. High molecular weight DNA fragments were digested with *EcoRI* endonuclease, modified with *EcoRI* methyltransferase and directionally cloned into pTARBAC2.1. Transformation was carried out by electroporating DH10B cells. Each BAC filter contains 18432 different BAC clones taken from 48 microtitre plates and each spotted in duplicate.

2.4.11.1 Pre-hybridisation

Chicken BAC filters were moistened with pre-hybridisation solution (200 µg per ml DNA in 10X SSC, 10X Denhardt's solution) (Sigma). Each filter was then rolled between two thin plastic meshes and placed in a glass roller bottle. A further 10 ml pre-hybridisation solution was added to each bottle and incubated overnight at 65°C in a hybridisation oven. Tubes were arranged symmetrically in a rotating rotisserie wheel to allow the filters to unwind. Pre-hybridisation solution contents are listed in Appendix III.

2.4.11.2 Synthesising a radio-labelled DNA probe

Using the random-primed DNA labelling kit (Roche), radio-labelled DNA probes were generated for BAC filter hybridisation. The theory behind this method is as follows: random hexanucleotide primers, present in all possible sequence combinations, anneal to denatured template DNA. This ensures templates are labelled equally along their entire length. Complementary strand synthesis then takes place from the 3' end of the hybridised primers using Klenow. During this synthesis, deoxycytidine triphosphate (dCTP) modified with ³²P becomes incorporated into the newly formed complementary strand.

Probe templates were generated by PCR amplification of genomic DNA or restriction digestion to release cDNA clones from a vector. They were then purified using the Qiaquick PCR purification kit. Templates were quantified by spectrophotometry, as described in section 2.4.3, and for each probe ≥25 ng DNA was denatured for 10 min at 99°C and then chilled on ice. This step created single-stranded DNA molecules.

To a 500 µl eppendorf tube on ice, the following were then added: 6 µl dATP, dGTP and dTTP (by mixing 2 µl of each of solutions 2, 4 and 5), 4 µl reaction mixture (solution 6; hexanucleotide primer mix in 10X reaction buffer), 18 µl denatured DNA, 2 µl Klenow enzyme (1 U/µl; solution 7) and 10 µl $\alpha^{32}\text{P}$ -dCTP (7.40 MBq). The reaction was incubated for 30 min at 37°C. The DNA was then denatured and the reaction stopped by incubating for 10 min at 95°C.

2.4.11.3 Hybridisation and washing

One quarter (10 µl) of the radio-labelled probe reaction mix was added to each of the four roller bottles containing CHORI-261 BAC filters 1-4, respectively. Bottles were incubated overnight at 65°C with rotation to facilitate hybridisation. Three washes with increasing stringency were performed following hybridisation. This was done to limit the amount of background radiation from unincorporated probe. Wash buffers were pre-warmed to 65°C and used to wash the filters as follows: wash 1: 2X SSC, 0.1% SDS; wash 2: 1X SSC, 0.1% SDS; and wash 3: 0.1X SSC, 0.1% SDS. Each wash was carried out at 65°C for 30 min. BAC filters were then removed from their roller bottles, sealed in plastic bags and placed in exposure cassettes containing two intensifying screens. Sealed filters were each overlaid with a single sheet of BioMax™ MR film (Kodak) before cassettes were transferred to -80°C for overnight exposure. Films were developed after 24 h using an X-ograph compact X4 automatic processor.

2.4.11.4 Identification of positive clones

Each BAC filter contains a total of 18432 distinct clones spotted in duplicate. Each filter was divided into 6 large panels and within each panel, a total of 384 boxes

(24 x 16) were present. Within each individual box there were a total of 8 clones spotted in duplicate. Hence 16 (spots) x 384 (boxes) x 6 (panels) = 36864 spots (18432 clones in duplicate) per filter. Each panel on any individual filter contained clones from 8 plates; hence 48 microtitre plates were represented on each filter. So for filter 1, plate #1 is spotted in panel 1, plate #2 is spotted in panel 2, plate #7 is spotted in panel 1 etc...up to plate #48 being spotted in panel 6. This pattern was maintained in the other 3 filters; for example, plate #49 is spotted in filter 2, panel 1, etc. To be able to interpret positive signals, a plastic overlay representing the gridded template described above was placed against a filter autoradiograph, using the label position for correct orientation. A positive hybridisation was denoted by a double spot within an individual box as each clone is spotted in duplicate within the same box. The relative orientation of positive duplicate spots in a box determined the range of plates where the clone came from. Combined with the panel and filter numbers, the exact plate could be identified. As each panel row is labelled 1-24, and column labelled A-P, the well coordinates of a positive clone could be determined. The exact identity of a positive clone was therefore established using the notation: plate number, column letter, and row number, e.g. clone 132E6. Positive clone ID's were submitted to CHORI, who supplied the clones in the form of bacterial cells on an agar plug. BAC DNA was purified as described in section 2.4.9.4.

2.4.12 Cell culture

2.4.12.1 Resurrecting cryopreserved cell lines

Cells were removed from liquid nitrogen and rapidly thawed in a 37°C water bath. They were then resuspended in 10 ml warm (37°C) growth medium and pelleted

by centrifugation at 216 x g for 5 min. After discarding the supernatant, cell pellets were washed in another 10 ml growth medium and centrifuged as before. Cells were then seeded at $1 \times 10^6/25 \text{ cm}^2$ flask in 5 ml growth medium, with cell densities scaled up accordingly for larger flasks. HD11 cells were routinely cultured in growth medium (contents listed in the appendix) at 41°C, 5% CO₂, whilst COS-7 cells were cultured in a different growth medium (contents listed in Appendix IV) at 37°C, 5% CO₂.

2.4.12.2 Passaging cells

Both HD11 and COS-7 cell lines were adherent and typically passaged every 2-3 days once flasks had become confluent. To passage cells, they were first washed with 2 x 10 ml warm PBS followed by a 1 in 10 solution of 0.25% trypsin/versene. For a 25 cm² flask, 5 ml trypsin/versene were added, with volumes scaled up for larger flasks. Trypsinisation detached adherent cells during a 4-5 min incubation at 37°C, after which trypsin was neutralised by adding a 2X volume of growth medium. Cells were pelleted by centrifugation at 216 x g for 5 min, supernatants discarded, and cells resuspended in 10 ml warm growth medium. Cell viability was determined using a 0.4% w/v solution of trypan blue, which is excluded by live cells but taken up by dead ones. A 20 µl aliquot of cell suspension was diluted 1 in 2 with trypan blue and cells were counted using a haemocytometer. Cells were reseeded at $1 \times 10^6/25 \text{ cm}^2$ flask in 5 ml growth medium.

2.4.12.3 Transfecting cells with pure chicken DNA

2.4.12.3.1 Transient protein expression in COS-7 cells

COS-7 cells were transiently transfected with chicken cDNA clones by the

DEAE/dextran method. The theory behind this method is as follows: DEAE/dextran is a positively charged polymer that binds to negatively charged DNA very tightly. This creates a DNA:polymer complex with an overall net positive charge. As cell membranes are negatively charged, this enables the complex to come into close contact with cell membranes facilitating uptake by endocytosis. DNA that has been taken up resides in endosomes that are capable of being acidified. This would lead to degradation of the DNA and therefore chloroquine is added to the transfection reagent to prevent this from happening.

To transfect, COS-7 cells were trypsinised, counted and re-seeded at 6×10^6 cells/75 cm² flask. Cells were then cultured for 18-24 h at 37°C, 5% CO₂. For each separate cDNA, a transfection mix for a 75 cm² flask was made containing: 15 ml serum-free medium, 112.5 µg DNA, 258 µg/ml chloroquine and 600 µg/ml DEAE/dextran. Cells were washed with 2 x 10 ml warm PBS followed by the addition of the transfection mix. Cells were incubated for 3 h at 37°C, 5% CO₂ to facilitate DNA uptake. The transfection mix was discarded and cells were washed with another 10 ml warm PBS. Next, a solution of PBS containing 10% DMSO was added for 2 min to shock the cells, increasing the efficiency of the transfection. The PBS/DMSO was then discarded and replaced with 15 ml growth medium. After incubating the cells for 16-24 h at 37°C, 5% CO₂, growth medium was changed for serum-free medium. Cell supernatants were harvested 72 h later. Some recombinant cytokines were not secreted and remained intracellular. Where this was suspected, COS-7 cells were trypsinised, resuspended in serum-free medium and frozen at -80°C. Cell lysates containing recombinant cytokines were generated by 3 repeated freeze-thaw cycles.

2.4.12.3.2 HEK293T cells

HEK293T cells were transiently transfected with chicken cDNA clones by the method of Aricescu, Lu et al. (2006) using polyethylenimine (PEI) transfection reagent. PEI, like DEAE/dextran, is also a cationic polymer so initiates transfection by the same method. It is also believed to buffer the endosomal pH, preventing acidification thus abrogating the need for chloroquine. HEK293T cells were routinely cultured in growth medium (contents listed in Appendix IV) at 37°C, 5% CO₂ and seeded at 90% confluence in 150 cm² flasks. For transfection, 50 µg pure plasmid DNA were added to 5 ml serum-free medium and mixed (scalable as necessary). Next, 75 µl of 1 mg/ml PEI were added, briefly mixed by inversion then incubated at room temperature for 10 min to permit DNA-PEI association. During this incubation, HEK293T growth medium was changed for 2% serum-containing growth medium. The DNA-PEI containing medium was added to the cells to finish. After 3 days, culture supernatants were harvested and replaced with fresh 2% serum-containing growth medium. This second batch of conditioned medium was harvested another 3 days later.

2.4.13 Purification of HIS-tagged recombinant proteins

2.4.13.1 Under native conditions

Crude HEK293T cell supernatants were concentrated in a stirred ultrafiltration cell using YM10 ultrafiltration membranes (NMWL: 10000) (both Millipore) followed by a buffer exchange with PBS. Concentrated proteins were purified under native conditions using 1.25 ml HIS-Select® high flow columns (Sigma). To purify, a column was mounted on a clamp stand and solutions were passed through at 1 ml/min using an EP-1 Econo Pump (Bio-rad). A modified version of the manufacturer's instructions was

followed as described. The storage solution was first removed using 10 ml sterile water. Next, the column was equilibrated with 10 ml wash buffer (20 mM imidazole in 0.3 M sodium chloride and 50 mM sodium phosphate at pH 8.0). Concentrated protein was then applied to the column followed by 10 ml of the same wash buffer to remove unbound proteins and impurities. The column was washed with increased stringency using 10 ml of a second wash buffer (30 mM imidazole in 0.3 M sodium chloride and 50 mM sodium phosphate at pH 8.0). Finally, pure proteins were eluted using 10 ml of elution buffer (250 mM imidazole in 0.3 M sodium chloride and 50 mM sodium phosphate at pH 8.0). All eluted fractions were saved for analysis.

2.4.13.2 Under denaturing conditions

The procedure was identical to purification under native conditions except for the following differences. Crude HEK293T cell supernatants were concentrated and buffer exchanged as above then solubilised using 8 M urea. Column equilibration and washes were carried out with a single denaturing wash buffer (0.1 M sodium phosphate at pH 8.0 with 8 M urea). Pure proteins were eluted using a denaturing elution buffer (250 mM imidazole in 0.1 M sodium phosphate at pH 8.0 with 8 M urea). Proteins were then refolded by stepwise dialysis against PBS for 24 h. Samples were dialysed to remove urea and imidazole using Slide-A-Lyzer G2 Dialysis Cassettes (10K MWCO) (Thermo Scientific).

2.4.14 Analysis of HIS-tagged recombinant proteins

2.4.14.1 SDS-polyacrylamide gel electrophoresis (SDS-PAGE)

SDS-PAGE analysis of pure recombinant proteins was carried out using a Mini-

PROTEAN® II electrophoresis cell (Bio-rad). To prepare the samples, 15 µl of protein were mixed with an equal volume of SDS-PAGE sample buffer (contents in the appendix) then denatured at 95°C for 5 min before being placed on ice. During the incubation step, a precast Tris-HCl Ready Gel, 4-15% (Bio-rad) was fitted into the clamp assembly and placed into the electrophoresis cell. Running buffer containing 25 mM Tris, 192 mM glycine and 0.1% SDS was added to the cell. Samples were loaded alongside a 6xHIS protein ladder (Qiagen) and electrophoresed at 150 V for 45 min.

2.4.14.2 Western blotting

Following electrophoresis, proteins were electroblotted onto a piece of Hybond ECL nitrocellulose membrane (Amersham) using a Mini Trans-Blot electrophoretic transfer cell (Bio-Rad). The SDS-PAGE gel was placed against the nitrocellulose membrane then sandwiched between double layers of 3 MM filter paper (Whatman), pre-soaked with transfer buffer. This assembly was sandwiched between pre-soaked fibre pads and secured in the gel holder cassette. The cassette was secured in the electrode module and placed in the buffer tank with the nitrocellulose membrane closest to the anode. Chilled transfer buffer containing 25 mM Tris.HCl, 192 mM glycine and 25% methanol was added to fill the tank. Electrophoresis was carried out at a constant 250 mA for 45 min. Proteins were then detected using the QIAexpress system (Qiagen) following the manufacturer's protocol. All incubations were performed at room temperature with shaking. After removal from the transfer cell, the membrane was washed twice with TBS buffer (see Appendix III) for 10 min each time. The membrane was then blocked for 1 h in blocking buffer (3% BSA (w/v) in TBS buffer). Two 10 min washes in TBS-Tween/Triton buffer (see Appendix III) were next followed by a 10 min wash in TBS. The membrane was then incubated for 1 h in a 1/2000 dilution of Penta-

HIS antibody (BSA-free; Qiagen) in blocking buffer. Two further 10 min washes in TBS-Tween/Triton buffer were next followed by another 10 min wash in TBS to remove unbound antibody. A secondary antibody (rabbit anti-mouse IgG conjugated to horseradish peroxidase (HRP); DAKO) was diluted 1/1000 in a solution of 10% non-fat dried milk in TBS. The membrane was then incubated in this antibody solution for 1 h followed by four further 10 min washes in TBS-Tween/Triton buffer. Proteins were detected by enhanced chemiluminescence using ECL™ Western Blotting Detection Reagents and Hyperfilm ECL (both Amersham). The HRP conjugated to the secondary antibody catalyses the oxidation of luminol, which becomes oxidised further by hydrogen peroxide and a chemical enhancer. This creates triplet carbonyl groups which decay to form single carbonyl groups that emit light. The membrane was covered with equal volumes of Detection Reagents solutions 1 and 2, incubated for 1 min and the excess drained off. After covering it in plastic wrap (Saran), the membrane was overlaid with a single sheet of Hyperfilm ECL and exposed for 30 s to 10 min at room temperature. The film was developed using an X-ograph compact X4 automatic processor.

2.4.15 HD11 bioassay

2.4.15.1 Pilot study

A pilot experiment was set up to determine the responsiveness of the HD11 cell line to recombinant mature chicken IL-1 β as described in Weining, Sick et al. (1998). Serial dilutions of recombinant mature chicken IL-1 β (kindly provided by Dr Benjamin Schusser, University of Munich, Germany) were pre-incubated for 2 h at 41°C with or without 30 μ l of anti-IL-1 β antibody (kindly provided by Dr Benjamin Schusser). HD11

cells were routinely cultured in growth medium at 41°C, 5% CO₂ as described in section 2.4.12.1 and then passaged and counted as outlined in section 2.4.12.2. Cells were reseeded at 1×10^6 /well in 1 ml growth medium in flat-bottomed 24-well culture plates. Cells were then cultured for 12-48 h at 41°C, 5% CO₂ in the presence of either serial dilutions of recombinant mature chicken IL-1 β pre-incubated with or without anti-IL-1 β antibody or media only. After 12-48 h, three 100 μ l aliquots of cell supernatant/well were harvested. The rest of the supernatant was discarded, cells were washed twice with warm PBS and trypsinised as outlined in section 2.4.12.2. Cells were pelleted by centrifugation at 1040 x g for 5 min and total RNA was extracted using the RNeasy mini kit (Qiagen).

2.4.15.2 Quantifying the biological response

2.4.15.2.1 Griess assay

Culture supernatants were harvested for the measurement of nitrite (NO₂⁻), the stable derivative product of nitric oxide (NO) breakdown, by the Griess reaction. Samples to create a standard curve were prepared by making a 1:200 dilution of 6.9 mg/ml NaNO₂ then double-diluting the stock a further 6 times. To a 96-well sterile culture plate, 100 μ l of six standard dilutions, alongside eighteen 100 μ l (i.e. one 24-well plate row (6 wells) of triplicate 100 μ l aliquots) aliquots of culture supernatant per individual treatment group were added. Griess reagent was prepared by mixing equal volumes of NED (Naphthylethylenediamine, 0.3 g/100 ml in 2.5% H₃PO₄) and sulphanilamide (1 g/100 ml in 2.5% H₃PO₄) reagents (both from Sigma) then adding 100 μ l to each well to be tested. Absorbance was measured after 5 min at 543 nm using a Biotek Elx 808 spectrophotometer (Biotek, Winooski, Vermont, USA).

2.4.15.3 Optimised bioassay conditions

2.4.15.3.1 Optimising the [pure rIL-1 β]

A preliminary assay was carried out to establish the optimal concentration of recombinant (mature) chicken IL-1 β (rchIL-1 β) (AMSBio, Abingdon, UK) to use in subsequent bioassays. To do this, HD11 cells were routinely cultured in growth medium at 41°C, 5% CO₂ as described in section 2.4.12.1 and then passaged and counted as in section 2.4.12.2. Cells were reseeded at 1 x 10⁶/well in 1 ml growth medium in flat-bottomed 24-well culture plates. Cells were then cultured for 12 h at 41°C, 5% CO₂ in the presence of a serial two-fold dilution of pure rchIL-1 β at a starting concentration of 166.6 ng/ml. Cell supernatant was assayed (in triplicate) for nitrite (NO₂⁻) using the Griess assay, as before.

2.4.15.3.2 Final bioassay conditions

To determine the antagonistic properties of recombinant chIL-1RN, bioassays were set up as follows: 1x10⁶ HD11 cells/well were seeded in flat-bottomed 24-well culture plates in 250 μ l medium with or without 500 μ l serial two-fold dilutions of ex-COS rIL-1RN (crude cell supernatant or cell lysate), purified rsIL-1RN or ricIL-1RN, ex-COS pCI-Neo (mock-transfected negative control) or media alone. To create the starting dilutions of pure chIL-1RNs, 500 μ l aliquots of both were concentrated to 30 μ l by centrifugation at 14000 x g for 15 min at 4°C using Amicon Ultra-0.5 centrifugal filters (Millipore). Starting dilutions were made by adding 15 μ l of concentrated protein to 985 μ l of growth media. After 4 h incubation at 41°C, 5% CO₂, 250 μ l of 40 ng/ml pure rIL-1 β (AMSBio) were added to all wells (except for 1 row of cells in media alone), followed by a further incubation for 12 h.

Cell supernatant was assayed (in triplicate) for nitrite (NO_2^-) using the Griess assay, as before. Cells were harvested, RNA extracted and IL-1 β , iNOS and 28S expression quantified by qRT-PCR (TaqMan®) as before.

2.4.16 HD11 time course stimulation assay

To determine the expression of chIL-1RN over a time course, HD11 cells were seeded in 25 cm² flasks at 2×10^6 in 5 ml growth medium, then stimulated for 0 (baseline control), 1, 2, 6, 12, 24 and 48 h with 200 ng/ μl LPS (Sigma) at 41°C, 5% CO₂. At each time-point, culture supernatant was discarded; cells were washed twice with warm PBS and lysed with 1.8 ml buffer RLT (Qiagen). Total RNA was extracted from cell lysates using the RNeasy mini kit (Qiagen). IL-1RN, IL-1 β and 28S mRNA levels were quantified by real-time quantitative RT-PCR (TaqMan®) as described in section 2.4.4.6. Results were standardized and calculated as previously.

2.4.17 Statistics

Statistical analyses were carried out using the Mann-Whitney U test within the Graphpad Prism software package. Tests were performed between different treatment groups within the HD11 bioassay. Within the gene expression analyses, tests were performed between groups of birds of different infection status. Statistical significance was determined with a P value ≤ 0.05 .

Chapter 3

Results 1: Analysis of the extent of the IL-1 family in chickens

3.1 Introduction

Cytokines are protein molecules produced by and able to act upon almost every cell in the body. They have an exceptionally broad repertoire of functions that influence numerous biological processes. Although widely acting, research into their function has been largely centred on their immune-related effects. Interleukins, a major subgroup of cytokines, were initially discovered and named according to their described production by and influence upon leukocytes. The first interleukin, IL-1, was described as a fever-inducing cytokine with multiple pro-inflammatory biological effects. Subsequent advances in molecular biology have led to the identification of genes for a further ten IL-1 family cytokines. All eleven ligands are structurally related; some have overlapping complementary functions, and others act to specifically antagonise these functions. The functional effects of the IL-1 ligands are mediated via a large group of IL-1 receptors and co-receptors that are characterised by a conserved intracellular Toll/IL-1R (TIR) domain. Novel IL-1 genes were originally discovered in humans and mice; however, annotation of latterly available mammalian genomes has identified most of these IL-1 ligands and receptors in other mammals. Some of these IL-1 genes in other mammals have been cloned, but most were identified *in silico*. Nine of these IL-1 genes are located in a cluster which is highly conserved across most mammalian species, except for mice, where *il-1f7* is absent and *il-1 α* and *il-1 β* genes are separated from the other six genes (Nicklin, Barton et al. 2002; Taylor, Renshaw et al. 2002). Similarly, over half of the IL-1 receptor genes are located at a single locus (Dale and Nicklin 1999). Due to a paucity of genomic and sequence resources, the extent of the IL-1 gene family in non-mammalian species is only beginning to become apparent. In birds, an IL-1 β gene was discovered in the chicken several years ago (Weining, Sick et

al. 1998); however, other avian orthologues were not found until more recently. The coding region of IL-1 β has now been cloned in duck, goose, turkey and pigeon (Wu, Liu et al. 2007). An IL-1 β orthologue has been found in several species of fish (Secombes, Wang et al. 2011), some of which encode more than one gene. IL-1 β has also been cloned in the African clawed frog (Zou, Bird et al. 2000).

Only one other IL-1 family ligand, IL-18, has been found in multiple non-mammalian species. The chicken IL-18 gene (Schneider, Puehler et al. 2000) was the first avian orthologue found, closely followed by turkey (Kaiser 2002). A partial IL-18 CDS has also been identified in the duck (Kaiser 2002). Compared with IL-1 β , fewer fish possess an identifiable IL-18 gene as only *Fugu* (Huising, Stet et al. 2004) and rainbow trout (Zou, Bird et al. 2004) orthologues have been cloned.

In addition to IL-1 β and IL-18, mammals possess up to a further nine IL-1 ligand genes. These genes have so far not been found in the chicken or in other non-mammalian species. The exception to this trend is in the rainbow trout where a novel IL-1F gene has been recently identified (Wang, Bird et al. 2009). Biologically, it functions as a receptor antagonist, although its gene structure, nt and aa sequences and overall size are markedly different from any of the mammalian IL-1RN genes. To date, a total of eight IL-1 receptors and three IL-1 co-receptors have been cloned in mammals. In the human genome, six of these reside in a cluster on chromosome 2 with the rest at discrete loci on different chromosomes. In the chicken, only two IL-1 receptors, chIL-1RI (Guida, Heguy et al. 1992) and chST2 (Iwahana, Hayakawa et al. 2004), have been cloned to date. Expression analysis of a further chIL-1R, SIGIRR/TIR8 (Riva, Polentarutti et al. 2009) has been carried out, although the cDNA was not cloned. Partial ESTs for the chicken IL-18R α , IL-1RAcP and TIGIRR-1 receptors have also been identified (Huising, Stet et al. 2004). In at least one species of

fish, the genes for the IL-1RI, IL-1RII, ST2 and IL-18R β receptors have been identified (Huising, Stet et al. 2004) so far.

Although fewer IL-1 family genes have been cloned in the chicken compared to mammals, there are clear discrepancies between the ligand and receptor genes found. For instance, a chIL-18 gene has been cloned, but the IL-18RAcP (IL-18 β) gene has not. Similarly, the chST2 cDNA has been isolated, but a gene for its ligand, IL-33, has yet to be identified.

In this Chapter the full extent of the IL-1 gene family in the most up-to-date assembled version (v2.1) of the chicken genome is described. Using a conserved synteny approach, several chIL-1 family receptor genes which have never been described in the literature were identified.

3.2 Methods

The ENSEMBL genome browser was initially screened using the search terms “IL-1” and “IL-18”. For all members of the human IL-1 family not identified in the chicken using that method, the full nt and aa sequences as well as the aa signature motif were used in BLAST searches. For the human IL-1 family genes which remained absent in the chicken, conserved synteny between their locations in the human genome and possible locations in the chicken were examined.

3.3 Results

3.3.1 IL-1 ligand genes in the chicken

The human IL-1 family consists of 11 ligand genes. To ascertain the extent of the chicken IL-1 ligand gene family, a search of the ENSEMBL chicken genome browser (v2.1) using the term “IL-1” was carried out. This identified the gene for chicken IL-1 β , located on chromosome 22, but did not provide evidence of any other ligand genes. The existence of this gene was already established (Weining, Sick et al. 1998). However, this search suggested a different genomic location to that given in previous reports. The gene was initially mapped to chromosome 2 (Kaiser, Rothwell et al. 2004), then reassigned to chromosome 4 in the 2006 release (v2.0) of the genome sequence (Kaiser 2007). In the v2.1 assembly, a limited degree of conserved synteny exists between the locus containing chicken IL-1 β and the human IL-1 gene cluster on chromosome 2. The human orthologues of two genes (SLC20A1 and CKAP2L) which flank the chIL-1 β gene are located adjacent to the huIL-1 gene locus (Figure 3.1). Neither of the previous attempts to map the chIL-1 β gene identified syntenic genes conserved with the human IL-1 locus. Whereas the huIL-1 gene cluster contains a further eight IL-1 ligand genes, these are all absent at the chicken locus. To determine if the avian orthologues of these other eight huIL-1 genes are located elsewhere in the chicken genome, TBLASTN searches of the chicken genome (v2.1) were carried out using full length and IL-1 family signature motif amino acid sequences. These did not identify any other chIL-1 genes.

The human genome contains genes for two other IL-1 ligands, IL-18 and IL-33, which are located on chromosomes 11 and 9, respectively. Searching the chicken genome in ENSEMBL with “IL-18” identified the only other known (Schneider,

Puehler et al. 2000) chicken ligand gene, IL-18, in this family on chicken chromosome 24 (location previously unknown). The amount of conserved synteny between the chicken and human IL-18 gene loci was examined and found to be substantial. A total of twelve genes including IL-18 are syntenically conserved at these loci.

Searching the chicken genome with “IL33” did not return any results. Similarly, a TBLASTN search of the chicken genome with the huIL-33 amino acid sequence did not return any significant results. The “multi-species view” tool in ENSEMBL showed that the huIL-33 gene is located in a region of the genome which lacks conserved synteny with any region of the chicken genome.

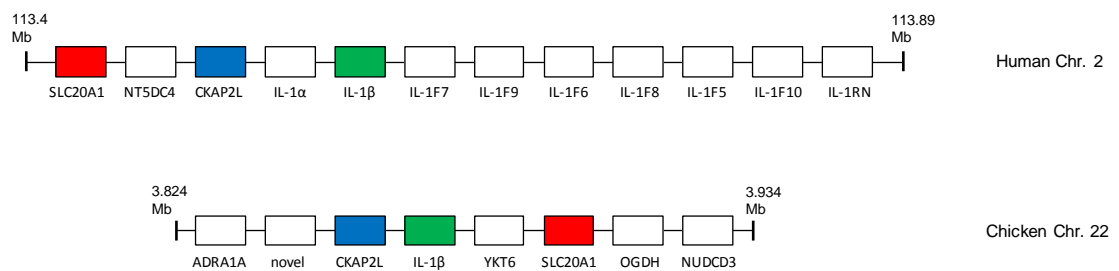


Figure 3.1 Schematic depicting an IL-1 gene family locus conserved between humans and chickens. A limited degree of conserved synteny exists between these two species at this region. The human locus on chromosome 2 contains nine IL-1 family genes, whereas only a single IL-1 family gene, IL-1 β , is found on chicken chromosome 22. Previous attempts to map the chIL-1 β gene did not identify the flanking genes SLC20A1 and CKAP2L present at both loci.

3.3.2 IL-1 receptor genes in the chicken

The human IL-1 family consists of eight receptor and three co-receptor genes. A search of the chicken genome (v2.1) in ENSEMBL with the term “IL-1” identified three

receptor genes present on chromosome 1: IL-1RI, IL-1RII and IL-1RL2. Searching with “IL-18” identified the IL-18R α gene at the same locus on chicken chromosome 1. In humans, IL-1RII, IL-1RI, IL-1RL2, ST2, IL-18R α and IL-18R β genes lie in a cluster on chromosome 2 in that order. Further examination of the chicken locus showed that this IL-1R gene cluster is fully conserved in the chicken on chromosome 1 (1: 137,942,100-138,163,150) (Figure 3.2). Previous studies reported the identification and cloning of the chIL-1RI (Guida, Heguy et al. 1992) and chST2 (Iwahana, Hayakawa et al. 2004) genes; however, neither provided a genomic location. A partial IL-18R α EST had already been identified (Huisling, Stet et al. 2004). Chicken orthologues of IL-1RII and IL-18R β have never been described.

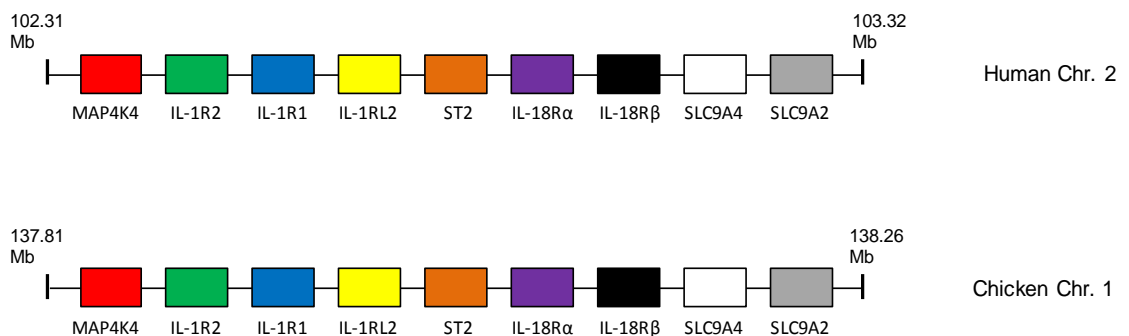


Figure 3.2 Schematic depicting an IL-1 receptor gene family locus conserved between humans and chickens. Complete conserved syntenicity exists between these two species at this region.

As the other members of the huIL-1R family reside elsewhere in the genome, conserved syntenicity between the two species was used to identify the remaining chIL-1R genes. The chicken gene for SIGIRR/TIR8 was found on chromosome 5, at a locus which is highly conserved with the SIGIRR/TIR8 locus on human chromosome 11. The chicken SIGIRR/TIR8 gene was identified following genome annotation by

ENSEMBL, but has never been cloned *in vitro*. Despite this, its global expression in the chicken has been analysed (Riva, Polentarutti et al. 2009). Full length chicken cDNAs of two other IL-1R (TIGIRR1, TIGIRR2) and two IL-1 co-receptors (IL-1RAcP and TILRR), present in humans, have never been isolated. Conserved synteny was used to identify these genes in the chicken. They were dispersed across the genome, as they are in humans. Human TIGIRR1/IL-1RAPL2, found on human chromosome X, has a chicken orthologue on chromosome 4 (4: 17,149,659-17,318,676). A partial chTIGIRR-1 EST had been previously identified (Huisling, Stet et al. 2004). Human TIGIRR2/IL-1RAPL1, which is also found on chromosome X, has an orthologue in the chicken genome on chromosome 1 (1: 119,540,327-120,167,775). Human IL-1RAcP is found on chromosome 3 at a locus syntenic with a region of chicken chromosome 9 which contains the chIL-1RAcP gene (9: 14,947,157-14,967,542). A partial chIL-1RAcP EST had been previously identified (Huisling, Stet et al. 2004). TILRR, a novel IL-1RI co-receptor recently discovered in human and mouse genomes, also has a chicken orthologue. The human gene lies on chromosome 9, with the chicken gene present on chromosome Z (Z: 31,415,596-31,473,831). An overview of the IL-1 receptor gene family in the human and chicken genomes is provided in Table 3.1.

Finally, a gene encoding the IL-18 binding protein (IL-18BP), a soluble protein which binds IL-18 to regulate its activity, is present on human chromosome 11. When conserved synteny with the chicken genome was examined, orthologues of three genes (NUMA1, RNF121 and XRCC1) which immediately flank the huIL-18BP gene were identified at a conserved locus on chicken chromosome 1. Between NUMA1 and XRCC1, where the chIL-18BP gene would be expected to be found is a large sequence gap spanning 2342 bp (Figure 3.3). The chIL-18BP gene may be present in this gap.

Human		Chicken		
Gene	Genomic location	Gene	Genomic location	cDNA clone
IL-1RII	2: 102,608,306-102,645,006	IL-1RII	1: 137,942,627-137,952,233	
IL-1RI	2: 102,681,004-102,796,334	IL-1RI	1: 138,002,937-138,026,152	Guida (1992)
IL-1RL2	2: 102,803,433-102,856,462	IL-1RL2	1: 138,039,834-138,053,899	
ST2	2: 102,927,962-102,968,497	ST2	1: 138,087,256-138,111,381	Iwahana (2004)
IL-18R α	2: 102,927,989-103,015,218	IL-18R α	1: 138,122,441-138,139,234	
IL-18R β	2: 103,035,149-103,069,025	IL-18R β	1: 138,147,956-138,161,221	
SIGIRR	11: 405,716-417,455	SIGIRR	5: 1,574,130-1,578,868	
TIGIRR1	X: 103,810,996-105,012,102	TIGIRR1	4: 17,149,659-17,318,676	
TIGIRR2	X: 28,605,516-29,974,840	TIGIRR2	1: 119,540,327-120,167,775	
IL-1RAcP	3: 190,231,840-190,375,843	IL-1RAcP	9: 14,947,157-14,967,542	
TILRR	9: 14,734,664-14,910,993	TILRR	Z: 31,415,596-31,473,831	

Table 3.1 The IL-1 receptor gene family in humans and chickens. Six members of the family are found at a locus with conserved synteny between human and chicken.

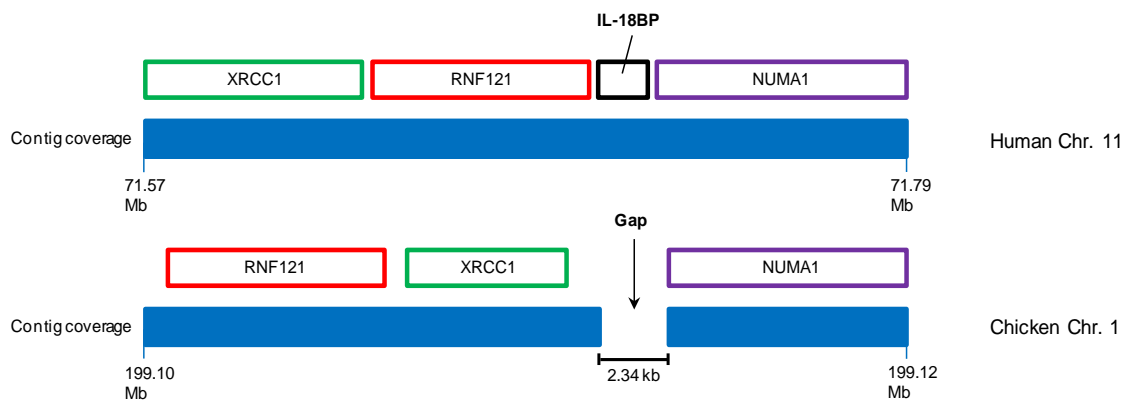


Figure 3.3 Schematic depicting the IL-18BP locus in humans and a region of the chicken genome with which it shares limited conserved synteny. Chicken chromosome 1 contains a large sequence gap where the chicken orthologue of IL-18BP may reside. The blue bars depict contig coverage in that part of the chromosome whilst the locations of the genes along the contig are indicated immediately above.

3.4 Discussion

To date, only two chIL-1 ligand cDNAs have been cloned: IL-1 β and IL-18. BLAST searches with the chIL-1 β and huIL-1F1-F11 sequences showed that no further members of IL-1 ligand family are present in v2.1 of the genome assembly. Examining conserved synteny between human and chicken chromosomes showed the nine IL-1 gene human cluster is represented by only a single chicken IL-1 gene, IL-1 β , at the equivalent chicken locus. In both the rainbow trout and puffer fish, a similar conserved locus encoding only IL-1 β exists. Both these fish also contain a gene encoding an IL-1RN-like protein, nIL-1F. These two genes are found at divergent loci in the two fish, on chromosomes 5 and 12, respectively. No other IL-1 genes are present at either locus in these fish. If the chicken contains any other IL-1 ligand genes, assuming the assembly of chicken chromosome 22 is correct, they may also lie at different loci, presumably in regions that are poorly assembled. The locus containing chIL-1 β does contain a number of sequence gaps. However, the equivalent locus in the zebra finch has the identical gene content and no sequence gaps.

Examining conserved synteny between the human IL-33 gene locus and the chicken genome did not identify an avian orthologue. Despite this, conserved synteny between large numbers of genes flanking huIL-33 and a region on chicken chromosome Z was evident. When evaluating the exact orthologous pairings between both species, it is clear that a chromosomal breakpoint has occurred and a potential chIL-33 gene has been lost or relocated. Avian orthologues of the two human genes (RANBP1 and TPD52L3) which immediately flank huIL-33 are located on chicken chromosomes 1 and 20, respectively. All other genes flanking this three gene cluster in both directions are completely syntenically conserved between human chromosome 9 and chicken

chromosome Z (Figure 3.4).

In stark contrast to the number of chIL-1 ligand genes, the chIL-1 receptor gene family contains all of the orthologues found in the human genome. Every receptor is located in a region of conserved synteny between both species. Some of the identified chIL-1R genes were assumed to exist because of their essential functional roles. For example, once a chicken IL-18 gene had been identified, it was inevitable the IL-18RacP gene would exist. Likewise, with both IL-1 β and IL-1RI genes already present, it was likely the IL-1RacP gene, essential for IL-1 β function, would be found. It is particularly interesting that the IL-1RL2 and ST2 receptors are found in the chicken. In mammals, IL-1F5, -F6, -F8 and -F9 bind to IL-1RL2, whilst IL-1F11 binds to ST2. This

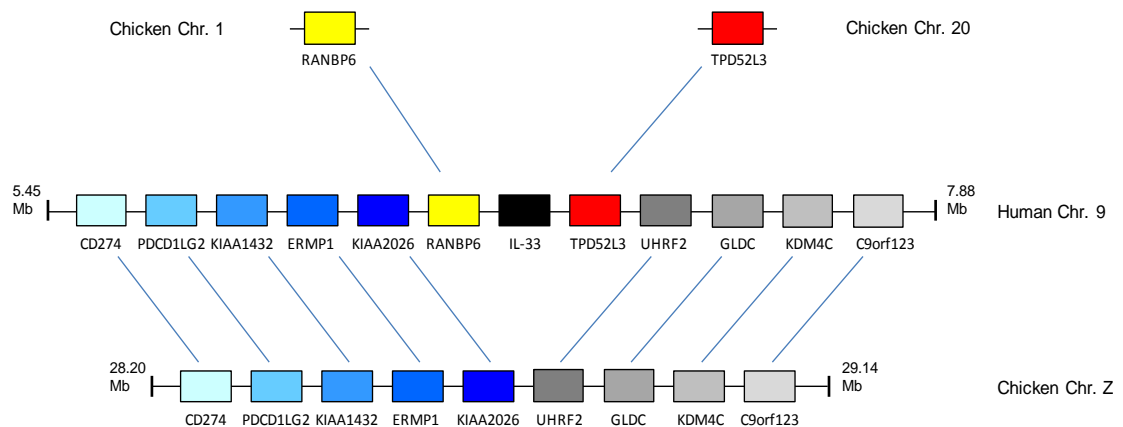


Figure 3.4 Schematic depicting the IL-33 locus in the human genome and a syntenic region of the chicken genome. Although considerable synteny exists at this locus, avian orthologues of two of the genes (RANBP6 and TPD52L3) on human chromosome 9 lie elsewhere in the chicken genome. An *IL-33* gene has yet to be identified in the chicken genome. Pairs of orthologous genes are indicated with lines and have identical shading.

suggests the chicken may also possess genes encoding these IL-1F ligands. It is also interesting to observe that both TIGIRR-1 (IL-1RAPL2) and TIGIRR-2 (IL-1RAPL1) genes are encoded in the chicken. The exact functional roles of these orphan receptors have yet to be comprehensively defined in humans, although IL-1RAPL1 appears to have a role in brain development as mutations in this gene are strongly associated with mental retardation (Pavlowsky, Zanchi et al. 2010). The existence of avian orthologues of both suggests they form part of a fundamental signalling network with important downstream functions.

The fact that all the receptors are present in the chicken but only two of the ligands have been found presents a somewhat paradoxical situation. It is possible that the chicken and human IL-1 ligand genes evolved from a single gene in a common ancestor which became duplicated at a single locus. Both species may have retained all eleven IL-1 genes, with nine of these remaining intact at a single locus in humans. Although the chicken may have retained all eleven genes, intense selective pressures may have led to significant chromosomal rearrangement, scattering the genes in the IL-1 locus across the genome. Should this be true then these genes presumably reside in areas of the genome which are too difficult to sequence with the current methods available. To date, a number of regions of the chicken genome have not been sequenced; in particular, coverage of the microchromosomes is negligible.

Alternatively, the chicken may contain 2-3 separate IL-1 loci (in addition to those identified) each containing several IL-1 genes. In mouse, the nine IL-1 genes clustered on human chromosome 2 are found on two separate loci. Assuming the three IL-1 loci in the human genome constitute regions containing paralogous genes, their inception could be traced to a single ancestral locus which underwent duplication. This primordial locus could have contained 2-3 IL-1 genes, which upon subsequent genome

duplication formed several paralogous IL-1 loci each encoding a copy of these few IL-1 ligand genes. Further duplications in the human genome may have expanded the size of the IL-1 gene family at one locus, whilst the other two loci may have contracted, conceivably leaving only single IL-1 gene loci containing IL-33 and IL-18. In the chicken, two of the loci could have respectively retained only single IL-1F genes, with IL-1 β at one locus and IL-18 at the other. Additional IL-1 loci could have lost these ligand genes, retained others and possibly undergone further duplications. If all nine (or even a few) of these “missing” genes are present in the chicken genome, their distribution would be atypical, compared to what is normally seen when comparisons are made with the human genome. In general, the distribution of the genes in a cytokine family in the human genome is mirrored in the chicken genome. For example, the IL-17 cytokine gene family is dispersed across the genomes of both species (Kaiser 2007). Similarly, the IL-10 family, although not completely conserved in the chicken, has the same pattern of gene distribution as that found in the human genome (Kaiser 2007).

An alternative hypothesis to explain gene absence is that the chicken has lost or is in the process of losing its IL-1 ligand genes and the receptors will also disappear over time. Considering the presumably indispensable functions of the IL-1 family to combat disease and ultimately sustain life, it is difficult to imagine functional redundancy leading to gene loss. Both humans and mice lacking the IL-1RN gene, for example, present with gross inflammatory disorders, which can be fatal in man. In mice overexpressing *il-1f6*, the prevailing inflammatory phenotype is significantly worsened when *il-1f5* is knocked out (Blumberg, Dinh et al. 2007). A further hypothesis is that the chicken has only ever had a limited IL-1 ligand family. Based on the approximate mutational rate of IL-1RN, it has been proposed that IL-1F5 is only found in mammals (Mulero, Nelken et al. 2000). This appears to be unlikely, however, given the presence

Chapter 3: Analysis of the extent of the IL-1 family in chickens

in the chicken genome of the receptor for IL-1F5, -F6, -F8 and -F9 (IL-1RL2).

Chapter 4

Results 2: Identification, cloning and characterisation of chicken interleukin-1 receptor antagonist (IL-1RN)

4.1 Introduction

For decades after its initial discovery in the 1940s, a substance described as “endogenous pyrogen” was known to induce fever when injected into animals. Advances in molecular biology eventually permitted the identification of two ligand genes responsible for these effects. Named IL-1 β (Auron, Webb et al. 1984) and IL-1 α (Lomedico, Gubler et al. 1984), these two agonist ligands were the first described members of the interleukin-1 cytokine family. Around the same time, several reports of a substance shown to inhibit IL-1 were published, prompting much research into its function. After showing its effects were IL-1 receptor-specific (Hannum, Wilcox et al. 1990), its cDNA (Eisenberg, Evans et al. 1990) was cloned and sequenced. Sequence analysis indicated a third IL-1 family gene had been found. Subsequent characterization of its bioactivity (Carter, Deibel et al. 1990) showed it specifically inhibited the actions of IL-1 β and IL-1 α , and was accordingly named IL-1 receptor antagonist (IL-1RN). Further studies confirmed that two major structural variants of this gene, secretory and intracellular, are formed through alternative splicing. Three protein isoforms of the intracellular variant (Haskill, Martin et al. 1991; Muzio, Polentarutti et al. 1995; Malyak, Guthridge et al. 1998) exist whose roles, whilst clearly antagonistic, remain inadequately defined. Since its discovery in humans, IL-1RN orthologues have been identified in 35 other mammalian genomes according to the ENSEMBL genome browser (personal search). However, it has continued to be absent in non-mammalian species, although an IL-1RN-like gene has recently been described in rainbow trout (Wang, Bird et al. 2009). Given the remarkable potency of IL-1 β in immune responses, it is difficult to conceive that any species possessing this gene would lack IL-1RN. As discussed in Chapter 3, examination of conserved synteny between human and chicken

chromosomes suggests that the chicken does not encode any other members of the IL-1 cytokine family at the relevant locus, including IL-1RN. However, we know that birds and mammals have evolved separately for ~310 Mya, and over time this has led to a striking divergence in the number, organisation and architecture of their chromosomes. Conservation of synteny therefore only indicates that the nine gene IL-1 cluster found in humans is absent at the equivalent genomic location in birds, apart from IL-1 β .

Significant progress has been made over the past decade to elucidate the repertoire of immune function genes in the chicken (Kaiser 2010). In particular, knowledge of the number of cytokine genes it possesses has grown rapidly, accelerated by the availability of the genome sequence (Wallis, Aerts et al. 2004). Whilst birds typically possess fewer members of individual cytokine gene families (Kaiser 2010), the essential functional role of IL-1RN made its existence likely in the chicken.

As comparative genomics would be a redundant approach for finding this gene, given its absence at the equivalent locus in the chicken, alternative sources of sequence information needed to be investigated. Around the time of the chicken genome sequence publication, several chicken EST sequencing projects were conducted (Savolainen, Fitzsimmons et al. 2005), providing thousands of novel transcript sequences.

In this Chapter the identification and molecular cloning of chicken IL-1RN is described. The procedure for screening EST databases which led to the identification of several novel chicken IL-1 sequences is also outlined. Further *in silico* characterization showed a number of these chIL-1 ESTs were most similar to the IL-1RN gene found in many other species. Once satisfied that chIL-1RN had been identified, RT-PCR was used to amplify chicken orthologues of the two major structural variants of IL-1RN found in mammals. Analyses of the chIL-1RN gene structure, as well as attempts to

determine its genomic location, were also carried out.

4.2 Methods

A combination of *in silico* and *in vitro* techniques were used to identify and clone a novel cytokine, chicken IL-1RN. General methods were carried out as outlined in Chapter 2. Additional methods and alterations to those described in Chapter 3 are detailed here.

4.2.1 In silico techniques

The NCBI EST database was initially screened as described in Chapter 2, section 2.2.2. This identified three putative chicken cytokine EST sequences from the IL-1 family. These sequences had significant homology with chIL-1 β , but were clearly different. A full length open reading frame cDNA was derived from combining two of these ESTs, which overlapped. Its nucleotide and predicted amino acid sequences were analysed and BLAST was used to confirm its identity as described in Chapter 2, section 2.2.3. Next, this amino acid sequence was used to attempt to uncover further chIL-1 ESTs. An EST with high identity to the query chIL-1RN sequence was identified which had an obviously different 5' end sequence and lacked a start codon. Latterly, a database of novel sequence reads, from efforts to resequence the chicken genome, became available. This database was screened, uncovering the missing start codon from this reciprocally mined EST sequence. Potential promoter regions were analysed with Softberry, a web-based tool which compares submitted promoter sequences with a database of published binding site consensus motifs. Further characterisation of chIL-1RN nucleotide and amino acid sequences was carried out to confirm the identity and

similarity of the chicken protein isoforms to their respective huIL-1RN sequences. Bioinformatics tools described in Chapter 2, section 2.1 were used for this analysis.

4.2.2 In vitro techniques

Using RT-PCR, both cDNA coding sequences were amplified, sequenced and cloned into the pTarget mammalian expression vector. For the RT-PCR, RNA isolated from LPS-stimulated HD11 cells was chosen as the template. HD11 cells were stimulated for 6 h with 200 ng/μl LPS (*E. coli*, Sigma). Sequence-specific primers for icIL-1RN and sIL-1RN (Table I in Appendix II) were designed from EST and Galgal 3.0 sequences. Cycling conditions were as described in Chapter 2, sections 2.4.4.2 (icIL-1RN) and 2.4.4.3 (sIL-1RN), with an annealing temperature of 60°C. HD11 cells are a chicken macrophage cell line (Beug, von Kirchbach et al. 1979), and were selected because monocytes and macrophages are the cells that predominantly express IL-1RN in mammals (Arend, Malyak et al. 1998). Of the many agents that induce mammalian IL-1RN expression, LPS is one of the most potent (Arend, Malyak et al. 1998). In a previous study, LPS activated NF-κB via chicken Toll-like receptor 4 (chTLR4) in HD11 cells (Keestra and van Putten 2008).

PCR amplification of chIL-1RN introns used custom primers designed from the coding sequence and optimised thermal cycling annealing temperatures. Details of both are in Table I in Appendix II.

To determine the genomic location of chIL-1RN, PCR analysis of the locus containing chIL-1β used a specific BAC clone (TAM32-21N6) for the template. This was acquired from the Institute for Plant Genomics & Biotechnology (Texas A&M University, Texas, USA) as a bacterial colony plug. A single colony of *E. coli* was

picked and used to inoculate 5 ml LB medium (containing 12.5 µg/ml chloramphenicol) which was incubated for 8 h at 37°C with shaking. This culture was used to seed 200 ml LB medium (+ 12.5 µg/ml chloramphenicol) followed by incubation at 37°C with shaking for 12 h. BAC DNA was purified from the bacterial cell pellet using the Nucleobond® PC100 kit (Macherey-Nagel) as described in Chapter 2, section 2.4.9.4. PCR amplification of chIL-1β and chIL-1RN used custom primers designed from the coding sequences and optimised thermal cycling annealing temperatures. Details of both are in Table I in Appendix II. An additional experiment to discover the genomic location of chIL-1RN used a ³²P-labelled (random-primed) probe to hybridize against BAC library filters. Four high-density BAC filters representing the complete v2.1 Red Jungle Fowl genome (CHORI-261 chicken BAC library) were acquired from the Children's Hospital Oakland Research Institute (CHORI), California, USA. IL-1RN probe templates were generated by *Eco*RI restriction digests to release the icIL-1RN and icIL-1RN SV2 clone inserts from pTarget. Restriction digests (40 µl) containing 28 µl dH₂O, 4 µl *Eco*RI and 8 µl DNA were incubated for 1 h at 37°C. Products were electrophoresed on an agarose gel at 100 V for 2 h and gel-purified using the QIAquick gel extraction kit (Qiagen). Purified DNA templates were quantified by spectrophotometry using the NanoDrop ND1000, radiolabelled and subsequently hybridised against the 4 BAC filters. Details of the filter preparation, probe preparation and hybridisation protocol are in Chapter 2, section 2.4.11.

4.3 Results

4.3.1 Identification and analysis of novel *chIL-1* expressed sequence tag (EST) sequences

The starting point for this project was a TBLASTN search of the NCBI EST database by a collaborator, Dr Steve Bird (University of Aberdeen). He identified three chicken ESTs representing putative *IL-1* genes, which were described as “similar to chicken IL-1 β ”. Two of these ESTs (Acc. Nos: CK613932 and BX257557) were combined to create a 554 bp sequence with potential start and stop codons as well as a polyadenylation (polyA) signal (AATAAA). I translated this combined EST and found the predicted protein sequence contained the IL-1 family signature motif (consensus: [FC]-x-S-[ASLV]-x(2)-P-x(2)-[FYLV]-[LI]-[SCA]-T-x(7)-[LIVM]; Bird, Zou et al. (2002)). Furthermore, the sequence had 20.6% identity with *chIL-1 β* , but was missing from v2.1 of the genome sequence. This predicted sequence was used to perform a TBLASTN analysis against all of the other eukaryotic genomes in ENSEMBL, which identified IL-1RN as the best hit in 22 other species (results in Table I in Appendix I).

To determine whether any further members of the *chIL-1* family were present in the NCBI EST database, reciprocal BLASTP analysis of this database using the predicted *chIL-1RN* amino acid sequence was performed. This uncovered twelve further EST sequences with significant homology (Table II in Appendix I). Three of these sequences were identical to the query IL-1RN sequence; however, one EST (BU214831.1) was similar but clearly differed at the 5' end. This 669 bp sequence also lacked a potential start codon. Unassembled, uncurated nucleotide sequence reads from the third build (Galgal 3.0) of the chicken genome were subsequently made available. A

TBLASTN search against these sequences was carried out and two contigs were identified (designated 81757.1 and 113837.1) from the “removed data” reads containing the majority of the coding sequence of chIL-1RN as well as some intronic sequence. Contig 81757.1 was aligned with the BU214831.1 EST sequence and additional 5' sequence was determined (that differed from the CK613932 and BX257557 ESTs) containing a single start codon (Figure 4.1).

4.3.2 Signal peptide analysis of predicted chIL-1RN amino acid sequences

Two similar chIL-1RN ESTs had been identified by screening the NCBI EST database. One of these ESTs (BU214831.1) was subsequently supplemented with further 5' end sequence from a contig (113837.1) mined from Galgal 3.0 (unassembled) sequence reads. Translating these two original ESTs produced two predicted chIL-1RN protein sequences that did not align at their NH₂-termini (Figure 4.2). The human IL-1RN gene is differentially spliced to create two structural variants that are identical to one another except for their 5' ends. This suggested that different structural variants may also exist in the chicken. Human IL-1RN structural variants are classified as either secretory or intracellular based on the existence of a signal peptide in the former. To determine if similar structural variants are synthesised in the two chIL-1RN sequences, they were analysed for the presence of a signal peptide using SignalP (Figure 4.3). The BU214831.1 EST (supplemented with further 5' end sequence from contig 113837.1) contained a 17 amino acid signal peptide and was designated secretory IL-1RN (sIL-1RN). The combined chIL-1RN EST (CK613932 & BX257557), however, did not contain a signal sequence and was therefore named intracellular IL-1RN (icIL-1RN) to reflect its likely identity.

Chapter 4: Identification, cloning and characterisation of chicken IL-1RN

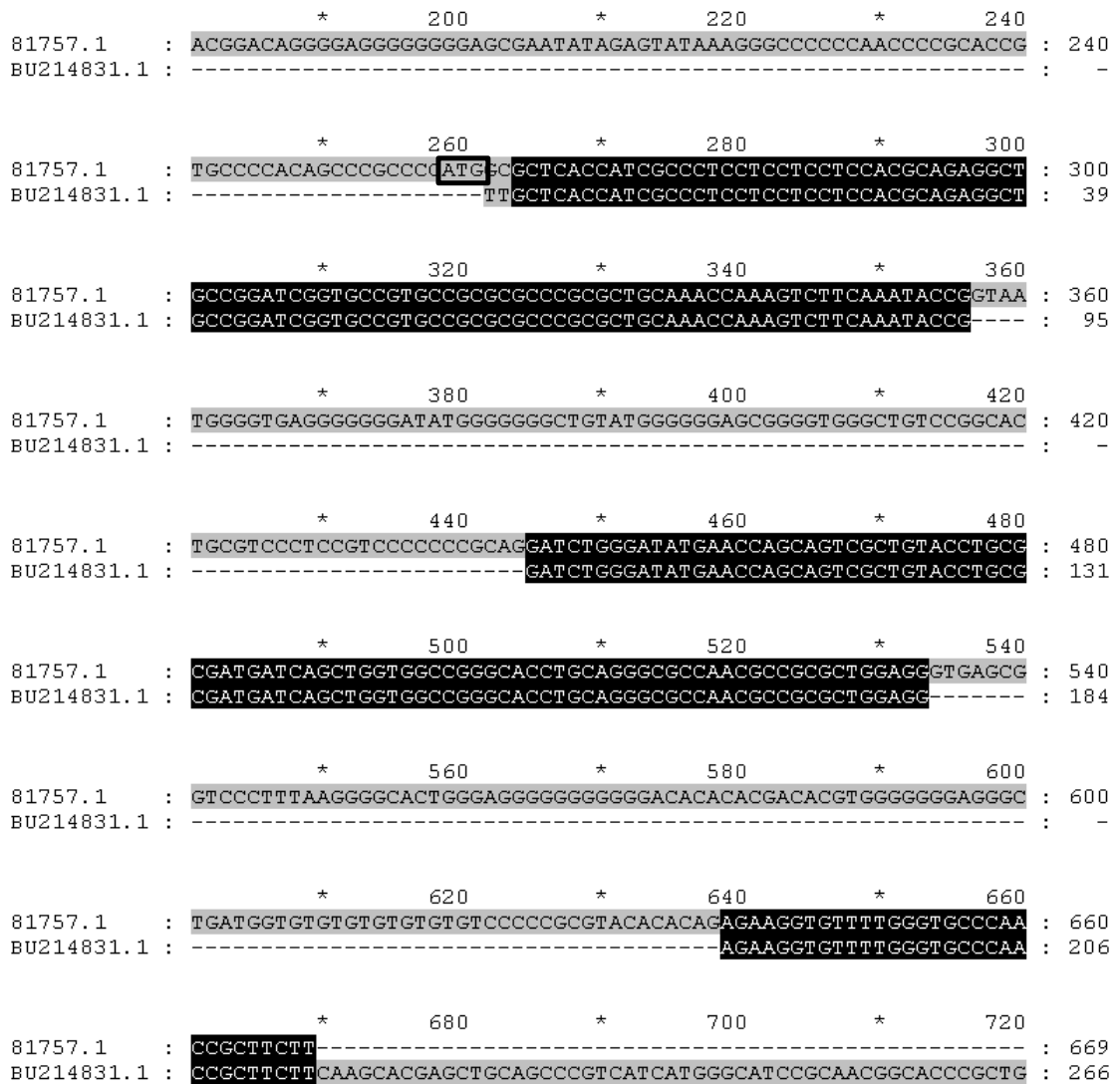


Figure 4.1 Nucleotide alignment between chIL-1RN EST BU214831.1 and Contig 81757.1. The single start codon missing from the EST is marked on the contig sequence. Once identified, it was then possible to design a forward primer against this EST/genomic sequence to amplify a full length CDS.

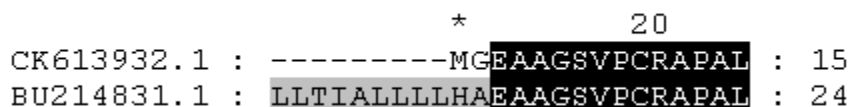


Figure 4.2 Amino acid alignment between 2 chIL-1RN ESTs differing at their 5' ends.

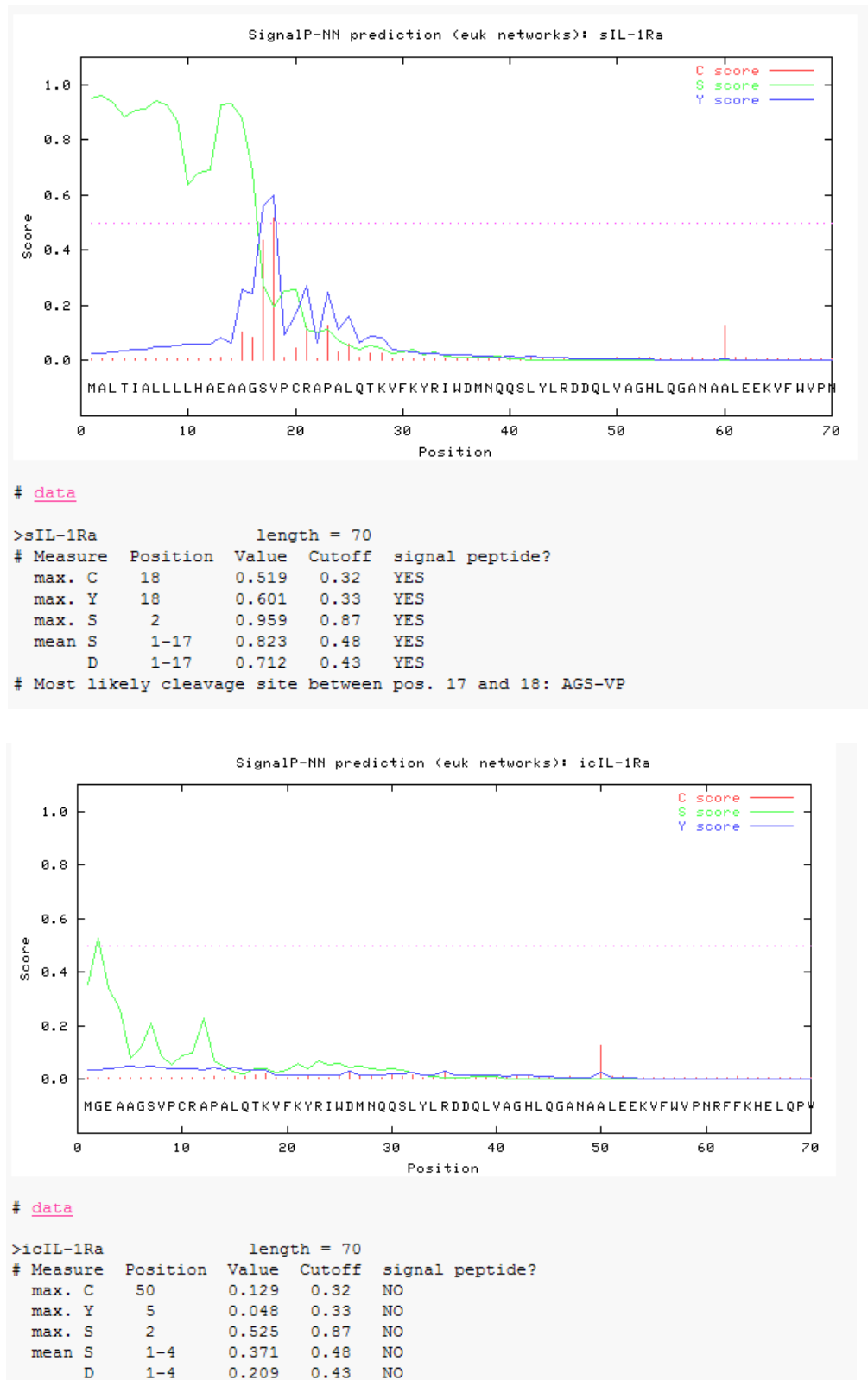


Figure 4.3 SignalP analysis of chIL-1RN amino acid sequences. *Top*, SignalP analysis of chicken sIL-1RN identifies a 17 amino acid signal peptide. *Bottom*, SignalP analysis of chicken icIL-1RN indicates no signal peptide is present.

4.3.3 Amplification and molecular cloning of chIL-1RN protein coding cDNA sequences

Primers were designed against the predicted sIL-1RN and icIL-1RN protein coding nucleotide sequences (CDS) derived from the ESTs. A full length icIL-1RN CDS was amplified by one-step reverse transcription-polymerase chain reaction (RT-PCR) using RNA from LPS-stimulated HD11 cells and ConA-stimulated splenocytes. Gel electrophoresis of the RT-PCR products revealed a double band consisting of a band of the expected size and a smaller additional band (see Figure 4.4). Both bands were gel-purified and TA-cloned into the pTarget mammalian expression vector. Clones were then screened by *EcoRI* restriction digestion. Agarose gel electrophoresis of released clone inserts suggested the small band present on the initial gel (Figure 4.4) was actually a doublet, as two clones with apparently different mobilities were isolated for this PCR product (Figure 4.5). All clones were sequenced by chain termination sequencing using T7 and revT7 (a custom reverse primer) vector primers (see Table 1 in the Appendix). Analysis of the clone sequences for the full length icIL-1RN CDS showed it was 492 bp in length and a 100% match with the IL-1RN EST sequence. Analysis of the clone sequences for the smaller band confirmed the existence of two distinct splice variants (SV) of the full length. Both aligned with the full length sequence but had regions where sequence was absent (Figure 4.6). As these truncated variants were specific, they were termed icIL-1RN SV1 and SV2. Their respective lengths were 400 bp and 420 bp.

A full length sIL-1RN ORF cDNA was amplified by PCR using cDNA made from LPS-stimulated HD11 RNA as template (Figure 4.7). As with icIL-1RN, agarose gel electrophoresis of the RT-PCR products revealed a double band - one at the expected size and a smaller additional band. Again, both bands were gel purified and

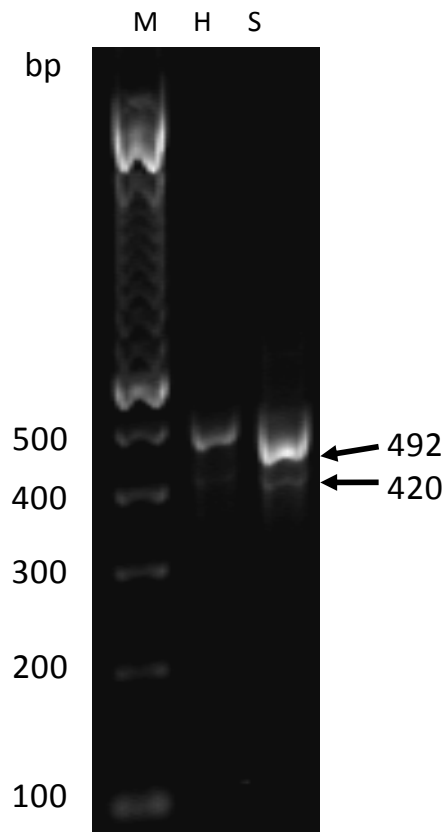


Figure 4.4 Agarose gel showing RT-PCR products from the amplification of the icIL-1RN CDS using ConA-stimulated splenocyte (S) and LPS-stimulated HD11 (H) macrophage cell line RNA as template. Expected band size = 492 bp. Both icIL-1RN splice variants are present in the smaller band at ~420 bp. M = 100 bp DNA ladder.

TA-cloned into the pTarget vector, followed by *EcoRI* restriction digestion to screen the clones. Agarose gel electrophoresis of the released clone inserts identified two splice variants of sIL-1RN in addition to the full length variant. Sequencing all of the clones with T7 and revT7 vector primers showed the two splice variants were specific and identical to those of the intracellular SVs at all of the splice sites, differing only in their 5' end sequences (Figure 4.8). This suggested a similar mechanism had led to their formation and they were subsequently named sIL-1RN SV1 and SV2. The CDS of full-length sIL-1RN is 522 bp in length, whilst SV1 and SV2 are 430 bp and 450 bp in length, respectively.

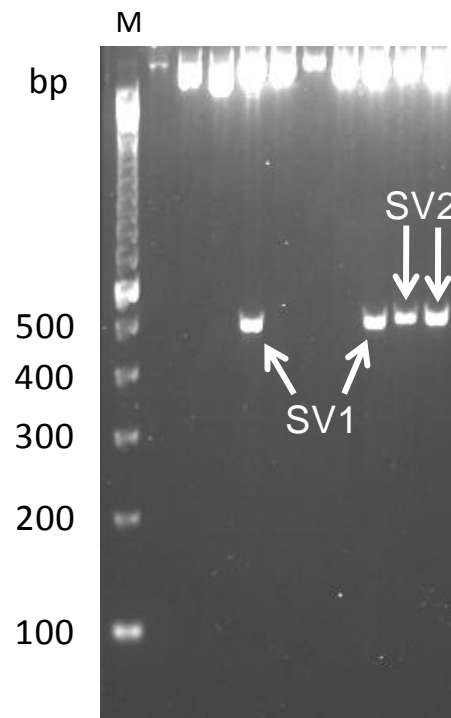


Figure 4.5 Agarose gel showing icIL-1RN splice variant clones released from pTarget by restriction digestion. Two different fragments are evident on this gel – SV1 and SV2. Size marker = 100 bp DNA ladder.

4.3.4 In silico analysis of chIL-1RN nucleotide and amino acid sequences

The full length chIL-1RN amino acid sequences were further characterized *in silico*.

The sIL-1RN and icIL-1RN ORF cDNAs encode predicted proteins of 173 and 163 amino acids, respectively, although sIL-1RN contains a predicted 17 amino acid signal peptide, so its predicted secreted mature protein is 156 amino acids. When aligned with mammalian IL-1RN sequences (Figure 4.9), both chIL-1RN sequences show relatively high amino acid identity for avian cytokines. Chicken sIL-1RN is very similar in length to the human and mouse sIL-1RN, sharing 38.3% and 37.9% sequence identity, respectively. Its predicted molecular weight (Mw) is 19.372 kDa with an isoelectric

Chapter 4: Identification, cloning and characterisation of chicken IL-1RN

```

          *           20           *           40           *           60
icSV2 : ATGGGTGAGGCTGCCGGATCGGTGCCGTGCCGCGCGCCCGCGCTGCAAACCAAAGTCTTC : 60
icFL  : ATGGGTGAGGCTGCCGGATCGGTGCCGTGCCGCGCGCCCGCGCTGCAAACCAAAGTCTTC : 60
icSV1 : ATGGGTGAGGCTGCCGGATCGGTGCCGTGCCGCGCGCCCGCGCTGCAAACCAAAGTCTTC : 60

          *           80           *           100          *           120
icSV2 : AAATACCGGATCTGGGATATGAACCAGCAGTCGCTGTACCTGCGCGATGATCAGCTGGTG : 120
icFL  : AAATACCGGATCTGGGATATGAACCAGCAGTCGCTGTACCTGCGCGATGATCAGCTGGTG : 120
icSV1 : AAATACC----- : 67

          *           140          *           160          *           180
icSV2 : GCCGGGCACCTGCAGGGCGCCAACGCCGCGCTGGAGGAGAAGGTGTTTTGGGTGCCAAC : 180
icFL  : GCCGGGCACCTGCAGGGCGCCAACGCCGCGCTGGAGGAGAAGGTGTTTTGGGTGCCAAC : 180
icSV1 : -----AAGGTGTTTTGGGTGCCAAC : 88

          *           200          *           220          *           240
icSV2 : CGCTTCTTCAAGCACGAGCTGCAGCCCGTCATCATGGGCATCCGCAACGGCACCCGCTGC : 240
icFL  : CGCTTCTTCAAGCACGAGCTGCAGCCCGTCATCATGGGCATCCGCAACGGCACCCGCTGC : 240
icSV1 : CGCTTCTTCAAGCACGAGCTGCAGCCCGTCATCATGGGCATCCGCAACGGCACCCGCTGC : 148

          *           260          *           280          *           300
icSV2 : CTGGCCTGCCCGGGCGGCCACAGCCCACCCTGCAGTCCA----- : 281
icFL  : CTGGCCTGCCCGGGCGGCCACAGCCCACCCTGCAGTCCAGGACGCCGACATCACGGAG : 300
icSV1 : CTGGCCTGCCCGGGCGGCCACAGCCCACCCTGCAGTCCAGGACGCCGACATCACGGAG : 208

          *           320          *           340          *           360
icSV2 : -----GGACGGG : 288
icFL  : CTGCCCCGACGCGGGCGCCGCTCCGCGCCGTTACCTTCTTCCGCACCTATAAGGACGGG : 360
icSV1 : CTGCCCCGACGCGGGCGCCGCTCCGCGCCGTTACCTTCTTCCGCACCTATAAGGACGGG : 268

          *           380          *           400          *           420
icSV2 : CTGTGGCGCTTCGAGTCGGCCGCCAACCCCGGATGGTTCTCTGCACCTCCGCCCGCGCC : 348
icFL  : CTGTGGCGCTTCGAGTCGGCCGCCAACCCCGGATGGTTCTCTGCACCTCCGCCCGCGCC : 420
icSV1 : CTGTGGCGCTTCGAGTCGGCCGCCAACCCCGGATGGTTCTCTGCACCTCCGCCCGCGCC : 328

          *           440          *           460          *           480
icSV2 : CACCAACCCCTGGGGCTCTCCCGGGCCCCGACGCCGCCACGTCCTGGATTTCTACTTC : 408
icFL  : CACCAACCCCTGGGGCTCTCCCGGGCCCCGACGCCGCCACGTCCTGGATTTCTACTTC : 480
icSV1 : CACCAACCCCTGGGGCTCTCCCGGGCCCCGACGCCGCCACGTCCTGGATTTCTACTTC : 388

          *
icSV2 : CAGCTGTGCTGA : 420
icFL  : CAGCTGTGCTGA : 492
icSV1 : CAGCTGTGCTGA : 400

```

Figure 4.6 Alignment between icIL-1RN (icFL), SV1 and SV2 CDS cDNA sequences using ClustalX. Blocks are shaded black to denote identical bases in all three sequences and grey to highlight identical bases in two of the sequences. This allows the exact locations of the splice junctions to be viewed more easily.

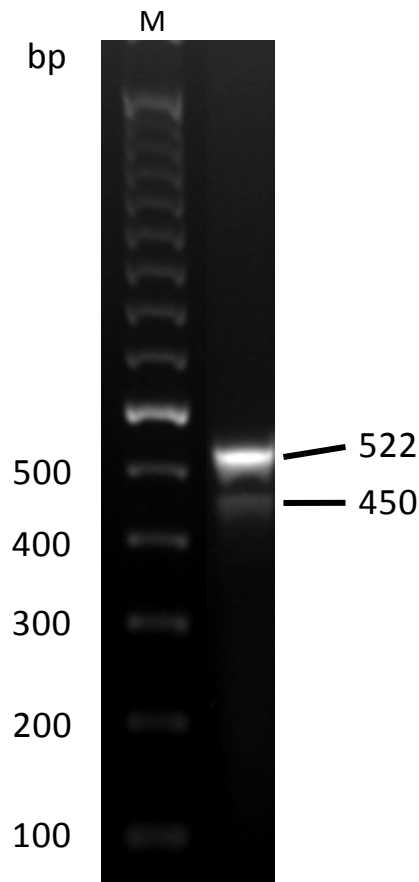


Figure 4.7 Agarose gel showing RT-PCR products from the amplification of the sIL-1RN CDS using LPS-stimulated HD11 (H) macrophage cell line RNA as template. Expected band size = 522 bp. Two sIL-1RN splice variants are present in the smaller band at ~450 bp. M = 100 bp DNA ladder.

point (pI) of 8.68. Chicken icIL-1RN, most similar to the human icIL-1RN1 isoform, has 38.2% and 40.4% amino acid identity with the respective human and mouse sequences. Its Mw is calculated as 18.299 kDa, with an identical pI to sIL-1RN of 8.68. The secondary structures of human and mouse IL-1 proteins have been characterized as β -trefoil folds comprised of 12 β -strands. Using PSIPRED, the secondary structure of chIL-1RN was predicted to have the same three-dimensional configuration, with the 12

Chapter 4: Identification, cloning and characterisation of chicken IL-1RN

```

*      20      *      40      *      60
icSV2 : -----ATGGGTGAGGCTGCCGGATCGGTGCCGTGC : 30
sSV2 : ATGGCGCTCACCATCGCCCTCCTCCTCCTCCACGCAGAGGCTGCCGGATCGGTGCCGTGC : 60
icFL : -----ATGGGTGAGGCTGCCGGATCGGTGCCGTGC : 30
sFL : ATGGCGCTCACCATCGCCCTCCTCCTCCTCCTCCACGCAGAGGCTGCCGGATCGGTGCCGTGC : 60
icSV1 : -----ATGGGTGAGGCTGCCGGATCGGTGCCGTGC : 30
sSV1 : ATGGCGCTCACCATCGCCCTCCTCCTCCTCCTCCACGCAGAGGCTGCCGGATCGGTGCCGTGC : 60

*      80      *      100     *      120
icSV2 : CGCGCGCCCGCGCTGCAAAACCAAAGTCTTCAAATACCGGATCTGGGATATGAACCAGCAG : 90
sSV2 : CGCGCGCCCGCGCTGCAAAACCAAAGTCTTCAAATACCGGATCTGGGATATGAACCAGCAG : 120
icFL : CGCGCGCCCGCGCTGCAAAACCAAAGTCTTCAAATACCGGATCTGGGATATGAACCAGCAG : 90
sFL : CGCGCGCCCGCGCTGCAAAACCAAAGTCTTCAAATACCGGATCTGGGATATGAACCAGCAG : 120
icSV1 : CGCGCGCCCGCGCTGCAAAACCAAAGTCTTCAAATACCGGATCTGGGATATGAACCAGCAG : 67
sSV1 : CGCGCGCCCGCGCTGCAAAACCAAAGTCTTCAAATACCGGATCTGGGATATGAACCAGCAG : 97

*      140     *      160     *      180
icSV2 : TCGCTGTACTGCGCGATGATCAGCTGGTGGCCGGGCACCTGCAGGGCGCCAAACGCCGCG : 150
sSV2 : TCGCTGTACTGCGCGATGATCAGCTGGTGGCCGGGCACCTGCAGGGCGCCAAACGCCGCG : 180
icFL : TCGCTGTACTGCGCGATGATCAGCTGGTGGCCGGGCACCTGCAGGGCGCCAAACGCCGCG : 150
sFL : TCGCTGTACTGCGCGATGATCAGCTGGTGGCCGGGCACCTGCAGGGCGCCAAACGCCGCG : 180
icSV1 : ----- : -
sSV1 : ----- : -

*      200     *      220     *      240
icSV2 : CTGGAGGACAAAGGTGTTTTGGGTGCCCAACCGCTTCTTCAAAGCAGGAGTGCAGCCCGTC : 210
sSV2 : CTGGAGGACAAAGGTGTTTTGGGTGCCCAACCGCTTCTTCAAAGCAGGAGTGCAGCCCGTC : 240
icFL : CTGGAGGACAAAGGTGTTTTGGGTGCCCAACCGCTTCTTCAAAGCAGGAGTGCAGCCCGTC : 210
sFL : CTGGAGGACAAAGGTGTTTTGGGTGCCCAACCGCTTCTTCAAAGCAGGAGTGCAGCCCGTC : 240
icSV1 : -----AAAGGTGTTTTGGGTGCCCAACCGCTTCTTCAAAGCAGGAGTGCAGCCCGTC : 118
sSV1 : -----AAAGGTGTTTTGGGTGCCCAACCGCTTCTTCAAAGCAGGAGTGCAGCCCGTC : 148

*      260     *      280     *      300
icSV2 : ATCATGGGCATCCGCAACGGCACCCGCTGCCTGGCCTGCCGGCGGCCCCACAGCCACC : 270
sSV2 : ATCATGGGCATCCGCAACGGCACCCGCTGCCTGGCCTGCCGGCGGCCCCACAGCCACC : 300
icFL : ATCATGGGCATCCGCAACGGCACCCGCTGCCTGGCCTGCCGGCGGCCCCACAGCCACC : 270
sFL : ATCATGGGCATCCGCAACGGCACCCGCTGCCTGGCCTGCCGGCGGCCCCACAGCCACC : 300
icSV1 : ATCATGGGCATCCGCAACGGCACCCGCTGCCTGGCCTGCCGGCGGCCCCACAGCCACC : 178
sSV1 : ATCATGGGCATCCGCAACGGCACCCGCTGCCTGGCCTGCCGGCGGCCCCACAGCCACC : 208

*      320     *      340     *      360
icSV2 : CTGCAGCTCCAGGAC----- : 286
sSV2 : CTGCAGCTCCAGGAC----- : 316
icFL : CTGCAGCTCCAGGACCCGACATCACGGAGCTGCCCGGCAGCGGGCGCCGCTCCGCGCCG : 330
sFL : CTGCAGCTCCAGGACCCGACATCACGGAGCTGCCCGGCAGCGGGCGCCGCTCCGCGCCG : 360
icSV1 : CTGCAGCTCCAGGACCCGACATCACGGAGCTGCCCGGCAGCGGGCGCCGCTCCGCGCCG : 238
sSV1 : CTGCAGCTCCAGGACCCGACATCACGGAGCTGCCCGGCAGCGGGCGCCGCTCCGCGCCG : 268

*      380     *      400     *      420
icSV2 : -----GGCTGTGGCGCTTCGAGTCGGCCGCCAACCC : 318
sSV2 : -----GGCTGTGGCGCTTCGAGTCGGCCGCCAACCC : 348
icFL : TTCACCTTCTCCGCACCTATAAGGACGGGCTGTGGCGCTTCGAGTCGGCCGCCAACCC : 390
sFL : TTCACCTTCTCCGCACCTATAAGGACGGGCTGTGGCGCTTCGAGTCGGCCGCCAACCC : 420
icSV1 : TTCACCTTCTCCGCACCTATAAGGACGGGCTGTGGCGCTTCGAGTCGGCCGCCAACCC : 298
sSV1 : TTCACCTTCTCCGCACCTATAAGGACGGGCTGTGGCGCTTCGAGTCGGCCGCCAACCC : 328

*      440     *      460     *      480
icSV2 : GGATGGTTCTCTGCACCTCCGCCCGGCCACCAACCCCTGGGGCTCTCCCGGGCCCC : 378
sSV2 : GGATGGTTCTCTGCACCTCCGCCCGGCCACCAACCCCTGGGGCTCTCCCGGGCCCC : 408
icFL : GGATGGTTCTCTGCACCTCCGCCCGGCCACCAACCCCTGGGGCTCTCCCGGGCCCC : 450
sFL : GGATGGTTCTCTGCACCTCCGCCCGGCCACCAACCCCTGGGGCTCTCCCGGGCCCC : 480
icSV1 : GGATGGTTCTCTGCACCTCCGCCCGGCCACCAACCCCTGGGGCTCTCCCGGGCCCC : 358
sSV1 : GGATGGTTCTCTGCACCTCCGCCCGGCCACCAACCCCTGGGGCTCTCCCGGGCCCC : 388

*      500     *      520
icSV2 : GACGCGCCACGTCCTGGATTTCTACTTCCAGCTGTGCTGA : 420
sSV2 : GACGCGCCACGTCCTGGATTTCTACTTCCAGCTGTGCTGA : 450
icFL : GACGCGCCACGTCCTGGATTTCTACTTCCAGCTGTGCTGA : 492
sFL : GACGCGCCACGTCCTGGATTTCTACTTCCAGCTGTGCTGA : 522
icSV1 : GACGCGCCACGTCCTGGATTTCTACTTCCAGCTGTGCTGA : 400
sSV1 : GACGCGCCACGTCCTGGATTTCTACTTCCAGCTGTGCTGA : 430

```

Figure 4.8 Alignment between the six chIL-1RN CDS cDNA sequences in ClustalX. *Previous page* Both secretory and intracellular splice variant sequences are identical at all of the splice sites. Blocks are shaded black to denote identical bases in all sequences and grey to highlight identical bases in four of the sequences.

β -strands located in almost identical regions to the huIL-1RN sequence (Figure 4.9).

These regions are the most highly conserved between species reflecting their likely functional/structural importance. Of the five cysteine residues in the chIL-1RN sequences, three of these are conserved in mammals, located in β -strands 6 and 10, and two will likely form disulphide bonds. A single potential N-glycosylation site (NGT) is found in icIL-1RN at positions 76-78 (86-88 in sIL-1RN); however, it is not conserved in mammalian sequences. Both chIL-1RN sequences were analysed for structural similarity to known protein domains in the ProDom database. Both sequences were most closely related to domains PDA1I6T8 (domain I.D: IL-1Ra; closest domains: rat IL-1Ra (to ch icIL-1RN) and rabbit IL-1Ra (to ch sIL-1RN); e-values: 2×10^{-9} and 4×10^{-9} for residues 2-62 and 15-69; with 49% and 52% amino acid identity, respectively); and PD002536 (IL-1; mouse IL-1F10; 2×10^{-18} ; 32-161/42-171; 37%). Upon examination of the IL-1RN SV nucleotide sequences, SV1 transcripts were apparently formed through use of an atypical splice donor site (GG). This resulted in the predicted protein sequence being out of frame and significantly truncated compared to the full length sequence (Figure 4.10). The modified amino acid sequence following the frameshift consists of a higher proportion of hydrophobic residues which may significantly affect the biochemical properties of the molecule. β -strands 2 and 3 have also been removed and the conserved cysteines found in the full length sequences are absent. The SV2 transcripts are apparently formed through use of an alternative splice acceptor site, with the predicted protein sequence in frame with the full length molecule. Although in

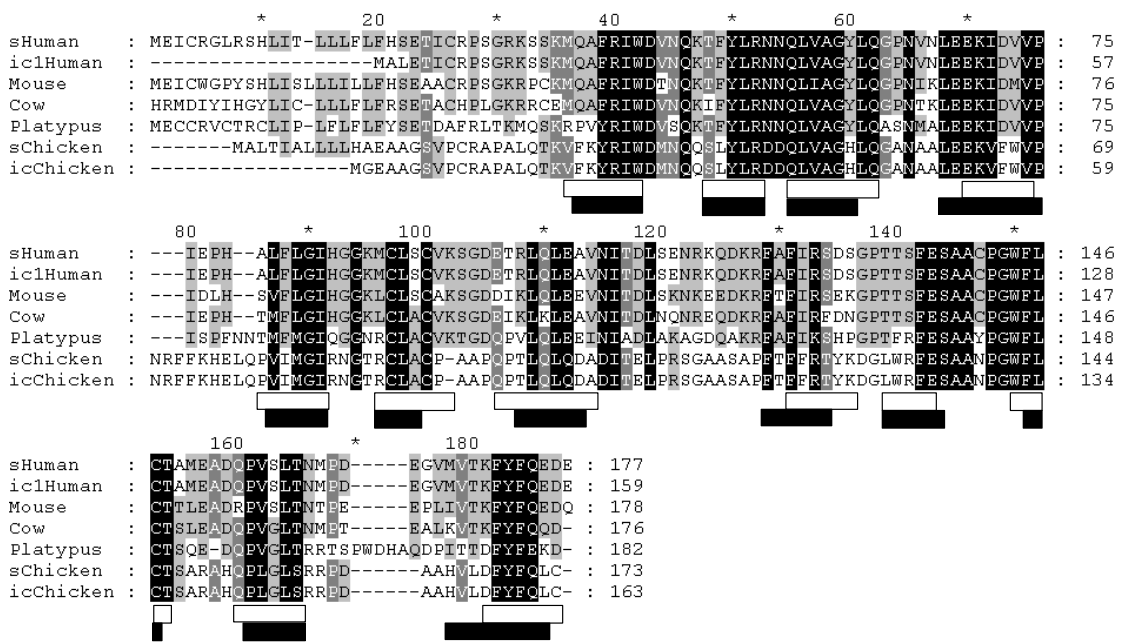


Figure 4.9 Amino acid alignment of chicken sIL-1RN and icIL-1RN with human (secretory and intracellular variant 1), mouse, cow, and platypus IL-1RN sequences. Identical residues between all five species at the same position are shaded black; identical residues between four species are shaded dark grey, those between three species shaded light grey; similar (structure) residues are shaded light grey. The secondary structure of IL-1 family proteins consists of 12 β -strands. The specific amino acid residues that comprise these 12 β -strands in humans (Schreuder 1997) are indicated by white blocks beneath the sequence. Their locations in the chicken, predicted by PSIPRED, are indicated by black blocks.

frame, the truncated sequence lacks β -strand 8 which may affect protein folding.

Using the full length chicken icIL-1RN and sIL-1RN amino acid sequences, phylogenetic analysis was carried out to determine an evolutionary relationship with mammalian IL-1RN. The initial large scale analysis incorporated the maximum number of known IL-1 amino acid sequences from the following species: human, mouse, platypus, chicken, zebra finch and lizard. The unrooted phylogenetic tree that was created showed both chicken IL-1 β and IL-18 sequences grouped within the major

```

      *      20      *      40      *      60      *      80      *
FL : MGEAAGSVPCRAPALQTRVFKYRIWDMNQSLYLRDDOLVAGHLQGANAALBEKVFVWPNRFFKHELQPVIMGIRNGTRCLACPAAPQPT : 90
SV2 : MGEAAGSVPCRAPALQTRVFKYRIWDMNQSLYLRDDOLVAGHLQGANAALBEKVFVWPNRFFKHELQPVIMGIRNGTRCLACPAAPQPT : 90
SV1 : MGEAAGSVPCRAPALQTRVFKYREGVLGAQPIQLQARAAARHHGHPQRHPLPGLPGGPTAHPAAPGRRHHGAAPQRRRLRAVHLLPHL--- : 87

      100      *      120      *      140      *      160
FL : LQLQDADITELPRSGAASAPFTFFRTYK DGLWRFE SAANPGWFLCT SARAHQPLGLSRRPDAAHVLD EYFQLC : 163
SV2 : LQLC-----DGLWRFE SAANPGWFLCT SARAHQPLGLSRRPDAAHVLD EYFQLC : 139
SV1 : ----- : -

```

Figure 4.10 Amino acid alignment between predicted icIL-1RN (icFL), SV1 & SV2 sequences. Due to use of an atypical splice donor site, the SV1 amino acid sequence is out of frame and truncated compared to the full length sequence.

clades for those genes, as previously shown (Huising, Stet et al. 2004). Both chIL-1RN formed a separate branch within the major IL-1 receptor antagonist subgroup (IL-1RN, IL-1F5 & IL-1F10) clade (Figure 4.11). A smaller scale analysis was carried out using only IL-1 β , IL-1RN, IL-1F5 and IL-1F10 from species possessing these genes, which again produced the same groupings. All IL-1 genes contain 3 highly conserved common exons which are always the last 3 in any transcript. The final common exon encodes the IL-1 family signature motif so is the most highly conserved region between all IL-1 genes across all species with identified orthologues. In an attempt to determine if chIL-1RN would group closer to its direct mammalian orthologues, analysis using only the amino acid sequence of common exon 3 was carried out. However, a similar tree topology to that previously seen was generated (data not shown).

4.3.5 Structural determination of chIL-1RN by PCR amplification, sequencing and in silico analysis

A combination of PCR and *in silico* analyses allowed the genomic structure of

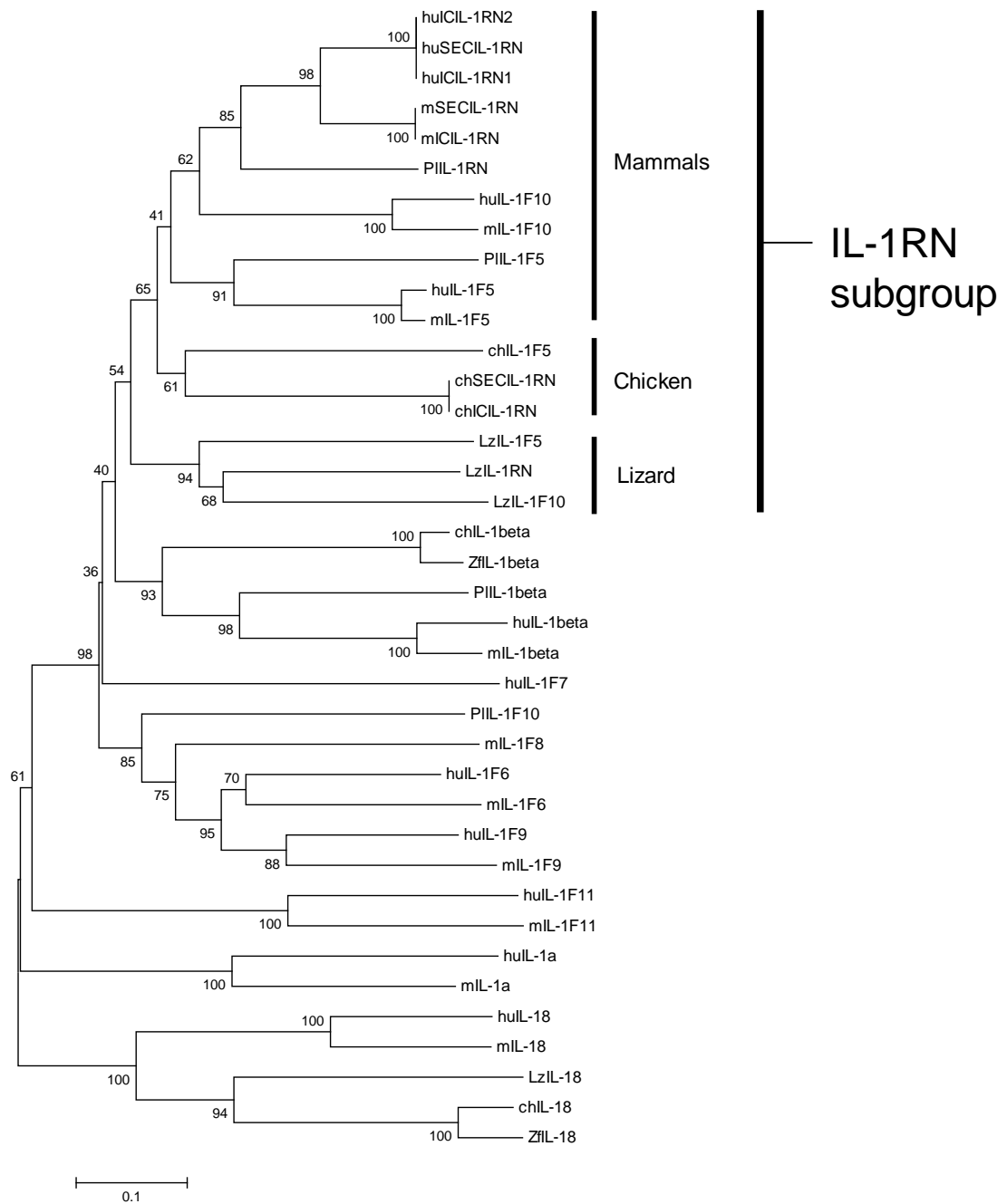


Figure 4.11 Phylogenetic analysis of chIL-1RN amino acid sequences using MEGA v5.0. Analysis was performed using the Neighbour-Joining (N-J) method. hu = human, m = mouse, Pl = platypus, ch = chicken, Lz = lizard, Zf = zebra finch. IC = intracellular; SEC = secretory.

chIL-1RN to be determined. The human *IL-1RN* gene consists of six exons, which, through differential splicing of the first three exons (ic1, ic2 and s1), creates three different transcripts: sIL-1RN, icIL-1RN1 and icIL-1RN2. All 3 transcripts include the common exons 2-4; and either all (sIL-1RN) or part (icIL-1RN1 and icIL-1RN2) of exon s1. The icIL-1RN1 transcript contains a further upstream exon (ic1) that is spliced into exon s1 through use of an internal splice acceptor site located within s1. This splice acceptor site is situated towards the 3' end of the sequence encoding the signal peptide, hence the icIL-1RN1 transcript does not possess a signal sequence. The icIL-1RN2 transcript contains all of the exons present in the icIL-1RN1 sequence, in addition to which a 63 bp exon (ic2) is inserted between ic1 and s1 (Figure 4.12). As the chromosomal location of the chIL-1RN gene remains unknown, the structure and full gene sequence are not present in any of the chicken genome browsers.

Avian cytokine genes are structurally very similar to their mammalian orthologues (Kaiser, 2004), so it is likely that the structure of the chIL-1RN gene resembles that of the huIL-1RN gene. Using knowledge of the huIL-1RN gene structure, the human and chicken IL-1RN cDNA sequences were aligned to predict the locations of the chicken introns (Figure 4.13). Primers were then designed from the exon sequences flanking the predicted intron-exon boundaries of the chicken transcripts. Only two chicken introns were successfully amplified using this approach. Using genomic DNA from lines 6₁ and N, a 354 bp PCR product was generated (the equivalent cDNA amplicon would be 161 bp) (Figure 4.14). Sequencing revealed this amplicon was comprised of intron 2, exon 3 and intron 3 of chIL-1RN. The size and sequence of exon 3 was already known, allowing the sizes of introns 2 and 3 to be accurately determined as being 88 bp and 105 bp in length, respectively. The

corresponding introns in the huIL-1RN gene are substantially larger, at 1835 bp and 1380 bp, respectively.

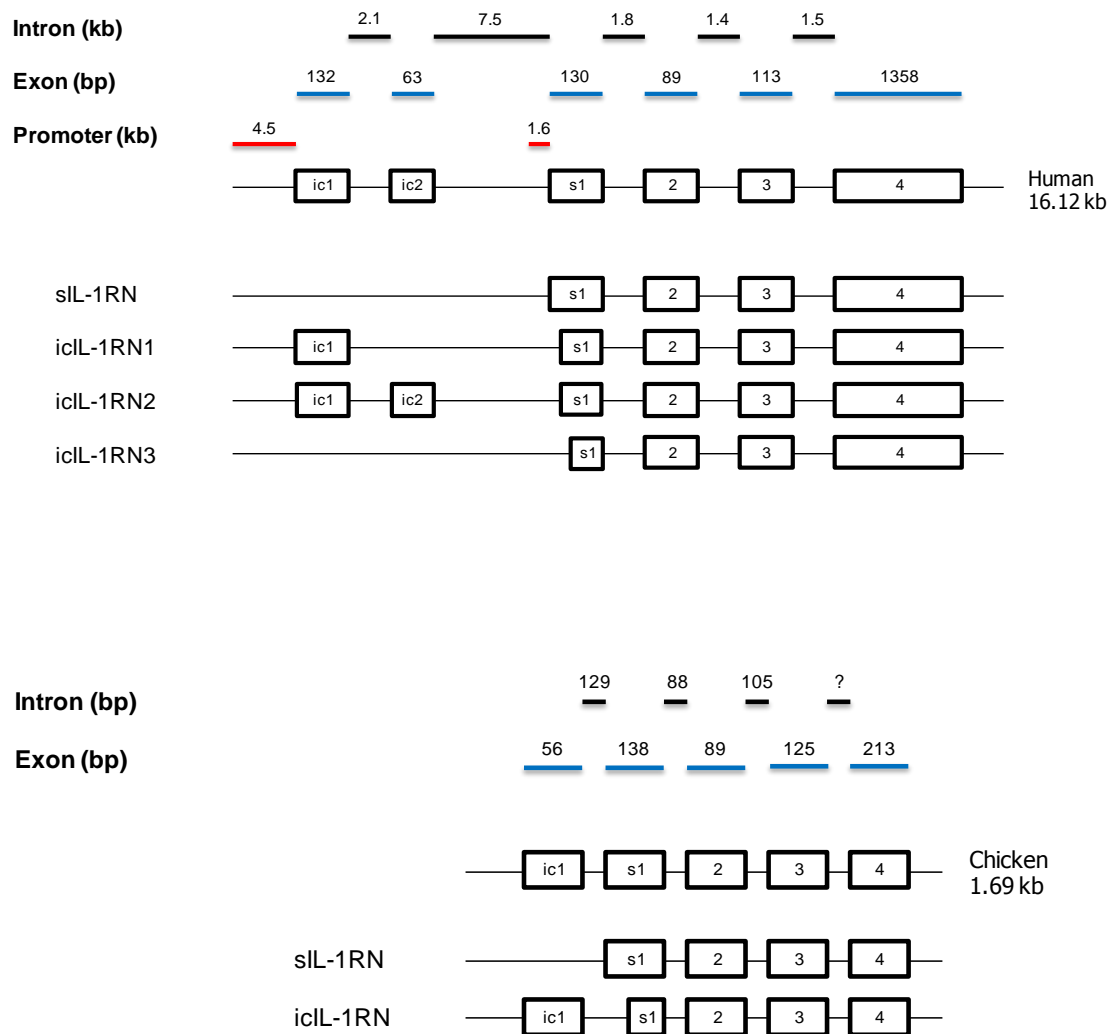


Figure 4.12 The structures and identified protein coding transcripts of chicken and human IL-1RN genes.

The subsequent availability of Galgal 3.0 unassembled sequence reads confirmed the sequencing results generated for introns 2 and 3 of chIL-1RN. Alignment of the chicken CDS with the genomic sequence in contigs 81757.1 and 113837.1 allowed the identification of the exact locations of each of the exons. The alignment also confirmed the full sequence of exons ic1, s1 and 2-4 and introns 1-3 (Figures 4.15 and 4.16), thus the only outstanding intron yet to be amplified was intron 4. Using

Chapter 4: Identification, cloning and characterisation of chicken IL-1RN

```

*           20           *           40           *           60
huicIL-1RN1 : -----*-----*-----*-----*----- : -
huicIL-1RN2 : ATGGCTTTAGCTGACTTGTATGAAGAAGGAGGTGGAGGAGGAGGAGAAGGTGAAGACAAAT : 60
huicIL-1RN3 : -----*-----*-----*-----*----- : -
husIL-1RN   : -----ATGGAATCTGCAGAGGCGCTCCGCAGTCACTAATCACTCTCCTCCTCTTC : 51
chicIL-1RN  : --CTCCCTCCTTCCCCAGGCTCCAGGGCGGGTGGCCTCCATTGGGGCATCTCATGGGTGA : 58
chsIL-1RN   : -----ATGGCGCTCACCATCGCCCTCCTCCTCCTCCACGCAGA : 38

IL-1RN Int1-2L1

*           80           *           100          *           120
huicIL-1RN1 : ---ATGGCTTTAGAGACGATCTGCCGACCCTCTGGGAGAAAAATCCAGCAAGATGCAAGCC : 57
huicIL-1RN2 : GCTGACTCAAAGGAGACGATCTGCCGACCCTCTGGGAGAAAAATCCAGCAAGATGCAAGCC : 120
huicIL-1RN3 : -----ATGCAAGCC : 9
husIL-1RN   : CTGTTCCATTGAGACGATCTGCCGACCCTCTGGGAGAAAAATCCAGCAAGATGCAAGCC : 111
chicIL-1RN  : GGCTGCCGG--ATCGGTGCCGTGCCGCGCGCCCGCGCTGCAAACCAA--AGTCTTCAA-- : 113
chsIL-1RN   : GGCTGCCGG--ATCGGTGCCGTGCCGCGCGCCCGCGCTGCAAACCAA--AGTCTTCAA-- : 93

IL-1RN Int2-3L2

*           140          *           160          *           180
huicIL-1RN1 : TTCAGAACTCTGGGATGTTAACCAGAAGACCTTCTATCTGAGGAACAACCAACTAGTTGCT : 117
huicIL-1RN2 : TTCAGAACTCTGGGATGTTAACCAGAAGACCTTCTATCTGAGGAACAACCAACTAGTTGCT : 180
huicIL-1RN3 : TTCAGAACTCTGGGATGTTAACCAGAAGACCTTCTATCTGAGGAACAACCAACTAGTTGCT : 69
husIL-1RN   : TTCAGAACTCTGGGATGTTAACCAGAAGACCTTCTATCTGAGGAACAACCAACTAGTTGCT : 171
chicIL-1RN  : TACCGGATCTGGGATATGAACCAGCAGTCGCTGTACCTGCGCGATGATCAGCTGGTGGCC : 173
chsIL-1RN   : TACCGGATCTGGGATATGAACCAGCAGTCGCTGTACCTGCGCGATGATCAGCTGGTGGCC : 153

*           200          *           220          *           240
huicIL-1RN1 : GGATACTTGCAAGGACCAAAATGTCAATTTAGAAGAAAAGATAGATGTGGTACCCATT--- : 174
huicIL-1RN2 : GGATACTTGCAAGGACCAAAATGTCAATTTAGAAGAAAAGATAGATGTGGTACCCATT--- : 237
huicIL-1RN3 : GGATACTTGCAAGGACCAAAATGTCAATTTAGAAGAAAAGATAGATGTGGTACCCATT--- : 126
husIL-1RN   : GGATACTTGCAAGGACCAAAATGTCAATTTAGAAGAAAAGATAGATGTGGTACCCATT--- : 228
chicIL-1RN  : GGCACCTGCAGGGCGCCAAACGCCGCGCTGGAGGAGAAGGTGTTTTGGGTGCCAACCCGC : 233
chsIL-1RN   : GGCACCTGCAGGGCGCCAAACGCCGCGCTGGAGGAGAAGGTGTTTTGGGTGCCAACCCGC : 213

*           260          *           280          *           300
huicIL-1RN1 : -----GAGCCTCATGCTCTGTTCTTGGGAATCCATGGAGGGAAGATGTGCCTG : 222
huicIL-1RN2 : -----GAGCCTCATGCTCTGTTCTTGGGAATCCATGGAGGGAAGATGTGCCTG : 285
huicIL-1RN3 : -----GAGCCTCATGCTCTGTTCTTGGGAATCCATGGAGGGAAGATGTGCCTG : 174
husIL-1RN   : -----GAGCCTCATGCTCTGTTCTTGGGAATCCATGGAGGGAAGATGTGCCTG : 276
chicIL-1RN  : TTCTTCAAGCAGGAGCTGCAGCCCGTCAATCATGGGCATCCGCAACGGCACCCCGCTGCCTG : 293
chsIL-1RN   : TTCTTCAAGCAGGAGCTGCAGCCCGTCAATCATGGGCATCCGCAACGGCACCCCGTGCCTG : 273

IL-1RN Int3-4R2

*           320          *           340          *           360
huicIL-1RN1 : TCCTGTGTCAAGTCTGGTGATGAGACCAGACTCCAGCTGGAGSCAGTTAACATCACTGAC : 282
huicIL-1RN2 : TCCTGTGTCAAGTCTGGTGATGAGACCAGACTCCAGCTGGAGSCAGTTAACATCACTGAC : 345
huicIL-1RN3 : TCCTGTGTCAAGTCTGGTGATGAGACCAGACTCCAGCTGGAGSCAGTTAACATCACTGAC : 234
husIL-1RN   : TCCTGTGTCAAGTCTGGTGATGAGACCAGACTCCAGCTGGAGSCAGTTAACATCACTGAC : 336
chicIL-1RN  : GCCTG---CCCGCGGCCCCACAGCCACCCCTGCAGCTCCAGSACGCCGACATCACGGAG : 350
chsIL-1RN   : GCCTG---CCCGCGGCCCCACAGCCACCCCTGCAGCTCCAGSACGCCGACATCACGGAG : 330

IL-1RN 130R

*           380          *           400          *           420
huicIL-1RN1 : CTGAGCGAGAACAGAAAGCAGGACAAGCGCTTCGCCTTCATCCGCTCAGACAGTGGCCCC : 342
huicIL-1RN2 : CTGAGCGAGAACAGAAAGCAGGACAAGCGCTTCGCCTTCATCCGCTCAGACAGTGGCCCC : 405
huicIL-1RN3 : CTGAGCGAGAACAGAAAGCAGGACAAGCGCTTCGCCTTCATCCGCTCAGACAGTGGCCCC : 294
husIL-1RN   : CTGAGCGAGAACAGAAAGCAGGACAAGCGCTTCGCCTTCATCCGCTCAGACAGTGGCCCC : 396
chicIL-1RN  : CTGCCCCGACGCGCGCCGCTCCGCGCGCTTACCTTCTCCGCACCTATAAGGACGGG : 410
chsIL-1RN   : CTGCCCCGACGCGCGCCGCTCCGCGCGCTTACCTTCTCCGCACCTATAAGGACGGG : 390

*           440          *           460          *           480
huicIL-1RN1 : ACCACCAGTTTTGAGTCTGCCGCTGCCCGGTTGGTTCTCTGCACAGCGATGGAAGCT : 402
huicIL-1RN2 : ACCACCAGTTTTGAGTCTGCCGCTGCCCGGTTGGTTCTCTGCACAGCGATGGAAGCT : 465
huicIL-1RN3 : ACCACCAGTTTTGAGTCTGCCGCTGCCCGGTTGGTTCTCTGCACAGCGATGGAAGCT : 354
husIL-1RN   : ACCACCAGTTTTGAGTCTGCCGCTGCCCGGTTGGTTCTCTGCACAGCGATGGAAGCT : 456
chicIL-1RN  : CTGTGGCGCTTCGAGTCGGCCGCCAACCCCGGATGGTTCTCTGCACCTCCGCCCCGCGC : 470
chsIL-1RN   : CTGTGGCGCTTCGAGTCGGCCGCCAACCCCGGATGGTTCTCTGCACCTCCGCCCCGCGC : 450

*           500          *           520          *           540
huicIL-1RN1 : GACCAGCCCGTCAGCCTCACCAATATGCCTGACGAAGGCGTCATGGTCACCAAATTTCTAC : 462
huicIL-1RN2 : GACCAGCCCGTCAGCCTCACCAATATGCCTGACGAAGGCGTCATGGTCACCAAATTTCTAC : 525
huicIL-1RN3 : GACCAGCCCGTCAGCCTCACCAATATGCCTGACGAAGGCGTCATGGTCACCAAATTTCTAC : 414
husIL-1RN   : GACCAGCCCGTCAGCCTCACCAATATGCCTGACGAAGGCGTCATGGTCACCAAATTTCTAC : 516
chicIL-1RN  : CACCAACCCCTGGGGCTCTCCCG-GCGCCC--CGAGCCCGCCACGTCCTGGATTCTAC : 527
chsIL-1RN   : CACCAACCCCTGGGGCTCTCCCG-GCGCCC--CGAGCCCGCCACGTCCTGGATTCTAC : 507

*
huicIL-1RN1 : TTCCAGGAGGACGAGTAG : 480
huicIL-1RN2 : TTCCAGGAGGACGAGTAG : 543
huicIL-1RN3 : TTCCAGGAGGACGAGTAG : 432
husIL-1RN   : TTCCAGGAGGACGAGTAG : 534
chicIL-1RN  : TTCCAGCTGTGCTGA--- : 542
chsIL-1RN   : TTCCAGCTGTGCTGA--- : 522

```

Figure 4.13 Alignment of human and chicken transcript sequences created to predict the locations of the chicken gene introns. *Previous page* Vertical lines indicate the location of introns in both species. In the chicken, the locations of primers used to amplify the 4 introns are indicated. Introns 1-4 were amplified with IL-1RN Int1-2L1 and IL-1RN 130R primers. Introns 2 and 3 were amplified with IL-1RN Int2-3L2 and IL-1RN Int3-4R2 primers.

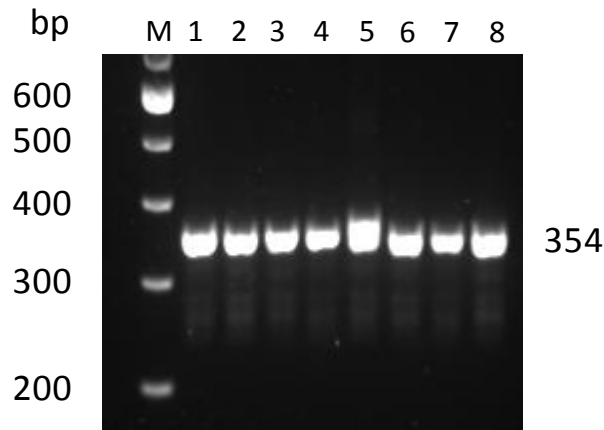


Figure 4.14 Agarose gel of PCR products containing intron 2, exon 3 and intron 3 of chIL-1RN. Products were amplified with IL-1RN Int2-3L2 and IL-1RN Int3-4R2 primers (see **Fig 4.13**). Lane M = 100 bp DNA ladder. Lanes 1-8 = products amplified from lines 6₁, 7₂, 15I, W, P, 0, RIR & N genomic DNA respectively.

previously unknown sequence from contig113837.1, several primer pairs were designed to generate a PCR product containing the “missing” intron 4. A ~1500 bp PCR product was amplified with Int1-2L1 and 130R primers (Figure 4.17), cloned and sequenced. Intron 4 of chIL-1RN is ~770 bp in length, ~1020 bp shorter than its human equivalent. In summary, the structure of chIL-1RN was found to be similar to that of its human orthologue (Figure 4.12). The coding region is comprised of five exons, which when translated are very similar in size to their corresponding human sequences. The introns of chIL-1RN, however, are significantly smaller than their human equivalents, resulting in the overall length of the gene being around one tenth (10.5%) that of huIL-1RN.

Chapter 4: Identification, cloning and characterisation of chicken IL-1RN

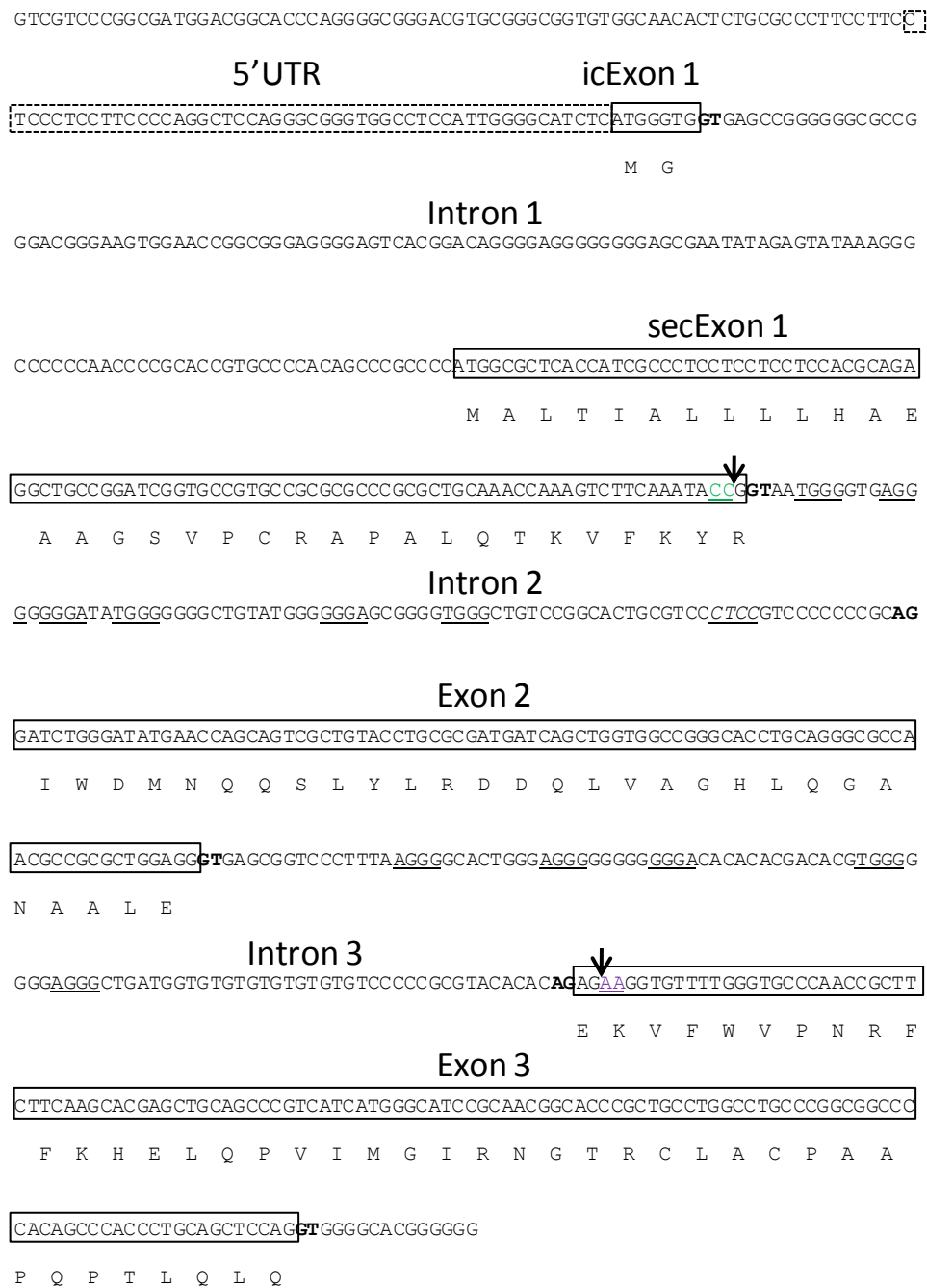


Figure 4.15 Structure of exon/intron 1-3 of chIL-1RN. Above Splicing that leads to the formation of SV1 transcripts is indicated. Intron 2 is usually spliced at the GT splice donor site (in bold), however, it is spliced 1 G nucleotide earlier in SV1 (splice site marked by an arrow) making **CC** the final nucleotides in the coding sequence. Intron 3 is usually spliced at the AG splice acceptor site (in bold), however, it is spliced 2 nucleotides later at the alternative but incorrect AG, making **AA** the first nucleotides in the continuing coding sequence. Several motifs associated with exon skipping in mammals are underlined in introns 2 and 3.

Chapter 4: Identification, cloning and characterisation of chicken IL-1RN

Below Exon skipping alters the reading frame of the amino acid, introducing a premature stop codon. Residues out of frame are shaded blue.

```
ATGGCGCTCACCATCGCCCTCCTCCTCCTCCACGCA
M A L T I A L L L L H A

GAGGCTGCCGGATCGGTGCCGTGCCGCGCGCCCGCG
E A A G S V P C R A P A

CTGCAAACCAAAGTCTTCAAATACCAAAGGTGTTTTG
L Q T K V F K Y Q G V L

GGTGCCCAACCGCTTCTTCAAGCACGAGCTGCAGCC
G A Q P L L Q A R A A A

CGTCATCATGGGCATCCGCAACGGCACCCGCTGCCT
R H H G H P Q R H P L P

GGCCTGCCCGGCGGCCCCACAGCCCACCCTGCAGCT
G L P G G P T A H P A A

CCAGGACGCCGACATCACGGAGCTGCCCCGAGCGG
P G R R H H G A A P Q R

CGCCGCTCCGCGCCGTTACCTTCTTCCGCACCTA
R R L R A V H L L P H L

TAAGGACGGGCTGTGGCGCTTCGAGTCGGCCGCAA
*

CCCCGATGGTTCCTCTGCACCTCCGCCCCGCGCCA
CCAACCCCTGGGGCTCTCCCGCGCCCCGAGCCCGC
CCACGTCTTGATTTCTACTTCCAGCTGTGCTGA
```

Establishing the genomic structure of chIL-1RN (above) allowed the sequences of the chIL-1RN splice variants to be revisited to decipher the alternative splicing events that generated them. SV1 was missing exon 3 and was formed through use of an atypical splice donor site (GG). This resulted in the predicted protein sequence being out of frame and significantly truncated compared to the full length amino acid (Figure 4.15). Analysis of the intron sequences flanking this missing exon identified several conserved sequence motifs associated with exon skipping in mammals (Miriami,

Margalit et al. 2003). These motifs were predominantly G-rich (AGGG or GGG(A/T)), with only a single C-rich (CTCC) motif present. Analysis of the type and position of these two motifs in mammalian intron sequences led to the proposal of a consensus pattern describing how they are arranged relative to a skipped exon (Miriami, Margalit et al. 2003). Complementary motifs appear in the same relative positions to one another in flanking introns, e.g. if, in the 5' direction from an exon there were a G-rich motif at -20 nt, a C-rich motif at -30 nt, a C-rich motif at -38 nt and a G-rich motif at -55, then in the 3' direction from the same exon you would see a C-rich motif at +20 nt, a G-rich motif at +30 nt, a G-rich motif at +38 nt and a C-rich motif at +55 nt. There is some leniency with this pattern, so the exact number of complementary motifs and the spacing may vary. The motifs in these chicken introns which are all G-rich except for a single C-rich motif (Figure 4.15) therefore do not fit this described pattern.

The SV2 transcript sequence was formed through use of an alternative splice acceptor site (AG) within exon 5 located 72 bp from its 5' end. In contrast to SV1, removal of this short stretch of nucleotides did not introduce a frameshift in the predicted protein sequence (Figure 4.15).

Contig 81757.1 also provided sufficient sequence at the 5' end of the gene to clarify how alternative splicing creates the two major structural variants of chIL-1RN. The icIL-1RN1 variant in humans is created following alternative splicing of an upstream exon into the 3' end of exon 1 of sIL-1RN, utilising an internal splice acceptor site. Analysis of Contig 81757.1 indicated that a similar mechanism takes place in the chicken, whereby an upstream exon is used to create the chicken icIL-1RN CDS previously identified (Figure 4.18).

3' end of Intron 4

AGGGCTGGGATGTGAGGGCTGAGCCGTGGTGC GGCCTGCCAGC**AG**GACGCCGACATCAC
 D A D I T

GGAGCTGCCCCGAGCGGC GCGCCTCCGCGCCGTT**CACCTTCTTCCGCACCTATA**AGGA
 E L P R S G A A S A P F T F F R T Y K D

CGGGCTGTGGCGCTTCGAGTCGGCCGCAACCCCGGATGGTTCCTCTGCACCTCCGCCCCG
 G L W R F E S A A N P G W F L C T S A R

Exon 4

CGCCACCAACCCCTGGGGCTCTCCCGCGCCCCGACGCCGCCACGTCCTGGATTTCTA
 A H Q P L G L S R R P D A A H V L D F Y

CTTCAGCTGTGCTGA**G**CCCATCCCCGGGCAATAAAGGCGCTCTGCTCCCCGTTGGGTGG
 F Q L C *

CACCGGCGTCGGTGC GCGCGCTTACCCACCGCGGCTGACGTGGGTGGTGGGGCTGCCCC
 GAAAGGGATGGGCACGGCCCTAAAATGGATGGGCACGGCCCTAAAATGGATGGGCACGGC
 CCTAAAATGGATGGGCACGGCCCCGAAAGGGATGGGCACGGCCCTTCCCGG

Figure 4.16 Structure of exon/intron 4 of chIL-1RN. Above Splicing that leads to the formation of SV2 transcripts is indicated. Intron 4 is usually spliced at the AG splice acceptor site (in bold). However, in SV2 it is spliced at an alternative splice acceptor site (in blue, arrow indicates splice) within exon 4. The polyadenylation signal (AATAAA) downstream of the final exon is underlined.

Next page Use of the alternative splice acceptor site in exon 4 truncates the amino acid sequence compared to that of full-length chIL-1RN.

Chapter 4: Identification, cloning and characterisation of chicken IL-1RN

ATGGCGCTCACCATCGCCCTCCTCCTCCTCCACGCA
M A L T I A L L L L H A

GAGGCTGCCGGATCGGTGCCGTGCCGCGCGCCCGCG
E A A G S V P C R A P A

CTGCAAACCAAAGTCTTCAAATACCGGATCTGGGAT
L Q T K V F K Y R I W D

ATGAACCAGCAGTCGCTGTACCTGCGCGATGATCAG
M N Q Q S L Y L R D D Q

CTGGTGGCCGGGCACCTGCAGGGCGCCAACGCCGCG
L V A G H L Q G A N A A

CTGGAGGAGAAGGTGTTTTGGGTGCCCAACCGCTTC
L E E K V F W V P N R F

TTCAAGCACGAGCTGCAGCCCGTCATCATGGGCATC
F K H E L Q P V I M G I

CGCAACGGCACCCGCTGCCTGGCCTGCCCGGGCGGCC
R N G T R C L A C P A A

CCACAGCCCACCCTGCAGCTCCAGGACGCCGACATC
P Q P T L Q L Q

ACGGAGCTGCCCCGCAGCGGGCGCCGCCTCCGCGCCG

TTACCTTCTTCCGCACCTATAAGGACGGGCTGTGG
D G L W

CGCTTCGAGTCGGCCGCCAACCCCGGATGGTTCCTC
R F E S A A N P G W F L

TGCACCTCCGCCCGCGCCACCAACCCCTGGGGCTC
C T S A R A H Q P L G L

TCCCGGCGCCCCGACGCCGCCACGTCCTGGATTTTC
S R R P D A A H V L D F

TACTTCCAGCTGTGCTGA
Y F Q L C *

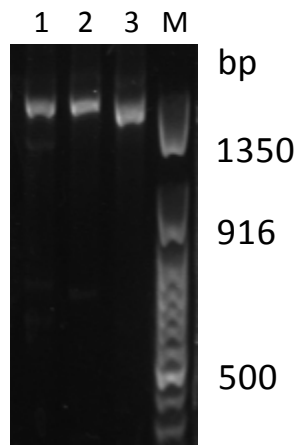


Figure 4.17 Agarose gel of PCR products containing introns 1-4 of chIL-1RN. Products were amplified with IL-1RN Int1-2L1 and IL-1RN 130R primers (see **Fig 4.13**). Lane 1-3 = products amplified from line N genomic DNA in each lane with identical thermal cycling conditions except for differing annealing temperatures of 54.0°C, 52.8°C and 52.0°C respectively. Lane M = 50 bp DNA ladder.

In humans, both first exons of ic and s variants are preceded by large promoters of 1680 bp and 1894 bp in length, respectively. Between exon 1 of icIL-1RN and exon 1 of sIL-1RN is a large intragenic region spanning 9.6 kb (Figure 4.12). In the chicken, however, examination of contig 81757.1 shows the genomic organization at the corresponding region of chIL-1RN differs markedly from this. Here only 129 bp separate the first exons of both variants. Analysis of this sequence using software that characterizes promoter sequences identified a TATA box at 40 nt upstream of the sIL-1RN start codon. This suggests this region may contain a minimal promoter sequence. No other known sequence motifs representing defined promoter elements were identified here (Figure 4.18). Three potential transcription factor binding sites (Sp1 and NF-IL-6 on the forward strand, PU.1 on the complementary strand) were identified upstream of the icIL-1RN start codon at -41 (PU.1), -69 (NF-IL-6) and -88 (Sp1). They may be part of the promoter controlling the sIL-1RN structural variant (Figure 4.18).

4.3.6 Identification of the genomic location

Nine of the human IL-1 genes (ordered centromere to telomere: IL-1 α , IL-1 β , IL-1F7, IL-1F9, IL-1F6, IL-1F8, IL-1F5, IL-1F10 and IL-1RN) are located in a cluster on human chromosome 2, with IL-18 (chromosome 11) and IL-1F11 (chromosome 9) located elsewhere in the genome. According to the chicken genome (v2.1), the chIL-1 β gene is encoded on chromosome 22 at a locus that possesses limited conserved synteny with the human IL-1 gene cluster on chromosome 2 (Chapter 3, Figure 3.1). The avian orthologues of two genes (SLC20A1 and CKAP2L) that flank the human IL-1 gene cluster are located adjacent to chicken IL-1 β , but no other genes are shared by the two loci. A TBLASTN search of this version of the chicken genome with both chIL-1RN amino acid sequence variants did not identify any positive hits. As this gene is present in the IL-1 gene cluster on human chromosome 2, it indicated that the present assembly of the chicken genome does not contain such an obvious locus containing multiple IL-1 family genes. A TBLASTN analysis of the chicken genome (v3.0, unassembled) with both full length chIL-1RN amino acid sequence variants identified two contigs (I.Ds: 81757.1 and 113837.1) containing the majority of the coding sequence as well as novel sequence flanking the first and final exons. These contigs, however, were mined from “removed data” sequence reads and are thus unplaced in the assembled genome; as such, the genomic location of chIL-1RN remains unknown.

Close examination of the locus containing chIL-1 β in build v.2.1 revealed the presence of four sequence gaps immediately adjacent to the 5' end of the gene. The sizes of sequence gaps in the v2.1 genome build are only estimated as 489, 100, 445 and 98 bp in length, respectively. The presence of further chIL-1 family genes in these gaps was investigated by PCR using a BAC, TAM32-21N6, which covers the entire region,

as template. To confirm specific amplification in the region covered by BAC TAM32-21N6, a control PCR to amplify chIL-1 β using this template was included. Positive control PCRs were also set up to amplify chIL-1 β and chIL-1RN using genomic DNA from line 0, 7₂ & 15I chickens, using the same primer pairs. The results confirmed the presence of chIL-1 β at this locus but chIL-1RN did not amplify, suggesting it is encoded elsewhere (Figure 4.19). A further BLASTN analysis of the v3.0 chicken genome build using the original 8.8 kb of sequence from v2.1, including these gaps, was carried out (Figure 4.20). This indicated 1147 bp of this region has been assigned to a contig in v3.0 but the remainder has yet to be assembled and is spread across numerous short contigs in the “removed data” (results not shown). It is not clear from this BLAST search, therefore, whether these sequence gaps will also be present in the third build of the genome.

Following confirmation by PCR that the chIL-1RN gene does not lie adjacent to that encoding IL-1 β , a BAC library representing the Red Jungle Fowl genome was screened with a ³²P-labelled 420 bp icIL-1RN SV2 CDS clone. No positive clones were identified. This experiment was repeated using the full length 492 bp icIL-1RN CDS as a probe, again without success.

4.3.7 Characterization of the 5' untranslated regions (5' UTRs) of icIL-1RN and sIL-1RN cDNA sequences

Attempts were made to determine the 5' UTRs of both chIL-1RN structural variants using 5' RACE, to accurately determine the exact sizes of both secretory and

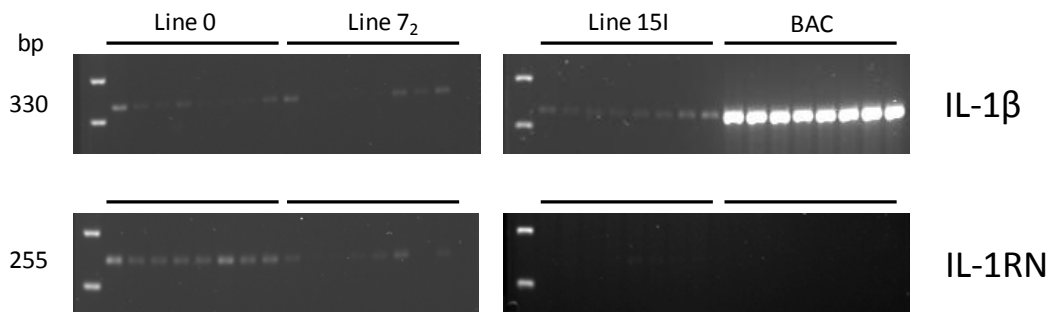


Figure 4.19 Agarose gel electrophoresis of IL-1 β and IL-1RN PCR products in lines 7₂, 15I & 0 genomic DNA and TAM32-21N6 BAC DNA. Examination of the locus containing chIL-1 β shows four sequence gaps are present immediately adjacent to the 5' end of the gene. The gaps were examined for further chIL-1 family genes by PCR using purified TAM32-21N6 bacterial artificial chromosome (BAC) clone DNA, which covers the entire region. To confirm specific amplification in the region covered by the BAC, a control PCR to amplify chIL-1 β using this template was included. Positive control PCRs were set up to amplify chIL-1 β and chIL-1RN in lines 0, 7₂ & 15I genomic DNA, using the same primer pairs as for the BAC DNA PCRs.

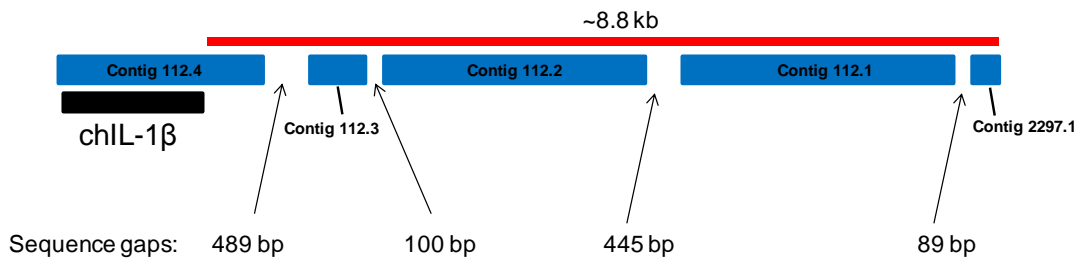


Figure 4.20 Diagram of the locus on chicken chromosome 22 (v2.1) containing IL-1 β and 4 adjacent sequence gaps. Estimated sizes of these gaps are indicated. Blue blocks denote contigs of known sequence. The black box denotes the location of chIL-1 β . The red line indicates coverage of the sequence used to perform a BLASTN search against v3.0 of the unassembled chicken genome sequence reads.

intracellular first exons and to establish how much of the 129 bp separating these exons was 5' UTR, as this could clarify if this region contains a promoter. Prior sequencing of s and ic coding regions revealed that only a very short amount of both 5' ends does not align. The first 36 bp of sIL-1RN and first 6 bp of icIL-1RN are dissimilar, after which the transcripts are identical. Therefore uncovering further unaligned 5' end sequence could provide sufficiently large regions to which variant-specific TaqMan primers and probes could be designed.

A pair of gene-specific primers was designed to amplify a product spanning part of exons 2-4 of the chIL-1RN coding sequence. The reverse primer was used to PCR amplify the 5' UTR, whilst the forward primer created a 219 bp amplicon with the reverse that acted as a positive control to ensure the target transcript was present in the cDNA template. Using RNA from LPS-stimulated HD11 cells as template, the icIL-1RN 5' UTR was amplified along with the positive control. Agarose gel electrophoresis of the PCR products revealed two bands, a larger band at ~ 480 bp and a smaller band at ~ 430 bp (Figure 4.21). Both bands were gel purified and TA-cloned into the pTarget mammalian expression vector; clones were screened by *EcoRI* restriction digestion and sequenced. Sequencing revealed both bands were icIL-1RN clones, with the smaller of the two corresponding to the icIL-1RN SV1 transcript previously identified. The chicken icIL-1RN 5' UTR was found to be 50 bp in length. This novel sequence was absent in all chIL-1 EST sequences mined from NCBI. By comparison, the 5' UTR of both human icIL-1RN1 and RN2 transcripts is longer at 122 bp. The PCR was repeated to attempt to elucidate the 5' UTR of the sIL-1RN transcript. To ensure the RACE PCR template contained this transcript, an RT-PCR using the total RNA isolated from LPS-stimulated HD11 cells was carried out in advance. The same primers and conditions

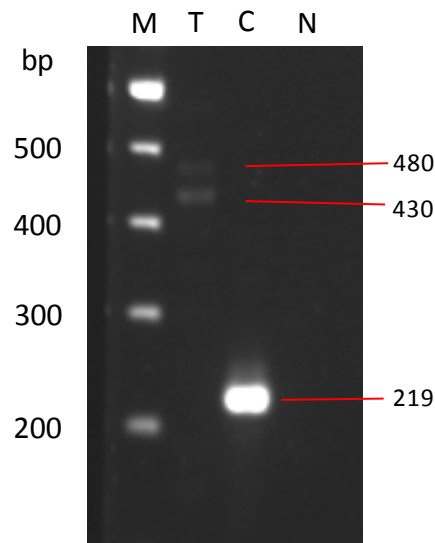


Figure 4.21 Agarose gel electrophoresis of 5' RACE PCR products. cDNA was made from RNA from LPS-stimulated HD11 cells using Superscript II reverse transcriptase. PCR was carried out to amplify the 5' UTR of chIL-1RN using gene-specific primers. M = 100 bp DNA ladder; T = test reaction. The 5' UTR of chicken icIL-1RN was amplified with the universal forward primer and the gene-specific reverse primer. C = positive control reaction to ensure the target transcript was present in the template used to make cDNA. ChIL-1RN was amplified from the cDNA template using a pair of gene-specific primers. N = negative control. The PCR set up for this reaction was identical to the test reaction except for the absence of the universal primer.

used to previously amplify the full length sIL-1RN coding region cDNA were used again, confirming this mRNA was present in the sample (Figure 4.22). Despite this, I was unable to subsequently amplify this 5' UTR, as this particular RACE PCR appears to always preferentially amplify the icIL-1RN variant.

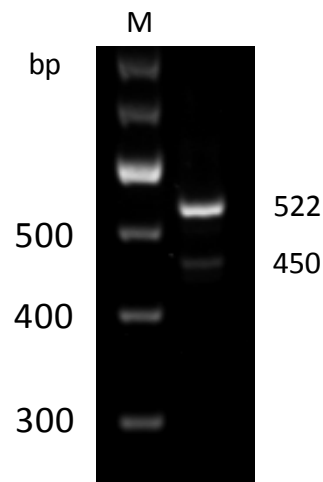


Figure 4.22 Agarose gel electrophoresis of sIL-1RN RT-PCR products. For the 5' RACE PCRs, cDNA was made from RNA from LPS-stimulated HD11 cells. Repeated attempts were unable to amplify the sIL-1RN 5' UTR using this template. To ensure the RACE PCR template contained the sIL-1RN transcript, RT-PCR using the total RNA isolated from HD11 cells was carried out in advance of cDNA synthesis. The same primers and thermal cycling conditions used to amplify the full length sIL-1RN coding region cDNA were used. M = 100 bp DNA ladder.

4.4 Discussion

The genomes of many eukaryotic species contain a pair of genes, IL-1 α and IL-1 β , whose proteins are responsible for multiple immune activities. Of these, their ability to induce inflammation has been the focus of most research efforts to characterise their biology. A naturally occurring receptor antagonist, IL-1RN, inhibits the bioactivity of IL-1 α and IL-1 β through cell surface receptor blocking. Subsequently identified isoforms act intracellularly to limit inflammation. The gene for IL-1RN has been found in many mammalian species and for years was considered to have arisen following gene duplication in the mammalian lineage.

In this Chapter, the identification and characterization of both secretory and intracellular variants of interleukin-1 receptor antagonist in the chicken is described. Whilst obvious similarities between the chicken gene and its mammalian orthologues exist, a number of notable differences were identified.

Given the potency of IL-1 β in immune responses, its regulation by IL-1RN is essential to avoid possible physical damage to the host organism. Humans either lacking or possessing mutations in the IL-1RN gene can die prematurely in the absence of treatment with synthetic IL-1RN (Aksentijevich, Masters et al. 2009). Following the identification of IL-1 β in the chicken (Weining, Sick et al. 1998), it was therefore likely that IL-1RN would also be present. The conserved locus containing chIL-1 β exhibits limited synteny with the human IL-1 gene locus but lacks any further IL-1 genes. TBLASTN analyses of the chicken genome with the chIL-1 β amino acid sequence did not reveal any further IL-1 gene loci. Using the chIL-1 β amino acid sequence, the NCBI databases were mined for ESTs encoding apparent novel chicken IL-1 genes. Using the predicted amino acid sequences of the ESTs, TBLASTN analysis identified them as the

chicken orthologue of IL-1RN. Further analysis of two IL-1RN ESTs differing at the 5' end identified both secretory and intracellular variants of the gene. Chicken sIL-1RN contains a predicted 17 amino acid signal peptide and is presumably secreted by the endoplasmic reticulum/golgi secretory pathway (Eisenberg, Evans et al. 1990; Walter and Johnson 1994). A relatively high degree of amino acid identity between the predicted chIL-1RNs and mammalian homologues was found. Further *in silico* analyses confirmed both chicken sequences are genuine IL-1 family members. Phylogenetic analysis was able to confirm they are distantly related to mammalian IL-1RN.

As both structural variants of human IL-1RN are expressed by macrophages (Arend, Malyak et al. 1998), RNA from LPS-stimulated HD11 cells (a macrophage-like cell line) was used to amplify full length chicken sIL-1RN and icIL-1RN CDS sequences. Two additional splice variants of both, designated SV1 and SV2, were identified upon examination of the resulting RT-PCR products. Both SV1 transcripts appear to be formed following exon skipping, whilst the SV2s utilise an alternative splice acceptor site in the final exon of the gene. A number of conserved sequence motifs synonymous with exon skipping (Miriami, Margalit et al. 2003) were identified in the introns adjacent to the spliced exon in SV1, although their relative locations and abundance did not conform to the described patterns found in mammalian introns. This exon skipping event caused the predicted amino acid sequence to change reading frame, introducing a premature stop codon, significantly truncating the molecule. Although the predicted SV2 amino acid sequences are in frame, potentially important residues corresponding to two β -sheets of the secondary structure have been removed by this splicing event. As yet, there are no reports of truncated splice variants of IL-1RN in mammals, suggesting a novel mechanism of regulating this gene has been found.

Alternatively, chIL-1RN may be prone to introducing splicing errors at the pre-mRNA stage.

Attempts to determine the genomic location of chIL-1RN were unsuccessful. Despite this, the identification on chromosome 22 of an IL-1 gene locus sheds new light on what is known regarding the evolution of this cytokine gene family. Firstly, the existence of IL-1RN in the chicken (in addition to IL-1 β) supports Eisenberg, Brewer et al. (1991) who predicted IL-1RN and IL-1 β evolved from a common ancestral gene ~350 million years ago. It is believed that the chicken and human have evolved separately for ~310 million years (Hedges, Parker et al. 1996). Results obtained in this study, however, do not support a straightforward explanation of IL-1 gene family evolution from a common ancestor. BLAST data confirmed both chicken gene variants are unquestionably IL-1 receptor antagonists. This was supported by clear evidence of secretory and intracellular variants and structural similarity with the human gene. However, chIL-1RN did not group with the orthologous mammalian genes in phylogenetic analysis. There are several hypotheses to explain this. It is possible that chIL-1RN and mammalian IL-1RN emerged by species-specific convergent evolution. Alternatively, the IL-1RNs evolved from a common ancestor followed by sequence, and possibly functional, divergence in the avian lineage. Although either is possible, I believe the latter is most likely given the number of structural similarities between the chicken and human genes. Cytokine genes are under extreme selective pressure and tend to evolve rapidly, so it is not surprising that avian cytokines exhibit limited sequence homology with mammalian equivalents. This has been a fundamental stumbling block to finding novel chicken cytokine orthologues, and as such, progress has been slow in this area compared to mammals (Kaiser, Poh et al. 2005). I therefore

believe the phylogenetic analysis reflects substantial sequence divergence in the genuine avian IL-1RN orthologue rather than the identification of a novel avian IL-1F gene.

The presence of IL-1RN in the chicken at a location elsewhere from IL-1 β suggests the evolution of the nine gene IL-1 cluster took place before the diversification of birds and mammals. An alternative hypothesis of differential gene loss within different species may also explain how IL-1RN has arisen at discordant loci in humans and chickens. Assuming the three human IL-1 loci constitute regions of the genome containing paralogous genes, their origins could be traced to a single ancestral locus which underwent duplication. This ancient locus could have contained both IL-1 β and IL-1RN, which upon subsequent genome duplication formed several paralogous IL-1 loci each encoding a copy of both genes. Additional duplications in the human genome may have expanded the size of the IL-1 gene family at one locus, whilst the other may have contracted, conceivably leaving only IL-33. In the chicken, one locus could have lost IL-1RN, whilst retaining IL-1 β ; with the opposite scenario taking place at a second locus.

It is interesting to observe that whilst the IL-1 locus in the chicken has become fragmented, it has remained relatively intact in most mammalian species for >300 million years. It would be interesting to investigate whether the human IL-1 locus has remained intact through genetic linkage. Additionally, the locus may also be under a degree of global regulation, such as that provided by an upstream locus control region. In either instance, the chicken presumably lacks any equivalent linkage or control mechanisms affecting its IL-1 ligand genes.

Elucidation of the chIL-1RN gene structure provided an interesting insight into how its regulation may differ from its mammalian orthologue. The expression of human

sIL-1RN is controlled by a 1680 bp promoter; however, the anticipated location of an equivalent promoter in the chicken, between exon 1 of sIL-1RN and exon 1 of icIL-1RN, was only 129 bp in length. A TATA box at -40 nt from the chicken sIL-1RN start codon suggested this variant may be driven by a minimal promoter sequence with a maximum length of 89 nt. No other known sequence motifs representing defined promoter elements were identified within this 89 nt region, suggesting different potential mechanisms for regulation of this chIL-1RN variant. Firstly, the human sIL-1RN promoter contains three LPS responsive elements (LRE) comprised of NF- κ B and PU.1 binding sites. These are completely absent between the TATA box and exon 1 of icIL-1RN in the chicken sequence. This sequence may not actually represent a promoter and chIL-1RN may, in fact, have evolved a different regulatory mechanism whereby both variants are controlled by a single promoter preceding exon 1 of icIL-1RN. The TATA box could, thus, be the remnants of where a promoter used to be. Alternatively, chicken sIL-1RN may only require a very short minimal promoter and may not, in contrast to mammals, need LREs to respond to LPS stimulation. Analysis of regulatory elements upstream of the icIL-1RN start codon identified three potential transcription factor binding sites (Sp1 and NF-IL-6 on the forward strand; PU.1 on the complementary strand) suggestive of a promoter sequence (Figure 4.18). Both Sp1 and NF-IL-6 binding sites were identified within the human icIL-1RN promoter (Jenkins, Drong et al. 1997). Further upstream genomic sequence is required for a thorough analysis of the potential promoter. It remains to be determined if this region only controls icIL-1RN transcripts or is also able to direct transcription of the sIL-1RN structural variant. In mammals, sIL-1RN and icIL-1RN expression are independently driven by separate promoters located proximally to their transcripts' first exons (see

Figure 4.12). It will be interesting to determine if chIL-1RN has evolved to accommodate a more promiscuous promoter. Interestingly, IL-1 α is an important regulator of icIL-1RN transcription in mouse keratinocytes (La, 2001). C/EBP and NF- κ B binding sites are essential for the modulation of this function. A chicken IL-1 α gene has yet to be identified, and neither C/EBP nor NF- κ B response elements are located in the first 123 bp upstream of the icIL-1RN start codon. Once the full genome sequence upstream of chIL-1RN is available, potential promoter regions could be cloned and functionally characterized in a reporter gene assay.

Further analysis of the chIL-1RN gene structure indicated the chicken may possess a relatively limited repertoire of IL-1RN protein isoforms compared to humans. Chicken icIL-1RN is most similar to human icIL-1RN1, containing a single upstream exon spliced into the 5' end of the sIL-1RN mRNA. Human icIL-1RN2 contains a further upstream exon spliced in between exons 1 and 2 of icIL-1RN1. This exon in the huIL-1RN gene is located between the first exons for icIL-1RN1 and sIL-1RN, but there is no equivalent in the chicken. This suggests the existence of a chicken icIL-1RN2-like transcript is unlikely. Human icIL-1RN3 is formed through use of an alternative translation initiation site within exon 1 of the sIL-1RN transcript. Amino acid alignments between the chicken and human show the chicken sequence contains a methionine separated by 7 residues from the icIL-1RN3 initiation site in the human sequence. At present, there is no evidence that a chicken icIL-1RN3 isoform exists.

Chapter 5

Results 3: Characterisation of expression and bioactivity of chicken IL-1RN

5.1 Introduction

Inflammation is an important process which forms part of an organism's response to restrict the impact of invading pathogens in order to maintain homeostasis. IL-1 α and IL-1 β are two examples of cytokines that induce inflammation by priming the innate immune response (Dinarello 2009). Their functional effects are exerted through a common, shared receptor, IL-1 receptor I (IL-1RI). In excess and without regulation, inflammation mediated by IL-1 α and IL-1 β can cause significant damage to the host. Their production at both mRNA and protein levels is therefore precisely controlled. In addition to this, a naturally occurring antagonist, IL-1 receptor antagonist (IL-1RN), acts to reduce IL-1 effects by physically occupying the IL-1RI (Carter, Deibel et al. 1990; Eisenberg, Evans et al. 1990; Hannum, Wilcox et al. 1990). This prevents signal transduction (Dripps, Brandhuber et al. 1991) and consequently gene transcription, as IL-1RN lacks the specific amino acids required to engage IL-1RAcP on the cell surface (Schreuder, Tardif et al. 1997; Wang, Zhang et al. 2010). The only apparent function of IL-1RN is to limit inflammation. It does not act as an agonist, as demonstrated by the lack of a response observed after administering humans with a million-fold excess (over IL-1 α and IL-1 β) of IL-1RN (Dinarello 1996).

In mammals, there are two major structural variants of *IL-1RN* – secretory (sIL-1RN) (Eisenberg, Evans et al. 1990) and intracellular (icIL-1RN). Alternative splicing of the *IL-1RN* gene gives rise to three protein isoforms of icIL-1RN in humans (Haskill, Martin et al. 1991; Muzio, Polentarutti et al. 1995; Malyak, Guthridge et al. 1998). The biological activity of IL-1RN has been quantified using a number of different methods. The first study to demonstrate IL-1RI-specific binding by sIL-1RN showed both

recombinant and native forms inhibited the binding of ^{125}I -labelled IL-1 α to EL4-6.1 cells, a murine thymoma cell line which is responsive to IL-1 stimulation (Hannum, Wilcox et al. 1990). An alternative bioassay was subsequently described, showing sIL-1RN inhibited IL-1 α and IL-1 β -mediated proliferation of PHA-stimulated murine thymocytes (Arend, Welgus et al. 1990). Characterisation of icIL-1RN1 bioactivity was based on the same principal (IL-1RI blocking), and showed this protein inhibited IL-1 β -mediated IL-2 production from the LBRM-33-1A5 murine thymoma cell line (Haskill, Martin et al. 1991). Recombinant icIL-1RN1 was expressed in COS-7 cells and both supernatants and lysates were tested in the assay. Results showed significantly more activity in the lysate, confirming this protein was a genuine intracellular isoform. The second major icIL-1RN isoform to be discovered (icIL-1RN2) inhibited the IL-1 β -mediated expression of E-selectin on cultured endothelial cells (Muzio, Polentarutti et al. 1995). As with icIL-1RN1, this cDNA was expressed in COS-7 cells with the majority of the protein found in the lysate. Of note, this protein has never been detected *in vivo* (Arend, Malyak et al. 1998; Arend, Palmer et al. 2008) beyond the original paper describing its discovery. Finally, the bioactivity of icIL-1RN3 (referred to as IL-1RaII in the paper) was established (Malyak, Guthridge et al. 1998) using the identical murine thymocyte proliferation assay previously described (Arend, Welgus et al. 1990).

Whilst the biological role of sIL-1RN appears to be limited to the blocking of IL-1RI on the cell surface, the icIL-1RN isoforms seem to function through any of three possible mechanisms. Firstly, icIL-1RN may exert intracellular effects in a non-classical (non-IL-1R-dependent) manner. For instance, when keratinocytes are cultured in the presence of IL-1 α , icIL-1RN1 binds to the third component of the COP9 signalosome, an important protein kinase involved in signal transduction. This causes inhibition of

downstream pro-inflammatory cytokine production (Banda, Guthridge et al. 2005).

Secondly, icIL-1RN1 may act within the nucleus to inhibit the effects of IL-1 α . Briefly, either full length IL-1 α (preIL-1 α) or its N-terminal propiece (NIL-1 α) increased the motility of ECV304 cells, a human endothelial cell line, following stable transfection. This effect was significantly attenuated when icIL-1RN was co-expressed with either (Merhi-Soussi, Berti et al. 2005). Thirdly, icIL-1RN isoforms may be released from cells and act in a similar way to sIL-1RN by antagonising membrane-bound IL-1RI (Corradi, Franzi et al. 1995; Levine, Wu et al. 1997; Yoon, Zhu et al. 1999; Evans, Dower et al. 2006).

The expression of *IL-1RN* has been studied in substantial depth in humans and mice and also in other mammals, although less thoroughly. Interestingly, although sIL-1RN mRNA has been predicted to be expressed in any cells able to transcribe IL-1 α and IL-1 β (Arend, Malyak et al. 1998), a global assessment of its expression in humans has never been carried out. The vast majority of studies have focussed on its expression in monocytes, macrophages, neutrophils and fibroblasts (Arend, Malyak et al. 1998). The expression of mammalian icIL-1RN is highly restricted, being found in only a narrow range of cell types. The icIL-1RN1 protein is predominantly found in endothelial cells, epithelial cells, fibroblasts, keratinocytes, and macrophages (Arend, Palmer et al. 2008), whereas icIL-1RN3 is mainly found in neutrophils, PBMCs (Malyak, Smith et al. 1998) and hepatocytes (Arend, Palmer et al. 2008). Although its expression *in vivo* has never been reported beyond the original study, icIL-1RN2 transcripts were detected in fibroblasts, keratinocytes, monocytes and polymorphonuclear cells (Muzio, Polentarutti et al. 1995).

The only published studies to date investigating global IL-1RN expression were

carried out in rabbits (Apostolopoulos, Ross et al. 1996; Matsukawa, Fukumoto et al. 1997) and mice (Gabay, Porter et al. 1997). Expression of sIL-1RN was constitutive in all nine tissues analysed in rabbits, with expression of icIL-1RN found in only caecum, kidney, skin and thymus (Matsukawa, Fukumoto et al. 1997). In mice, expression of IL-1RN was not ubiquitous, with sIL-1RN undetectable in unstimulated tissues and icIL-1RN only expressed in skin. LPS stimulation of the same tissues induced sIL-1RN expression in liver, lung and spleen and increased the amount of icIL-1RN expression in skin (Gabay, Porter et al. 1997). This study used a ribonuclease protection assay to quantify expression levels and so may have lacked the degree of sensitivity obtained with real-time qRT-PCR. Although the data were not shown, icIL-1RN transcripts were also amplified by RT-PCR in kidney, liver and spleen tissues stimulated with LPS (Gabay, Porter et al. 1997). Expression of a novel IL-1F gene (IL-1RN-like) was quantified by real-time qRT-PCR in rainbow trout and was constitutive in the eight tissues examined (Wang, Bird et al. 2009).

An enormous number of different agents induce IL-1RN expression with LPS, adherent IgG and the cytokines GM-CSF and IL-4 the most effective substances *in vitro* (Arend, Malyak et al. 1998). A similarly broad number of agents induce IL-1RN production *in vivo*. These include virtually all known bacteria and viruses, many fungi, as well as numerous cytokines, enzymes and plasma proteins (Dinarello 1996). IL-1RN protein levels also increase in many disease states including autoinflammation, autoimmunity, allergies, and injury (amongst others) (Arend, Malyak et al. 1998).

Of the many agents known to increase IL-1RN expression, the response to LPS-stimulation is the most comprehensively understood. In particular, the kinetics of IL-1RN expression *in vitro* has been resolved in detail. After LPS stimulation, human

blood monocytes rapidly express sIL-1RN, with protein apparent in the Golgi around 4-6 h later as transcript levels begin to decline. After 12 h, icIL-1RN expression starts to increase, becoming the predominant transcript by 24 h (Dinarello 1996). In monocytes and macrophages stimulated with LPS for a sustained period, tolerance develops leading to decreased cytokine production upon subsequent stimulation. Unlike certain cytokines, such as IL-10 and TNF α whose levels decline, the expression of IL-1RN remains unaffected, continuing to increase in response to endotoxin challenge (Randow, Syrbe et al. 1995).

The differential expression of IL-1RN and IL-1 β has also been examined in LPS-stimulated leukocytes. In freshly isolated monocytes, mRNA and protein levels of both IL-1RN and IL-1 β are almost identical following LPS stimulation. Following *in vitro* differentiation into macrophages, relative mRNA expression levels alter markedly in these cells. Increased constitutive expression of IL-1RN is observed; however, IL-1 β expression is lower both constitutively and after LPS stimulation (Arend, Smith et al. 1991).

In this Chapter, thorough analyses of both chIL-1RN expression and biological activity are described.

5.2 Methods

5.2.1 Sources of chicken tissues and cells

All chicken tissues and cells were acquired, sorted and stimulated as described in Chapter 2, section 2.4.1.1. Tissues and cells were acquired from SPF chickens challenged with bacteria or virus as described in Chapter 2, section 2.4.1.2.

5.2.2 HD11 time course stimulation

HD11 cells were routinely cultured as described in Chapter 2, section 2.4.12.1 and 2.4.12.2. Cells were stimulated with LPS as described in Chapter 2, section 2.4.16.

5.2.3 Transfecting cells with pure chicken DNA

5.2.3.1 Transient protein expression in COS-7 cells

COS-7 cells were transiently transfected by the DEAE/dextran method with endotoxin-free chicken sIL-1RN SV1, sIL-1RN SV2, icIL-1RN, icIL-1RN SV1 and icIL-1RN SV2 clones (in pTargetT) and pCI-neo (lacking an insert) as described in Chapter 2, section 2.4.12.3.1. COS cell lysates were generated as described in Chapter 2, section 2.4.12.3.1.

5.2.3.2 Transient protein expression in HEK293T cells

HEK293T cells were transiently transfected with endotoxin-free chicken mature sIL-1RNpHLSec and icIL-1RNpHLSec clones as described in Chapter 2, section 2.4.12.3.2.

5.2.4 Purification and analysis of HIS-tagged recombinant proteins

Recombinant mature sIL-1RNpHLSec and icIL-1RNpHLSec proteins were purified from crude HEK293T culture supernatants under native conditions as described in Chapter 2, section 2.4.13.1. Proteins were analysed by SDS-PAGE and Western blotting as described in Chapter 2, sections 2.4.14.1 and 2.4.14.2. Pure proteins were quantified using the Bradford assay. Briefly, a series of protein standards (0, 250, 500, 750 and 1500 µg BSA/ml) in 0.15 M NaOH (both Sigma) and a 10-fold serial dilution series of the chIL-1 proteins were generated. To a 100 µl aliquot of each of the standard and test samples, 5 µl of Coomassie Brilliant Blue (Bio-rad) were added, mixed, and the absorbance measured at 595 nm. ChIL-1 protein concentrations were calculated from the standard curve.

5.2.5 HD11 bioassay

5.2.5.1 Pilot assay set up

To determine the suitability of the HD11 cell line for characterisation of chIL-1RN bioactivity, a pilot study was carried out, testing the ability of the cell line to respond to stimulation with chIL-1β as described in Chapter 2, section 2.4.15.1.

The optimal concentration of recombinant chicken IL-1β (rchIL-1β) (AMSBio) to use in “test” assays was determined. HD11 cells were seeded in a 24-well plate at 1×10^6 cells/well. The cells were stimulated with a double dilution series of rchIL-1β (range: 166.6-5.21 ng/ml) and cultured overnight at 41°C, 5% CO₂. The next day, culture media was tested for nitrite using the Griess reaction as outlined in Chapter 2, section 2.4.15.2.1.

To test the ability of rchIL-1 β (AMSBio) to stimulate HD11 cells and sustain IL-1 β mRNA levels for 24 h, seven T25 flasks of HD11 cells were seeded at 2×10^6 /flask and cultured overnight at 41°C, 5% CO₂. The next day, culture media were replaced with fresh media containing 200 ng/ml LPS and cells were stimulated for 0, 1, 2, 4, 8, 12 and 24 h. At each time-point, cells were lysed with 600 μ l RLT buffer (Qiagen) and lysates frozen at -80°C.

5.2.5.2 Final bioassay conditions

Optimal bioassay conditions were determined empirically and all assays described in this Chapter were carried out under these conditions as outlined in Chapter 2, section 2.4.15.3.2.

5.2.5.3 Quantifying the biological response

The concentration of nitrites (NO₂⁻) was measured in HD11 culture supernatants by the Griess reaction as outlined in Chapter 2, section 2.4.15.2.1. IL-1 β and iNOS mRNA levels were quantified by TaqMan® as described in Chapter 2, sections 2.4.4.6 and 2.4.15.3.2 and this Chapter, section 5.2.6. Primer and probe sequences are provided in Appendix II.

5.2.6 Total RNA isolation and real-time qRT-PCR (TaqMan®) analysis of chicken mRNA expression

RNA was extracted from the tissues and cells used in this Chapter as described in Chapter 2, sections 2.4.2.1 and 2.4.2.2.

Primers and probes to detect expression of IL-1 β , iNOS and 28S were designed

using Primer Express (Applied Biosystems) as described in Chapter 2, section 2.4.4.6. For chIL-1RN, it was not possible to design TaqMan® assays with sufficiently long amplicons to distinguish between each of the 6 identified variants. This was due to a combination of the GC-rich nature of chIL-1RN transcripts and the stringent primer and probe design parameters. Three different TaqMan® primer/probe sets were designed to detect expression of full-length (IL-1RN_{fl}), splice variant 1 (IL-1RN_{SV1}) and splice variant 2 (IL-1RN_{SV2}) transcripts. Standard probes labelled at the 5' end with 5- or 6-carboxyfluorescein (FAM) fluorophore, and at the 3' end with tetramethylrhodamine (TAMRA) quencher dye were used to detect IL-1RN_{fl} expression. Probes used to detect IL-1RN_{SV1} and IL-1RN_{SV2} transcripts were labelled with FAM at the 5' end and dihydrocyclopyrroloindole tripeptide minor groove binder (MGB) at the 3' end. Assays were performed as described in Chapter 2, section 2.4.4.6.

5.3 Results

5.3.1 Analysis of IL-1RN mRNA expression in unstimulated tissues by real-time qRT-PCR

The expression of IL-1RN_{fl} mRNA was determined in a broad range of chicken tissues by qRT-PCR (Figure 5.1). Expression of full-length IL-1RN was ubiquitous, with highest levels in lymphoid tissues in the bone marrow and blood. These findings are consistent with IL-1RN production in mammals which is highest in monocytes and macrophages (Arend, Malyak et al. 1998). In non-lymphoid tissues, expression was highest in brain and lung. Constitutive expression of IL-1RN has been detected in rat brain (van Dam, Poole et al. 1998) and human bronchial epithelial cells (Coulter, Wewers et al. 1999).

5.3.2 Analysis of IL-1RN mRNA expression by real-time qRT-PCR in sorted lymphocyte subsets

Constitutive expression of IL-1RN_{fl} was detected in the entire cell panel. Of the 20 different populations investigated, KUL01⁺ cells (macrophages) and blood-derived monocytes (with or without LPS stimulation) showed the highest expression levels (Figure 5.2). Stimulation of several cell subsets with LPS did not lead to an increase in expression levels except in the monocyte population. In bone marrow-derived dendritic cells (BM-DC) and bone marrow-derived macrophages (BM-MØ), LPS stimulation decreased expression levels of IL-1RN_{fl}. LPS-stimulation had no effect on expression levels in heterophils.

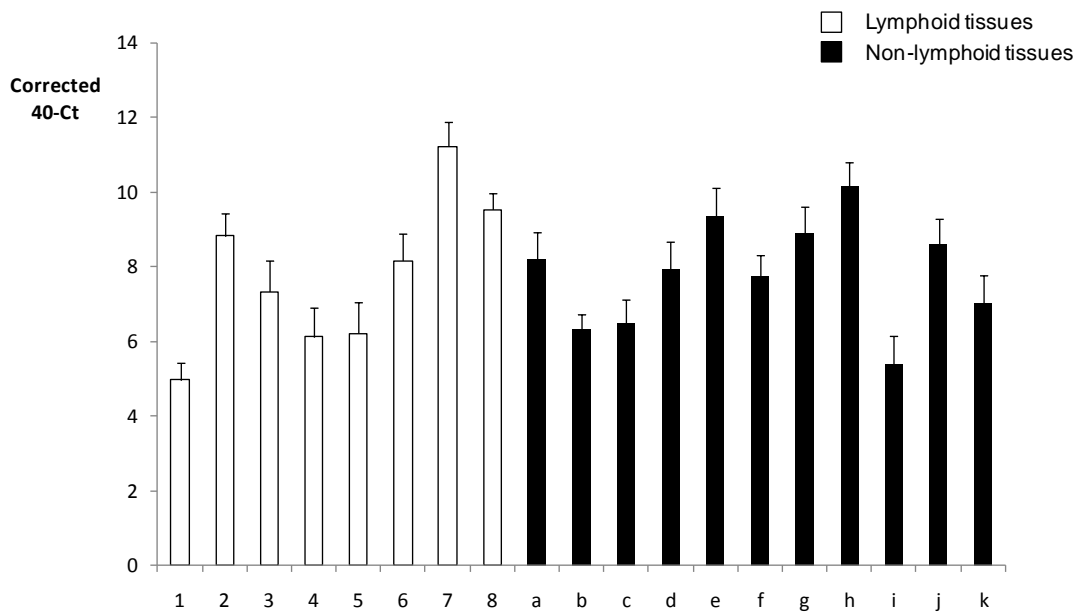


Figure 5.1 IL-1RN_{fl} expression in lymphoid and non-lymphoid tissues as measured by real-time qRT-PCR. Results are expressed as corrected 40-Ct +SEM of three replicates from a single sample. Lymphoid: 1, bursa of Fabricius; 2, caecal tonsil; 3, Meckel's diverticulum; 4, spleen; 5, thymus; 6, Harderian gland; 7, bone marrow; 8, blood; Non-lymphoid: a, lower gastrointestinal tract (GIT); b, mid-GIT; c, upper GIT; d, kidney; e, lung; f, heart; g, muscle; h, brain; i, skin; j, caecal wall; k, liver.

5.3.3 Analysis of IL-1RN mRNA expression across a time course in three different populations of stimulated macrophages

To gain an understanding of IL-1RN mRNA expression across a time course, three different populations of macrophages were stimulated in culture. Expression was assessed in *in vitro* cultured HD11 cells stimulated with LPS from 0-24 h. Expression was also measured in two *ex vivo* populations, bone marrow-derived macrophages (BM-MØ) and blood monocyte-derived macrophages (Mo-MØ), stimulated with LPS or CD40L for 1-48 h.

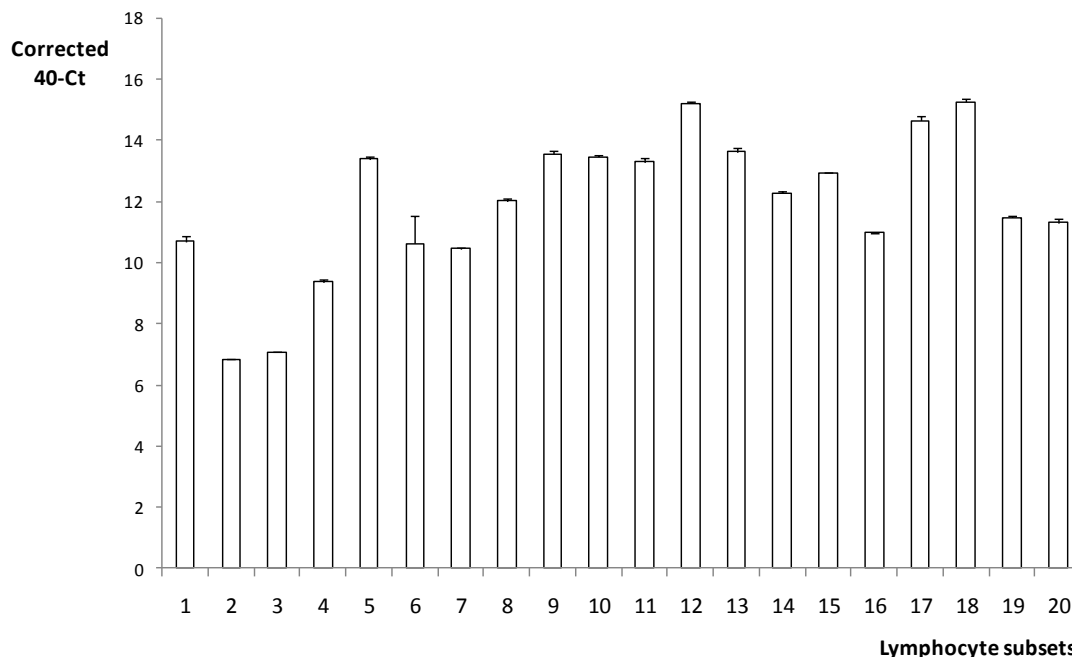


Figure 5.2 IL-1RN_{fl} expression in sorted chicken lymphocyte subsets as measured by real-time qRT-PCR. Results are expressed as corrected 40-Ct +SEM of three replicates from a single sample. Bars represent expression in: 1, splenocytes; 2, bursal cells; 3, PMA-stimulated bursal cells; 4, thymocytes; 5, CD4+ cells; 6, CD8 α + cells; 7, CD8 β + cells; 8, TCR1+ cells; 9, TCR2+ cells; 10, TCR3+ cells; 11, Bu-1+ cells; 12, KULO1+ cells; 13, BM-DC; 14, LPS-stimulated BM-DC; 15, BM-M Φ ; 16, LPS-stimulated BM-M Φ ; 17, blood-derived monocytes; 18, LPS-stimulated blood-derived monocytes; 19, heterophils; 20, LPS-stimulated heterophils.

In the HD11 macrophage cell line, full length IL-1RN (IL-1RN_{fl}) expression remained constant from 0-24 h (Figure 5.3), seemingly unaffected by the presence of LPS at any of the time-points investigated. At 48 h post-stimulation (hps), substantial cell death had occurred (data not shown), effectively ending the assay. By contrast, the expression of IL-1 β in the same cells was significantly affected by LPS, increasing by >300-fold after 1 hps. Expression remained constant from 1-12 hps, and began to noticeably decrease by 24 hps.

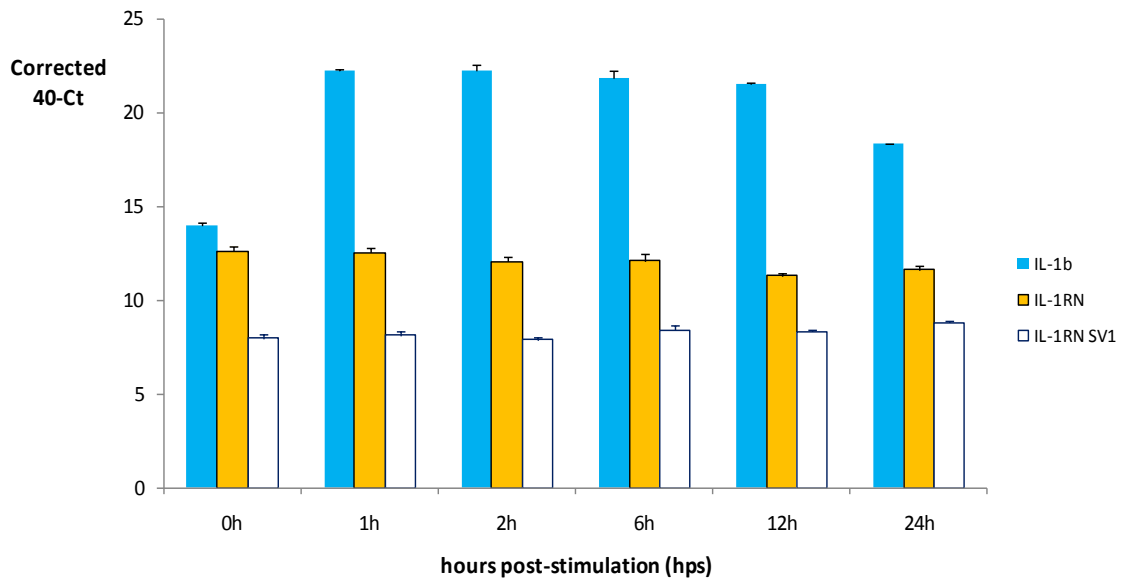


Figure 5.3 Expression of IL-1RN_{fl}, IL-1RN_{SV1} and IL-1β in the HD11 macrophage cell line following stimulation with LPS as measured by real-time qRT-PCR. Results are expressed as corrected 40-Ct ± SEM of three samples from single flasks.

In primary BM-MØ stimulated with LPS or CD40L, IL-1RN_{fl} expression did not significantly increase when compared with unstimulated controls over the entire 48 h period (Figure 5.4). IL-1RN splice variant 1 expression (IL-1RN_{SV1}), whilst relatively lower at all of the time-points, exhibited a similar expression profile to IL-1RN_{fl} (Figure 5.5). At 2 hps, IL-1RN_{SV1} expression in both LPS-stimulated and CD40L-stimulated cells was >2-fold greater than control cells; however, this difference was not statistically significant. A similar magnitude of difference in IL-1RN_{SV1} expression was observed between LPS-stimulated and control cells at 4 hps, which again was not significant.

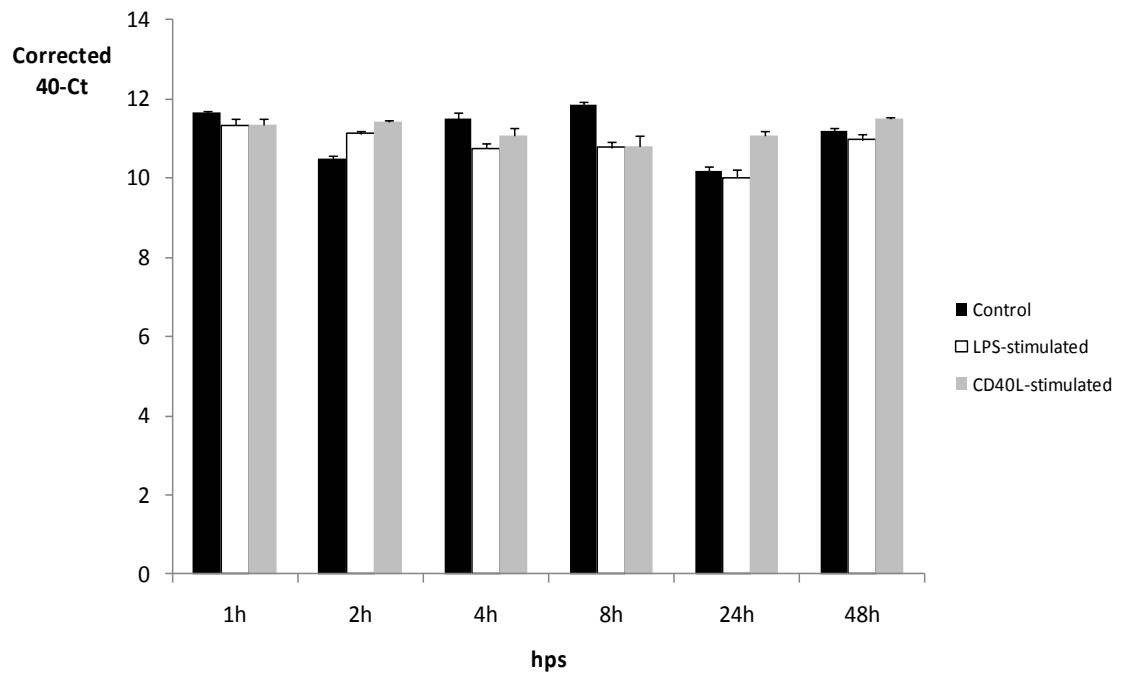


Figure 5.4 Expression of IL-1RN_{fl} in BM-MØ stimulated with LPS or CD40L. Results are expressed as corrected 40-Ct ± SEM of three replicates from a single sample. hps = hours post-stimulation.

A similar profile to that for BM-MØ was also observed for IL-1RN_{fl} expression in Mo-MØ stimulated with LPS or CD40L (Figure 5.6). A noticeable difference in expression (2.6-fold) was seen between control cells and cells stimulated for 24 h with CD40L, however, it was not statistically significant. At all other time-points with both stimuli, there were no statistically significant differences in expression levels from those in control cells. The expression of IL-1RN_{SV1} mRNA in Mo-MØ (Figure 5.7) was distinctly different to its expression in BM-MØ and to IL-1RN_{fl} expression in the same cells. LPS-stimulation at 1, 2, 8 and 12 hps led to a large increase in expression (from 3- to 4.3-fold) compared with controls, although this was not statistically significant. At 4 hps, however, LPS-stimulated Mo-MØ exhibited lower IL-1RN_{SV1} mRNA expression. By 24 h, IL-1RN_{SV1} expression levels were 2.8-fold lower in LPS- stimulated Mo-MØ

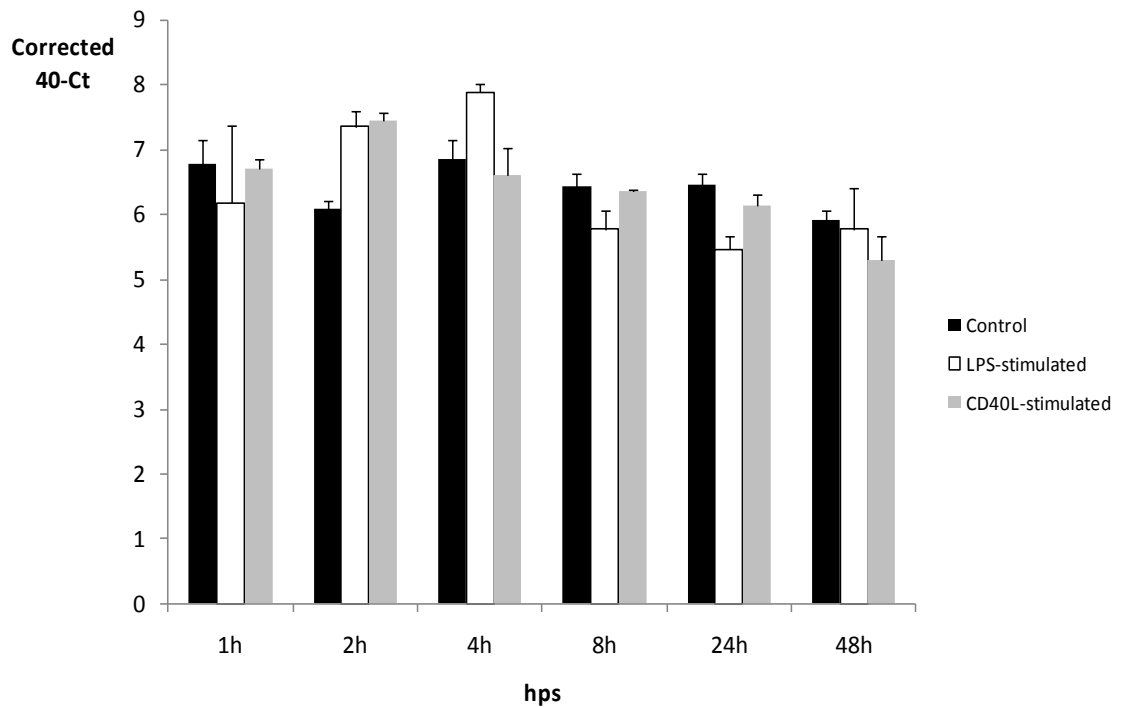


Figure 5.5 Expression of IL-1RN_{SV1} in BM-MØ stimulated with LPS or CD40L. Results are expressed as corrected 40-Ct ± SEM of three replicates from a single sample. hps = hours post-stimulation.

compared to control cells. This difference was even greater at 48 hps, being equivalent to a 3.95-fold decrease. Following CD40L stimulation, IL-1RN_{SV1} expression was higher than in control cells at 4, 8 and 12 hps, although relative increases were lower than in LPS-stimulated Mo-MØ. As with LPS, expression levels following CD40L stimulation were much lower than in control cells at 48 hps.

5.3.4 Analysis of IL-1RN expression in vivo by qRT-PCR following bacterial or viral challenge

IL-1RN mRNA expression was determined by qRT-PCR in a common viral and a common bacterial challenge model.

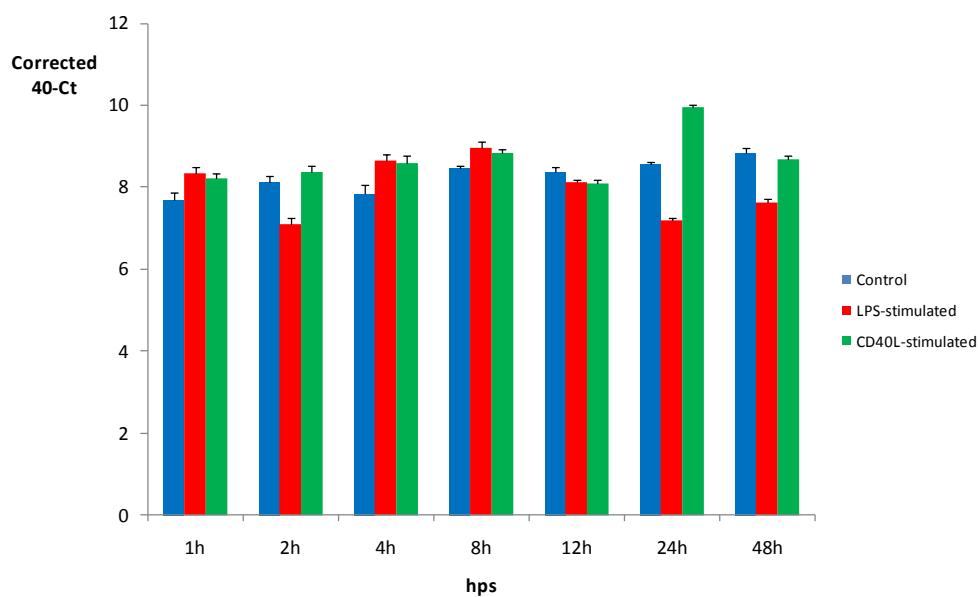


Figure 5.6 Expression of IL-1RN_{fi} in Mo-MØ stimulated with LPS or CD40L for 1-48 h. Results are expressed as corrected 40-Ct ± SEM of three replicates from a single sample. hps = hours post-stimulation.

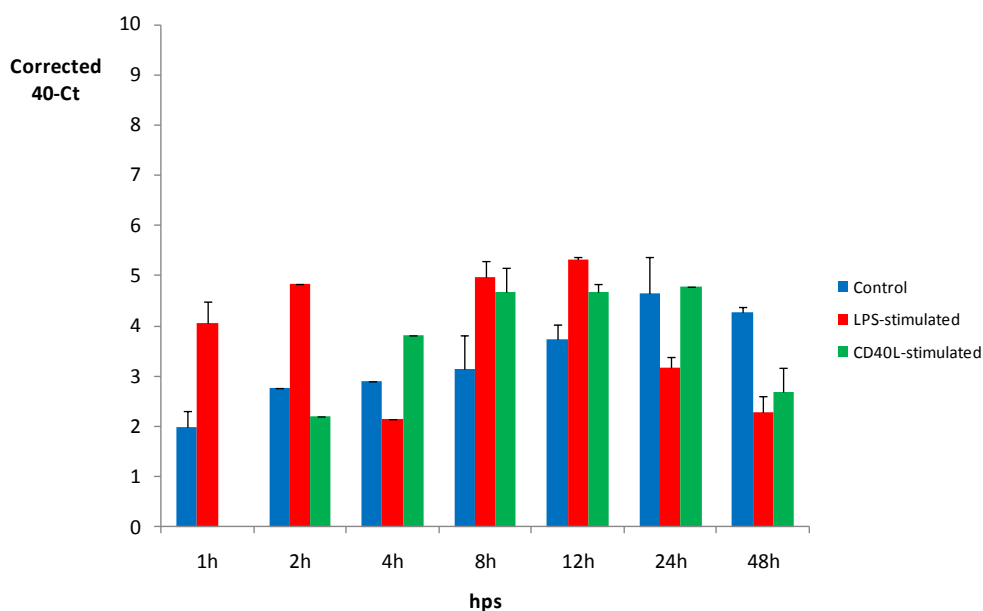


Figure 5.7 Expression of IL-1RN_{sv1} in Mo-MØ stimulated with LPS or CD40L for 1-48 h. Results are expressed as corrected 40-Ct ± SEM of three replicates from a single sample. hps = hours post-stimulation.

5.3.4.1 Infectious Bursal Disease Virus

Birds known to be either resistant (line 6₁) or susceptible (Brown Leghorn, BrL) to infectious bursal disease virus (IBDV) were challenged as outlined in Chapter 2, section 2.4.1.2. At 2 days post-infection (dpi), levels of expression of IL-1RN_{fl} were not statistically significantly different between infected and control birds of either line. By 3 dpi, relative expression in both groups of infected birds had increased compared to the controls, but again the differences were not statistically significant. At 4 dpi, the difference in IL-1RN_{fl} expression between infected and uninfected birds had increased even further in both lines. In the resistant birds, expression was 2.1 Ct greater (4.3-fold) which was statistically significant. A 1.7 Ct (3.3-fold) difference was observed in the susceptible line birds (Figure 5.8), but this was not statistically significant.

By comparison, there were no statistically significant differences in IL-1RN_{SV1} expression between both groups of infected and uninfected birds at any time-point (Figure 5.9). The pattern of IL-1RN_{SV2} expression was almost identical to that for IL-1RN_{fl} expression (Figure 5.10). At 2 dpi there were no statistically significant differences between control and infected birds in both groups. By 3 dpi, however, greater levels of expression (2.7-fold) were found in both groups of infected birds compared with respective control groups, although neither was statistically significant. The biggest differences were observed between infected and control birds at 4 dpi. In line 6₁ birds, mRNA expression was 2.5-fold higher in the infected subgroup, which was statistically significant. Although a 3.2-fold difference in expression was found between the two groups of BrL birds, this was not significant due to a single infected bird skewing the results (Figure 5.10).

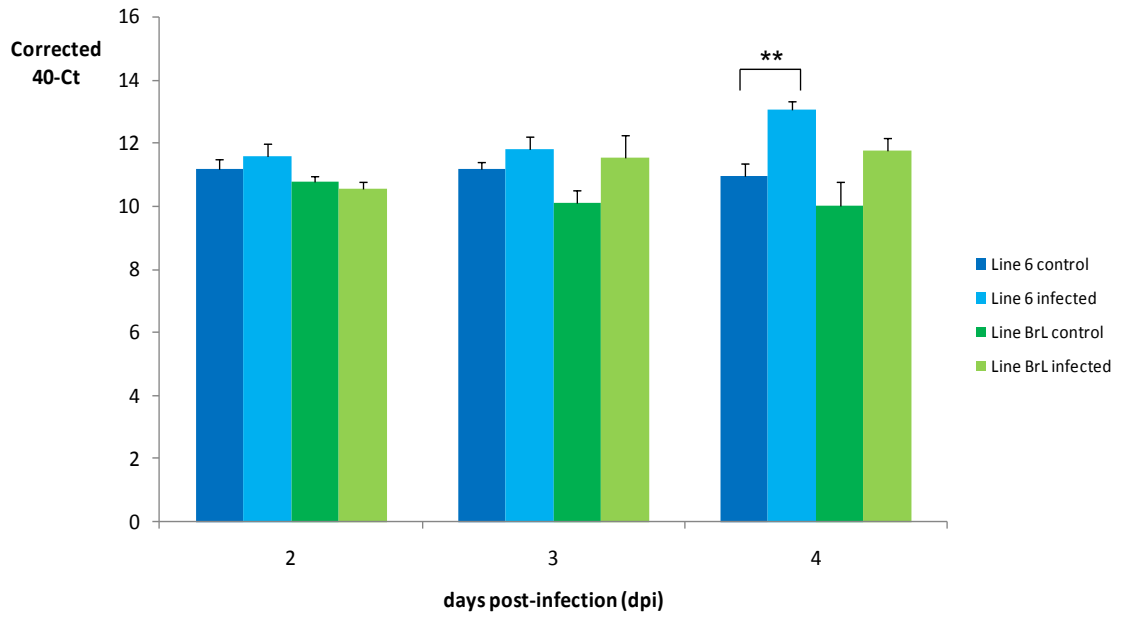


Figure 5.8 Expression of IL-1RN_{fl} mRNA in bursal cells from line 6₁ (resistant) and BrL (susceptible) chickens infected with IBDV. Results are expressed as mean corrected 40-Ct ± SEM of five birds per individual group. **P<0.01.

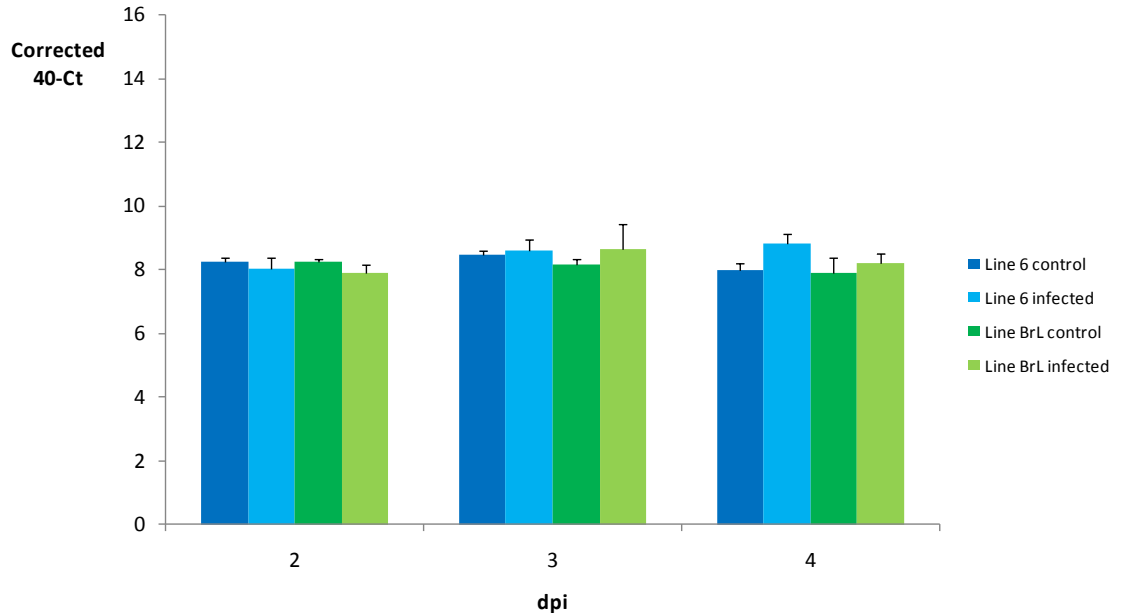


Figure 5.9 Expression of IL-1RNSV1 mRNA in bursal cells from line 6₁ (resistant) and BrL (susceptible) chickens infected with IBDV. Results are expressed as mean corrected 40-Ct ± SEM of five birds per individual group. dpi = days post-infection.

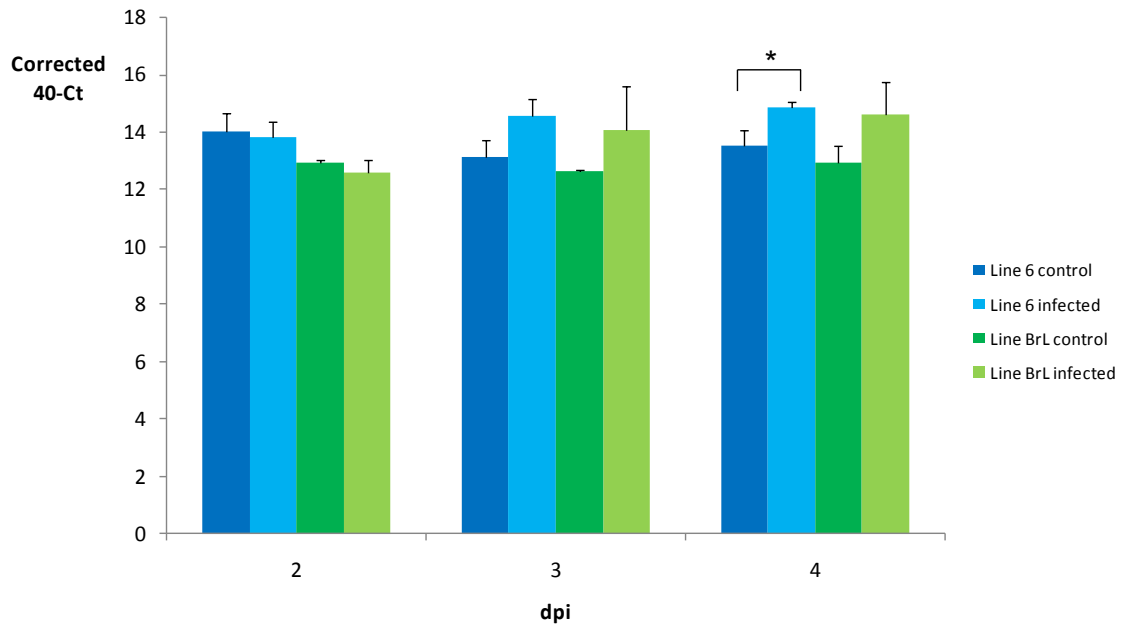


Figure 5.10 Expression of IL-1RNSV2 mRNA in bursal cells from line 6₁ (resistant) and BrL (susceptible) chickens infected with IBDV. Results are expressed as mean corrected 40-Ct \pm SEM of five birds per individual group. *P<0.05. dpi = days post-infection.

5.3.4.2 *Salmonella Typhimurium* strain F98 *Nal^R*

The expression of IL-1RN_{fl}, IL-1RN_{SV1}, and IL-1RN_{SV2} transcripts was assessed following oral infection with *Salmonella Typhimurium* (*S.Typhi*) strain F98 *Nal^R* across a 28 day period (Figure 5.11). Splenocyte RNA from infected and uninfected age-matched outbred RIR birds was assayed at 3, 7, 14, 21 and 28 dpi. IL-1RN_{fl} mRNA expression was 1.93-fold higher in the spleen of infected birds compared to the uninfected controls at 3 dpi, which was statistically significant. By 7 dpi, however, expression levels in both groups of birds were similar and remained so for the duration of the experiment. A comparable pattern of IL-1RN_{SV1} expression was observed, with a

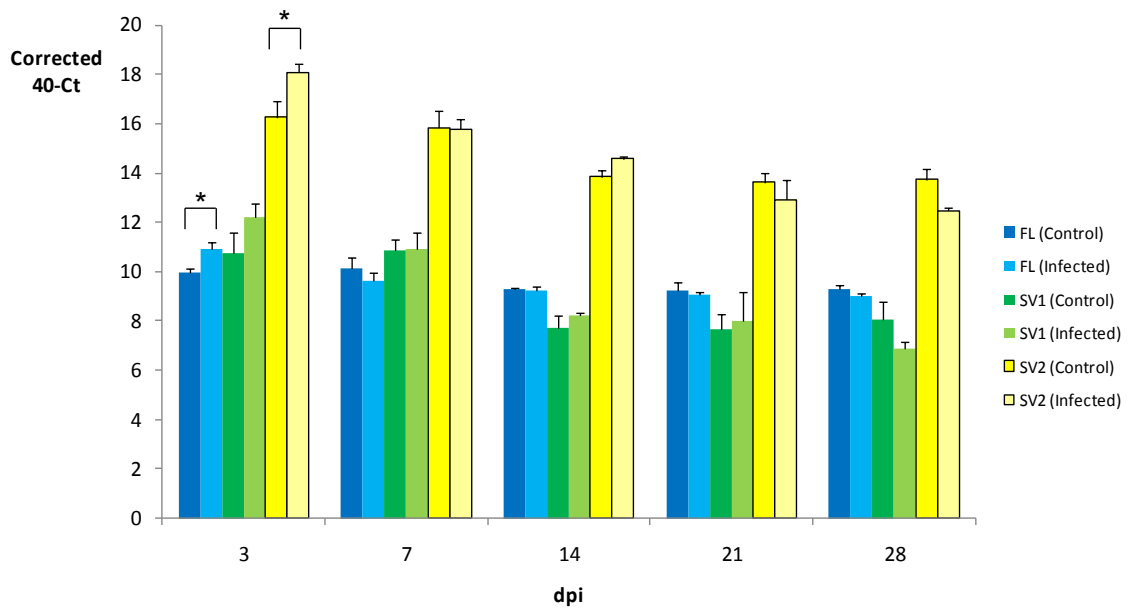


Figure 5.11 IL-1RN expression in splenocytes from RIR chickens following infection with *Salmonella Typhimurium* strain F98 NaI^R. Blue bars = IL-1RN_{FL} expression, green bars = IL-1RN_{SV1} expression, yellow bars = IL-1RN_{SV2} expression. Results are expressed as mean corrected 40-Ct ± SEM of four birds per individual group. *P<0.05. dpi = days post-infection.

2.7-fold increase (infected compared to uninfected) at 3 dpi. Between 7 and 28 dpi, there were no statistically significant differences in IL-1RN_{SV1} expression between the groups. Again, a similar pattern of expression was found for the IL-1RN_{SV2} variant, with the largest differences at 3 dpi between infected and control birds. A 3.5-fold difference was measured, which was statistically significant. As with the other two IL-1RN splice variants, IL-1RN_{SV2} expression in both groups of birds was similar by 7 dpi and remained so until 28 dpi.

5.3.5 Characterization of the bioactivity of *chIL-1RN*

The antagonistic activity of *chIL-1RN* was determined by its ability to

effectively inhibit the IL-1 β -mediated upregulation of IL-1 β and iNOS genes in HD11 cells. In several different types of human cells, IL-1 β induces its own production (Schindler, Ghezzi et al. 1990). The amount of IL-1 β mRNA in IL-1 β -stimulated cells remains high for over 24 h. By contrast, IL-1 β mRNA levels begin to fall after 4 h in LPS-stimulated cells (Dinarello 2009).

We initially sought to establish whether the HD11 cell line was responsive to IL-1 β stimulation, and if this also induced IL-1 β expression over a sustained period as is seen in mammals.

5.3.5.1 Pilot study

As the chicken HD11 cell line had never previously been used to carry out such an assay, a pilot experiment was performed to establish its suitability. Its ability to respond to stimulation with rchIL-1 β was tested. As a control, a doubling dilution series of rchIL-1 β was incubated for 2 h with a uniform volume of neutralizing antibody. HD11 cells were then either stimulated for 24 h with rchIL-1 β \pm antibody or cultured in media only. Both IL-1 β and iNOS mRNA expression were upregulated in rchIL-1 β -stimulated cells compared with no stimulation. In cells cultured with rchIL-1 β + antibody, IL-1 β and iNOS mRNA expression were initially equivalent to rchIL-1 β -stimulated cells; however, sufficient dilution of the cytokine allowed the antibody to neutralize its activity. This resulted in a decrease in IL-1 β and iNOS expression to levels equivalent to those in unstimulated cells (Figure 5.12).

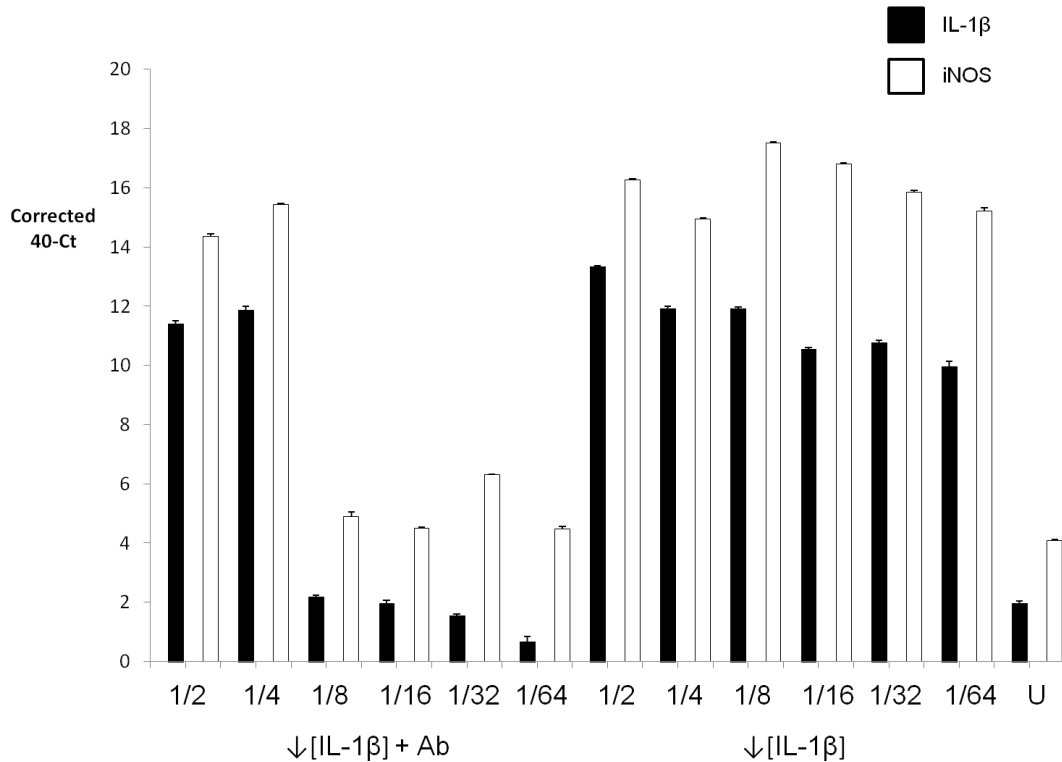


Figure 5.12 IL-1 β and iNOS expression in IL-1 β -stimulated HD11 cells. A doubling dilution series of recombinant chIL-1 β was pre-incubated \pm a uniform volume of anti-IL-1 β antibody for 2 h at 41°C. HD11 cells were then either stimulated for 24 h with rchIL-1 β \pm antibody or cultured in media only. RNA was extracted from the HD11 cells and assayed for IL-1 β and iNOS expression by real-time qRT-PCR.

To ensure the optimal rchIL-1 β concentration was used in subsequent bioassays, HD11 cells were stimulated with a doubling dilution series of rchIL-1 β as described in this Chapter, section 5.2.5.1. Culture supernatants were tested for nitrite content by the Griess reaction as outlined in Chapter 2, section 2.4.15.2.1. A rchIL-1 β concentration of 10 ng/ μ l was deemed optimal (Figure 5.13).

For all subsequent “test” assays, a commercially produced stock of rchIL-1 β was purchased from AMSBio (Abingdon, UK). To test its ability to stimulate HD11 cells and sustain IL-1 β mRNA levels for 24 h, HD11 cells were cultured as described in

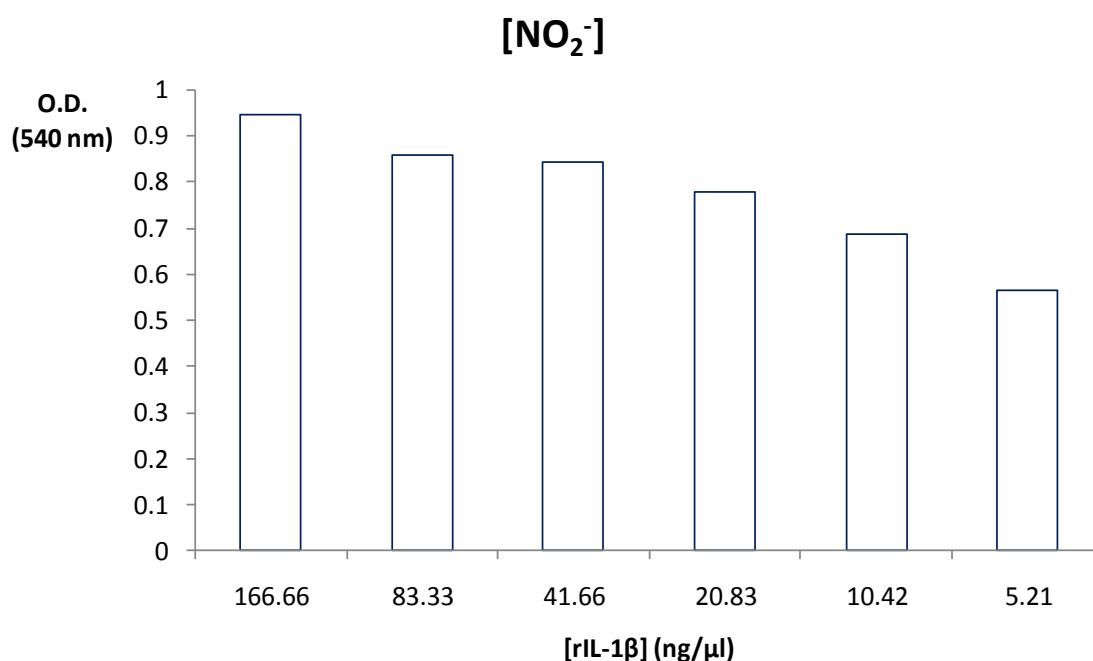


Figure 5.13 Establishing the optimal [rchIL-1β] required to stimulate HD11 cells. HD11 cells were routinely cultured and stimulated overnight with a doubling dilution series of rchIL-1β as indicated. The next day, supernatants were assayed using the Griess reaction. Bars denote the O.D. of culture supernatants at 540 nm, as a representation of the [NO₂⁻]. O.D₅₄₀ (media only control) = 0.118.

Chapter 2, section 2.4.12.1, and stimulated as described in this Chapter, section 5.2.5.1.

IL-1β expression levels were determined at 0, 1, 2, 4, 8, 12 and 24 hps by real-time qRT-PCR (Figure 5.14). Results indicated the stock of rchIL-1β was able to stimulate HD11 cells, increasing IL-1β expression. Increased IL-1β mRNA levels were sustained across a 24 h period.

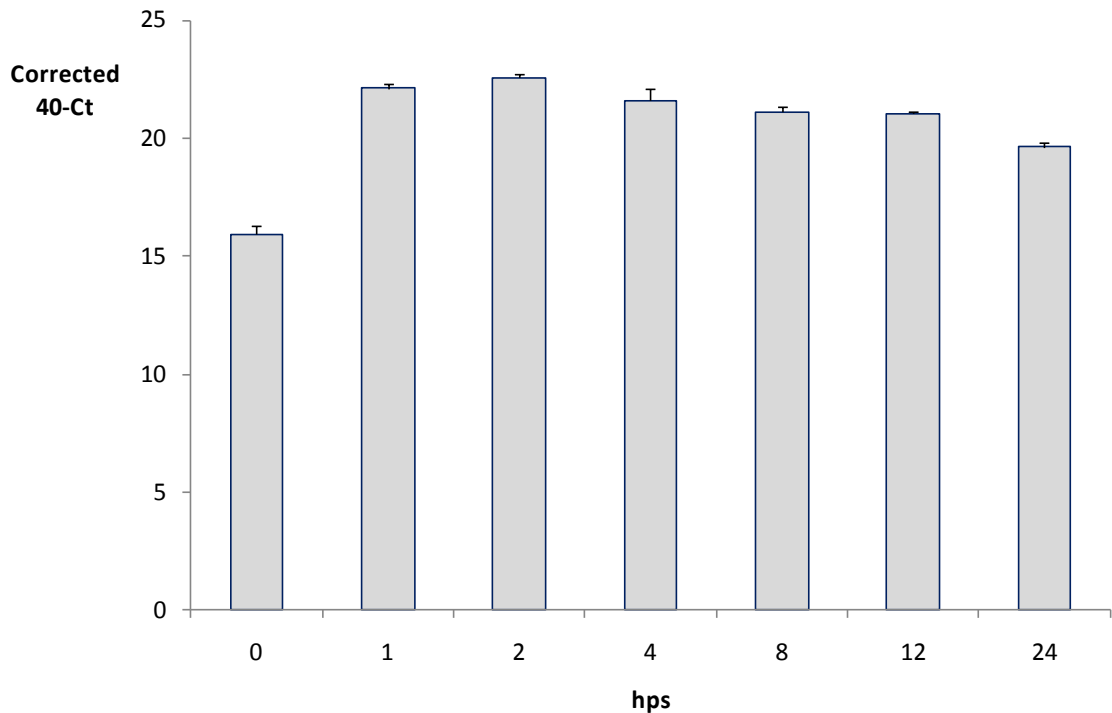


Figure 5.14 IL-1 β mRNA expression in IL-1 β -stimulated HD11 cells. HD11 cells were routinely cultured at 41°C, 5% CO₂ for 0, 1, 2, 4, 8, 12 and 24 h in medium supplemented with 10 ng/ μ l rchIL-1 β . RNA was extracted from the HD11 cells and assayed for IL-1 β expression by real-time qRT-PCR. Results are represented as mean corrected 40-Ct \pm SEM of two samples from individual flasks. hps = hours post-stimulation.

5.3.5.2 Characterization of the bioactivity of pure secretory and intracellular IL-1RN (purified recombinant proteins)

Recombinant chicken sIL-1RN and icIL-1RN were successfully expressed in HEK293T cells (Figure 5.15). The ability of rchIL-1RN to inhibit the biological activity of IL-1 β was assessed in a HD11 cell bioassay. The antagonistic activity of both chIL-1RN was determined by their ability to effectively inhibit the IL-1 β -mediated upregulation of IL-1 β and iNOS genes. In HD11 cells incubated for 4 h with either sIL-

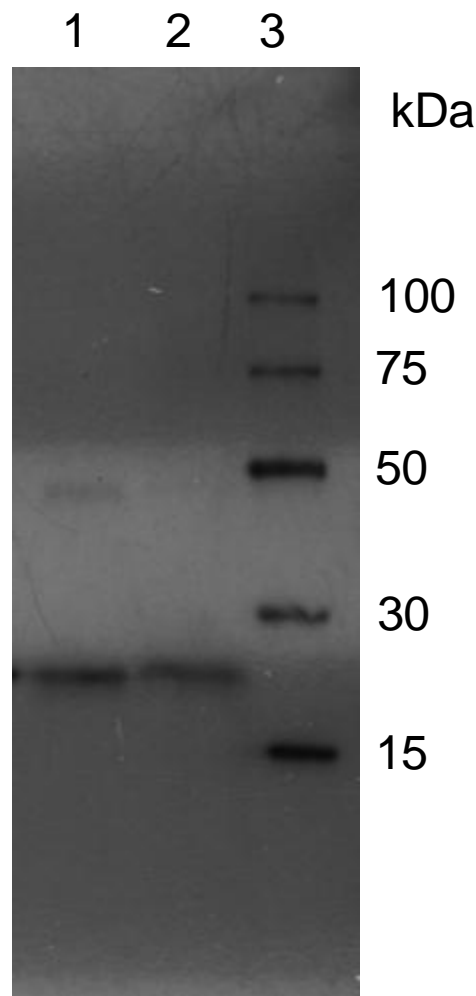


Figure 5.15 Western blot of purified recombinant chIL-1RN proteins expressed in HEK293T cells. Samples were electrophoresed by SDS-PAGE on a 4-15% Mini-PROTEAN TGX gel. Lane 1 = recombinant mature sIL-1RNpHLSec; calculated Mw = 21.857 kDa. Lane 2 = recombinant icIL-1RNpHLSec; calculated Mw = 22.329 kDa. Lane 3 = 6xHIS protein ladder (Qiagen).

1RN or icIL-1RN prior to the addition of rchIL-1 β , the upregulation of IL-1 β and iNOS mRNA expression levels was effectively inhibited (Figure 5.16). In cells stimulated with IL-1 β alone, IL-1 β and iNOS mRNA expression levels increased significantly compared to expression levels in unstimulated cells. The antagonistic effect of both chIL-1RN gradually declined as they were titrated out in the presence of a fixed

concentration of rchIL-1 β . Griess assay results correlated with the qRT-PCR data throughout the experiment (Figure 5.17).

5.3.5.3 Characterization of the bioactivity of ex-COS secretory and intracellular IL-1RN splice variant proteins

The biological activity of the four identified splice variants of chIL-1RN was tested in the same HD11 bioassay. The bioactivities of cell supernatants and lysates from COS cells transfected with each IL-1RN splice variant were compared with similar mock-transfected controls of pCI-neo vector lacking a cDNA insert. At their highest concentration, ex-COS lysates containing either icIL-1RN SV1 or SV2 gave greater inhibition of IL-1 β -mediated upregulation of proinflammatory genes than their respective supernatants. When compared with ex-COS lysates of pCI-neo controls, however, no significant differences in IL-1 β and iNOS expression were found following rchIL-1 β stimulation (Figures 5.18-5.21). When titrated out, there were no differences in bioactivity between any of the icIL-1RN SV cell lysates and their respective pCI-neo controls. Lysates and supernatants (ex-COS) of both sIL-1RN splice variants, similarly, showed no bioactivity when compared with pCI-neo controls. These results indicate all four splice variants of chIL-1RN do not act as functional antagonists of IL-1 β in this bioassay.

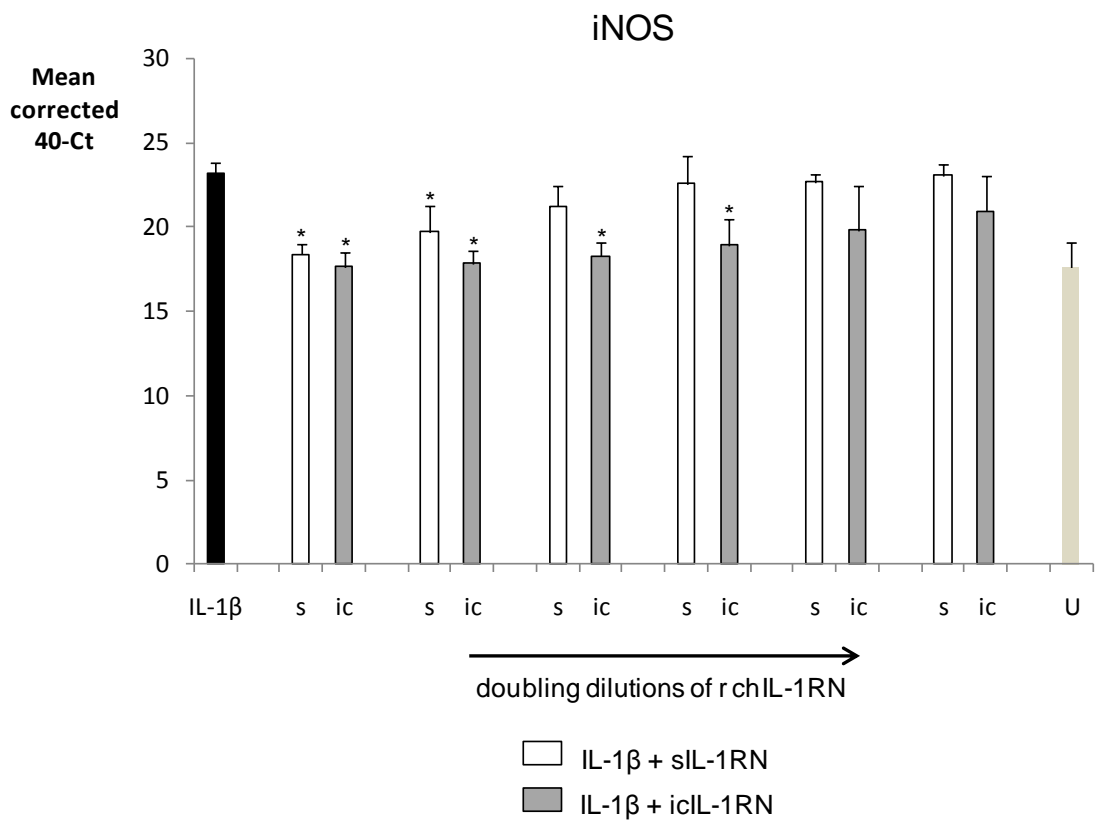
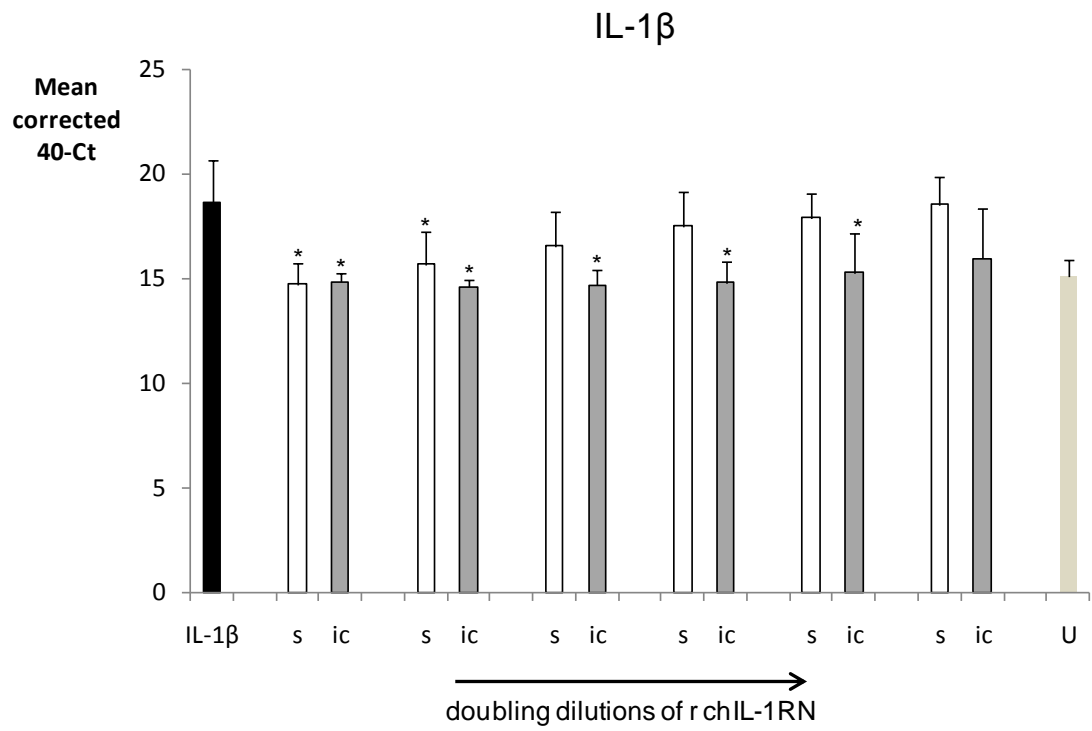


Figure 5.16 Full length chIL-1RN are bioactive as determined by TaqMan.

Previous page. Both secretory and intracellular variants of purified recombinant chIL-1RN antagonise the stimulatory effects of recombinant chIL-1 β in HD11 cells, in a dose-dependent manner. Doubling dilutions of recombinant proteins from 225 $\mu\text{g/ml}$ (sIL-1RN) and 194 $\mu\text{g/ml}$ (icIL-1RN). Bars denote IL-1 β and iNOS expression in HD11 cells pre-incubated with either pure sIL-1RN (s) or icIL-1RN (ic) for 4 h prior to the addition of rchIL-1 β for 12 h. Results are represented as the mean corrected 40-Ct \pm SD of three independent experiments. U = unstimulated cells. IL-1 β = cells stimulated with IL-1 β without IL-1RN. *P<0.05 of the rchIL-1 β + IL-1RN treatment groups compared to the rchIL-1 β only treatment.

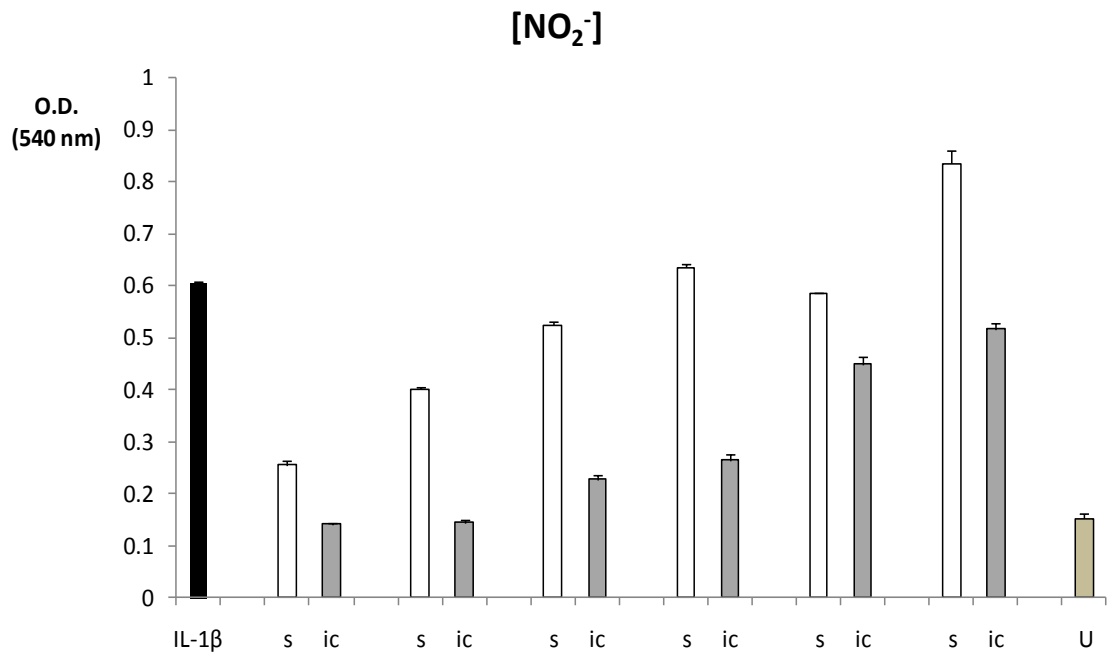


Figure 5.17 Full length chIL-1RN are bioactive as determined by the Griess assay.

Both secretory and intracellular variants of purified recombinant chIL-1RN antagonise the stimulatory effects of recombinant chIL-1 β in HD11 cells, in a dose-dependent manner. Bars denote O.D. of culture supernatant from HD11 cells pre-incubated with either pure sIL-1RN (s) or icIL-1RN (ic) for 4 h prior to the addition of rchIL-1 β for 12 h. Results are represented as the mean \pm SEM of 9 replicates (triplicate measurements from three independent experiments). U = unstimulated cells. IL-1 β = cells stimulated with IL-1 β without IL-1RN.

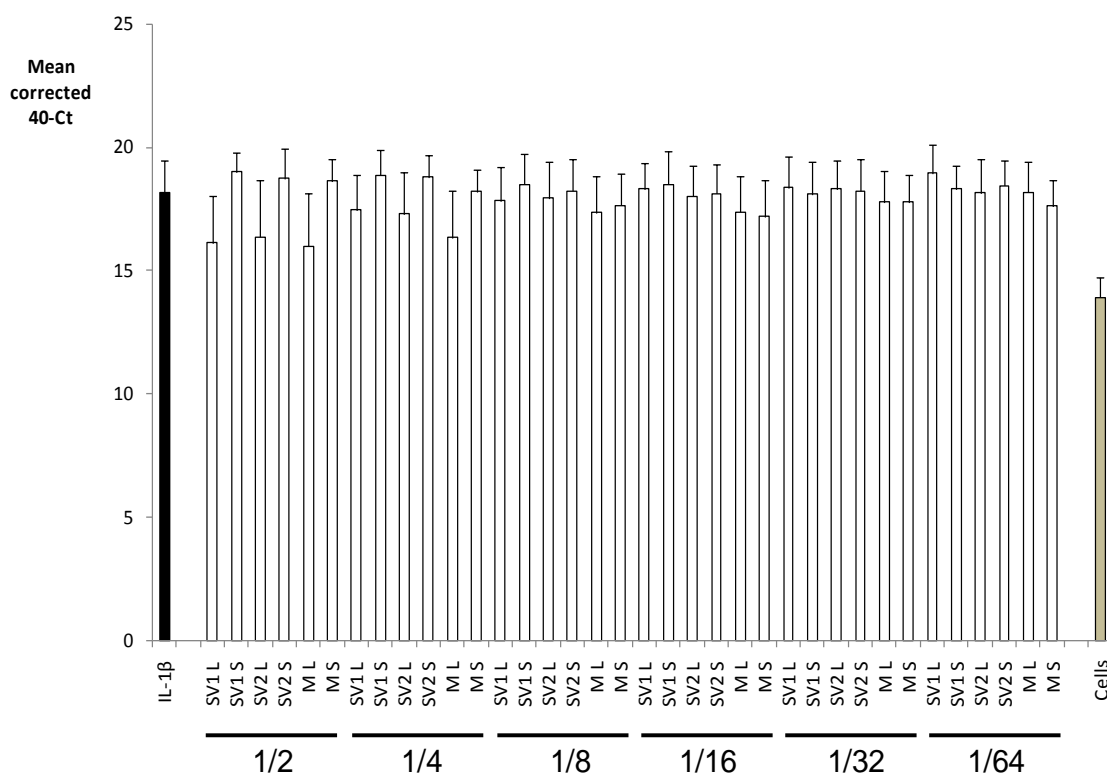


Figure 5.18 Chicken icIL-1RN splice variants do not antagonise IL-1β-mediated IL-1β expression. Bars indicate IL-1β expression in HD11 cells pre-incubated with either ex-COS icIL-1RN SV1 or SV2 (cell lysate (L) or supernatant (S)) or ex-COS cell lysate or supernatant (mock transfected cells, M) for 2 h prior to the addition of rhIL-1β for 12 h. Dilutions of crude ex-COS supernatants and lysates are indicated beneath the x-axis. Results are represented as mean corrected 40-Ct ± SEM of three independent experiments.

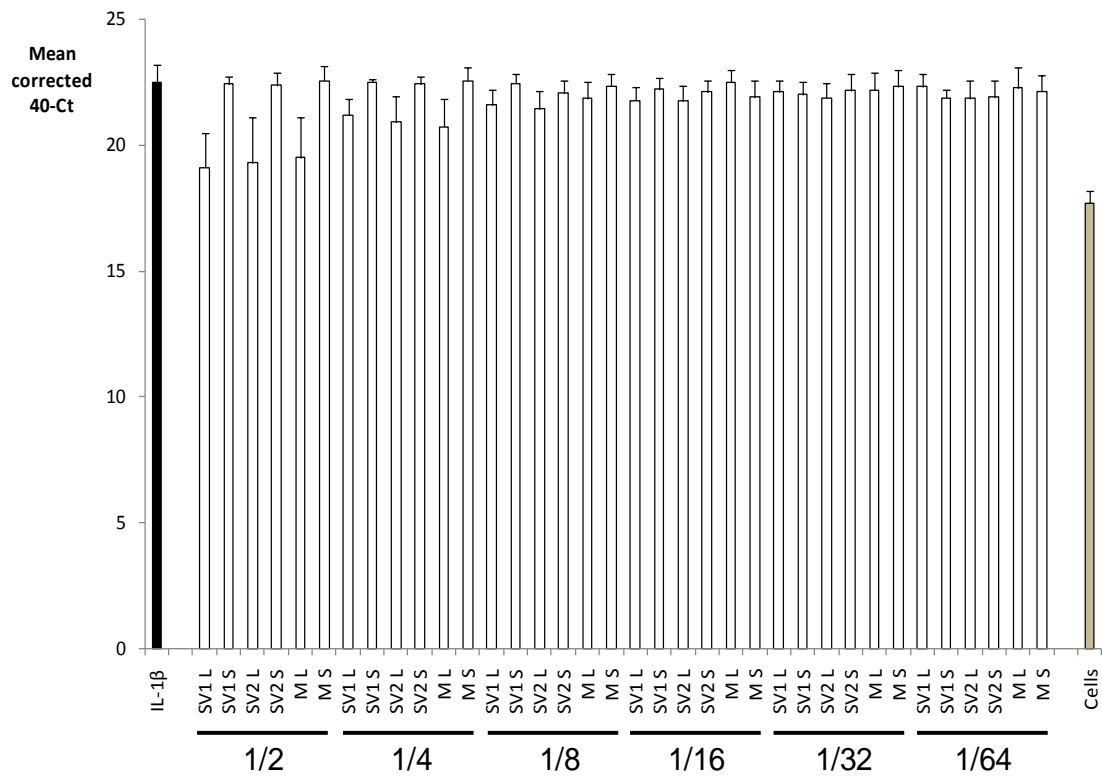


Figure 5.19 Chicken icIL-1RN splice variants do not antagonise IL-1β-mediated iNOS expression. Bars indicate iNOS expression in HD11 cells pre-incubated with either ex-COS icIL-1RN SV1 or SV2 (cell lysate or supernatant) or ex-COS cell lysate or supernatant (mock transfected cells, M) for 2 h prior to the addition of rchIL-1β for 12 h. Dilutions of crude ex-COS supernatants and lysates are indicated beneath the x-axis. Results are represented as mean corrected 40-Ct ± SEM of three independent experiments.

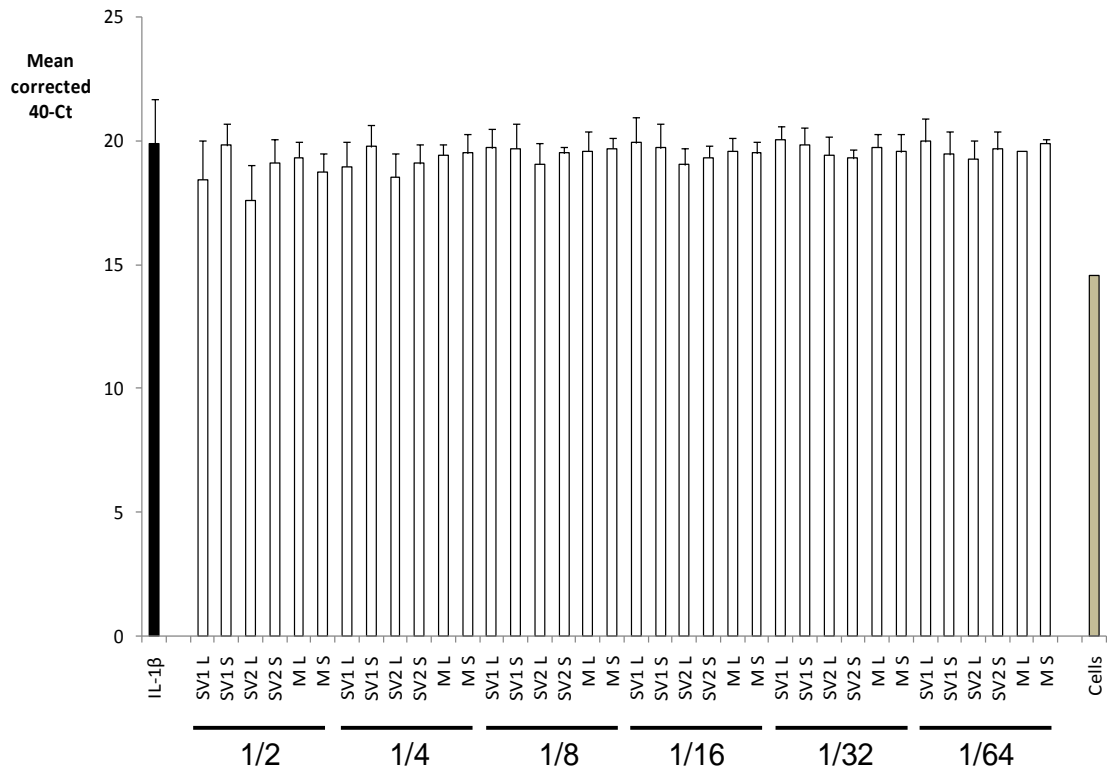


Figure 5.20 Chicken sIL-1RN splice variants do not antagonise IL-1 β -mediated IL-1 β expression. Bars indicate IL-1 β expression in HD11 cells pre-incubated with either ex-COS sIL-1RN SV1 or SV2 (cell lysate or supernatant) or ex-COS cell lysate or supernatant (mock transfected cells, M) for 2 h prior to the addition of rhIL-1 β for 12 h. Dilutions of crude ex-COS supernatants and lysates are indicated beneath the x-axis. Results are represented as mean corrected 40-Ct \pm SEM of three independent experiments.

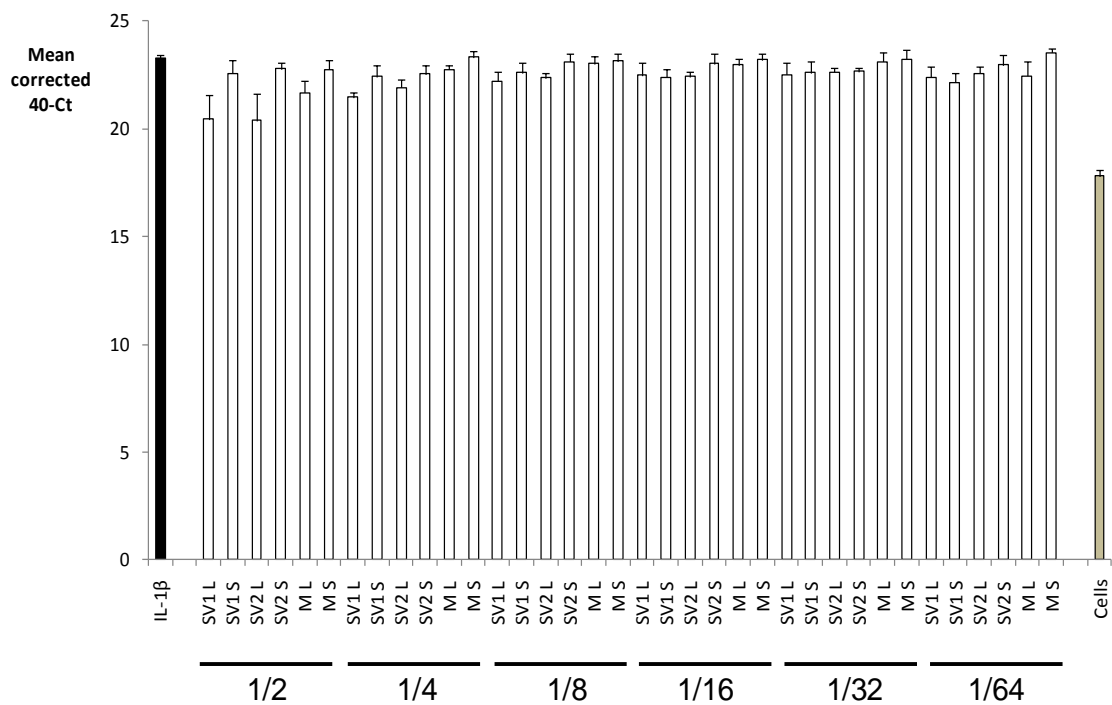


Figure 5.21 Chicken sIL-1RN splice variants do not antagonise IL-1β-mediated iNOS expression. Bars indicate iNOS expression in HD11 cells pre-incubated with either ex-COS sIL-1RN SV1 or SV2 (cell lysate or supernatant) or ex-COS cell lysate or supernatant (mock transfected cells, M) for 2 h prior to the addition of rchIL-1β for 12 h. Dilutions of crude ex-COS supernatants and lysates are indicated beneath the x-axis. Results are represented as mean corrected 40-Ct ± SEM of 3 independent experiments.

5.4 Discussion

The biological activity of human and mouse IL-1RN has been repeatedly characterised in assays which show it acts as an antagonist of IL-1RI. It physically occupies this receptor preventing IL-1 β or IL-1 α from binding. However, this does not lead to signal transduction. Although IL-1RN is sufficiently similar to IL-1 β to facilitate IL-1RI binding, several key differences account for its inability to activate signalling. IL-1 β has two binding sites termed A (bsA) and B (bsB). It binds domains I and II of IL-1RI with bsA leading to a conformational change allowing bsB to bind domain III of IL-1RI. This activates the intracellular signalling cascade. IL-1RN has bsA but lacks bsB. It therefore only binds domains I and II of IL-1RI, facilitating blocking (Gosavi, Whitford et al. 2008). This binding event leads to the creation of an angle between domains II and III of IL-1RI which prevents any contact between IL-1RN and domain III of IL-1RI. This completely abolishes its capacity to recruit MyD88 to activate signalling (Sims and Smith 2010). In addition, IL-1RN lacks the specific amino acids required to engage IL-1RAcP on the cell surface (Schreuder, Tardif et al. 1997; Wang, Zhang et al. 2010). The extent to which IL-1RN is similar to the agonist IL-1 β has been shown following site-directed mutagenesis of IL-1RN at a single codon. The resulting substitution, making IL-1RN differ from the wild type by only a single amino acid, conferred partial agonist activity (Ju, Labriola-Tompkins et al. 1991).

Both full length chicken sIL-1RN and icIL-1RN recombinant proteins were able to antagonize the IL-1 β -mediated upregulation of IL-1 β and iNOS genes, and as such exhibited biological activity analogous to their mammalian orthologues.

Bioinformatic analysis of the four chIL-1RN SVs in Chapter 4, section 4.3.4

suggested they would be functionally redundant given the potential importance of missing residues. Ex-COS recombinant SV proteins were tested in the HD11 bioassay in parallel with vector controls, and lacked any biological activity. Although ex-COS lysates of both SV1 and SV2 proteins contained more activity than their respective supernatants, when compared with mock control ex-COS lysates, differences were not statistically significant. Any differences between lysates and supernatants were therefore unlikely to be IL-1-mediated. These bioassay results suggest a possible control mechanism may exist to regulate chIL-1RN expression, and hence bioactivity, by creating SV transcripts that encode functionally redundant proteins. It is possible the SV proteins were misfolded in COS-7 cells and subsequently degraded by the ubiquitin-proteasome system (Hershko and Ciechanover 1998). Alternatively, SV mRNAs may have been inefficiently translated which could have led to defective protein synthesis. To determine whether this occurred, a polysome profile of the transfected COS-7 cells followed by Northern blotting could be carried out (Beilharz and Preiss 2004).

Expression of IL-1RN_{fl} is ubiquitous and constitutive in the range of cells and tissues examined, although the assay does not differentiate between sIL-1RN and icIL-1RN mRNAs. Previous studies have assessed global IL-1RN expression in mice (Gabay, Porter et al. 1997) and rabbits (Apostolopoulos, Ross et al. 1996; Matsukawa, Fukumoto et al. 1997), and found it was not constitutive in all mouse tissues. Analyses in mice used an RNase protection assay which lacks sensitivity compared to TaqMan, so IL-1RN expression may be more widespread than reported in that species. As in humans, rabbit sIL-1RN expression was ubiquitous but icIL-1RN expression was restricted. The highest levels of chicken IL-1RN_{fl} expression were found in monocytes and macrophages. Human equivalents of these leukocytes also exhibit high levels of

huIL-1RN expression, suggesting the predominance of chIL-1RN in these cells reflects a similar requirement at sites of immune activation *in vivo*.

Chicken IL-1RN_{fl} expression is increased *in vivo* following bacterial or viral infection, reflecting a typical response to that seen in experimental models of disease in mammalian species. For IBDV, IL-1RN_{fl} expression was highest at 4 dpi, which was also observed for IL-1 β expression in the bursae of out-bred RIR chickens infected with the same strain of virus (Eldaghayes, Rothwell et al. 2006).

Stimulation of three distinct monocyte/macrophage populations with LPS did not affect the expression of IL-1RN_{fl}, a response that differs from previous observations in human monocytes. Following LPS stimulation, human blood-derived monocytes express sIL-1RN in less than an hour, with detectable levels of protein present after 4 h. The icIL-1RN1 transcript is subsequently expressed after ~12-15 h, and is the principal IL-1RN isoform after 24 h (Dinarello 1996). Despite our assay being unable to distinguish structural variants, it was somewhat unexpected that LPS did not increase the expression of IL-1RN_{fl} up to 24 hps in any of the macrophage populations. In the HD11 cell line, LPS robustly activates NF- κ B via chicken Toll-like receptor 4 (chTLR4) (Keestra and van Putten 2008). We were satisfied a similar LPS response had taken place in the HD11 cells in this experiment, reflected by the vast increase in IL-1 β expression after only 1 h. The pattern of IL-1RN_{SV1} expression was consistent with IL-1RN_{fl} expression in HD11 cells, showing no increase following exposure to LPS. Given that both chicken sIL-1RN and icIL-1RN cDNAs were amplified from LPS-stimulated HD11 cells, it must be assumed the promoter region of chIL-1RN and cell machinery required to initiate chIL-1RN transcription are intact in HD11 cells. Thus, the apparent non-existent response to LPS in these cells is surprising and demonstrates the

transcriptional response of chIL-1RN *in vitro* is strikingly different from findings in mammals.

In contrast to HD11s, IL-1RN_{SV1} expression in both BM-MØ and Mo-MØ was noticeably upregulated following LPS stimulation at 2 and 4 hps, and 1, 2, 4 and 12 hps, respectively. It is interesting to observe the contrast with IL-1RN_{fl} expression in these cells perhaps lending weight to the idea that a control mechanism is regulating chIL-1RN expression. For instance, the chicken may be preferentially splicing a significant proportion of full length transcripts into SV transcripts in response to stimulation. It seems rather futile to be deliberately splicing full length transcripts that normally encode proteins which are biologically inert, unless of course chIL-1RN is functionally promiscuous. This was not apparent in the bioassay, although the assay may not provide an accurate reflection of alternative function(s).

Another interesting observation in these stimulated BM-MØ and Mo-MØ was the apparently large differences in expression of the same transcript in the two different cell types. In Mo-MØ, IL-1RN_{fl} expression was, compared with the levels determined in BM-MØ, relatively lower. A difference of around 2-3 Ct values (4 to 8-fold) was evident at any of the given time-points. The absolute Ct values for IL-1RN_{SV1} mRNA expression in Mo-MØ were also considerably smaller than those determined in BM-MØ. Although it is difficult to imagine why chIL-1RN expression is much lower in cells isolated from the blood than the bone marrow, it is undoubtedly an observation with implications for experimental interpretation. Considering the wide-reaching influence of IL-1-mediated effects in macrophages, it may be important to consider that the activation status of a cell, cell surface marker expression, motility, and production of many other cytokines (amongst countless other effects) is being innately suppressed to a

greater extent in blood-derived Mo-MØ.

In conclusion, *in vitro* analyses of IL-1RN expression did not identify any statistically significant differences between stimulated and unstimulated cell populations. By contrast, in two distinct *in vivo* challenge models, significant differences in IL-1RN expression were found between infected and uninfected birds. Specifically, the expression of both full length and SV2 transcripts were statistically significantly elevated in birds infected with either IBDV or *S.Typhi* compared with uninfected controls. It was not evident why there was such a discrepancy between *in vitro* and *in vivo* models, and consequently, it warrants further investigation.

Chapter 6

Results 4: Identification, cloning and characterisation of chicken interleukin-1F5 (IL-1F5)

6.1 Introduction

Rapid advances in genomics-based molecular techniques vastly increased the availability of sequence data around the start of this century. This led to the emergence of the human genome sequence, and greatly expanded our knowledge of the repertoires of genes we possess. Screening EST and cDNA sequence databases prior to the human genome assembly led to many novel genes being discovered. This was the case with the IL-1 gene family which up until 1999 was only thought to contain four genes (IL-1 β , IL-1 α , IL-1RN and IL-18). Studies conducted by several different groups culminated in concurrent reports of six “new” genes in the huIL-1 family, all of which clustered with IL-1 β , IL-1 α and IL-1RN on chromosome 2 (Mulero, Pace et al. 1999; Barton, Herbst et al. 2000; Kumar, McDonnell et al. 2000; Smith, Renshaw et al. 2000; Bensen, Dawson et al. 2001; Lin, Ho et al. 2001; Pan, Risser et al. 2001). These were named IL-1F5-F10 (Sims, Nicklin et al. 2001), although this has since been replaced with an updated nomenclature (Dinarello, Arend et al. 2010). Some degree of biological function has been assigned to all of these except for IL-1F10. The number of published studies looking at these cytokines, however, remains very small and it is possible they may possess additional, as yet undefined functions.

IL-1F5 is evidently an antagonistic cytokine – its two major roles being as a receptor antagonist of IL-1RL2 (Debets, Timans et al. 2001) and a suppressor of inflammation through an (as yet unelucidated) interaction with the orphan receptor, SIGIRR (Costelloe, Watson et al. 2008). Since its discovery in humans, IL-1F5 orthologues have been identified in 31 other mammalian genomes according to the ENSEMBL genome browser (personal search). However, it remains absent in non-mammalian species, although an apparent IL-1F5 orthologue is present in the Anole

lizard genome (unpublished observations). The proximity of these nine IL-1 genes at a single locus, their phylogeny, and their similar sequences and structures suggest they arose by gene duplication. Analysis of the IL-1 α , IL-1 β and IL-1RN sequences proposed that IL-1RN arose through gene duplication ~350 Mya, after which a successive duplication ~285 Mya formed the IL-1 β and IL-1 α genes. Using the calculated mutational rate of IL-1RN since it was formed (Eisenberg, Brewer et al. 1991), it was predicted that IL-1F5 emerged later, at ~190-210 Mya (Mulero, Nelken et al. 2000). If accurate, this would have precluded its existence in non-mammalian species. The apparent absence of a large multigene IL-1 locus in non-mammalian species with an assembled genome sequence lends weight to this hypothesis.

This chapter describes the identification and molecular cloning of chicken IL-1F5. After screening EST databases to find a novel IL-1 sequence, it was comprehensively characterised *in silico*, which showed it was most similar to the IL-1F5 gene found in mammals. Once this EST had been unequivocally identified as chIL-1F5, it was amplified by PCR directly from its cDNA clone. Analyses of the chIL-1F5 gene structure, genomic location and chicken-specific sequence features were also carried out.

6.2 Methods

General methods were carried out as outlined in Chapter 2. Additional methods and alterations to those described in Chapter 2 are detailed here.

Both *in silico* and *in vitro* techniques were used to identify and clone a novel cytokine, chicken IL-1F5. The NCBI database was initially screened as described in Chapter 2, section 2.2.2. This identified a putative chicken cytokine EST sequence from the IL-1 family. The sequence had significant homology with chIL-1 β and chIL-1RN; however, it appeared to lack the IL-1 signature motif and was truncated at the 3' end. Analyses of its nucleotide and predicted amino acid sequence were carried out whilst BLAST was used to confirm its identity as described in Chapter 2, section 2.2.3. Its amino acid sequence was used to identify further chIL-1 ESTs.

In order to obtain a full-length clone of IL-1F5, the original EST clone (ChEST734c4/ BU247129.1) was ordered from MRC geneservice (<http://www.geneservice.co.uk/products/cdna/chickenEST.jsp>). The clone was provided as a bacterial stab and re-streaked onto solid LB medium (+ 50 μ g/ml carbenicillin) then incubated overnight at 37°C. Ten single colonies were picked and grown in LB broth (+ 50 μ g/ml carbenicillin + 8% glycerol) overnight with shaking at 37°C. A 1.5 ml stock of each culture was then frozen at -70°C for 24 h. All 10 stock cultures were streaked out onto solid LB (+ 100 μ g/ml ampicillin) and incubated overnight at 37°C. Ten single colonies were picked and grown in LB broth (+ 100 μ g/ml ampicillin) and incubated overnight at 37°C. Plasmid DNA was isolated using the QIAprep spin miniprep kit (Qiagen). Clones were sequenced using the M13 and revM13 sequencing primers (Sigma-Genosys) on the CEQ™ 8000 Genetic Analysis System (Beckman Coulter). Using PCR, the IL-1F5 CDS was amplified, sequenced and cloned into the pTarget

mammalian expression vector. For the PCR, the EST clone was used as the template and thermal cycling conditions were: one cycle of 94°C for 2 min, then 30 cycles of 94°C for 30 s, 69°C for 30 s, and 72°C for 2 min. Sequence-specific primers (Table 1 in the Appendix) were designed from the full-length EST sequence (missing sequence in the NCBI submission was obtained from sequencing the clones with M13 and revM13 sequencing primers).

Further bioinformatic characterization of chIL-1F5 nucleotide and amino acid sequences was carried out to confirm the avian gene's identity and similarity to the orthologous human and mouse IL-1F5 sequences. PCR amplification of chIL-1F5 introns used custom primers designed from the coding sequence (Table 1 in the Appendix). Cycling conditions were as described in Chapter 2, section 2.4.4.3 with an initial annealing temperature of 70°C for the five touchdown cycles.

To determine the genomic location of chIL-1F5, PCR analysis of the locus containing chIL-1 β was performed using a specific BAC clone (TAM32-21N6) for the template as described in Chapter 4, section 4.2.2. An additional experiment to discover the genomic location of chIL-1F5 used a ³²P-labelled (random-primed) probe to hybridize against BAC library filters as described in Chapter 4, section 4.2.2.

6.3 Results

6.3.1 Identification and analysis of a novel *chIL-1* EST sequence

A TBLASTN search of the NCBI expressed sequence tag (EST) database by a collaborator, Dr Steve Bird (University of Aberdeen), identified a chicken EST representing a putative novel chicken IL-1 gene. This EST (Acc. No. BU247129.1) was an 811 bp sequence with 3 potential start codons but lacked both a stop codon and a polyA signal. Translation of this EST showed that the predicted protein sequence did not contain the highly conserved IL-1 family motif, but had significant identity with *chIL-1 β* (17.5%) and *ic chIL-1RN* (32.4%) amino acid sequences when aligned using ClustalX. Next, TBLASTN analysis against all of the genomes in ENSEMBL showed it was missing from the chicken genome (v2.1), but exhibited significant identity with IL-1F5 (IL-36RN) in 19 other species (results in Table III in Appendix I). When aligned with the human, macaque, mouse and cow IL-1F5 sequences, the chicken sequence was clearly truncated at the 3' end (Figure 6.1). Several unsuccessful attempts were made to amplify the 3' end of the IL-1F5 cDNA using 3' RACE.

To determine whether any similar *chIL-1* family sequences were present in the NCBI EST database; a reciprocal BLASTP analysis of this database using the predicted *chIL-1F5* amino acid sequence was carried out. This did not identify any further ESTs with significant homology, other than those already identified in this study (listed in Table II in Appendix I).

The NCBI record for this EST (<http://www.ncbi.nlm.nih.gov/nucest/BU247129.1>) indicated it had only been sequenced from the 5' end. Therefore, it was possible the BU247129.1 EST

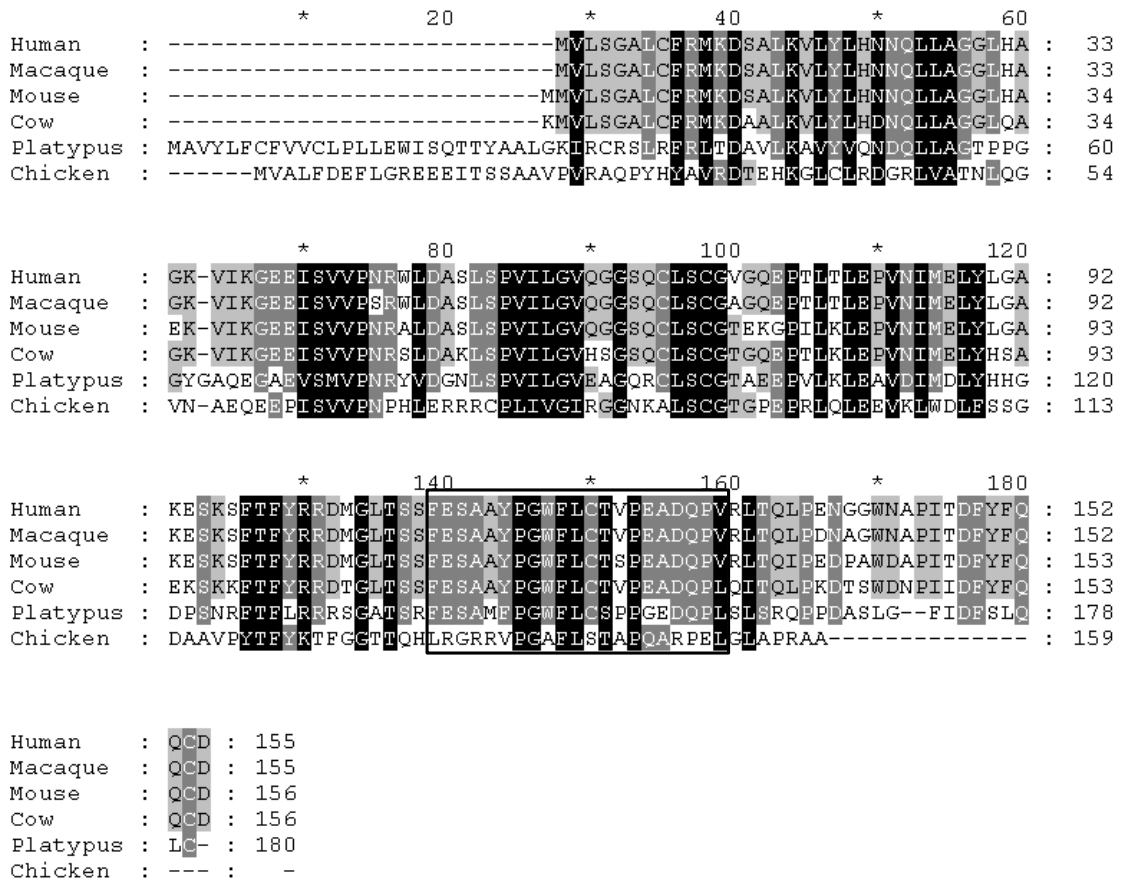


Figure 6.1 Amino acid alignment of truncated chicken IL-1F5 with the full length human, macaque, mouse, cow and platypus IL-1F5 sequences. Identical residues between all 5 species at the same position are shaded black; identical residues between 4 species are shaded dark grey, those between 3 species shaded light grey; similar (structure) residues are shaded light grey. The chicken sequence is incorrect as the IL-1 family signature motif (indicated with a box) is not conserved. The chicken sequence is also incomplete as it is truncated at the 3' end.

(ChEST734c4) was longer than the published 811 nt sequence. The cDNA clone was acquired, fully sequenced and found to be 1059 nt in length. Sequence analysis identified the previously missing stop codon and polyA signal. It also uncovered a number of errors in the submitted BU247129.1 sequence towards the 3' end (Figure 6.2). Consequently, translation of the correct EST sequence altered the reading frame of

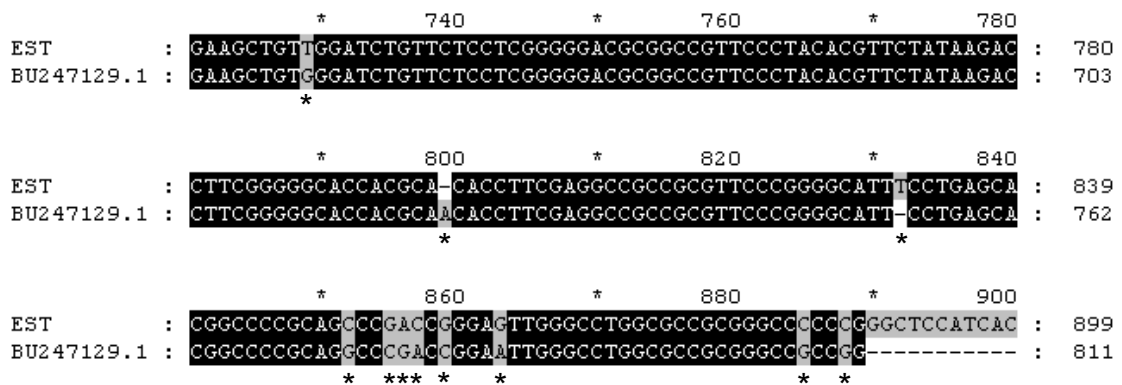


Figure 6.2 Nucleotide sequence alignment between the 3' end of the chIL-1F5 EST (BU247129.1) present in the NCBI database and the clone of the identical EST (ChEST734c4) after being fully sequenced in both directions. A number of incorrect, missing or inserted nucleotides in the BU247129.1 sequence were identified. They are indicated with an asterisk below the alignment.

the protein sequence such that a conserved IL-1 signature motif was now apparent (Figure 6.3). This predicted chIL-1F5 amino acid sequence now had higher identity with the chIL-1 β (20.4%) and chIL-1RN (34.1%) sequences, as well as with the 19 other species to which it was previously aligned. Figure 6.3 shows the correct chicken sequence aligned with human, mouse, cow, macaque & platypus IL-1F5 sequences.

Unassembled, uncurated nucleotide sequence reads from the third assembly (Galgal 3.0) of the chicken genome were subsequently made available. A TBLASTN analysis of these sequences was carried out which identified two contigs (designated 110035.1 and 162436.1) from the “removed data” reads containing ~80% of the coding region of chIL-1F5 as well as some intronic sequence. A third contig (designated 166095.1) was identified which contained two exons from the apparent 5' UTR of the gene. This contig aligned with the 5' end of the full-length EST clone sequence.

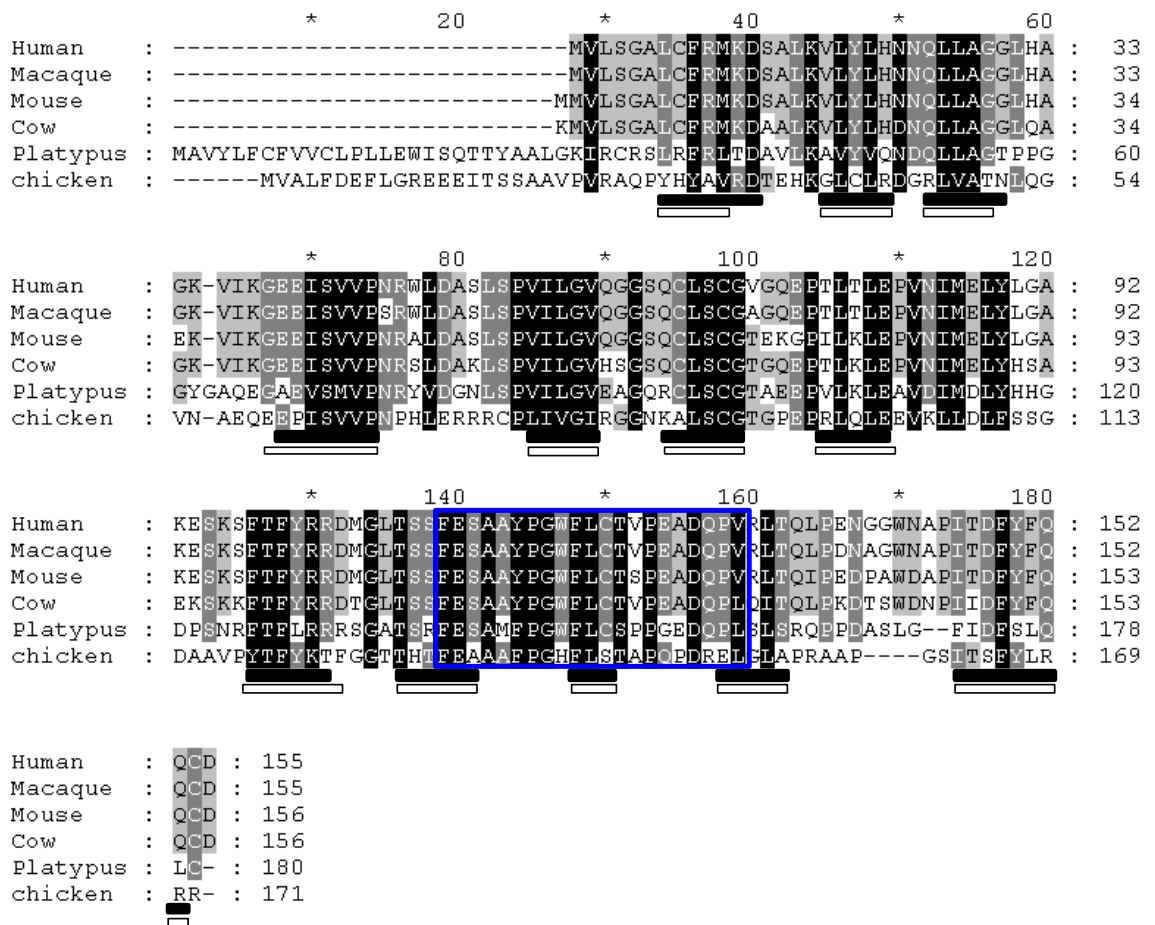


Figure 6.3 Amino acid alignment of chicken IL-1F5 with the human, macaque, mouse, cow and platypus IL-1F5 sequences. Identical residues between all 5 species at the same position are shaded black; identical residues between 4 species are shaded dark grey, those between 3 species shaded light grey; similar (structure) residues are shaded light grey. The original translation of the chIL-1F5 EST was truncated at the 3' end and did not contain the conserved IL-1 family signature motif (**Figure 6.1**). Both errors and missing sequence were identified following full-length sequencing of the chIL-1F5 EST. Translation of the correct full length CDS sequence changed the reading frame such that the IL-1 family signature motif (indicated with a blue box) was now well conserved. The secondary structure of IL-1 family proteins consists of 12 β -strands. The specific amino acid residues that comprise these 12 β -strands in humans (Schreuder 1997) are indicated by black blocks beneath the sequence. Their locations in the chicken, predicted by PSIPRED, are indicated by white blocks.

6.3.2 Characterization of the putative processed form of chIL-1F5

Human IL-1F5 lacks a signal peptide and apparent pro-domain, and its mode of secretion thus remains unknown. Despite this, unpublished observations indicate human IL-1F5 truncated at the N-terminus has increased biological activity. The predicted chIL-1F5 amino acid sequence was, therefore, examined for potential cleavage sites that may indicate a particular mechanism of secretion. Analysis using PeptideCutter (ExpASY) predicted that chicken IL-1F5 would not be cleaved by signal peptidase or caspase-1, i.e. it does not contain either a signal peptide or a pro-domain. Although chIL-1F5 possesses aspartic acid (D) residues (caspase-1 cut site) at positions 6, 34 and 44 at the NH₂-terminus, adjacent residues do not conform to any of the published consensus sequences for this enzyme. None of the other 17 enzymes queried with PeptideCutter were predicted to process chIL-1F5. These findings correlate with a similar analysis for huIL-1F5.

6.3.3 Amplification and molecular cloning of the chIL-1F5 coding sequence

cDNA

The translated ChEST734c4 sequence contained three potential start codons. Alignment of the predicted chIL-1F5 amino acid sequence with 19 other species indicated only one likely candidate for the genuine initiation codon. Primers were designed against the predicted IL-1F5 CDS sequence derived from the EST. A full length 516 bp IL-1F5 CDS cDNA was amplified by PCR using purified ChEST734c4 DNA. This EST clone was generated from a liver cDNA library. Several initial attempts were made to amplify the full length CDS by RT-PCR in skin, spleen, lung and bone

marrow; however, these were unsuccessful. It was therefore amplified directly from the EST clone. Gel electrophoresis of the PCR products revealed a single band of the expected size (Figure 6.4). Products were TA-cloned into the pTarget mammalian expression vector, and clones were screened by *EcoRI* restriction digestion. All clones were sequenced by chain termination sequencing using T7 and revT7 vector primers. Analysis of the clone sequences revealed a 100% match with the IL-1F5 ChEST734c4 sequence.

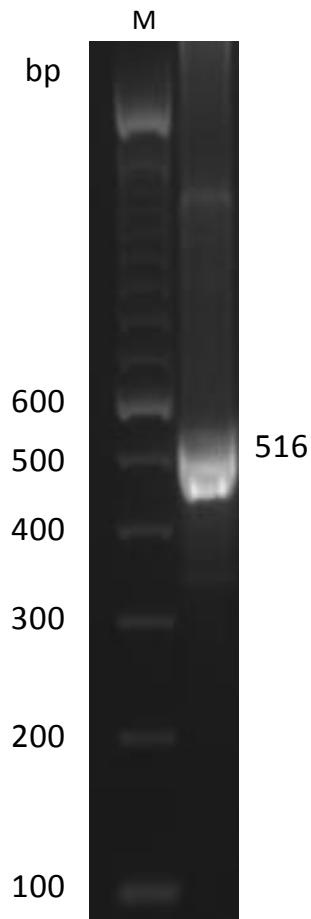


Figure 6.4 Agarose gel showing PCR products from the amplification of the IL-1F5 CDS using ChEST734c4 DNA as template. Expected band size = 516 bp. Size marker = 100 bp DNA ladder.

6.3.4 *In silico* analysis of the chIL-1F5 amino acid sequence

The full length chIL-1F5 amino acid sequence was further characterized *in silico*. The CDS cDNA encodes a predicted protein of 171 amino acid residues in length. When aligned with mammalian IL-1F5 sequences (Figure 6.3), chIL-1F5 shares 31.2% amino acid identity with both its human and mouse homologues. The chicken sequence, however, is significantly longer (>20 aa) at its 5' end when compared with the human and mouse proteins, which may affect its function. Its calculated Mw is 18.748 kDa with a theoretical pI of 6.52. The secondary structures of human and mouse IL-1 proteins have been elucidated as β -trefoil folds comprised of 12 β -strands. The crystal structure of mouse IL-1F5 has been resolved, with the analysis showing this cytokine also adopts the same β -trefoil fold. In addition, the study identified several major differences between the composition and conformation of the other structural features of IL-1F5 compared to those found on IL-1RN and IL-1 β . Using PSIPRED, the secondary structure of chIL-1F5 was predicted to contain 12 β -strands, located in almost identical regions to the mouse IL-1F5 sequence (Figure 6.3). Three cysteine residues are present in the chIL-1F5 sequence, although only one of these is conserved with mammals, located in β -strand 6. The mouse IL-1F5 sequence contains four cysteine residues of which two are linked by a disulphide bond. These are found at the NH₂- and COOH-termini (Cys8 and Cys155, respectively) of the protein. When aligned with mouse IL-1F5, one of the cysteines in chIL-1F5 is located 12 amino acids in the 3' direction from Cys8. However, neither of the other 2 cysteine residues (Cys76 and Cys91) in the chicken sequence is situated close to the C-terminus. This makes it difficult to speculate with any confidence which two cysteines will form a disulphide bond in the chicken amino acid. No potential N-linked glycosylation sites were located

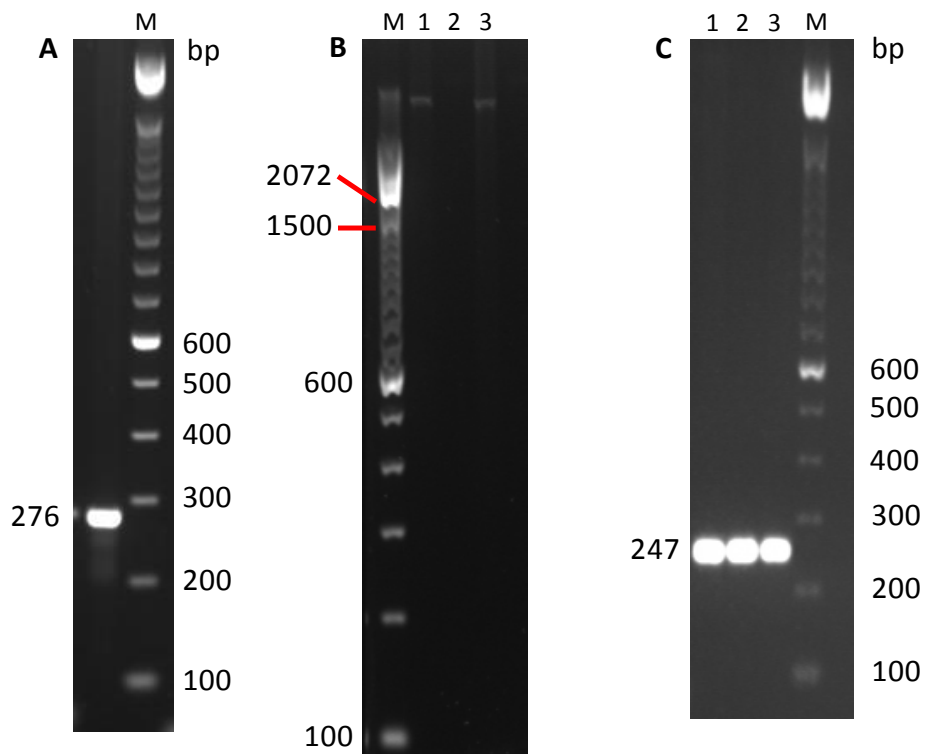
in chIL-1F5, consistent with their absence in mammalian sequences. The chIL-1F5 sequence was analysed for structural similarity to known protein domains in the ProDom database. The sequence was most closely related to domain PD002536 (domain I.D: IL-1; closest domain: human IL-1F5; e-value: 1×10^{-13} for residues 78-170; amino acid identity: 39%). The sequence was further examined for other functional motifs. Using the NetNES prediction server, chIL-1F5 was found to possess a nuclear export sequence (LQLEEVKLLDL) at positions 99-109. Analysis of both human and mouse IL-1F5 sequences did not detect a similar motif in either species. This motif may be non-functional, as most proteins <50 kDa are able to diffuse freely across nuclear membranes.

Using the full length chicken IL-1F5 amino acid sequence, phylogenetic analysis was performed to determine an evolutionary relationship with mammalian IL-1F5. Analysis was performed exactly as described in Chapter 4, section 4.3.4. As shown in Figure 4.11, chIL-1F5 formed a separate branch (with the chIL-1RN sequences) within the major IL-1 receptor antagonist subgroup (IL-1RN, IL-1F5, IL-1F10) clade.

6.3.5 Structural determination by PCR amplification, sequencing and in silico analysis

A combination of PCR and *in silico* analyses allowed the genomic structure of chIL-1F5 to be partially determined. The human IL-1F5 gene consists of six exons, which through use of alternative first exons (1a and 1b), creates two different five exon-containing transcripts (Figure 6.5D). These transcripts only differ in their 5' UTRs and encode exactly the same protein sequence. As the chromosomal location of the chIL-1F5 gene remains unknown, the structure and full gene sequence is not present in any of

Chapter 6: Identification, cloning and characterisation of chicken IL-1F5



D

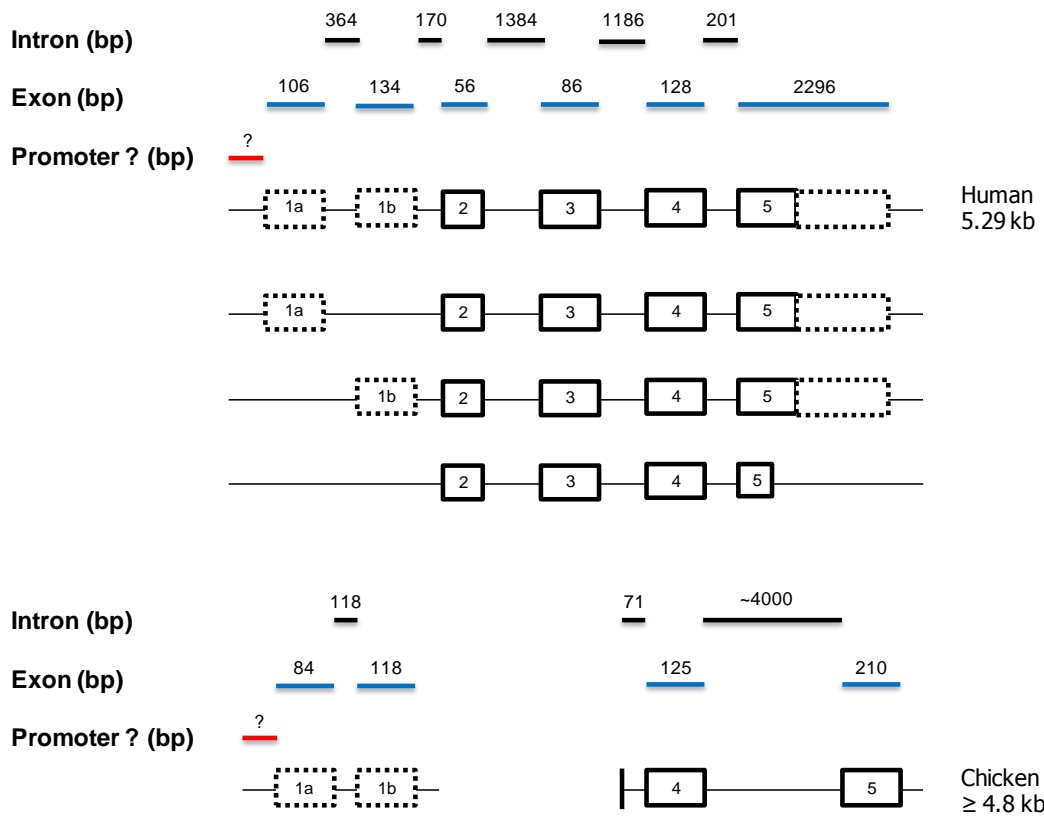


Figure 6.5 Determination of the gene structure of chicken IL-1F5.

Previous page **A.** Agarose gel of PCR products containing Intron 4 of chIL-1F5. Products were amplified from genomic DNA from line 6₁ with IL-1F5 332L and IL-1F5 437R primers. M = 100 bp DNA ladder. **B.** Agarose gel of PCR products containing Intron 5 of chIL-1F5. Products were amplified with IL-1F5 Int5F and IL-1F5 Int5R primers. M = 100 bp DNA ladder, lanes 1 & 3 = products amplified from lines 6₁ and N, respectively, lane 2 = empty. **C.** Agarose gel of PCR products containing Intron 1 of chIL-1F5. Products were amplified with IL-1F5 Int1F and IL-1F5 Int1R primers. M = 100 bp DNA ladder, lanes 1-3 = products amplified from lines 6₁, N and 15I respectively. **D.** The structures and identified protein coding transcripts of chicken and human IL-1F5 genes. The chicken gene structure is only partially known.

the chicken genome browsers.

A similar approach to the one employed for the chIL-1RN gene was used to establish the locations of the chIL-1F5 introns. The cDNA sequences of human, platypus and chicken IL-1F5 were aligned to verify the approximate intron-exon boundaries in the chicken. Platypus cDNAs were aligned because the chicken and platypus transcripts encode an additional 16 and 25 amino acids respectively at their NH₂-termini that are absent in other mammalian sequences (Figure 6.3). It was possible any platypus introns in this region may also be present in the chicken. As before, primers were designed from the exon sequences flanking the predicted chicken exon-intron boundaries.

This approach enabled three chicken introns to be successfully amplified. Using genomic DNA from line 6₁ as a template, a ~280 bp PCR product was amplified (the equivalent cDNA amplicon would be 205 bp) with the primers IL-1F5 332L and 437R (Figure 6.5A). Sequencing revealed this amplicon contained a 71 bp intron of chIL-1F5. Its location indicated it was intron 4 and was thus much smaller than the 1186 bp human intron 4. To amplify a second intron, the primers IL-1F5 Int5 F and IL-1F5 Int5 R were used. A ~4 kb PCR product (the equivalent cDNA amplicon would be 117 bp) was

generated using genomic DNA from line N as template (Figure 6.5B). This product was TA-cloned into pTarget and sequenced from both ends with T7 and revT7 vector primers to confirm it was specific. Its location in the gene indicated it was intron 5 and was therefore substantially larger than its 201 bp human equivalent. The subsequent availability of Galgal 3.0 sequence reads confirmed the sequencing results for intron 4 of chIL-1F5. For intron 5, 381 bp at the 5' end and 90 bp at the 3' end were also verified.

Previous BLASTN analysis with the full length ChEST734c4 sequence against Galgal3.0 reads identified a contig (166095.1) containing the likely 5' UTR sequence. This contig is 531 bp long comprising, 5'-3', 170 bp of upstream (possible promoter) sequence, an 84 bp exon, a 118 bp intron, a 118 bp exon and finally 41 bp of (likely) intron sequence. To verify that the 118 bp intron sequence was correct, it was amplified by PCR and then sequenced. Using genomic DNA from lines 6₁, N and 15I as template, a 247 bp PCR product was generated (the equivalent cDNA amplicon would be 129 bp) with the primers IL-1F5 Int1 F and IL-1F5 Int1 R (Figure 6.5C). Sequencing the line 6₁ product revealed a 100% match with the sequence in contig 166095.1. It was already known this was intron 1 and is thus much smaller than its 364 bp human equivalent. Alignment of the combined chicken CDS and intron sequences with the genomic sequence in contigs 110035.1, 162436.1 and 166095.1 allowed the exact locations of four of the exons to be identified. From the initial alignment of chicken, human, mouse and platypus transcript sequences, it was apparent the chIL-1F5 gene would be likely to contain four exons. With the addition of two further 5' UTR exons, it is likely that the chIL-1F5 gene, as with that of mammals, consists of six exons in total. This means that up to two further introns, separating coding region exons, have yet to be amplified.

The incomplete chIL-1F5 gene structure is shown in Figure 6.5D. In summary, the exact sizes of two exons (designated exons 4 and 5) at the 3' end of the chIL-1F5 coding region are known. When translated, the amino acid sequences of these two exons are very similar in size to the corresponding human sequences. Chicken exon 5 is much smaller than its human homologue which contains a long 3' UTR. The polyadenylation signal in exon 5 of chIL-1F5 is found 24 nt after the stop codon. RNA is usually cleaved 10-30 nt after the polyA signal. Therefore, the 3' UTR of chIL-1F5 is very short compared to the 3' UTR of huIL-1F5 (which is 2071 nt long). The probable chIL-1F5 5' UTR is encoded by two exons, which are both smaller than their equivalents in human. Both of these exons appeared in the chIL-1F5 EST, which is in contrast to the situation in humans, in which 2 different transcripts, each containing only one of two alternative 5' UTR exons, are encoded. The mouse, however, encodes an IL-1F5 transcript containing both its 5' UTR exons. The introns of chIL-1F5 are generally smaller than their human equivalents, except for intron 5 which is much larger (4 kb compared to 201 bp). The overall length of chIL-1F5 is no shorter than 4.8 kb, so it is atypically (for a chicken cytokine gene) similar in size to the 5.29 kb huIL-1F5 gene.

6.3.6 Identification of the genomic location

An identical procedure to that carried out for chIL-1RN in Chapter 4, section 4.3.6 was used to elucidate the genomic location of chIL-1F5. A TBLASTN search of the chicken genome (v2.1) with the chIL-1F5 amino acid sequence did not return any positive hits. This offered further indication that the present assembly of the chicken genome does not contain an IL-1 gene cluster resembling the locus found in humans. A

TBLASTN search of the chicken genome (Galgal3.0, unassembled) with the full length chIL-1F5 amino acid sequence identified two contigs (110035.1 and 162436.1) containing the coding sequence from residues 35-171, the 71 bp intron and 184 bp novel sequence beyond the stop codon. An additional BLASTN search with the full length ChEST734c4 sequence against the same reads identified a further contig (166095.1) containing the likely 5' UTR sequence. These contigs were mined from "removed data" sequence reads and are thus unplaced, indicating the third build of the genome sequence may not provide the location of chIL-1F5.

As for chIL-1RN, the four sequence gaps adjacent to chIL-1 β were analysed for the presence of chIL-1F5 by PCR using purified TAM32-21N6 BAC clone DNA. Specific amplification in the region covered by BAC TAM32-21N6 was confirmed with a control PCR to amplify chIL-1 β using this template. Positive control PCRs were also set up to amplify chIL-1 β and chIL-1F5 in genomic DNA from line 6₁ using the same primer pairs. The results confirmed the presence of chIL-1 β at this locus but chIL-1F5 did not amplify from the BAC, suggesting it is encoded elsewhere (Figure 6.6).

Following confirmation by PCR that the chIL-1F5 gene does not lie adjacent to chIL-1 β , the CHORI261 BAC library was screened with a radiolabelled DNA probe. To synthesise the probe, IL-1F5 was amplified by PCR from genomic DNA from line 6₁ as template with primers IL-1F5 332L and IL-1F5 437R, yielding a product of 276 bp. This probe identified three apparent positive clones (Figure 6.7) which corresponded to the following BAC clones: 70B9, 132E6 & 161B7. Two of these clones had previously been placed in the chicken genome at chr2:96,686,393-96,852,271 (70B9) and chr2:55,324,685-55,545,707 (132E6). In the genome, the region covered by BAC 70B9 is fully sequenced except for two gaps predicted to span 784 bp and 810 bp,

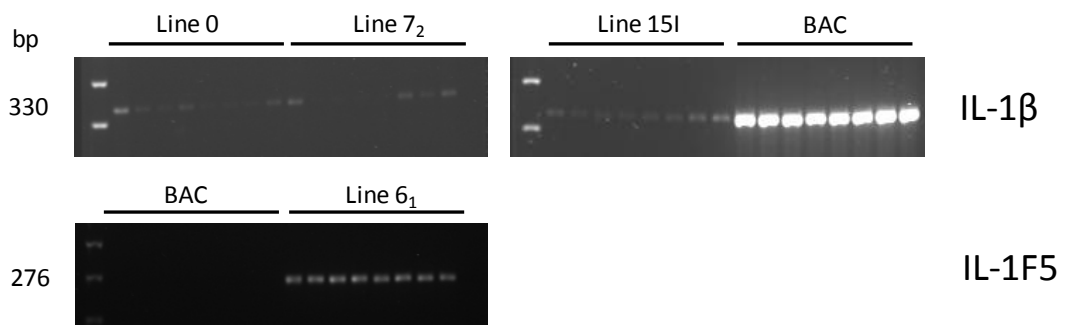


Figure 6.6 Agarose gel electrophoresis of IL-1 β and IL-1F5 PCR products in lines 7₂, 15I, 0 (IL-1 β) and line 6₁ (IL-1F5) genomic DNA and TAM32-21N6 BAC DNA. Examination of the locus containing chIL-1 β shows four sequence gaps are present immediately adjacent to the 5' end of the gene. The gaps were examined for further chIL-1 family genes by PCR using purified TAM32-21N6 bacterial artificial chromosome (BAC) clone DNA, which covers the entire region, as template. To confirm specific amplification in the region covered by the BAC, a control PCR to amplify chIL-1 β using this template was included. Positive control PCRs were set up to amplify chIL-1 β and chIL-1F5 in genomic DNA, using the same primer pairs as for the BAC DNA PCRs.

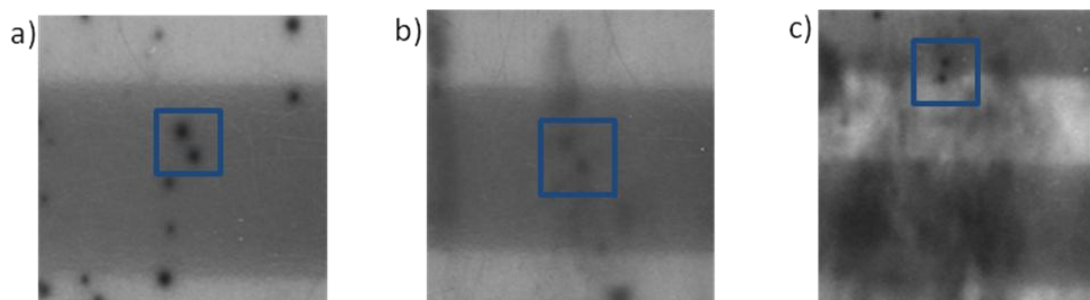


Figure 6.7 Screening a BAC library to elucidate the genomic location of chIL-1F5.

The CHORI261 BAC library was screened with a radiolabelled DNA probe corresponding to 276 bp of chIL-1F5. This probe identified 3 apparent positive clones which corresponded to the following BAC clones: a) 70B9, b) 132E6 & c) 161B7.

respectively. Again, for BAC 132E6 the genome sequence coverage is extensive but the locus also contains gaps of predicted size 640 bp, 312 bp and 1058 bp. BAC 161B7 is unplaced in the current build of the chicken genome (v2.1). All three BAC clones were acquired from CHORI and DNA was purified as described in the methods. BACs were screened by PCR to establish whether the identified sequence gaps contained chIL-1F5. Although all of the gaps at both loci on chromosome 2 are much smaller than the full length chIL-1F5 gene, the specified sizes of sequence gaps in the genome build are only estimates. Using the same primers from which the probe was synthesised, five PCRs were set up; a positive control to amplify genomic DNA from line 6₁; a no template control, and reactions with the three BAC DNA templates. A single band of the correct size was apparent following agarose gel electrophoresis of the positive control and test (BAC) PCR products (Figure 6.8). When repeated using brand new PCR reagents and new BAC DNA preparations, this product was no longer amplified from BAC DNA, but continued to be synthesised from genomic DNA (Figure 6.9). None of the clones corresponding to positive hybridisation signals, therefore, contained the chIL-1F5 gene.

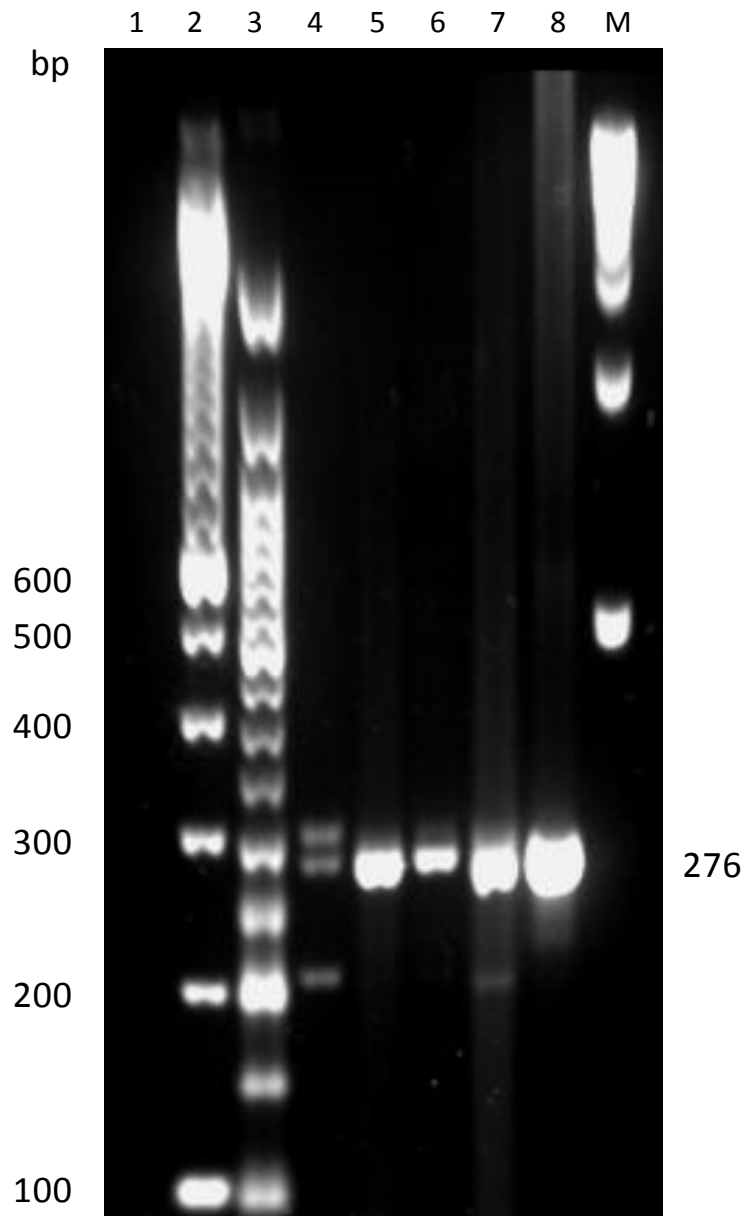


Figure 6.8 Agarose gel showing PCR products from the amplification of IL-1F5 using BAC DNA and genomic DNA from line 6₁. Products were amplified with the IL-1F5 332L & 437R primers. A negative (no template) control reaction was also set up. Lane 1 = negative control, 2 = 100 bp DNA ladder, 3 = 50 bp DNA ladder, 4 = clone 70B9, 5 = clone 132E6, 6 = clone 161B7 (prep 1), 7 = clone 161B7 (prep 2), 8 = positive control (line 6₁ genomic DNA), M = 1 kb ladder.

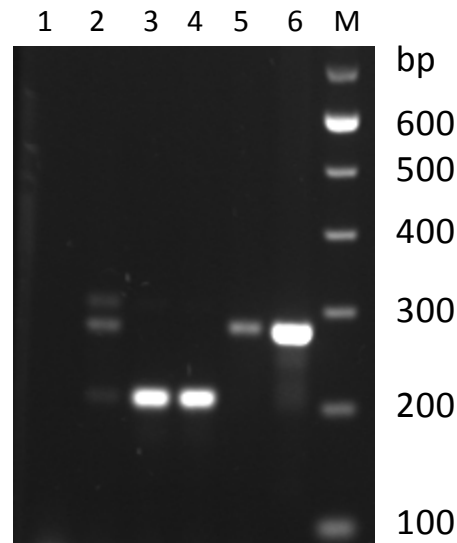


Figure 6.9 Agarose gel showing PCR products from the repeated amplification of **IL-1F5** using **BAC DNA** and **genomic DNA from line 6₁**. Products were amplified with the IL-1F5 332L & 437R primers. A negative (no template) control reaction was also set up. Lane 1 = negative control, 2 = clone 70B9 (original prep), 3 = clone 132E6 (new prep), 4 = clone 161B7 (new prep), 5 = 161B7 (original prep), 6 = positive control (line 6₁ genomic DNA), M = 100 bp ladder.

6.4 Discussion

Early studies into the interleukin-1 gene cytokine family identified and characterized the protein products of three ligand genes: IL-1 β , IL-1 α and IL-1RN. For almost another decade, only a single novel IL-1 ligand (IL-18) (Okamura, Tsutsi et al. 1995) was found. However, during this same period an increasing number of orphan receptors with IL-1R-like features were discovered. The availability of the human genome sequence revealed a further six IL-1 family ligand genes (IL-1F5-F10) clustered with the original three members on human chromosome 2. Subsequent work has attributed most of these ligands to IL-1 family receptors, with some formerly orphaned receptors now having defined roles. One of these more recently discovered members, IL-1F5 (IL-36RN), suppresses inflammation through its role as a receptor antagonist of IL-1RL2 (IL-1Rrp2) (Debets, Timans et al. 2001). This prevents the agonists IL-1F6 (IL-36 α), IL-1F8 (IL-36 β) and IL-1F9 (IL-36 γ) from binding this receptor to initiate gene transcription via NF- κ B and MAP kinases. As with IL-1RN, IL-1F5 fails to recruit IL-1RAcP on the cell surface. IL-1F5 can also downregulate inflammation through an (as yet unelucidated) interaction with the orphan receptor, SIGIRR (Costelloe, Watson et al. 2008). The gene for IL-1F5 is present in the genome sequence of many mammalian species and is considered to have arisen following gene duplication from IL-1RN in the mammalian lineage.

This Chapter describes the identification and characterization of IL-1F5 in the chicken. Whilst many similarities between the chicken gene and its mammalian orthologues exist, several contrasting features were identified.

The locus containing chIL-1 β exhibits limited conserved synteny with the human IL-1 gene locus but lacks any further IL-1 genes. TBLASTN searches of the

chicken genome with the chIL-1 β amino acid sequence did not reveal any further IL-1 gene loci. The same sequence was also used to mine the NCBI database for ESTs encoding novel chicken IL-1 genes. This search identified a novel EST, whose predicted amino acid sequence was shown to most closely resemble IL-1F5 following subsequent BLASTP analysis. A moderate degree of amino acid identity (31.2%) between the predicted chIL-1F5 sequence and human and mouse IL-1F5 was found. Chicken cytokines typically share 25-40% amino acid identity with their mammalian homologues. Additional *in silico* analyses supported the BLASTP results to unequivocally establish the identity of the gene. Phylogenetic analysis was able to confirm it is distantly related to mammalian IL-1F5. Analysis of the predicted secondary structure of chIL-1F5 identified 12 β -strands located in almost identical regions to the mouse IL-1F5 sequence; the only experimentally resolved IL-1F5.

Attempts to determine the genomic location of chIL-1F5 were unsuccessful. PCR results indicated chIL-1F5 does not lie adjacent to chIL-1 β as it does in mammals. Despite this, limited conserved synteny with the human, anole lizard and zebrafish genomes implies the IL-1 locus on chicken chromosome 22 may have had a common ancestral origin with the larger IL-1 loci in those species. For example, the avian orthologues of 2 genes (SLC20A1 and CKAP2L) that flank the human cluster are located adjacent to chicken IL-1 β , although no other genes are shared by the two loci (see Chapter 3, Figure 3.1). Similarly, the avian orthologues of three genes (YKT6, NUDCD3 and OGDH) situated next to the lizard IL-1 cluster (containing IL-1RN, IL-1F5, IL-1F10) are located adjacent to chicken IL-1 β . In the zebrafish, NUDCD3 and OGDH are also found adjacent to its IL-1 β gene. How these loci have arisen and evolved to represent their current compositions, however, cannot be explained with a

simple answer. Perhaps the most logical explanation is that all IL-1 genes evolved from a common ancestor followed by substantial sequence divergence within each species. The majority of single locus multigene families are conserved between humans and chickens and are likely to have arisen this way. As this is not the case with the chIL-1 family, significant chromosomal rearrangement must have taken place in the chicken at some point, leading to the separation of IL-1F5 (and IL-1RN) from IL-1 β . If the IL-1 family has emerged this way, then gene duplication from a common ancestral gene would have to precede the divergence of birds and mammals which took place ~310 Mya. This would comprehensively disprove Mulero, Nelken et al. (2000) who speculated IL-1F5 evolved following divergence from the IL-1RN sequence around the time mammals emerged ~200 Mya. An alternative hypothesis for the origin of IL-1F5 in three species as diverse as human, chicken and lizard, is species-specific convergent evolution. Despite the number of similar structural features between the human and chicken IL-1F5 genes appearing to be relatively low (compared with similarities between huIL-1RN and chIL-1RN genes), this would still represent an extraordinary occurrence.

A hypothesis of differential gene loss within different species may also explain how IL-1F5 has arisen at discordant loci in humans and chickens. Assuming the three human IL-1 loci constitute regions of the genome containing paralogous genes, their origins could be traced to a single ancestral locus which underwent duplication. This ancient locus could have contained both IL-1 β and IL-1F5, which upon subsequent genome duplication formed several paralogous IL-1 loci each encoding a copy of both genes. Additional duplications in the human genome may have expanded the size of the IL-1 gene family at one locus, whilst the other may have contracted, conceivably

leaving only IL-33. In the chicken, one locus could have lost IL-1F5 (and IL-1RN), whilst retaining IL-1 β ; with the opposite scenario taking place at a second locus.

Efforts to elucidate the mechanism by which the IL-1F5, F6, F8 and F9 proteins are secreted from cells have so far been inconclusive. None of the four genes encode a signal peptide like IL-1RN, nor have an obvious pro-domain like IL-1 β and IL-1 α . Only a single report to date has described the secretion of IL-1F5, from trophoblastic JEG-3 cells, although the mechanism remains unknown (Barton, Herbst et al. 2000). Another study has attempted to characterize the mechanism by which murine IL-1F6 is released from bone marrow-derived macrophages (Martin, Scholler et al. 2009). It revealed export was not constitutive, but was increased significantly in response to LPS/ATP stimulation of cell surface P2X₇ receptors. No evidence of proteolytic cleavage was found as IL-1F6 from conditioned medium was exactly the same size as that found in cell lysates. Unpublished observations in two other recent papers imply proteolytic cleavage may take place to yield mature proteins with increased specific activity. For instance, a truncated mutant of murine IL-1F6 with Arg8 as its first amino acid has ~10000-fold greater specific activity than the full length molecule (Blumberg, Dinh et al. 2010). Likewise, an IL-1F9 truncation mutant starting at Gly13 exhibits similarly enhanced activity (Blumberg, Dinh et al. 2010). NH₂-terminally cleaved IL-1F5 and IL-1F8 also exhibit increased bioactivity (Sims and Smith 2010). The fact that neither IL-1F6 nor IL-1F9 mutants are cleaved at an aspartic acid residue (the caspase-1 cleavage site) may mean they are processed independently of the inflammasome. The classical model of enzymatic cleavage incorporates this consensus sequence: P4-P3-P2-P1|P1'-P2'-P3'-P4', whereby the protein is cleaved between P1 and P1'. The chIL-1F5 protein is not predicted to be cleaved by caspase-1 as it does not contain any sites that fully

conform to the published P4-P1 consensus ([F/W/Y/L]-N-[H/A/T]-D for human proteins). Despite this, it does contain three aspartic acid residues at positions 6, 34 and 44 at the N-terminus. The P4-P1 sequences are ALFD, AVR D and CLRD at these sites, respectively. A degree of homology is shared between these sites and the caspase-1 cut sites of huIL-1 β and IL-33. The two IL-1 β cut sites are FEAD and YVHD. Examining the four residues at the Asp34 site of chIL-1F5 shows those at the P3 (V) and P1 (D) positions are identical to those within the YVHD huIL-1 β sequence. Even greater similarity exists between the huIL-33 caspase-1 cut site of ALHD and the Asp6 site of chIL-1F5 (ALFD), which are identical at positions P4, P3 and P1. Caspase-1 cleavage of IL-33 at this site inactivates this cytokine (Cayrol and Girard 2009), although there still remains much contention and conflicting evidence concerning exactly how it is processed (Sims and Smith 2010). The published consensus sequence for caspase-1 is for human proteins and it may be the case that chicken caspase-1, with which it shares 41% identity, exhibits moderately divergent substrate specificity for residues P4-P2 when P1 = D.

A number of striking differences between the chicken and human sequences at both nt and aa levels were noted during this study. For instance, the chIL-1F5 aa sequence has a much longer NH₂-terminus than the human protein, which may have a functional consequence. The platypus IL-1F5 aa also has a longer 5' end, although, this is uncharacteristically predicted (for this cytokine) to contain a signal peptide. The chIL-1F5 aa sequence contains a nuclear export sequence (NES). This motif may not be functional as most proteins <50 kDa are able to diffuse freely across nuclear membranes (Fahrenkrog and Aebi 2003). However, proteins with defined nuclear roles are considered to be transported in a controlled manner (la Cour, Kiemer et al. 2004).

Whether this NES is functional will have to be investigated *in vitro*. This would also raise the question as to how IL-1F5 accumulates in the nucleus such that it is required to be exported and why? To date, within the IL-1 family, only huIL-1 α is actively transported across the nuclear membrane, although in the opposite direction, as it contains a nuclear localization signal (NLS) (Wessendorf, Garfinkel et al. 1993). Human IL-1 β , IL-1F7b and IL-33 also have nuclear functionality, although how they arrive in the nucleus is not known (Luheshi, Rothwell et al. 2009).

Chapter 7

Results 5: Characterisation of expression and bioactivity of chicken IL-1F5

7.1 Introduction

Discovery of the novel IL-1F genes expanded the repertoire of cytokines coordinating innate and inflammatory immune responses, increasing our knowledge of the depth and complexity of this highly sophisticated signalling network.

A high degree of sequence identity with IL-1RN suggested IL-1F5 would be an antagonist; however, initial studies examining its biology were unable to ascribe an obvious function. The purified recombinant form did not, for instance, possess either agonist or antagonist activity in NF- κ B reporter assays, bioassays conducted in primary osteoblasts or in any T cell lines used in earlier assays characterizing IL-1 bioactivity (Busfield, Comrack et al. 2000). Similarly, using either fibroblasts or endothelial cells, IL-1F5 did not stimulate IL-6 production or attenuate IL-1 α /IL-1 β -mediated upregulation of the same proinflammatory cytokine. It also failed to either stimulate IFN- γ production in the human myelomonocytic KG-1 cell line, or suppress its induction following PHA/IL-18 co-stimulation (Barton, Herbst et al. 2000). Interestingly, both these studies expressed IL-1F5 in COS-7 cells and found significantly more recombinant protein in the supernatants than was present in the lysates. Supernatant from cultured JEG-3 cells, a human tumour cell line which constitutively expresses IL-1F5, was also found to contain much more rIL-1F5 than the lysate following immunoprecipitation (Barton, Herbst et al. 2000). As IL-1F5 lacks a signal peptide, pro-domain and N-linked glycosylation sites, this consistent observation strongly implies an unorthodox mode of secretion.

A major breakthrough only a year later conclusively determined the biological function of IL-1F5 as a receptor antagonist of the IL-1RL2 (IL-1Rrp2) (Debets, Timans

et al. 2001). In this study, Jurkat T cells transiently transfected with IL-1RL2 were stimulated with IL-1F9, leading to NF- κ B activation. This response was effectively antagonized by IL-1F5. Typically, a 100- to 1000-fold excess of IL-1RN over IL-1 β /IL-1 α is required to effectively antagonise IL-1RI, whereas this study showed equimolar concentrations of IL-1F5 and IL-1F9 were sufficient for inhibition of IL-1RL2 activation (Debets, Timans et al. 2001). This work also highlighted the short comings of previous studies (Barton, Herbst et al. 2000; Busfield, Comrack et al. 2000) which failed to investigate orphan receptors or novel IL-1F agonist ligands. Another of the original papers describing the novel IL-1F members disagreed with the findings of Debets, Timans et al. (2001). These studies investigated ligand-receptor binding interactions between orphan receptor Fc fusion proteins and IL-1F5-F8 but were unable to observe any, including IL-1F5 being unable to bind to IL-1RL2 (Smith, Renshaw et al. 2000). In another study, Towne, Garka et al. (2004) only found partial IL-1RL2 antagonism by IL-1F5 in Jurkat cells transfected with the receptor, and this was not consistently observed. Interestingly, although IL-1F6, -F8 and -F9 activated NF- κ B and MAPKs in a reporter assay using IL-1RL2 transfected cells, none of the ligands bound this receptor when it was fixed on a BIAcore chip (Towne, Garka et al. 2004). In synovial fibroblasts and articular chondrocytes stimulated with IL-1F8, antagonism of this response by IL-1F5 was only transient (Magne, Palmer et al. 2006). A subsequent study provided a more robust assessment of the role of IL-1F5, examining the effects of knocking the gene out. In transgenic mice overexpressing *il-1f6*, an abnormal skin phenotype develops. The severity of this phenotype is worsened in *il-1f5* deficient mice, underlining its role as an antagonist of inflammation (Blumberg, Dinh et al. 2007). It is possible the previous evidence investigating the role of IL-1F5 was inconsistent due to

inadequate or suboptimal experimental conditions. It is difficult, however, to argue with the results of the knockout model.

A recent review has stated IL-1F5 is definitely a receptor antagonist, binding IL-1RL2 and preventing recruitment of IL-1RAcP, although these are unpublished observations (Sims and Smith 2010). Its nomenclature has now been revised to IL-36 receptor antagonist (IL-36RN) to reflect this function (Dinarello, Arend et al. 2010). Since the review by Sims and Smith (2010) was published, two more recent reports have provided further evidence of the antagonistic role of IL-36RN. In a cohort of patients containing a homozygous missense mutation in IL-36RN, an aberrant protein which has lower affinity for IL-1RL2 is expressed at low levels. This leads to unregulated inflammation and chronic pustular psoriasis, which can be fatal (Marrakchi, Guigue et al. 2011). More recently, a new study appears to have comprehensively shown that IL-36RN is definitely the antagonist of IL-1RL2 (Vigne, Palmer et al. 2011). Multiple stimulatory effects induced by IL-36 α , - β and - γ in bone marrow-derived DCs and CD4⁺ T cells were dose-dependently antagonised by IL-36RN (Vigne, Palmer et al. 2011). In the same cells stimulated with IL-1 β , preincubation with IL-36RN has no effect on the induction of proinflammatory effects (Vigne, Palmer et al. 2011). An additional, as yet unpublished, study (referred to in the discussion of Vigne, Palmer et al. 2011) has also characterised IL-36RN and observed the same general effect (Towne, unpublished).

The second major functional role of IL-1F5 is as an anti-inflammatory cytokine able to downregulate IL-1 β - and LPS-mediated immune responses. This has so far been exclusively reported in the brain of mice and rats, and apparently does not take place in mouse macrophages or DCs. This effect appears to be mediated through its interaction

with the orphan receptor SIGIRR which induces IL-4 production. Both the SIGIRR interaction and the production of IL-4 are integral to this particular function of IL-1F5, as it is abrogated in either IL-4^{-/-} or SIGIRR^{-/-} mice (Costelloe, Watson et al. 2008).

There have been no further studies investigating the function of IL-1F5. Despite only a small number of reports, with some discordant findings, IL-1F5 is evidently involved in downregulating the immune response.

IL-1F5 appears to be broadly expressed in humans and mice with transcripts detectable in most major organs and several cell subsets. Initial studies used Northern blotting and *in situ* hybridisation to quantify expression as restricted to a very narrow range of tissues, namely skin, placenta, uterus, thymus and keratinocytes (Barton, Herbst et al. 2000; Busfield, Comrack et al. 2000). Subsequent analyses using RT-PCR and both EST and cDNA library screening identified significantly more tissues expressing the cytokine (Barton, Herbst et al. 2000; Smith, Renshaw et al. 2000). To date, only bone marrow, liver and small and large intestine have failed to show IL-1F5 expression. Distinct populations of human cells expressing IL-1F5 include THP-1 (monocytic leukaemia cell) ±PMA ±LPS, PBMCs ±PHA ±LPS, LPS-stimulated monocytes, *in vitro* differentiated macrophages, B-cells ± SAC and CD40L and IL-4, NK cells and LPS-stimulated dendritic cells (Mulero, Pace et al. 1999; Barton, Herbst et al. 2000; Busfield, Comrack et al. 2000; Smith, Renshaw et al. 2000). In human bronchial epithelial cells, both IL-4 and IFN- γ significantly decrease IL-1F5 expression (Chustz, Nagarkar et al. 2011).

The expression of IL-1F5 *in vivo* has been incompletely studied with only a very small number of reports available to date. Initial studies showed IL-1F5 was highly expressed in skin (Debets, Timans et al. 2001) and this observation has seemed to direct

the focus of further studies making inflammatory skin conditions the only disease model examined. In various forms of human psoriatic skin, IL-1F5 expression is greatly increased compared with levels found in normal skin (Debets, Timans et al. 2001; Blumberg, Dinh et al. 2007; Johnston, Xing et al. 2011). Similarly, in the inflammatory psoriasis-like skin condition which develops in il-1f6 transgenic mice (Blumberg, Dinh et al. 2007), and the involved skin of mouse psoriasis (Johnston, Xing et al. 2011), IL-1F5 is highly expressed. The expression of IL-1F5 following viral, fungal or parasitic infection has not been described. Beyond stimulation with LPS, responses to other bacterial agents are also unknown.

In this Chapter, thorough analyses of both chIL-1F5 expression and biological activity are described. Attempts to characterise the bioactivity of full length recombinant chicken IL-1F5 were unsuccessful. The transcriptional profile of chIL-1F5 provided some novel observations on possible regulation of the cytokine at sites of immune activation and, in particular, disease states.

7.2 Methods

7.2.1 Sources of chicken tissues and cells

All chicken tissues and cells were acquired, sorted and stimulated as described in Chapter 2, section 2.4.1.1. Tissues and cells were acquired from SPF chickens challenged with bacteria or virus as described in Chapter 2, section 2.4.1.2.

7.2.2 HD11 time course stimulation

HD11 cells were routinely cultured as described in Chapter 2, section 2.4.12.1 and 2.4.12.2. Cells were stimulated with LPS as described in Chapter 2, section 2.4.16.

7.2.3 Transfecting cells with pure chicken DNA

HEK293T cells were transiently transfected with a pure chicken IL-1F5pHLSec CDS clone as described in Chapter 2, section 2.4.12.3.2.

7.2.4 Purification and analysis of HIS-tagged recombinant proteins

Recombinant IL-1F5pHLSec protein was purified from crude HEK293T culture supernatants under denaturing conditions as described in Chapter 2, section 2.4.13.2, as initial attempts to purify under native conditions repeatedly resulted in loss of the protein (determined by SDS-PAGE and Western blotting). Purified proteins were analysed by SDS-PAGE and Western blot as described in Chapter 2, sections 2.4.14.1 and 2.4.14.2. Pure proteins were quantified using the Bradford assay as described in Chapter 5, section 5.2.4.

7.2.5 HD11 bioassay

7.2.5.1 LPS optimisation assay

A pilot study was set up to quantify the optimal concentration of LPS to use in subsequent “test” assays. Two rows of a 24-well plate were seeded with 5×10^5 HD11 cells/well and cultured overnight at 41°C, 5% CO₂. The next day, HD11 cells were stimulated with LPS (strain: *Klebsiella pneumoniae*) across the following concentration range: 5000, 2500, 1000, 500, 250, 100, 50, 25, 10 and 1 ng/ml, and incubated for 12 h overnight. The concentration of nitrites (NO₂⁻) was measured in HD11 culture supernatants by the Griess reaction as outlined in Chapter 2, section 2.4.15.2.1.

7.2.5.2 Final bioassay conditions

HD11 cells were seeded in a 24-well plate at 1×10^6 cells/well and cultured with a doubling dilution series of pure rIL-1F5 (range: 625-19.53 µg/ml) for 4 h at 41°C, 5% CO₂. Next, cells were stimulated with 200 ng/ml LPS and cultured overnight at 41°C, 5% CO₂. The next day, culture media was tested for nitrites by the Griess reaction as outlined in Chapter 2, section 2.4.15.2.1. The rest of the supernatant was discarded, cells were lysed with 600 µl RLT buffer and lysates were used immediately or frozen at -80°C. Optimal bioassay conditions were determined empirically and all assays described in this Chapter were carried out under these conditions.

7.2.5.3 Quantifying the biological response

The concentration of nitrites (NO₂⁻) was measured in HD11 culture supernatants by the Griess reaction as outlined in Chapter 2, section 2.4.15.2.1. IL-1β and iNOS

mRNA levels were quantified by TaqMan® as described in Chapter 2, sections 2.4.4.6 and 2.4.15.3.2 and this Chapter, section 7.2.6.

7.2.6 Total RNA isolation and real-time qRT-PCR (TaqMan®) analysis of chicken mRNA expression

RNA was extracted from the tissues and cells used in this Chapter as described in Chapter 2, sections 2.4.2.1 and 2.4.2.2.

Primers and probes to detect expression of IL-1F5, IL-1 β , iNOS and 28S were designed using Primer Express (Applied Biosystems) as described in Chapter 2, section 2.4.4.6. Standard probes labelled at the 5' end with 5- or 6-carboxyfluorescein (FAM) fluorophore, and at the 3' end with tetramethylrhodamine (TAMRA) quencher dye were used to detect IL-1 β , iNOS and 28S expression. The probe used to detect IL-1F5 transcripts was labelled with FAM at the 5' end and dihydrocyclopyrroloindole tripeptide minor groove binder ligand (MGB) at the 3' end. Assays were performed as described in Chapter 2, section 2.4.4.6.

7.3 Results

7.3.1 Analysis of IL-1F5 mRNA expression in unstimulated tissues by real-time qRT-PCR

The expression profile of chIL-1F5 was examined in a broad range of chicken tissues and cells by qRT-PCR (TaqMan®) (Figure 7.1). Expression was ubiquitous with highest levels, in lymphoid tissues, in the blood, spleen and thymus. In non-lymphoid tissues, expression was highest in lung and skin. By contrast, the expression of mammalian IL-1F5 appears to be restricted to skin, brain, spleen, leukocytes (Mulero, Pace et al. 1999), and placenta, thymus, macrophages and LPS-stimulated monocytes (Barton, Herbst et al. 2000).

7.3.2 Analysis of IL-1F5 mRNA expression by real-time qRT-PCR in sorted cells which were either unstimulated or stimulated

Constitutive expression of IL-1F5 was detected in all 20 subsets of sorted chicken lymphocytes. In heterophils (\pm LPS stimulation) and LPS-stimulated blood-derived monocytes, IL-1F5 expression was substantially higher than in the rest of the panel (Figure 7.2). DCs and macrophages derived from bone marrow were also stimulated with LPS; however, this did not lead to an increase in IL-1F5 expression.

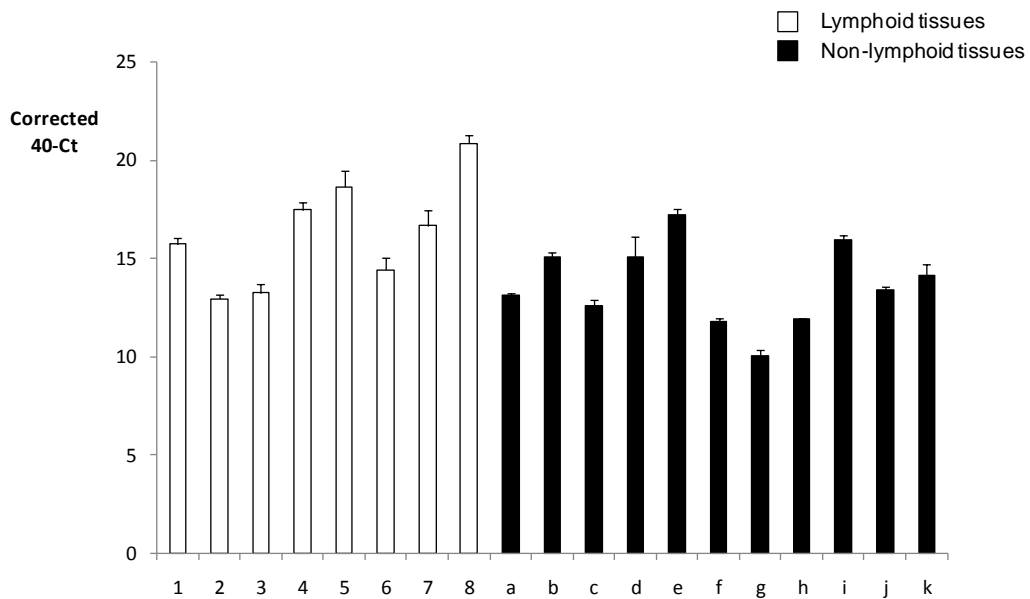


Figure 7.1 IL-1F5 expression in lymphoid and non-lymphoid tissues as measured by real-time qRT-PCR. Results are expressed as corrected 40-Ct +SEM. Lymphoid: 1, bursa of Fabricius; 2, caecal tonsil; 3, Meckel’s diverticulum; 4, spleen; 5, thymus; 6, Harderian gland; 7, bone marrow; 8, blood. Non-lymphoid: a, lower gastrointestinal tract (GIT); b, mid-GIT; c, upper GIT; d, kidney; e, lung; f, heart; g, muscle; h, brain; i, skin. j, caecal wall; k, liver.

7.3.3 Analysis of IL-1F5 mRNA expression across a time course by real-time qRT-PCR in three different populations of stimulated macrophages

As described in Chapter 5, section 5.3.3, three different populations of macrophages were stimulated in culture from 0-48 h. IL-1F5 expression was assessed in *in vitro* cultured HD11 cells stimulated with LPS from 0-24 h. Expression was also measured in two *ex vivo* populations; bone marrow-derived macrophages (BM-MØ) and blood monocyte-derived macrophages (Mo-MØ), stimulated with LPS or CD40L for 1-48 h. In the HD11 macrophage cell line, IL-1F5 expression increased by 1.75-fold at 1 hps. This level of expression was sustained at 2 hps, but then noticeably declined by 6 hps, being 2.6 fold lower. The level of expression then remained constant for the

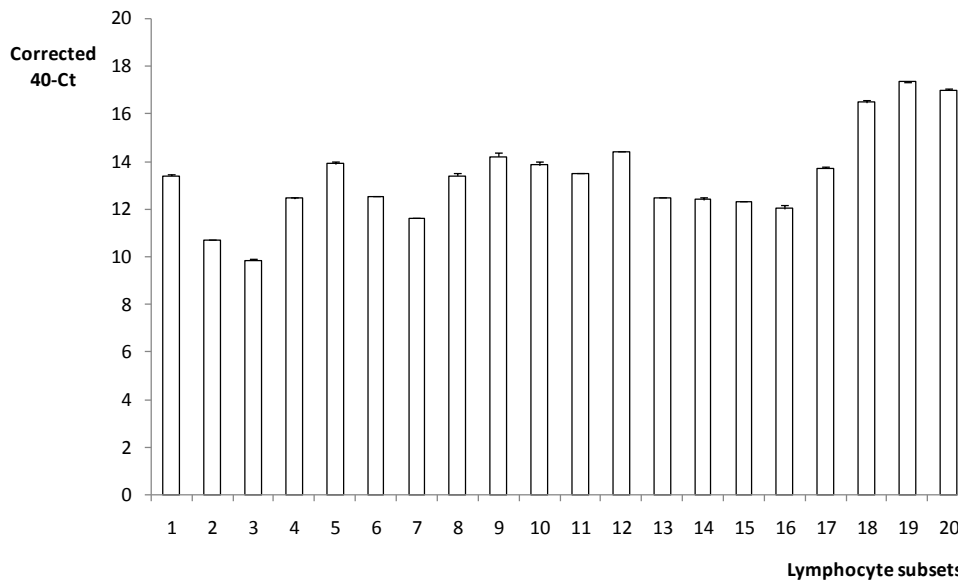


Figure 7.2 IL-1F5 expression in sorted chicken lymphocyte subsets as measured by real-time qRT-PCR. Results are expressed as corrected 40-Ct \pm SEM. Bars represent expression in: 1, splenocytes; 2, bursal cells; 3, PMA-stimulated bursal cells; 4, thymocytes; 5, CD4+ cells; 6, CD8 α + cells; 7, CD8 β + cells; 8, TCR1+ cells; 9, TCR2+ cells; 10, TCR3+ cells; 11, Bu-1+ cells; 12, KULO1+ cells; 13, BM-DC; 14, LPS-stimulated BM-DC; 15, BM-M Φ ; 16, LPS-stimulated BM-M Φ ; 17, blood-derived monocytes; 18, LPS-stimulated blood-derived monocytes; 19, heterophils; 20, LPS-stimulated heterophils.

duration of the experiment (Figure 7.3).

In BM-M Φ , large differences in IL-1F5 expression were observed between LPS-stimulated and unstimulated control cells. At 1 hps, mRNA expression was 1.5-fold higher in stimulated cells. By 2 and 4 hps, an even bigger difference was observed as expression had increased to 3.2-fold higher than in control cultures (Figure 7.4). At 8 hps, however, LPS-stimulated BM-M Φ exhibited identical IL-1F5 expression to the control cells, an inconsistent result relative to the sampled time-points before and after. Expression was again increased in LPS-stimulated cells at 24 h and 48 h to levels ~1.6-fold higher than the controls. Stimulation with CD40L, however, did not affect IL-1F5

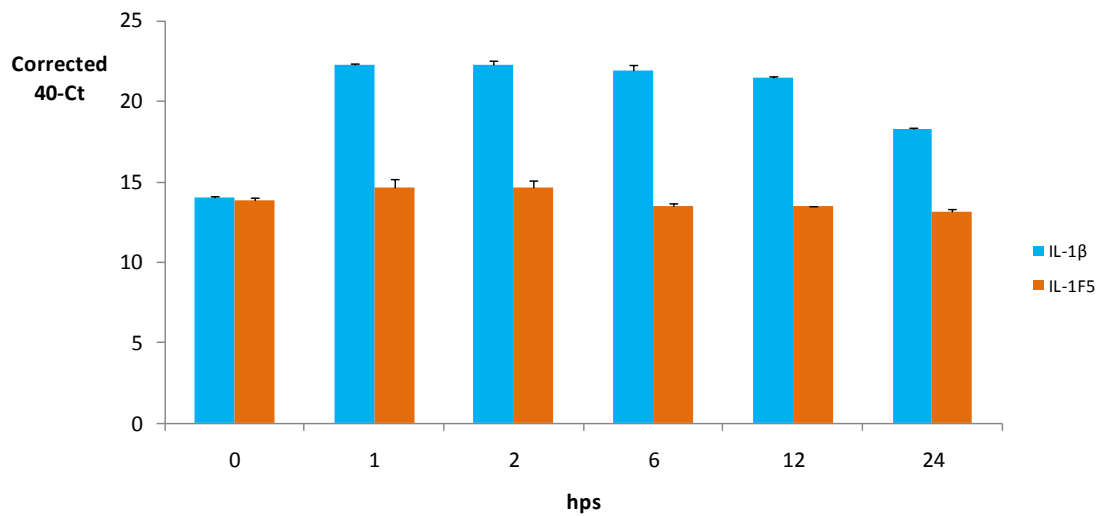


Figure 7.3 Expression of IL-1F5 and IL-1 β in the HD11 macrophage cell line following stimulation with LPS as measured by real-time qRT-PCR. Results are expressed as corrected 40-Ct \pm SEM of three samples from single flasks. hps = hours post-stimulation.

expression in this population. None of the observed differences in expression were statistically significant.

A similar, albeit delayed response to LPS was observed in Mo-M \emptyset . Here, LPS-stimulation led to 1.5 and 1.7-fold increases at 1 and 2 hps compared with unstimulated cells. A substantial increase in expression was apparent after 4 h (7.2-fold), which remained high at 8 h (4.4-fold) post-stimulation, but declined thereafter. In contrast to the findings in BM-M \emptyset , CD40L stimulation led to an upregulation in IL-1F5 expression in Mo-M \emptyset throughout the experiment (Figure 7.5). A gradual rise in expression was observed in stimulated cells at 1, 2 and 4 hps, increasing by 1.9, 2.6 and 4.2-fold respectively, relative to controls. Expression was no higher than in unstimulated cells at 8 hps (1.1-fold). However, at both 12 h and 24 h a difference of >2-fold was apparent in CD40L-stimulated cells, compared to control cultures. Again, none of the observed

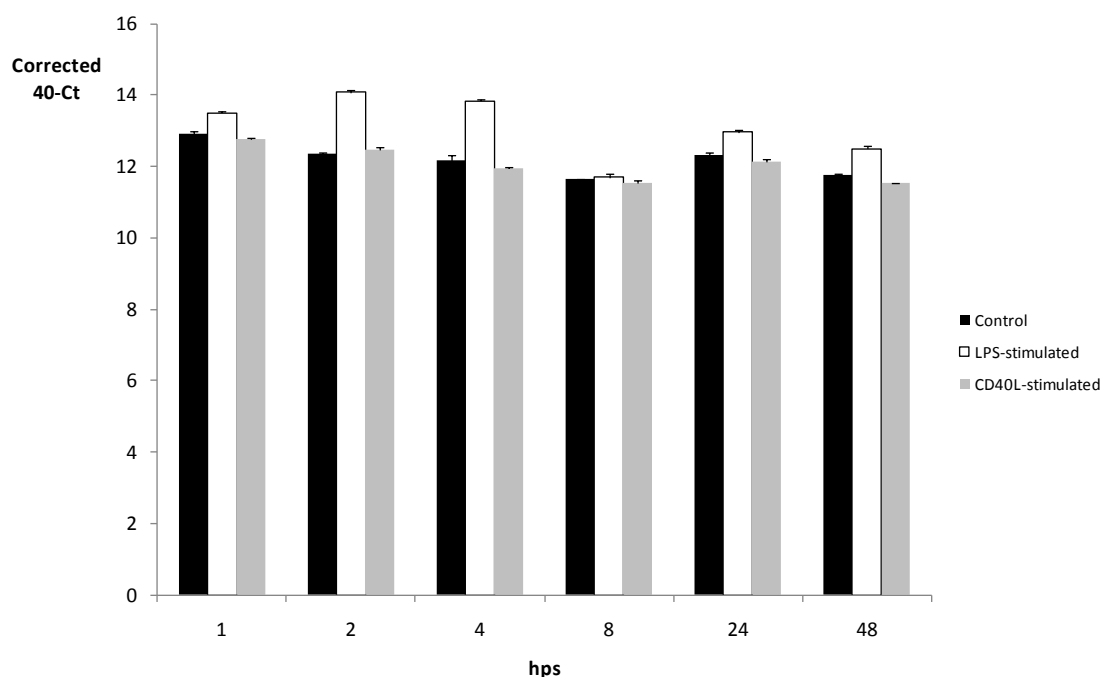


Figure 7.4 Expression of IL-1F5 in BM-MØ stimulated with LPS or CD40L. Results are expressed as corrected 40-Ct \pm SEM of three replicates from a single sample. hps = hours post-stimulation.

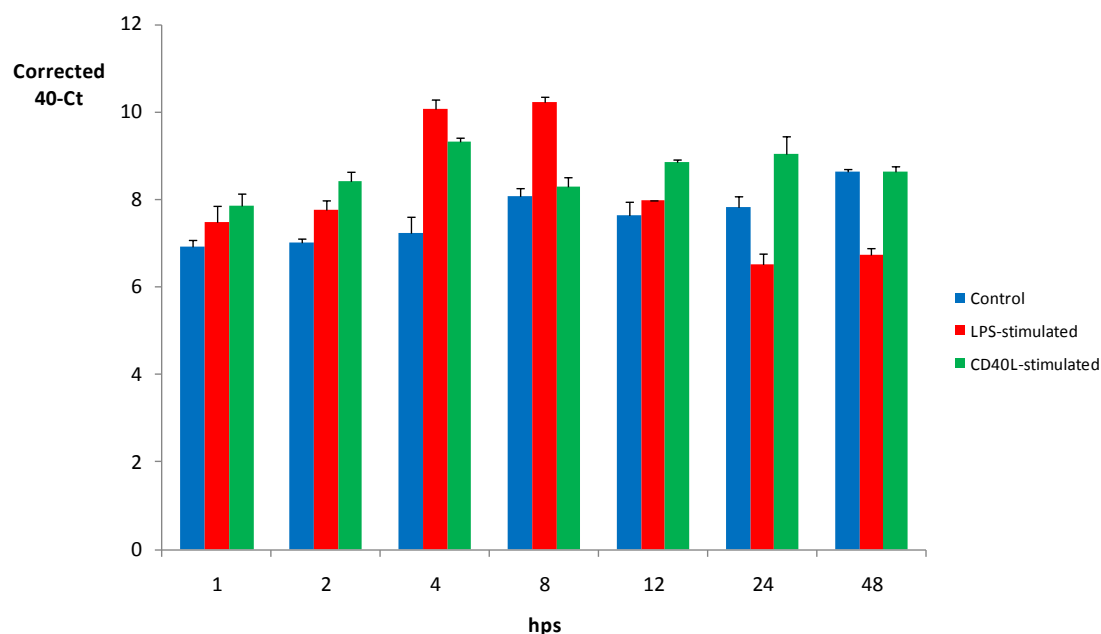


Figure 7.5 Expression of IL-1F5 in Mo-MØ stimulated with LPS or CD40L. Results are expressed as corrected 40-Ct \pm SEM of three replicates from a single sample. hps = hours post-stimulation.

differences in expression were statistically significant.

7.3.4 Analysis of IL-1F5 expression in vivo by real-time qRT-PCR following bacterial or viral challenge

7.3.4.1 Infectious Bursal Disease Virus

Chickens which have either increased resistance (line 6₁) or susceptibility (BrL) to infectious bursal disease virus (IBDV) were challenged as outlined in Chapter 2, section 2.4.1.2. RNA was extracted from bursae of Fabricius and assayed for IL-1F5 expression at 2, 3 and 4 dpi (Figure 7.6). In contrast to the pattern of IL-1RN_{fl} expression found in this tissue (Chapter 5, section 5.3.4.1), IBDV infection consistently downregulated IL-1F5 mRNA expression throughout the experiment. At 2 dpi there was no statistically significant difference (-1.23-fold) in expression between line 6₁ infected and control birds. By contrast, a statistically significant decrease in IL-1F5 expression in infected BrL birds compared with controls was observed (-4.24-fold). Again at 3 dpi, differences between control and infected line 6₁ birds were not statistically significant, although expression was lower in the infected birds by 1.4-fold. A bigger difference in expression between both groups of BrL birds was again apparent at 3 dpi, being 3.46-fold lower in the infected cohort. This was also statistically significant. Finally, at 4 dpi, the largest differences in mRNA expression between control and infected birds of both lines were found. For the resistant line, 2.86-fold lower expression was detected in the infected birds relative to controls; whilst the infected susceptible birds exhibited a 6.65-fold decrease in expression compared with uninfected birds. At this time-point,

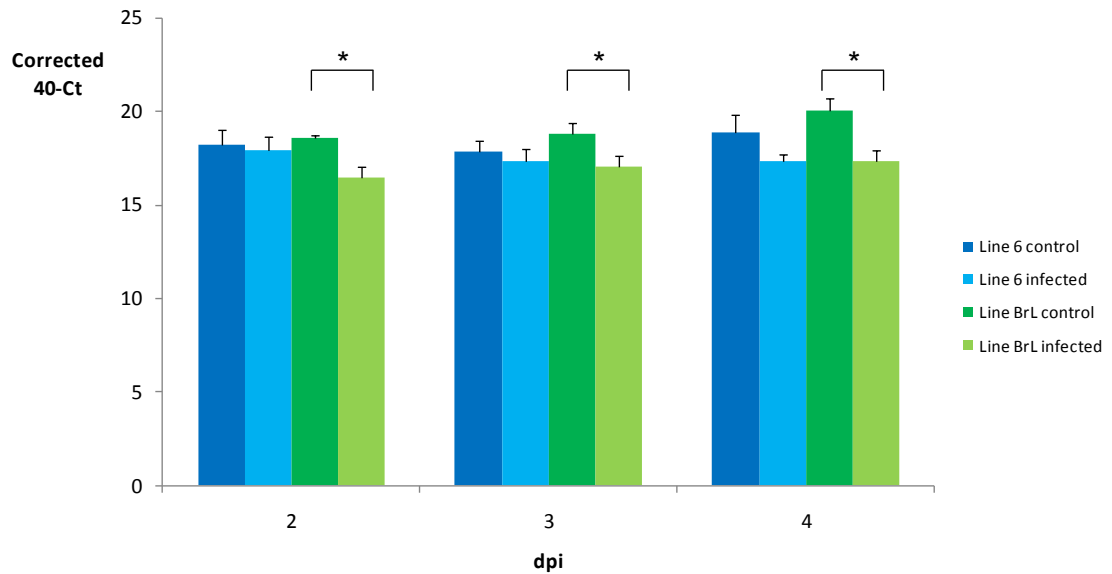


Figure 7.6 Expression of IL-1F5 mRNA in bursal cells from line 6₁ (resistant) and BrL (susceptible) chickens infected with IBDV. Results are expressed as mean corrected 40-Ct \pm SEM of five birds per individual group. *P<0.05. dpi = days post-infection.

differences in expression were again only statistically significant in the BrL line.

7.3.4.2 *S. Typhimurium* strain F98 *Nal*^R

The expression of IL-1F5 mRNA, as with IL-1RN, was assessed following infection of outbred RIR chickens with *S. Typhimurium* strain F98 *Nal*^R across a 28 day period (Figure 7.7). Splenocyte RNA from infected and uninfected age-matched RIR birds was quantified at 3, 7, 14, 21 and 28 dpi. A similar expression profile to that seen with IL-1RN (Chapter 5, section 5.3.4.2) was observed for this gene. At 3 dpi, IL-1F5 mRNA expression was 4.52-fold higher in the spleen of infected birds compared to the uninfected controls. This result was statistically significant. For the remainder of the

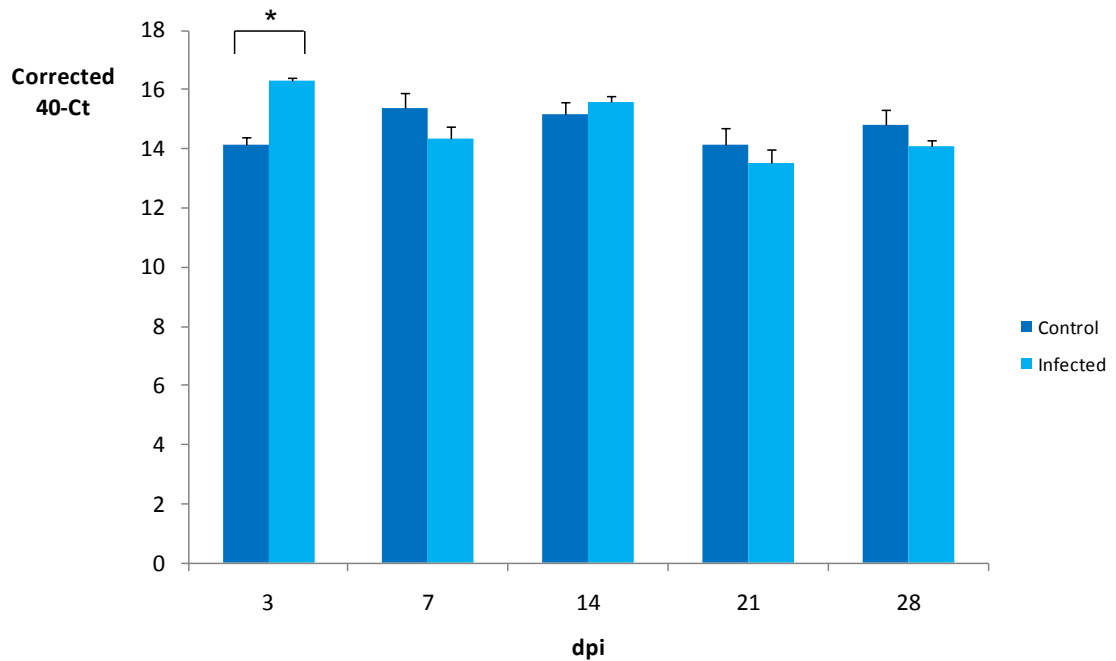


Figure 7.7 IL-1F5 expression in splenocytes from RIR chickens following infection with *S. Typhimurium* strain F98 Nal^R. Results are expressed as mean corrected 40-Ct \pm SEM of four birds per individual group. *P<0.05. dpi = days post-infection.

experiment, differences in expression between infected and uninfected birds were small (range: -1.6 to 1.3-fold) and not statistically significant.

7.3.5 Characterization of the bioactivity of IL-1F5

7.3.5.1 Characterization of the bioactivity of pure IL-1F5

Recombinant chicken IL-1F5 was successfully expressed in HEK293T cells (Figure 7.8). Full length chIL-1F5 was cloned into the pHLSec expression vector as described in Chapter 2, section 2.4.7.4. Following transfection into HEK293T cells, recombinant chicken IL-1F5 was initially detected in crude cell supernatant by western blot (Figure 7.8A, lane 2). However, following concentration of the supernatant and

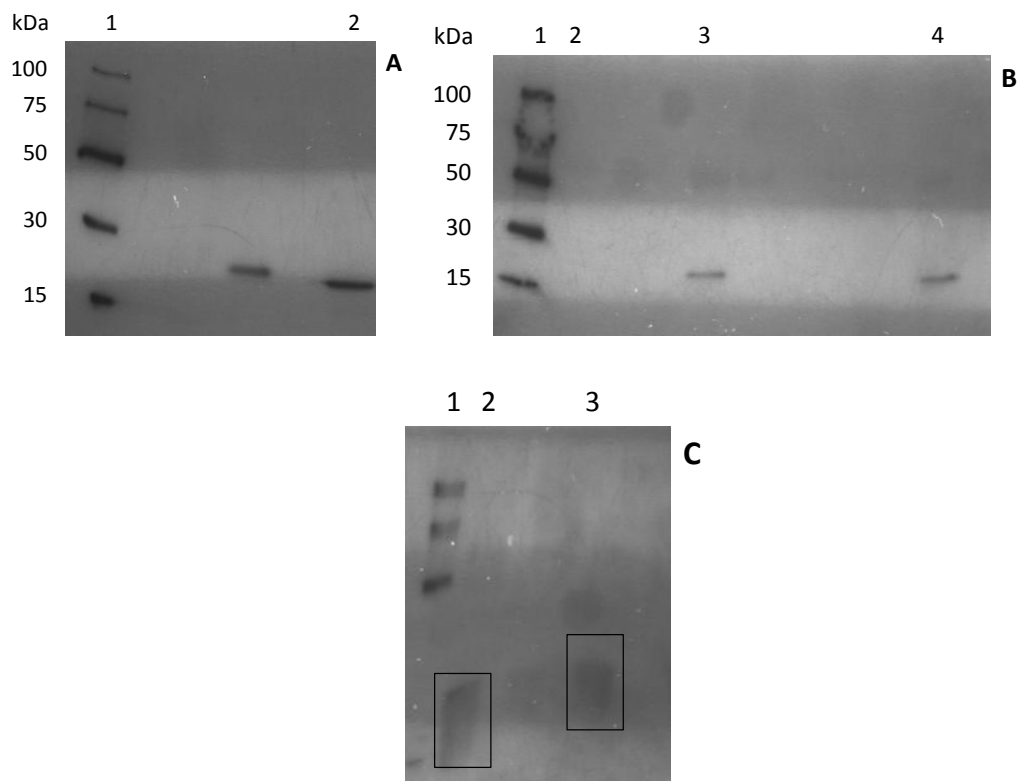


Figure 7.8 Western blot of pure recombinant chIL-1F5 protein expressed in HEK293T cells. Samples were electrophoresed on a 4-15% Mini-PROTEAN TGX gel under denaturing conditions then purified under denaturing conditions. Urea was removed by stepwise dialysis. **A.** Lane 1 = 6xHIS protein ladder (Qiagen); Lane 2 = crude HEK293T culture supernatant containing rchIL-1F5pHLSec. **B.** Lane 1 = 6xHIS protein ladder (Qiagen); Lane 2 = crude HEK293T culture supernatant containing rchIL-1F5pHLSec (precipitated); Lane 3 = Denatured re-solubilised crude rchIL-1F5pHLSec in PBS + 8M urea (the identical sample from lane 2 with added urea); Lane 4 = Purified rchIL-1F5pHLSec (in PBS with imidazole and urea). **C.** Lane 1 = 6xHIS protein ladder (Qiagen); Lane 2 = crude HEK293T culture supernatant containing rchIL-1F5; Lane 3 = dialysed, urea-free purified rchIL-1F5pHLSec. Purification and dialysis led to a loss of protein as shown by the unclear band in this lane. Protein concentration = 2 mg/ml. Calculated Mw (chIL-1F5pHLSec) = 22.8 kDa.

buffer exchange with PBS, the recombinant protein became precipitated and was no longer detectable by western blot (Figure 7.8B, lane 2). It was therefore necessary to purify chIL-1F5 under denaturing conditions. To do this, precipitated rchIL-1F5 was initially denatured with 8 M urea, which resolubilised the protein (Figure 7.8B, lane 3).

Following washing, purified rchIL-1F5 was detectable by western blot (Figure 7.8B, lane 4). To remove the urea and refold rchIL-1F5, the sample was dialysed against PBS then detected by western blot (Figure 7.8C, lane 3). This confirmed that dialysis had not caused precipitation of the protein.

In mammals, IL-1F5 acts as an antagonist of the IL-1RL2 receptor.

Proinflammatory immune responses are modulated via this receptor by the agonists IL-1F6 (IL-36 α), IL-1F8 (IL-36 β) and IL-1F9 (IL-36 γ). As yet, these ligands have not been identified in the chicken, so it was not possible to determine the antagonistic activity of chIL-1F5 in a straightforward ligand-receptor interaction bioassay. Transgenic technology is in its infancy in this species, ruling out the use of knockout chickens to establish function. Although unsuccessful in mouse macrophages, we assessed the ability of pure recombinant chIL-1F5 to downregulate LPS-mediated inflammation in a HD11 (macrophage) cell bioassay. The activity of IL-1F5 was determined by its ability to abrogate the LPS-mediated upregulation of IL-1 β and iNOS genes. In cells stimulated with LPS alone, IL-1 β and iNOS mRNA expression increased significantly compared to expression levels in unstimulated cells (Figure 7.9). Preincubation with different dilutions of rchIL-1F5 for 4 h prior to the addition of LPS had no effect, in that levels of IL-1 β and iNOS mRNA expression were the same as in those cells stimulated with LPS alone.

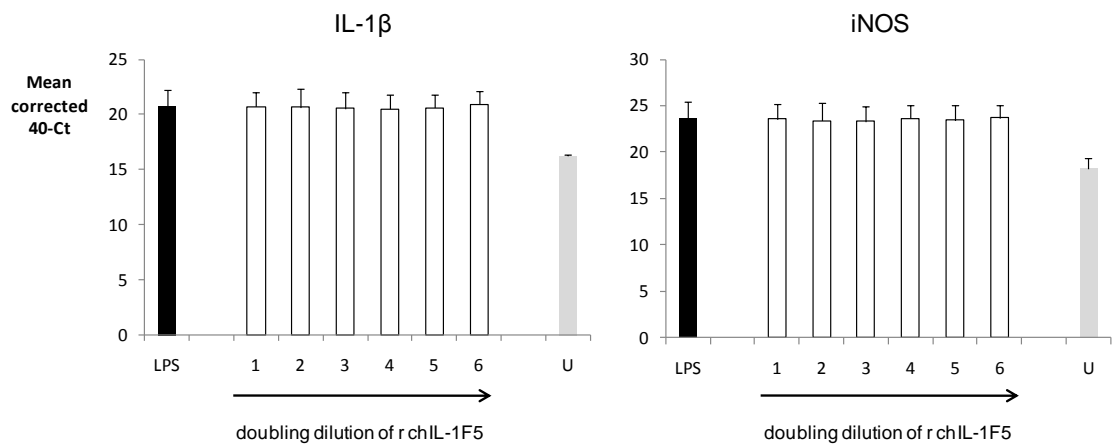


Figure 7.9 Full length chIL-1F5 does not downregulate LPS-induced inflammation in HD11 cells. Doubling dilution of rchIL-1F5 from 250 $\mu\text{g}/\text{ml}$. Bars denote IL-1 β and iNOS expression in HD11 cells pre-incubated with pure rchIL-1F5 for 4 hours prior to the addition of LPS for 12 hours. Results are represented as the mean corrected 40-Ct \pm SD of 3 independent experiments. U = unstimulated cells. LPS = cells stimulated with LPS without IL-1F5.

7.4 Discussion

The biological activity of human and mouse IL-1F5 has been characterised in NF- κ B reporter assays showing it acts as an antagonist of IL-1RL2 (Debets, Timans et al. 2001), although not all groups are able to replicate these findings (Towne, Garka et al. 2004; Magne, Palmer et al. 2006). It is assumed to physically occupy this receptor preventing IL-1F6, -F8 and -F9 from binding (Sims and Smith 2010). Although bioassays have shown it does not initiate signal transduction, resolution of its crystal structure actually suggested it was more likely to operate as an agonist (Dunn, Gay et al. 2003). As IL-1F6, -F8 and -F9 ligands remain absent in the chicken, it was not possible to determine the antagonistic activity of chIL-1F5 in a ligand-receptor interaction bioassay. Other potential methods of investigation such as a knockout model to establish function are also unavailable in the chicken at present. We therefore sought to replicate a previous assay carried out in mice, by preincubating cells in culture with IL-1F5 prior to the addition of LPS. In mouse glial cells, IL-1F5 potently downregulated the effects of subsequent LPS-stimulation; however, this effect was not observed in macrophages or DCs (Costelloe, Watson et al. 2008). With limited scope for an alternative, we investigated the ability of pure recombinant chIL-1F5 to downregulate LPS-mediated inflammation in a HD11 (macrophage) cell bioassay. Chicken IL-1F5 contains an additional 16 amino acids (than mouse IL-1F5) at its NH₂-terminus, a potential nuclear export sequence, and exceptionally low amino acid identity with mouse IL-1F5 at both NH₂- and COOH-termini. It therefore cannot be assumed to possess identical biological function to the mammalian protein. It did not suppress LPS-mediated increases in IL-1 β and iNOS mRNA expression.

Purification of chIL-1F5 was initially unsuccessful under native conditions due

to precipitation. This was predicted to be due to the theoretical pI of chIL-1F5 being very similar to the pH of the HEK293T culture medium. Purification of chIL-1F5 was therefore performed under denaturing conditions. This meant stepwise dialysis was required to purge the sample of urea and to refold the recombinant protein. It is possible the protein did not refold properly, which would make it unable to bind its receptor. It is also possible HD11 cells do not express IL-1RL2 or SIGIRR. ChIL-1F5 may just not function in these cells even if it is able to downregulate LPS-induced inflammation in other cell types. The IL-1RL2 agonist ligands are required to facilitate a more comprehensive assessment of function.

Expression of IL-1F5 was ubiquitous and constitutive in the range of cells and tissues examined. Previous studies have assessed global IL-1F5 expression in humans and mice (Mulero, Pace et al. 1999; Barton, Herbst et al. 2000; Busfield, Comrack et al. 2000; Smith, Renshaw et al. 2000) and found it was not present in all tissues. The highest constitutive levels of chicken IL-1F5 expression were in blood, thymus and spleen, reflecting a likely requirement for high levels of IL-1F5 production from leukocytes upon activation. Similar to IL-1RN, IL-1F5 was also highly expressed in KUL01+ cells and LPS-stimulated blood-derived monocytes, although expression in heterophils was markedly divergent. In these avian-specific cells, IL-1RN_{fl} exhibited relatively low expression whereas high levels of IL-1F5 were found. As heterophils migrate to sites of infection more rapidly than other cell types (Wu and Kaiser 2011), being the dominant subset during the first 6-12 h post-infection (Harmon 1998), large amounts of IL-1F5 are likely to be produced during acute inflammation. There are no reports as yet of IL-1F5 expression in neutrophils, the mammalian equivalent of avian heterophils.

Stimulation of three distinct monocyte/macrophage populations with LPS led to large increases in the expression of IL-1F5 in BM-MØ and Mo-MØ, sharply contrasting with IL-1RN_{fl} expression in the identical samples, which was unaffected. In both of these *ex vivo* populations, expression was much higher than the controls at 4 hps, as well as at 2 hps in BM-MØ and at 8 hps in Mo-MØ. At all time-points after 8 hps, IL-1F5 mRNA levels were similar in control and LPS-stimulated cells. These novel findings suggest IL-1F5 is a *bona fide* innate immune response gene in the chicken. Expression of IL-1F5 has never been examined over a time course *in vitro* in any other species. As was seen for IL-1RN_{fl} and IL-1RN_{SV1}, IL-1F5 expression did not significantly increase after LPS-stimulation in the HD11 cell line.

Chicken IL-1F5 expression was significantly increased following infection with *S. Typhimurium*. As befits an innate immune response gene, expression was much higher in infected than uninfected splenocytes at 3 dpi. By 7 dpi, expression was similar in both groups following the onset of the adaptive immune response. This expression profile correlated with that of IL-1RN_{fl} in these samples.

Infection with IBDV led to a striking decrease in IL-1F5 mRNA expression in both lines throughout the entire experiment. In the resistant line, differences between infected and uninfected birds were modest at 2 and 3 dpi. By 4 dpi, expression was much lower in the infected birds relative to the uninfected group, although not significantly so. In the susceptible line, the differences in IL-1F5 expression between infected and uninfected birds were much bigger than differences in the resistant line. Relative differences were statistically significant at 2, 3 and 4 dpi in the susceptible birds. It is interesting to observe such a discrepancy between the two lines of birds. It is not possible to say whether differences in IL-1F5 expression are caused by differential

resistance to IBDV, whether expression differences lead to disease resistance or whether neither is causative. The IL-1F5 gene or genes which regulate its expression in brown Leghorn birds may contain certain polymorphisms which affect the amount of mRNA produced. Whatever the cause, these are significant and novel findings when compared with the results obtained for IL-1RN_{fl} and IL-1RN_{SV1}, and with IL-1F5 expression following *S. Typhimurium* infection, and from them we can form certain hypotheses.

Firstly, there is some degree of regulation of IL-1F5 expression which must differ from the control of IL-1RN (and IL-1 β) expression. It may be possible that some form of subversion or downregulation of the intracellular signalling pathway is taking place. If so, this would suggest an alternative pathway to that regulating IL-1 β or IL-1RN is being utilised as expression of both these genes is increased following IBDV infection (Eldaghayes, Rothwell et al. 2006). However, the likelihood of this is difficult to predict.

Secondly, a viral-specific factor, either directly or indirectly, may regulate IL-1F5 expression, for example a secreted protein binding to its promoter. The IL-1F5 gene may be directly influenced in response to viral infection. As its expression has never been assessed in response to any type of virus in any other species, there are no simple models for how this could occur. IL-1F5 may be at the end of a cascade of gene-gene interactions and so would be indirectly influenced by IBDV, but again, there is no precedent for this. Related to both original points, IBDV may encode a microRNA which degrades IL-1F5 mRNA, leading to reduced expression levels in infected birds. Regardless of the cause, these findings represent the first ever study of IL-1F5 expression in response to viral infection.

Chapter 8

Discussion

8.1 Discussion

The major aim of this study was to determine the extent of the IL-1 gene family in the chicken. Once novel chIL-1 genes had been identified, the aim was to clone and thoroughly characterise them at the genomic, transcriptional and translational levels. In humans, eleven IL-1 ligand genes encoding proteins with both pro- and anti-inflammatory activities have been identified. Prior to this study, avian orthologues of only two IL-1 family agonist ligands, IL-1 β and IL-18, had been characterised. None of the anti-inflammatory IL-1 genes, or any of the IL-1F agonists most recently discovered in man, had been identified in the chicken. The number of IL-1 receptor genes identified in the chicken was similarly small when compared with the size of the IL-1R family in mammals. Due to the exceptional potency of IL-1 agonist ligands such as IL-1 β , it was surprising that the chicken appeared to lack any of the genes encoding IL-1 ligands and receptors that regulate inflammation. In particular, the absence of IL-1RN and the IL-1RII and SIGIRR receptors was conspicuous, given their critical functional roles in limiting IL-1 activity.

An initial examination of the IL-1 ligand and receptor gene repertoires in the chicken used conserved synteny and BLAST searches to fully interrogate the most up-to-date (although incomplete) assembly (v2.1) of the chicken genome. This failed to uncover any further ligands beyond the two already known, but did identify a different genomic location to those previously reported for IL-1 β . This appeared to be a genuine IL-1 locus, as it shared a limited degree of conserved synteny with the major IL-1 ligand gene locus in the human genome. The human locus contains a further eight IL-1 ligand genes, but the chicken locus clearly does not. No other areas of the chicken

Chapter 8: Discussion

genome provided any evidence of IL-1 ligand genes. This indicated the chicken either lacks these genes entirely or that some or all of them are present in areas of the genome that have yet to be sequenced. The latter scenario was predicted to be the most likely, based on the absence of fundamentally important members of the family. At the genomic level, this would represent an atypical situation in the chicken, assuming the v2.1 build was assembled correctly. In general, although chickens characteristically possess fewer members of multigene families than are found in mammals, their genomic locations tend to be conserved. Clearly, this does not extend to the IL-1 family in the chicken.

In contrast to the small number of identifiable IL-1 ligand genes, all of the IL-1 receptor genes identified in the human genome are present in v2.1 of the chicken genome. Additionally, they are all found in regions of conserved synteny between both species. The degree of conserved synteny at each of these loci is very high and strongly suggests this receptor family was formed in a common ancestor prior to the divergence of birds and mammals. Assuming this is true, the persistence in the chicken of the IL-1RL2 and ST2 receptors over 300 million years later implies they may continue to serve a purpose. This provides compelling evidence for the existence of avian orthologues of their ligands, IL-1F5, -F6, -F8, -F9 and -F11.

Whilst comparative genomics did not identify additional IL-1 ligand genes in the chicken, EST library screening uncovered sequences for IL-1RN and IL-1F5. Thorough analyses of both genes showed they retained certain features that were similar to those found in their mammalian orthologues, alongside some quite significant differences.

The coding sequences of both secretory and intracellular IL-1RN cDNAs were present in the NCBI chicken EST library. Both were subsequently cloned from RNA

Chapter 8: Discussion

from LPS-stimulated HD11 cells and examined *in silico*. The predicted amino acid sequences were analysed by SignalP, confirming the two major structural variants of the mammalian gene are conserved in the chicken. Both protein sequences contain the IL-1 signature motif, have a similar secondary structure to human IL-1RN, and share relatively high amino acid identity (for a chicken cytokine) with their human isoforms. Functionally, they both comprehensively antagonised IL-1 β activity.

The full chIL-1RN gene sequence was obtained by PCR and sequence reads from the latterly available unassembled third build of the chicken genome. This revealed a number of significant differences with the human gene, most prominently at the 5' end. In this region of the chicken gene, there are two exons, ic1 and s1, separated by only 129 bp. By contrast, the human gene contains exons ic1, ic2 and s1 with 2.1 kb separating the intracellular exons and 7.5 kb between ic2 and s1. This latter region contains a 1.6 kb promoter proximal to s1 which drives transcription of the secretory transcript. Within the chicken gene, there is no obvious secretory-specific promoter in the respective location. This suggests the regulation of chIL-1RN transcription may differ from that of the human orthologue. The absence of upstream sequence in the genome meant it was not possible to fully characterise any putative promoter upstream of ic1 in the chicken. The chicken gene was also evidently missing an ic2 exon, suggesting fewer intracellular isoforms are present in this species. These key differences show the evolution of IL-1RN in the chicken has been distinctively different to that of the human orthologue. IL-1RN was predicted to emerge around 350 Mya, following duplication of an ancestral gene (Eisenberg, Brewer et al. 1991). As the major speciation event which led to the formation of birds and mammals happened around 40 million years later, this suggests both human and chicken IL-1RN evolved from a

common ancestor. This implies that the ic2 exon was either present in the original gene and was then lost in birds, or it was gained independently during the evolution of mammals.

Examination of the other 33 mammalian IL-1RN sequences indicates that they are, not surprisingly, much more closely related to huIL-1RN than chIL-1RN. Despite this similarity, only three of these mammals (chimpanzee, gibbon and gorilla) appear to possess the ic2 exon. The gene structures of the other 30 mammals may have been incorrectly predicted or curated. Alternatively, this exon has arisen in the primate lineage; however, this theory is inconsistent as orang-utans, which lack ic2, diverged from their ancestor after the divergence of gibbons but before the divergence of gorillas and chimpanzees. Clearly, the identification of IL-1RN in many more non-mammalian species is required to determine whether ic2 is genuinely confined to the mammalian lineage.

Identification and characterisation of IL-1F5 (IL-36RN) in the chicken provided some novel observations as well as expanding the current thinking on evolution of the IL-1 cytokine family. Initial BLAST and phylogenetic analyses provided unequivocal confirmation of the exact identity of the cytokine. IL-1F5 in mammals acts as an antagonist of the IL-1RL2 receptor. As yet, the agonists of this receptor, IL-1F6, -F8 and -F9, have not been identified in the chicken, which eliminated the possibility of demonstrating receptor blockade with IL-1F5. With limited alternatives, the ability of chIL-1F5 to downregulate LPS-mediated inflammation in a macrophage cell line (HD11 cells) was examined. This particular property of IL-1F5 had only previously been shown in rodent glial cells but not in macrophages or DCs. Although pre-incubating cells with chIL-1F5 did not abrogate the effects of subsequent LPS

Chapter 8: Discussion

stimulation, it did not invoke a response prior to endotoxin exposure, confirming it lacks agonist activity. Despite a previous lack of reproducibility in studies carried out by different research groups, a new study has comprehensively shown that IL-1F5 is definitely the antagonist of IL-1RL2 (Vigne, Palmer et al. 2011). Multiple stimulatory effects induced by IL-1F6, -F8 and -F9 (IL-36 α , - β and - γ , respectively) in bone marrow-derived DCs and CD4⁺ T cells were antagonised by IL-1F5 in a dose-dependent manner (Vigne, Palmer et al. 2011). An additional study (alluded to in Vigne, Palmer et al. (2011)) has also characterised IL-1F5 and observed the same general effect (Towne, unpublished). These studies indicate that chicken orthologues of the mammalian IL-36 ligands are needed, should they exist, to assess the function of chIL-36RN.

As previously discussed, these genes have not been found in the chicken genome or EST libraries. Intuitively, a receptor antagonist would be expected to be expressed in the same tissues that express the agonists. This is clearly the case for IL-1RN, which is detectable in all tissues that express IL-1 β and IL-1 α . The EST library containing chIL-1F5 was made from the liver so it is not unreasonable to presume this tissue may also express IL-36 α , - β and - γ , although they were not apparent. Interestingly, the liver cells that were used to make this EST library were unstimulated. Whilst we have shown the expression of the biologically inert IL-36RN is constitutive in all chicken tissues examined, this may not extend to IL-1RL2 agonists capable of multiple stimulatory effects. If the chicken does possess IL-36 α , - β and - γ , these may be inducible genes so may not be expressed in an unstimulated tissue. Previous studies have consistently shown that IL-36 α , - β and - γ expression is not constitutive in many tissues (Busfield, Comrack et al. 2000; Kumar, McDonnell et al. 2000; Smith, Renshaw et al. 2000; Debets, Timans et al. 2001); most tellingly IL-36 α and IL-36 β were not constitutively

expressed in the liver in one of these studies (Smith, Renshaw et al. 2000). In the study discussed above (Vigne, Palmer et al. 2011) real-time qRT-PCR showed that the IL-1RL2 ligands were not expressed constitutively in all cells. The presence of IL-1RL2 and its antagonist IL-36RN in the chicken strongly suggest the agonist ligand genes may also be present. There is of course the possibility that these ligand genes were formed in an ancient ancestor, present in the earliest birds and then lost during evolution. For this to happen, the robustness of the bird would have to be maintained by genetic redundancy whereby other genes, presumably IL-1 paralogues, performed the same set of functions. These paralogues would then be able to compensate for the loss of dispensable IL-1RL2 ligands. This would certainly fit with the pattern of a reduced gene repertoire in the minimalist avian immune genome; however, if minimalism is the prevailing genetic hallmark of birds, it would not explain why the genes for IL-1RL2 and IL-36RN are maintained. Given the increasingly apparent importance of IL-36 α , - β and - γ in mammals, it seems likely their deletion without functional compensation would seriously compromise the fitness of any species, including birds.

Prior to the commencement of this study, only two of the IL-1 family agonist ligands and six of the IL-1 receptor genes found in man had been identified in the chicken. The findings of this study have shown the IL-1 receptor family is completely conserved in the chicken genome. These chicken genes presumably retain similar functions as part of the essential signalling network of the IL-1 family. The number of known IL-1 ligand genes in the chicken has also been expanded following the identification of both receptor antagonists, IL-1RN and IL-36RN, found in humans. Before this study began, IL-1RN was thought to be confined to mammals; however, this gene has since been found in rainbow trout and now the chicken. This has demonstrated

Chapter 8: Discussion

that regulation in the IL-1 cytokine family is a fundamental requirement, with the IL-1RN gene having been maintained in these two species despite millions of years of separate evolution and a significant amount of genomic reorganisation. The extent of this rearrangement within the chicken genome is clearly reflected in the observable differences between chIL-1RN and its mammalian orthologues. For example, chIL-1RN is separated from IL-1 β , appears to lack a secretory-specific promoter and appears to be differentially regulated through splice variant formation. It is more than likely there are other non-mammalian species, containing an IL-1 β gene, that also possess IL-1RN. Identification of chIL-36RN has provided further evidence of the need to regulate IL-1 activity and has also shown that predictions of greater functional complexity in the IL-1 family being confined to mammals (Mulero, Nelken et al. 2000) may have been overstated.

This study has added two new cytokines to the growing number identified in birds which have previously been found in humans. A total of 27 interleukins have now been discovered in the chicken, compared with 41 in man. Although the minimalist immune genome is at present the accepted paradigm in the chicken, this is beginning to look less minimalist as more avian cytokine orthologues are being discovered. This is also expanding our understanding of the functional complexity of the immune system in the chicken. It remains to be seen how many of the 41 mammalian interleukins are actually present in this species.

This study has also raised many questions concerning the extent to which the genetic and functional repertoires of the IL-1 family in man and mouse are conserved in birds. For instance, in humans IL-1 α regulates transcription of icIL-1RN by controlling its promoter (La and Fischer 2001). A single report has also shown a degree of

regulation of IL-1 α by icIL-1RN (Merhi-Soussi, Berti et al. 2005). As icIL-1RN has been identified in the chicken, this raises the possibility of the existence of IL-1 α in the chicken. Alternatively, it may have lost this function, never had it in the first place or it may have been conserved in a paralogue. Only a single intracellular variant of icIL-1RN was found in the chicken, but further variants may exist. The genomic structure suggests icIL-1RN2 may be missing in birds; however, icIL-1RN3, formed through alternative translation initiation may be present.

As discussed previously, the large discrepancy between the number of chIL-1 receptor and ligand genes currently annotated in the genome may not be true, as the chicken genome may contain all of the ligands in as yet unsequenced regions. Identifying the genomic location of IL-1RN and IL-36RN may be a catalyst for finding some of these.

8.2 Future work

There are a number of ways this project could have been improved, as well as several other approaches which could be attempted to find further novel IL-1 genes in the chicken.

Although the chIL-1F5 bioassay was possibly flawed (if the chicken orthologue is, as in mammals, a receptor antagonist) there are several improvements and alternative strategies which could be attempted to prove functionality. To establish whether the recombinant chIL-1F5 was correctly refolded, the protein could be analysed by nuclear magnetic resonance (NMR) spectroscopy.

To overcome problems associated with mis-folded or precipitated recombinant

Chapter 8: Discussion

chIL-1F5, HD11 cells could be transfected with an expression vector containing the chIL-1F5 cDNA (alongside mock-transfected cells). Both groups of transfected cells could then be subsequently stimulated with IL-1 β or LPS. Alternatively, siRNA knockdown of IL-1F5 alongside a scrambled siRNA control could be attempted in leukocytes. Cells could then be stimulated with LPS or IL-1 β to establish if this leads to enhanced responses in the IL-1F5 knockdowns. This may also overcome problems with mis-folded protein and confirm if chIL-1F5 possesses endogenous anti-inflammatory activity. Unpublished observations (discussed in Sims and Smith (2010)) have also indicated that human IL-1F5 truncated at the NH₂-terminus has increased biological activity. The transfection strategy outlined above could therefore also be attempted with a series of NH₂-terminal truncation mutants of chIL-1F5. Cloning chIL-1F5 into an expression vector containing a GFP-tag prior to transfection would allow the movement of the protein to be monitored using laser scanning confocal microscopy. This may provide an insight into whether this protein is translocated to the nucleus and if it is subsequently exported as free ligand. This could reveal a role for the putative nuclear export sequence discussed in Chapter 6, section 6.3.4.

None of the chIL-1RN splice variants appeared to be bioactive in the assays carried out. This could be a genuine effect or could be due to problems with translation or correct folding of the proteins. The efficiency of mRNA translation can be measured by the extent to which transcripts associate with ribosomes. Those mRNAs which are being efficiently translated are physically bound by numerous ribosomes (polysomes), whereas mRNAs being inadequately translated are associated with a single ribosome (monosome) (Ingolia, Ghaemmaghami et al. 2009; Esposito, Mateyak et al. 2010). These distinct pools of ribosome-bound mRNAs can be separated and then analysed by

Chapter 8: Discussion

Northern blotting. A polysome profile of the COS cells transfected with IL-1RN splice variant cDNAs could thus be carried out alongside a profile of cells transfected with full length IL-1RN.

Chickens which are either resistant (line 6₁) or susceptible (BrL) to infectious bursal disease virus (IBDV) were challenged with the virus as outlined in Chapter 2, section 2.4.1.2. As discussed in Chapter 7, section 7.3.4.1, this led to a noticeable decrease in IL-1F5 mRNA expression in both lines throughout the entire experiment. In the BrL line, the differences in expression between infected and uninfected birds were much greater than differences in line 6₁. The IL-1F5 gene in BrL birds may contain SNPs which affect the amount of mRNA produced, or mRNA half-life, and thus contribute to disease susceptibility. It would therefore be interesting to fully sequence the coding region, 5' UTR, 3' UTR and putative promoter of the IL-1F5 gene in both lines to identify possible differences.

It may be possible that further variants of icIL-1RN exist in the chicken. As icIL-1RN3 is formed through alternative translation initiation and has 100% nucleotide sequence identity with other intracellular isoforms, a molecular biology approach is not feasible. Raising a monoclonal antibody to chicken icIL-1RN should permit detection of all potential isoforms of this variant, if targeted against a region of the protein likely to be present in all isoforms. As any equivalent icIL-1RN3 isoform would have a much lower molecular weight than the isoforms created through alternative transcriptional splicing, distinguishing between the isoforms could then be possible using western blotting. Avian equivalents of the cell types which predominantly express icIL-1RN3 in mammals would be the first cells to test.

The genomic locations of chIL-1RN and chIL-1F5 were not identified during

this study. An alternative approach to those tried would be to use fluorescence *in situ* hybridisation (FISH). Generating probes as close as possible in length to both full length gene sequences would be required to achieve specific hybridization.

A number of possible strategies could be attempted to uncover novel IL-1 ligands in the chicken. Firstly, all IL-1 ligands in mammals have several regions within their cDNA sequences which are highly similar. These include the three common final exons in every transcript; the areas which correspond to the β -sheets of the protein secondary structure and the region containing the IL-1 family signature motif which has the highest homology between paralogues. For each IL-1 gene, cDNA and amino acid alignments should be created between all species possessing that orthologue. Regions with the highest homology between species would then be identified and degenerate primers designed against these regions. Multiple degenerate primers can then be used to attempt to amplify IL-1 ligand genes in the chicken. Although avian cytokines typically share 25-40% sequence identity with their mammalian equivalents, both chIL-1F5 and IL-1RN contain a number of short regions with 80-100% identity with the mammalian sequences. These are visible in Chapter 4, Figure 4.9 and Chapter 6, Figure 6.3. It is also apparent that, for any particular IL-1 gene, the signature motif is highly conserved between all species. For example, the motif in IL-1 β is well conserved in mammals, birds, fish and amphibians (Bird, Zou et al. 2002). When attempting to amplify novel chicken orthologues, it would be prudent to design the reverse primers in the signature motif region.

A proteomic screen of supernatants from stimulated avian cells may be useful for identifying novel chicken IL-1 ligands. In murine macrophage cultures stimulated with LPS and ATP, IL-1F6 was released into the supernatant (Martin, Scholler et al.

2009). This has also been repeatedly shown to induce IL-1 β secretion into cell culture supernatants. The underlying mechanism is that of passive release following activation of the P2X₇ receptor on the cell surface. A similar experiment could be attempted with avian macrophages that express the P2X₇ receptor. These cells could be similarly stimulated with LPS and ATP and pools of proteins in the supernatants could be detected by mass spectrometry. It may be possible to identify passively secreted novel IL-1 proteins by *de novo* peptide sequencing of the entire pool of secreted proteins.

At present, the chicken genome sequence is incomplete and poorly annotated throughout. The majority of chromosomes contain sequence gaps, some of which are likely to contain missing genes. With higher sequencing throughput, reduced costs and better chemistries, this may improve the overall sequence coverage, potentially uncovering many novel genes. This may lead to identification of further IL-1 family members in the chicken.

8.3 Conclusion

In summary, the chicken orthologues of *IL-1RN* and *IL-36RN* have been identified. Functionally, chIL-1RN exhibited biological activity resembling that of its mammalian homologues; however, the function of chIL-36RN remained undetermined. The expression of both genes was increased following bacterial infection; however, chIL-36RN mRNA expression decreased whilst chIL-1RN expression increased in a viral challenge model. Attempts to identify the genomic locations of both genes revealed they were not clustered at a conserved locus with chIL-1 β . Although their exact locations were not identified, the absence of an IL-1 gene cluster similar to the

Chapter 8: Discussion

one found in humans suggested the evolution of the chIL-1 family has been distinctly different to that in mammals.

References

- Agostini, L., F. Martinon, et al. (2004). "NALP3 forms an IL-1beta-processing inflammasome with increased activity in Muckle-Wells autoinflammatory disorder." *Immunity* **20**(3): 319-325.
- Aksentijevich, I., S. L. Masters, et al. (2009). "An autoinflammatory disease with deficiency of the interleukin-1-receptor antagonist." *N Engl J Med* **360**(23): 2426-2437.
- Ali, S., M. Huber, et al. (2007). "IL-1 receptor accessory protein is essential for IL-33-induced activation of T lymphocytes and mast cells." *Proc Natl Acad Sci U S A* **104**(47): 18660-18665.
- Allakhverdi, Z., D. E. Smith, et al. (2007). "Cutting edge: The ST2 ligand IL-33 potently activates and drives maturation of human mast cells." *J Immunol* **179**(4): 2051-2054.
- Andersson, J., L. Bjork, et al. (1992). "Lipopolysaccharide induces human interleukin-1 receptor antagonist and interleukin-1 production in the same cell." *Eur J Immunol* **22**(10): 2617-2623.
- Apostolopoulos, J., S. Ross, et al. (1996). "Interleukin-1 receptor antagonist: characterisation of its gene expression in rabbit tissues and large-scale expression in eucaryotic cells using a baculovirus expression system." *J Immunol Methods* **199**(1): 27-35.
- Arend, W. P. and C. J. Guthridge (2000). "Biological role of interleukin 1 receptor antagonist isoforms." *Ann Rheum Dis* **59 Suppl 1**: i60-64.
- Arend, W. P., M. Malyak, et al. (1998). "Interleukin-1 receptor antagonist: role in biology." *Annu Rev Immunol* **16**: 27-55.
- Arend, W. P., G. Palmer, et al. (2008). "IL-1, IL-18, and IL-33 families of cytokines." *Immunol Rev* **223**: 20-38.
- Arend, W. P., M. F. Smith, Jr., et al. (1991). "IL-1 receptor antagonist and IL-1 beta production in human monocytes are regulated differently." *J Immunol* **147**(5): 1530-1536.
- Arend, W. P., H. G. Welgus, et al. (1990). "Biological properties of recombinant human monocyte-derived interleukin 1 receptor antagonist." *J Clin Invest* **85**(5): 1694-1697.
- Aricescu, A. R., W. Lu, et al. (2006). "A time- and cost-efficient system for high-level protein production in mammalian cells." *Acta Crystallogr D Biol Crystallogr* **62**(Pt 10): 1243-1250.
- Aruffo, A. (2002). "Transient expression of proteins using COS cells." *Curr Protoc Mol Biol* **Chapter 16**: Unit 16 12.
- Auron, P. E., A. C. Webb, et al. (1984). "Nucleotide sequence of human monocyte interleukin 1 precursor cDNA." *Proc Natl Acad Sci U S A* **81**(24): 7907-7911.
- Avery, S., L. Rothwell, et al. (2004). "Characterization of the first nonmammalian T2 cytokine gene cluster: the cluster contains functional single-copy genes for IL-3, IL-4, IL-13, and GM-CSF, a gene for IL-5 that appears to be a pseudogene, and a gene encoding another cytokinelike transcript, KK34." *J Interferon Cytokine Res* **24**(10): 600-610.

References

- Banda, N. K., C. Guthridge, et al. (2005). "Intracellular IL-1 receptor antagonist type 1 inhibits IL-1-induced cytokine production in keratinocytes through binding to the third component of the COP9 signalosome." *J Immunol* **174**(6): 3608-3616.
- Barber, M. R., J. R. Aldridge, Jr., et al. (2010). "Association of RIG-I with innate immunity of ducks to influenza." *Proc Natl Acad Sci U S A* **107**(13): 5913-5918.
- Barton, J. L., R. Herbst, et al. (2000). "A tissue specific IL-1 receptor antagonist homolog from the IL-1 cluster lacks IL-1, IL-1ra, IL-18 and IL-18 antagonist activities." *Eur J Immunol* **30**(11): 3299-3308.
- Beilharz, T. H. and T. Preiss (2004). "Translational profiling: the genome-wide measure of the nascent proteome." *Brief Funct Genomic Proteomic* **3**(2): 103-111.
- Bendtsen, J. D., H. Nielsen, et al. (2004). "Improved prediction of signal peptides: SignalP 3.0." *J Mol Biol* **340**(4): 783-795.
- Bensen, J. T., P. A. Dawson, et al. (2001). "Identification of a novel human cytokine gene in the interleukin gene cluster on chromosome 2q12-14." *J Interferon Cytokine Res* **21**(11): 899-904.
- Bettelli, E., Y. Carrier, et al. (2006). "Reciprocal developmental pathways for the generation of pathogenic effector TH17 and regulatory T cells." *Nature* **441**(7090): 235-238.
- Bettini, M. L. and D. A. Vignali (2010). "Development of thymically derived natural regulatory T cells." *Ann N Y Acad Sci* **1183**: 1-12.
- Beug, H., A. von Kirchbach, et al. (1979). "Chicken hematopoietic cells transformed by seven strains of defective avian leukemia viruses display three distinct phenotypes of differentiation." *Cell* **18**(2): 375-390.
- Bigler, C. F., D. A. Norris, et al. (1992). "Interleukin-1 receptor antagonist production by human keratinocytes." *J Invest Dermatol* **98**(1): 38-44.
- Bird, S., J. Zou, et al. (2002). "Evolution of interleukin-1beta." *Cytokine Growth Factor Rev* **13**(6): 483-502.
- Black, R. A., S. R. Kronheim, et al. (1988). "Generation of biologically active interleukin-1 beta by proteolytic cleavage of the inactive precursor." *J Biol Chem* **263**(19): 9437-9442.
- Blumberg, H., H. Dinh, et al. (2010). "IL-1RL2 and its ligands contribute to the cytokine network in psoriasis." *J Immunol* **185**(7): 4354-4362.
- Blumberg, H., H. Dinh, et al. (2007). "Opposing activities of two novel members of the IL-1 ligand family regulate skin inflammation." *J Exp Med* **204**(11): 2603-2614.
- Bombara, C. J. and R. L. Taylor, Jr. (1991). "Signal transduction events in chicken interleukin-1 production." *Poult Sci* **70**(6): 1372-1380.
- Boraschi, D. and A. Tagliabue (2006). "The interleukin-1 receptor family." *Vitam Horm* **74**: 229-254.
- Born, T. L., L. A. Morrison, et al. (2000). "A poxvirus protein that binds to and inactivates IL-18, and inhibits NK cell response." *J Immunol* **164**(6): 3246-3254.
- Born, T. L., E. Thomassen, et al. (1998). "Cloning of a novel receptor subunit, AcPL, required for interleukin-18 signaling." *J Biol Chem* **273**(45): 29445-29450.
- Bourque, G., E. M. Zdobnov, et al. (2005). "Comparative architectures of mammalian and chicken genomes reveal highly variable rates of genomic rearrangements across different lineages." *Genome Res* **15**(1): 98-110.
- Brint, E. K., D. Xu, et al. (2004). "ST2 is an inhibitor of interleukin 1 receptor and Toll-like receptor 4 signaling and maintains endotoxin tolerance." *Nat Immunol* **5**(4): 373-379.

References

- Brownlie, R., J. Zhu, et al. (2009). "Chicken TLR21 acts as a functional homologue to mammalian TLR9 in the recognition of CpG oligodeoxynucleotides." Mol Immunol **46**(15): 3163-3170.
- Bru, C., E. Courcelle, et al. (2005). "The ProDom database of protein domain families: more emphasis on 3D." Nucleic Acids Res **33**(Database issue): D212-215.
- Bufler, P., T. Azam, et al. (2002). "A complex of the IL-1 homologue IL-1F7b and IL-18-binding protein reduces IL-18 activity." Proc Natl Acad Sci U S A **99**(21): 13723-13728.
- Bufler, P., F. Gamboni-Robertson, et al. (2004). "Interleukin-1 homologues IL-1F7b and IL-18 contain functional mRNA instability elements within the coding region responsive to lipopolysaccharide." Biochem J **381**(Pt 2): 503-510.
- Busfield, S. J., C. A. Comrack, et al. (2000). "Identification and gene organization of three novel members of the IL-1 family on human chromosome 2." Genomics **66**(2): 213-216.
- Calderara, S., Y. Xiang, et al. (2001). "Orthopoxvirus IL-18 binding proteins: affinities and antagonist activities." Virology **279**(1): 22-26.
- Carrie, A., L. Jun, et al. (1999). "A new member of the IL-1 receptor family highly expressed in hippocampus and involved in X-linked mental retardation." Nat Genet **23**(1): 25-31.
- Carriere, V., L. Roussel, et al. (2007). "IL-33, the IL-1-like cytokine ligand for ST2 receptor, is a chromatin-associated nuclear factor in vivo." Proc Natl Acad Sci U S A **104**(1): 282-287.
- Carter, D. B., M. R. Deibel, Jr., et al. (1990). "Purification, cloning, expression and biological characterization of an interleukin-1 receptor antagonist protein." Nature **344**(6267): 633-638.
- Cayrol, C. and J. P. Girard (2009). "The IL-1-like cytokine IL-33 is inactivated after maturation by caspase-1." Proc Natl Acad Sci U S A **106**(22): 9021-9026.
- Chackerian, A. A., E. R. Oldham, et al. (2007). "IL-1 receptor accessory protein and ST2 comprise the IL-33 receptor complex." J Immunol **179**(4): 2551-2555.
- Chavez, L. L., S. Gosavi, et al. (2006). "Multiple routes lead to the native state in the energy landscape of the beta-trefoil family." Proc Natl Acad Sci U S A **103**(27): 10254-10258.
- Cheng, C. S., W. T. Chen, et al. (2011). "Structural and functional comparison of cytokine interleukin-1 beta from chicken and human." Mol Immunol **48**(6-7): 947-955.
- Chuammitri, P., J. Ostojic, et al. (2009). "Chicken heterophil extracellular traps (HETs): novel defense mechanism of chicken heterophils." Vet Immunol Immunopathol **129**(1-2): 126-131.
- Chung, Y., S. H. Chang, et al. (2009). "Critical regulation of early Th17 cell differentiation by interleukin-1 signaling." Immunity **30**(4): 576-587.
- Chustz, R. T., D. R. Nagarkar, et al. (2011). "Regulation and Function of the IL-1 Family Cytokine IL-1F9 in Human Bronchial Epithelial Cells." Am J Respir Cell Mol Biol **45**(1): 145-153.
- Colotta, F., S. K. Dower, et al. (1994). "The type II 'decoy' receptor: a novel regulatory pathway for interleukin 1." Immunol Today **15**(12): 562-566.
- Coltey, M., R. P. Bucy, et al. (1989). "Analysis of the first two waves of thymus homing stem cells and their T cell progeny in chick-quail chimeras." J Exp Med **170**(2): 543-557.

References

- Corradi, A., A. T. Franzi, et al. (1995). "Synthesis and secretion of interleukin-1 alpha and interleukin-1 receptor antagonist during differentiation of cultured keratinocytes." *Exp Cell Res* **217**(2): 355-362.
- Costelloe, C., M. Watson, et al. (2008). "IL-1F5 mediates anti-inflammatory activity in the brain through induction of IL-4 following interaction with SIGIRR/TIR8." *J Neurochem* **105**(5): 1960-1969.
- Coulter, K. R., M. D. Wewers, et al. (1999). "Extracellular regulation of interleukin (IL)-1beta through lung epithelial cells and defective IL-1 type II receptor expression." *Am J Respir Cell Mol Biol* **20**(5): 964-975.
- Cui, X., F. N. Rouhani, et al. (2003). "Shedding of the type II IL-1 decoy receptor requires a multifunctional aminopeptidase, aminopeptidase regulator of TNF receptor type 1 shedding." *J Immunol* **171**(12): 6814-6819.
- Cullinan, E. B., L. Kwee, et al. (1998). "IL-1 receptor accessory protein is an essential component of the IL-1 receptor." *J Immunol* **161**(10): 5614-5620.
- Dale, M. and M. J. Nicklin (1999). "Interleukin-1 receptor cluster: gene organization of IL1R2, IL1R1, IL1RL2 (IL-1Rrp2), IL1RL1 (T1/ST2), and IL18R1 (IL-1Rrp) on human chromosome 2q." *Genomics* **57**(1): 177-179.
- Davidson, N. J. and R. L. Boyd (1992). "Delineation of chicken thymocytes by CD3-TCR complex, CD4 and CD8 antigen expression reveals phylogenically conserved and novel thymocyte subsets." *Int Immunol* **4**(10): 1175-1182.
- Debets, R., J. C. Timans, et al. (2000). "IL-18 receptors, their role in ligand binding and function: anti-IL-1RAcPL antibody, a potent antagonist of IL-18." *J Immunol* **165**(9): 4950-4956.
- Debets, R., J. C. Timans, et al. (2001). "Two novel IL-1 family members, IL-1 delta and IL-1 epsilon, function as an antagonist and agonist of NF-kappa B activation through the orphan IL-1 receptor-related protein 2." *J Immunol* **167**(3): 1440-1446.
- Degen, W. G., N. Daal, et al. (2005). "Th1/Th2 polarization by viral and helminth infection in birds." *Vet Microbiol* **105**(3-4): 163-167.
- Dinarello, C., W. Arend, et al. (2010). "IL-1 family nomenclature." *Nat Immunol* **11**(11): 973.
- Dinarello, C. A. (1996). "Biologic basis for interleukin-1 in disease." *Blood* **87**(6): 2095-2147.
- Dinarello, C. A. (2000). "Proinflammatory cytokines." *Chest* **118**(2): 503-508.
- Dinarello, C. A. (2009). "Immunological and inflammatory functions of the interleukin-1 family." *Annu Rev Immunol* **27**: 519-550.
- Dinarello, C. A. (2011). "Interleukin-1 in the pathogenesis and treatment of inflammatory diseases." *Blood* **117**(14): 3720-3732.
- Dripps, D. J., B. J. Brandhuber, et al. (1991). "Interleukin-1 (IL-1) receptor antagonist binds to the 80-kDa IL-1 receptor but does not initiate IL-1 signal transduction." *J Biol Chem* **266**(16): 10331-10336.
- Dunn, E. F., N. J. Gay, et al. (2003). "High-resolution structure of murine interleukin 1 homologue IL-1F5 reveals unique loop conformations for receptor binding specificity." *Biochemistry* **42**(37): 10938-10944.
- Eisenberg, S. P., M. T. Brewer, et al. (1991). "Interleukin 1 receptor antagonist is a member of the interleukin 1 gene family: evolution of a cytokine control mechanism." *Proc Natl Acad Sci U S A* **88**(12): 5232-5236.

References

- Eisenberg, S. P., R. J. Evans, et al. (1990). "Primary structure and functional expression from complementary DNA of a human interleukin-1 receptor antagonist." Nature **343**(6256): 341-346.
- Eldaghayes, I., L. Rothwell, et al. (2006). "Infectious bursal disease virus: strains that differ in virulence differentially modulate the innate immune response to infection in the chicken bursa." Viral Immunol **19**(1): 83-91.
- Emanuelsson, O., S. Brunak, et al. (2007). "Locating proteins in the cell using TargetP, SignalP and related tools." Nat Protoc **2**(4): 953-971.
- Esposito, A. M., M. Mateyak, et al. (2010). "Eukaryotic polyribosome profile analysis." J Vis Exp(40).
- Evans, I., S. K. Dower, et al. (2006). "Action of intracellular IL-1Ra (Type 1) is independent of the IL-1 intracellular signalling pathway." Cytokine **33**(5): 274-280.
- Fahrenkrog, B. and U. Aeberli (2003). "The nuclear pore complex: nucleocytoplasmic transport and beyond." Nat Rev Mol Cell Biol **4**(10): 757-766.
- Fenton, M. J., J. A. Buras, et al. (1992). "IL-4 reciprocally regulates IL-1 and IL-1 receptor antagonist expression in human monocytes." J Immunol **149**(4): 1283-1288.
- Fettelschoss, A., M. Kistowska, et al. (2011). "Inflammasome activation and IL-1beta target IL-1alpha for secretion as opposed to surface expression." Proc Natl Acad Sci U S A **108**(44): 18055-18060.
- Fukui, A., N. Inoue, et al. (2001). "Molecular cloning and functional characterization of chicken toll-like receptors. A single chicken toll covers multiple molecular patterns." J Biol Chem **276**(50): 47143-47149.
- Gabay, C., B. Porter, et al. (1997). "Mouse IL-1 receptor antagonist isoforms: complementary DNA cloning and protein expression of intracellular isoform and tissue distribution of secreted and intracellular IL-1 receptor antagonist in vivo." J Immunol **159**(12): 5905-5913.
- Gabay, C., B. Porter, et al. (1999). "Interleukin-4 (IL-4) and IL-13 enhance the effect of IL-1beta on production of IL-1 receptor antagonist by human primary hepatocytes and hepatoma HepG2 cells: differential effect on C-reactive protein production." Blood **93**(4): 1299-1307.
- Gao, W., S. Kumar, et al. (2003). "Innate immunity mediated by the cytokine IL-1 homologue 4 (IL-1H4/IL-1F7) induces IL-12-dependent adaptive and profound antitumor immunity." J Immunol **170**(1): 107-113.
- Garlanda, C., H. J. Anders, et al. (2009). "TIR8/SIGIRR: an IL-1R/TLR family member with regulatory functions in inflammation and T cell polarization." Trends Immunol **30**(9): 439-446.
- Germain, R. N. (1994). "MHC-dependent antigen processing and peptide presentation: providing ligands for T lymphocyte activation." Cell **76**(2): 287-299.
- Ghayur, T., S. Banerjee, et al. (1997). "Caspase-1 processes IFN-gamma-inducing factor and regulates LPS-induced IFN-gamma production." Nature **386**(6625): 619-623.
- Gibson, M. S., P. Kaiser, et al. (2009). "Identification of chicken granulocyte colony-stimulating factor (G-CSF/CSF3): the previously described myelomonocytic growth factor is actually CSF3." J Interferon Cytokine Res **29**(6): 339-343.
- Glimcher, L. H. and K. M. Murphy (2000). "Lineage commitment in the immune system: the T helper lymphocyte grows up." Genes Dev **14**(14): 1693-1711.

References

- Gobel, T. W., K. Schneider, et al. (2003). "IL-18 stimulates the proliferation and IFN-gamma release of CD4+ T cells in the chicken: conservation of a Th1-like system in a nonmammalian species." *J Immunol* **171**(4): 1809-1815.
- Gosavi, S., P. C. Whitford, et al. (2008). "Extracting function from a beta-trefoil folding motif." *Proc Natl Acad Sci U S A* **105**(30): 10384-10389.
- Gottlieb, A. B., F. Chamian, et al. (2005). "TNF inhibition rapidly down-regulates multiple proinflammatory pathways in psoriasis plaques." *J Immunol* **175**(4): 2721-2729.
- Gracie, J. A., S. E. Robertson, et al. (2003). "Interleukin-18." *J Leukoc Biol* **73**(2): 213-224.
- Graham, F. L., J. Smiley, et al. (1977). "Characteristics of a human cell line transformed by DNA from human adenovirus type 5." *J Gen Virol* **36**(1): 59-74.
- Granowitz, E. V., R. Porat, et al. (1992). "Pharmacokinetics, safety and immunomodulatory effects of human recombinant interleukin-1 receptor antagonist in healthy humans." *Cytokine* **4**(5): 353-360.
- Graves, B. J., M. H. Hatada, et al. (1990). "Structure of interleukin 1 alpha at 2.7-A resolution." *Biochemistry* **29**(11): 2679-2684.
- Griffin, D. K., L. B. Robertson, et al. (2007). "The evolution of the avian genome as revealed by comparative molecular cytogenetics." *Cytogenet Genome Res* **117**(1-4): 64-77.
- Gu, Y., K. Kuida, et al. (1997). "Activation of interferon-gamma inducing factor mediated by interleukin-1beta converting enzyme." *Science* **275**(5297): 206-209.
- Guida, S., A. Heguy, et al. (1992). "The chicken IL-1 receptor: differential evolution of the cytoplasmic and extracellular domains." *Gene* **111**(2): 239-243.
- Guo, L., G. Wei, et al. (2009). "IL-1 family members and STAT activators induce cytokine production by Th2, Th17, and Th1 cells." *Proc Natl Acad Sci U S A* **106**(32): 13463-13468.
- Gyorffy, Z., A. Ohnemus, et al. (2003). "Truncated chicken interleukin-1beta with increased biologic activity." *J Interferon Cytokine Res* **23**(5): 223-228.
- Hammerberg, C., W. P. Arend, et al. (1992). "Interleukin-1 receptor antagonist in normal and psoriatic epidermis." *J Clin Invest* **90**(2): 571-583.
- Hannum, C. H., C. J. Wilcox, et al. (1990). "Interleukin-1 receptor antagonist activity of a human interleukin-1 inhibitor." *Nature* **343**(6256): 336-340.
- Harmon, B. G. (1998). "Avian heterophils in inflammation and disease resistance." *Poult Sci* **77**(7): 972-977.
- Haskill, S., G. Martin, et al. (1991). "cDNA cloning of an intracellular form of the human interleukin 1 receptor antagonist associated with epithelium." *Proc Natl Acad Sci U S A* **88**(9): 3681-3685.
- Hayari, Y., K. Schauenstein, et al. (1982). "Avian lymphokines, II: interleukin-1 activity in supernatants of stimulated adherent splenocytes of chickens." *Dev Comp Immunol* **6**(4): 785-789.
- Hedges, S. B., P. H. Parker, et al. (1996). "Continental breakup and the ordinal diversification of birds and mammals." *Nature* **381**(6579): 226-229.
- Hershko, A. and A. Ciechanover (1998). "The ubiquitin system." *Annu Rev Biochem* **67**: 425-479.
- Higgs, R., P. Cormican, et al. (2006). "Induction of a novel chicken Toll-like receptor following *Salmonella enterica* serovar Typhimurium infection." *Infect Immun* **74**(3): 1692-1698.

References

- Higuchi, M., A. Matsuo, et al. (2008). "Combinational recognition of bacterial lipoproteins and peptidoglycan by chicken Toll-like receptor 2 subfamily." Dev Comp Immunol **32**(2): 147-155.
- Holtkamp, G. M., A. F. de Vos, et al. (1999). "Expression of multiple forms of IL-1 receptor antagonist (IL-1ra) by human retinal pigment epithelial cells: identification of a new IL-1ra exon." Eur J Immunol **29**(1): 215-224.
- Hong, J., S. Bae, et al. (2011). "Identification of constitutively active interleukin 33 (IL-33) splice variant." J Biol Chem **286**(22): 20078-20086.
- Hong, Y. H., H. S. Lillehoj, et al. (2006). "Changes in immune-related gene expression and intestinal lymphocyte subpopulations following *Eimeria maxima* infection of chickens." Vet Immunol Immunopathol **114**(3-4): 259-272.
- Huising, M. O., R. J. Stet, et al. (2004). "The molecular evolution of the interleukin-1 family of cytokines; IL-18 in teleost fish." Dev Comp Immunol **28**(5): 395-413.
- ICGSC (2004). "Sequence and comparative analysis of the chicken genome provide unique perspectives on vertebrate evolution." Nature **432**(7018): 695-716.
- Igyarto, B. Z., E. Lacko, et al. (2006). "Characterization of chicken epidermal dendritic cells." Immunology **119**(2): 278-288.
- Ingolia, N. T., S. Ghaemmaghami, et al. (2009). "Genome-wide analysis in vivo of translation with nucleotide resolution using ribosome profiling." Science **324**(5924): 218-223.
- Iqbal, M., V. J. Philbin, et al. (2005). "Expression patterns of chicken Toll-like receptor mRNA in tissues, immune cell subsets and cell lines." Vet Immunol Immunopathol **104**(1-2): 117-127.
- Iqbal, M., V. J. Philbin, et al. (2005). "Identification and functional characterization of chicken toll-like receptor 5 reveals a fundamental role in the biology of infection with *Salmonella enterica* serovar typhimurium." Infect Immun **73**(4): 2344-2350.
- Iwahana, H., M. Hayakawa, et al. (2004). "Molecular cloning of the chicken ST2 gene and a novel variant form of the ST2 gene product, ST2LV." Biochim Biophys Acta **1681**(1): 1-14.
- Janson, R. W., K. R. Hance, et al. (1991). "Production of IL-1 receptor antagonist by human in vitro-derived macrophages. Effects of lipopolysaccharide and granulocyte-macrophage colony-stimulating factor." J Immunol **147**(12): 4218-4223.
- Jenkins, J. K., R. F. Drong, et al. (1997). "Intracellular IL-1 receptor antagonist promoter: cell type-specific and inducible regulatory regions." J Immunol **158**(2): 748-755.
- Jobling, S. A., P. E. Auron, et al. (1988). "Biological activity and receptor binding of human prointerleukin-1 beta and subpeptides." J Biol Chem **263**(31): 16372-16378.
- Johnson, A. L., J. T. Bridgham, et al. (1998). "Characterization of the chicken interleukin-1beta converting enzyme (caspase-1) cDNA and expression of caspase-1 mRNA in the hen." Gene **219**(1-2): 55-62.
- Johnson, V. J., B. Yucesoy, et al. (2005). "Prevention of IL-1 signaling attenuates airway hyperresponsiveness and inflammation in a murine model of toluene diisocyanate-induced asthma." J Allergy Clin Immunol **116**(4): 851-858.

References

- Johnston, A., X. Xing, et al. (2011). "IL-1F5, -F6, -F8, and -F9: a novel IL-1 family signaling system that is active in psoriasis and promotes keratinocyte antimicrobial peptide expression." *J Immunol* **186**(4): 2613-2622.
- Ju, G., E. Labriola-Tompkins, et al. (1991). "Conversion of the interleukin 1 receptor antagonist into an agonist by site-specific mutagenesis." *Proc Natl Acad Sci U S A* **88**(7): 2658-2662.
- Kaiser, P. (2002). "Turkey and chicken interleukin-18 (IL18) share high sequence identity, but have different polyadenylation sites in their 3' UTR." *Dev Comp Immunol* **26**(8): 681-687.
- Kaiser, P. (2007). "The avian immune genome--a glass half-full or half-empty?" *Cytogenet Genome Res* **117**(1-4): 221-230.
- Kaiser, P. (2010). "Advances in avian immunology--prospects for disease control: a review." *Avian Pathol* **39**(5): 309-324.
- Kaiser, P., T. Y. Poh, et al. (2005). "A genomic analysis of chicken cytokines and chemokines." *J Interferon Cytokine Res* **25**(8): 467-484.
- Kaiser, P., L. Rothwell, et al. (2000). "Differential cytokine expression in avian cells in response to invasion by *Salmonella typhimurium*, *Salmonella enteritidis* and *Salmonella gallinarum*." *Microbiology* **146 Pt 12**: 3217-3226.
- Kaiser, P., L. Rothwell, et al. (2004). "The chicken proinflammatory cytokines interleukin-1beta and interleukin-6: differences in gene structure and genetic location compared with their mammalian orthologues." *Anim Genet* **35**(3): 169-175.
- Kaiser, P., G. Underwood, et al. (2003). "Differential cytokine responses following Marek's disease virus infection of chickens differing in resistance to Marek's disease." *J Virol* **77**(1): 762-768.
- Karpala, A. J., C. Stewart, et al. (2011). "Characterization of chicken Mda5 activity: regulation of IFN-beta in the absence of RIG-I functionality." *J Immunol* **186**(9): 5397-5405.
- Kaufman, J., J. Jacob, et al. (1999). "Gene organisation determines evolution of function in the chicken MHC." *Immunol Rev* **167**: 101-117.
- Kaufman, J., S. Milne, et al. (1999). "The chicken B locus is a minimal essential major histocompatibility complex." *Nature* **401**(6756): 923-925.
- Kawai, T. and S. Akira (2010). "The role of pattern-recognition receptors in innate immunity: update on Toll-like receptors." *Nat Immunol* **11**(5): 373-384.
- Keestra, A. M., M. R. de Zoete, et al. (2007). "The central leucine-rich repeat region of chicken TLR16 dictates unique ligand specificity and species-specific interaction with TLR2." *J Immunol* **178**(11): 7110-7119.
- Keestra, A. M. and J. P. van Putten (2008). "Unique properties of the chicken TLR4/MD-2 complex: selective lipopolysaccharide activation of the MyD88-dependent pathway." *J Immunol* **181**(6): 4354-4362.
- Klasing, K. C. and R. K. Peng (1987). "Influence of cell sources, stimulating agents, and incubation conditions on release of interleukin-1 from chicken macrophages." *Dev Comp Immunol* **11**(2): 385-394.
- Klasing, K. C. and R. K. Peng (2001). "Soluble type-I interleukin-1 receptor blocks chicken IL-1 activity." *Dev Comp Immunol* **25**(4): 345-352.
- Kobayashi, Y., K. Yamamoto, et al. (1990). "Identification of calcium-activated neutral protease as a processing enzyme of human interleukin 1 alpha." *Proc Natl Acad Sci U S A* **87**(14): 5548-5552.

References

- Kogut, M. H., L. Rothwell, et al. (2005). "IFN-gamma priming of chicken heterophils upregulates the expression of proinflammatory and Th1 cytokine mRNA following receptor-mediated phagocytosis of *Salmonella enterica* serovar enteritidis." *J Interferon Cytokine Res* **25**(2): 73-81.
- Kumar, H., T. Kawai, et al. (2011). "Pathogen recognition by the innate immune system." *Int Rev Immunol* **30**(1): 16-34.
- Kumar, S., C. R. Hanning, et al. (2002). "Interleukin-1F7B (IL-1H4/IL-1F7) is processed by caspase-1 and mature IL-1F7B binds to the IL-18 receptor but does not induce IFN-gamma production." *Cytokine* **18**(2): 61-71.
- Kumar, S., P. C. McDonnell, et al. (2000). "Identification and initial characterization of four novel members of the interleukin-1 family." *J Biol Chem* **275**(14): 10308-10314.
- Kurowska-Stolarska, M., P. Kewin, et al. (2008). "IL-33 induces antigen-specific IL-5+ T cells and promotes allergic-induced airway inflammation independent of IL-4." *J Immunol* **181**(7): 4780-4790.
- Kurt-Jones, E. A., D. I. Beller, et al. (1985). "Identification of a membrane-associated interleukin 1 in macrophages." *Proc Natl Acad Sci U S A* **82**(4): 1204-1208.
- la Cour, T., L. Kiemer, et al. (2004). "Analysis and prediction of leucine-rich nuclear export signals." *Protein Eng Des Sel* **17**(6): 527-536.
- La, E. and S. M. Fischer (2001). "Transcriptional regulation of intracellular IL-1 receptor antagonist gene by IL-1 alpha in primary mouse keratinocytes." *J Immunol* **166**(10): 6149-6155.
- Lang, D., J. Knop, et al. (1998). "The type II IL-1 receptor interacts with the IL-1 receptor accessory protein: a novel mechanism of regulation of IL-1 responsiveness." *J Immunol* **161**(12): 6871-6877.
- Leveque, G., V. Forgetta, et al. (2003). "Allelic variation in TLR4 is linked to susceptibility to *Salmonella enterica* serovar Typhimurium infection in chickens." *Infect Immun* **71**(3): 1116-1124.
- Levine, S. J., T. Wu, et al. (1997). "Extracellular release of the type I intracellular IL-1 receptor antagonist from human airway epithelial cells: differential effects of IL-4, IL-13, IFN-gamma, and corticosteroids." *J Immunol* **158**(12): 5949-5957.
- Liew, F. Y., N. I. Pitman, et al. (2010). "Disease-associated functions of IL-33: the new kid in the IL-1 family." *Nat Rev Immunol* **10**(2): 103-110.
- Lin, H., A. S. Ho, et al. (2001). "Cloning and characterization of IL-1HY2, a novel interleukin-1 family member." *J Biol Chem* **276**(23): 20597-20602.
- Lomedico, P. T., U. Gubler, et al. (1984). "Cloning and expression of murine interleukin-1 cDNA in *Escherichia coli*." *Nature* **312**(5993): 458-462.
- Lonnemann, G., S. Endres, et al. (1989). "Differences in the synthesis and kinetics of release of interleukin 1 alpha, interleukin 1 beta and tumor necrosis factor from human mononuclear cells." *Eur J Immunol* **19**(9): 1531-1536.
- Luheshi, N. M., N. J. Rothwell, et al. (2009). "Dual functionality of interleukin-1 family cytokines: implications for anti-interleukin-1 therapy." *Br J Pharmacol* **157**(8): 1318-1329.
- Magne, D., G. Palmer, et al. (2006). "The new IL-1 family member IL-1F8 stimulates production of inflammatory mediators by synovial fibroblasts and articular chondrocytes." *Arthritis Res Ther* **8**(3): R80.
- Malyak, M., J. M. Guthridge, et al. (1998). "Characterization of a low molecular weight isoform of IL-1 receptor antagonist." *J Immunol* **161**(4): 1997-2003.

References

- Malyak, M., M. F. Smith, Jr., et al. (1998). "The differential production of three forms of IL-1 receptor antagonist by human neutrophils and monocytes." *J Immunol* **161**(4): 2004-2010.
- Mantovani, A., M. A. Cassatella, et al. (2011). "Neutrophils in the activation and regulation of innate and adaptive immunity." *Nat Rev Immunol* **11**(8): 519-531.
- Marrakchi, S., P. Guigue, et al. (2011). "Interleukin-36-receptor antagonist deficiency and generalized pustular psoriasis." *N Engl J Med* **365**(7): 620-628.
- Martin, U., J. Scholler, et al. (2009). "Externalization of the leaderless cytokine IL-1F6 occurs in response to lipopolysaccharide/ATP activation of transduced bone marrow macrophages." *J Immunol* **183**(6): 4021-4030.
- Martinon, F., A. Mayor, et al. (2009). "The inflammasomes: guardians of the body." *Annu Rev Immunol* **27**: 229-265.
- Matsukawa, A., T. Fukumoto, et al. (1997). "Detection and characterization of IL-1 receptor antagonist in tissues from healthy rabbits: IL-1 receptor antagonist is probably involved in health." *Cytokine* **9**(5): 307-315.
- Merhi-Soussi, F., M. Berti, et al. (2005). "Intracellular interleukin-1 receptor antagonist type 1 antagonizes the stimulatory effect of interleukin-1 alpha precursor on cell motility." *Cytokine* **32**(3-4): 163-170.
- Miriami, E., H. Margalit, et al. (2003). "Conserved sequence elements associated with exon skipping." *Nucleic Acids Res* **31**(7): 1974-1983.
- Mosley, B., D. L. Urdal, et al. (1987). "The interleukin-1 receptor binds the human interleukin-1 alpha precursor but not the interleukin-1 beta precursor." *J Biol Chem* **262**(7): 2941-2944.
- Moulin, D., O. Donze, et al. (2007). "Interleukin (IL)-33 induces the release of pro-inflammatory mediators by mast cells." *Cytokine* **40**(3): 216-225.
- Mulero, J. J., S. T. Nelken, et al. (2000). "Organization of the human interleukin-1 receptor antagonist gene IL1HY1." *Immunogenetics* **51**(6): 425-428.
- Mulero, J. J., A. M. Pace, et al. (1999). "IL1HY1: A novel interleukin-1 receptor antagonist gene." *Biochem Biophys Res Commun* **263**(3): 702-706.
- Murzin, A. G., A. M. Lesk, et al. (1992). "beta-Trefoil fold. Patterns of structure and sequence in the Kunitz inhibitors interleukins-1 beta and 1 alpha and fibroblast growth factors." *J Mol Biol* **223**(2): 531-543.
- Muzio, M., N. Polentarutti, et al. (1995). "Cloning and characterization of a new isoform of the interleukin 1 receptor antagonist." *J Exp Med* **182**(2): 623-628.
- Nair, V. (2005). "Evolution of Marek's disease -- a paradigm for incessant race between the pathogen and the host." *Vet J* **170**(2): 175-183.
- Nakanishi, K., T. Yoshimoto, et al. (2001). "Interleukin-18 is a unique cytokine that stimulates both Th1 and Th2 responses depending on its cytokine milieu." *Cytokine Growth Factor Rev* **12**(1): 53-72.
- Neill, D. R., S. H. Wong, et al. (2010). "Neutrophils represent a new innate effector leukocyte that mediates type-2 immunity." *Nature* **464**(7293): 1367-1370.
- Nicklin, M. J., J. L. Barton, et al. (2002). "A sequence-based map of the nine genes of the human interleukin-1 cluster." *Genomics* **79**(5): 718-725.
- Nold, M. F., C. A. Nold-Petry, et al. (2010). "IL-37 is a fundamental inhibitor of innate immunity." *Nat Immunol* **11**(11): 1014-1022.
- Nonaka, M. and A. Kimura (2006). "Genomic view of the evolution of the complement system." *Immunogenetics* **58**(9): 701-713.

References

- Novick, D., S. H. Kim, et al. (1999). "Interleukin-18 binding protein: a novel modulator of the Th1 cytokine response." *Immunity* **10**(1): 127-136.
- O'Neill, L. A. and A. G. Bowie (2010). "Sensing and signaling in antiviral innate immunity." *Curr Biol* **20**(7): R328-333.
- Oboki, K., T. Ohno, et al. (2010). "IL-33 and IL-33 receptors in host defense and diseases." *Allergol Int* **59**(2): 143-160.
- Ohno, T., K. Oboki, et al. (2009). "Caspase-1, caspase-8, and calpain are dispensable for IL-33 release by macrophages." *J Immunol* **183**(12): 7890-7897.
- Okamura, H., H. Tsutsi, et al. (1995). "Cloning of a new cytokine that induces IFN-gamma production by T cells." *Nature* **378**(6552): 88-91.
- Ozinsky, A., D. M. Underhill, et al. (2000). "The repertoire for pattern recognition of pathogens by the innate immune system is defined by cooperation between toll-like receptors." *Proc Natl Acad Sci U S A* **97**(25): 13766-13771.
- Palmer, G., B. P. Lipsky, et al. (2008). "The IL-1 receptor accessory protein (AcP) is required for IL-33 signaling and soluble AcP enhances the ability of soluble ST2 to inhibit IL-33." *Cytokine* **42**(3): 358-364.
- Pan, G., P. Risser, et al. (2001). "IL-1H, an interleukin 1-related protein that binds IL-18 receptor/IL-1Rrp." *Cytokine* **13**(1): 1-7.
- Paramithiotis, E. and M. J. Ratcliffe (1993). "Bursa-dependent subpopulations of peripheral B lymphocytes in chicken blood." *Eur J Immunol* **23**(1): 96-102.
- Pavlovsky, A., A. Zanchi, et al. (2010). "Neuronal JNK pathway activation by IL-1 is mediated through IL1RAPL1, a protein required for development of cognitive functions." *Commun Integr Biol* **3**(3): 245-247.
- Philbin, V. J., M. Iqbal, et al. (2005). "Identification and characterization of a functional, alternatively spliced Toll-like receptor 7 (TLR7) and genomic disruption of TLR8 in chickens." *Immunology* **114**(4): 507-521.
- Priestle, J. P., H. P. Schar, et al. (1989). "Crystallographic refinement of interleukin 1 beta at 2.0 A resolution." *Proc Natl Acad Sci U S A* **86**(24): 9667-9671.
- Pushparaj, P. N., H. K. Tay, et al. (2009). "The cytokine interleukin-33 mediates anaphylactic shock." *Proc Natl Acad Sci U S A* **106**(24): 9773-9778.
- Qu, Y., L. Franchi, et al. (2007). "Nonclassical IL-1 beta secretion stimulated by P2X7 receptors is dependent on inflammasome activation and correlated with exosome release in murine macrophages." *J Immunol* **179**(3): 1913-1925.
- Random, F., U. Syrbe, et al. (1995). "Mechanism of endotoxin desensitization: involvement of interleukin 10 and transforming growth factor beta." *J Exp Med* **181**(5): 1887-1892.
- Ratcliffe, M. J. (2006). "Antibodies, immunoglobulin genes and the bursa of Fabricius in chicken B cell development." *Dev Comp Immunol* **30**(1-2): 101-118.
- Riva, F., N. Polentarutti, et al. (2009). "The expression pattern of TIR8 is conserved among vertebrates." *Vet Immunol Immunopathol* **131**(1-2): 44-49.
- Roach, J. C., G. Glusman, et al. (2005). "The evolution of vertebrate Toll-like receptors." *Proc Natl Acad Sci U S A* **102**(27): 9577-9582.
- Rogers, S. L., B. C. Viertlboeck, et al. (2008). "Avian NK activities, cells and receptors." *Semin Immunol* **20**(6): 353-360.
- Roux-Lombard, P., C. Modoux, et al. (1989). "Production of interleukin-1 (IL-1) and a specific IL-1 inhibitor during human monocyte-macrophage differentiation: influence of GM-CSF." *Cytokine* **1**(1): 45-51.

References

- Rozen, S. and H. Skaletsky (2000). "Primer3 on the WWW for general users and for biologist programmers." Methods Mol Biol **132**: 365-386.
- Sana, T. R., R. Debets, et al. (2000). "Computational identification, cloning, and characterization of IL-1R9, a novel interleukin-1 receptor-like gene encoded over an unusually large interval of human chromosome Xq22.2-q22.3." Genomics **69**(2): 252-262.
- Savolainen, P., C. Fitzsimmons, et al. (2005). "ESTs from brain and testis of White Leghorn and red junglefowl: annotation, bioinformatic classification of unknown transcripts and analysis of expression levels." Cytogenet Genome Res **111**(1): 79-87.
- Schindler, R., B. D. Clark, et al. (1990). "Dissociation between interleukin-1 beta mRNA and protein synthesis in human peripheral blood mononuclear cells." J Biol Chem **265**(18): 10232-10237.
- Schindler, R., P. Ghezzi, et al. (1990). "IL-1 induces IL-1. IV. IFN-gamma suppresses IL-1 but not lipopolysaccharide-induced transcription of IL-1." J Immunol **144**(6): 2216-2222.
- Schmitz, J., A. Owyang, et al. (2005). "IL-33, an interleukin-1-like cytokine that signals via the IL-1 receptor-related protein ST2 and induces T helper type 2-associated cytokines." Immunity **23**(5): 479-490.
- Schneider, K., F. Puehler, et al. (2000). "cDNA cloning of biologically active chicken interleukin-18." J Interferon Cytokine Res **20**(10): 879-883.
- Schreuder, H., C. Tardif, et al. (1997). "A new cytokine-receptor binding mode revealed by the crystal structure of the IL-1 receptor with an antagonist." Nature **386**(6621): 194-200.
- Sebzda, E., S. Mariathasan, et al. (1999). "Selection of the T cell repertoire." Annu Rev Immunol **17**: 829-874.
- Secombes, C. J., T. Wang, et al. (2011). "The interleukins of fish." Dev Comp Immunol.
- Shanmugasundaram, R. and R. K. Selvaraj (2011). "Regulatory T cell properties of chicken CD4+CD25+ cells." J Immunol **186**(4): 1997-2002.
- Sharma, S., N. Kulk, et al. (2008). "The IL-1 family member 7b translocates to the nucleus and down-regulates proinflammatory cytokines." J Immunol **180**(8): 5477-5482.
- Shields, J., L. M. Bernasconi, et al. (1990). "Production of a 26,000-dalton interleukin 1 inhibitor by human monocytes is regulated by granulocyte-macrophage colony-stimulating factor." Cytokine **2**(2): 122-128.
- Shini, S., A. Shini, et al. (2010). "Cytokine and chemokine gene expression profiles in heterophils from chickens treated with corticosterone." Stress **13**(3): 185-194.
- Shortman, K. and L. Wu (1996). "Early T lymphocyte progenitors." Annu Rev Immunol **14**: 29-47.
- Sijben, J. W., K. C. Klasing, et al. (2003). "Early in vivo cytokine genes expression in chickens after challenge with Salmonella typhimurium lipopolysaccharide and modulation by dietary n-3 polyunsaturated fatty acids." Dev Comp Immunol **27**(6-7): 611-619.
- Sims, J. E. (2010). "Accessory to inflammation." Nat Immunol **11**(10): 883-885.
- Sims, J. E., C. J. March, et al. (1988). "cDNA expression cloning of the IL-1 receptor, a member of the immunoglobulin superfamily." Science **241**(4865): 585-589.
- Sims, J. E., M. J. Nicklin, et al. (2001). "A new nomenclature for IL-1-family genes." Trends Immunol **22**(10): 536-537.

References

- Sims, J. E. and D. E. Smith (2010). "The IL-1 family: regulators of immunity." Nat Rev Immunol **10**(2): 89-102.
- Smith, D. E. (2011). "The biological paths of IL-1 family members IL-18 and IL-33." J Leukoc Biol **89**(3): 383-392.
- Smith, D. E., R. Hanna, et al. (2003). "The soluble form of IL-1 receptor accessory protein enhances the ability of soluble type II IL-1 receptor to inhibit IL-1 action." Immunity **18**(1): 87-96.
- Smith, D. E., B. P. Lipsky, et al. (2009). "A central nervous system-restricted isoform of the interleukin-1 receptor accessory protein modulates neuronal responses to interleukin-1." Immunity **30**(6): 817-831.
- Smith, D. E., B. R. Renshaw, et al. (2000). "Four new members expand the interleukin-1 superfamily." J Biol Chem **275**(2): 1169-1175.
- Smith, V. P., N. A. Bryant, et al. (2000). "Ectromelia, vaccinia and cowpox viruses encode secreted interleukin-18-binding proteins." J Gen Virol **81**(Pt 5): 1223-1230.
- Smithgall, M. D., M. R. Comeau, et al. (2008). "IL-33 amplifies both Th1- and Th2-type responses through its activity on human basophils, allergen-reactive Th2 cells, iNKT and NK cells." Int Immunol **20**(8): 1019-1030.
- Stevenson, F. T., S. L. Bursten, et al. (1993). "The 31-kDa precursor of interleukin 1 alpha is myristoylated on specific lysines within the 16-kDa N-terminal propeptide." Proc Natl Acad Sci U S A **90**(15): 7245-7249.
- Subramaniam, S., C. Stansberg, et al. (2004). "The interleukin 1 receptor family." Dev Comp Immunol **28**(5): 415-428.
- Tabolacci, E., M. G. Pomponi, et al. (2006). "A truncating mutation in the IL1RAPL1 gene is responsible for X-linked mental retardation in the MRX21 family." Am J Med Genet A **140**(5): 482-487.
- Talabot-Ayer, D., C. Lamacchia, et al. (2009). "Interleukin-33 is biologically active independently of caspase-1 cleavage." J Biol Chem **284**(29): 19420-19426.
- Taylor, S. L., B. R. Renshaw, et al. (2002). "Genomic organization of the interleukin-1 locus." Genomics **79**(5): 726-733.
- Towne, J. E., K. E. Garka, et al. (2004). "Interleukin (IL)-1F6, IL-1F8, and IL-1F9 signal through IL-1Rrp2 and IL-1RAcP to activate the pathway leading to NF-kappaB and MAPKs." J Biol Chem **279**(14): 13677-13688.
- Vainio, O., C. Koch, et al. (1984). "B-L antigens (class II) of the chicken major histocompatibility complex control T-B cell interaction." Immunogenetics **19**(2): 131-140.
- van Asseldonk, E. J., R. Stienstra, et al. (2010). "The effect of the interleukin-1 cytokine family members IL-1F6 and IL-1F8 on adipocyte differentiation." Obesity (Silver Spring) **18**(11): 2234-2236.
- van Dam, A. M., S. Poole, et al. (1998). "Effects of peripheral administration of LPS on the expression of immunoreactive interleukin-1 alpha, beta, and receptor antagonist in rat brain." Ann N Y Acad Sci **840**: 128-138.
- van de Veerdonk, F. L., M. G. Netea, et al. (2011). "Inflammasome activation and IL-1beta and IL-18 processing during infection." Trends Immunol **32**(3): 110-116.
- Vannier, E., L. C. Miller, et al. (1992). "Coordinated antiinflammatory effects of interleukin 4: interleukin 4 suppresses interleukin 1 production but up-regulates gene expression and synthesis of interleukin 1 receptor antagonist." Proc Natl Acad Sci U S A **89**(9): 4076-4080.

References

- Vigne, S., G. Palmer, et al. (2011). "IL-36R ligands are potent regulators of dendritic and T cells." Blood.
- Wallis, J. W., J. Aerts, et al. (2004). "A physical map of the chicken genome." Nature **432**(7018): 761-764.
- Walter, P. and A. E. Johnson (1994). "Signal sequence recognition and protein targeting to the endoplasmic reticulum membrane." Annu Rev Cell Biol **10**: 87-119.
- Wang, D., S. Zhang, et al. (2010). "Structural insights into the assembly and activation of IL-1beta with its receptors." Nat Immunol **11**(10): 905-911.
- Wang, P., B. Meinhardt, et al. (2005). "The interleukin-1-related cytokine IL-1F8 is expressed in glial cells, but fails to induce IL-1beta signalling responses." Cytokine **29**(6): 245-250.
- Wang, T., S. Bird, et al. (2009). "Identification of a novel IL-1 cytokine family member in teleost fish." J Immunol **183**(2): 962-974.
- Weining, K. C., C. Sick, et al. (1998). "A chicken homolog of mammalian interleukin-1 beta: cDNA cloning and purification of active recombinant protein." Eur J Biochem **258**(3): 994-1000.
- Wessendorf, J. H., S. Garfinkel, et al. (1993). "Identification of a nuclear localization sequence within the structure of the human interleukin-1 alpha precursor." J Biol Chem **268**(29): 22100-22104.
- Wu, Y. F., H. J. Liu, et al. (2007). "Sequence and phylogenetic analysis of interleukin (IL)-1beta-encoding genes of five avian species and structural and functional homology among these IL-1beta proteins." Vet Immunol Immunopathol **116**(1-2): 37-46.
- Wu, Z., T. Hu, et al. (2010). "Cloning and characterisation of the chicken orthologue of dendritic cell-lysosomal associated membrane protein (DC-LAMP)." Dev Comp Immunol **34**(2): 183-188.
- Wu, Z. and P. Kaiser (2011). "Antigen presenting cells in a non-mammalian model system, the chicken." Immunobiology.
- Xiang, Y. and B. Moss (2001). "Correspondence of the functional epitopes of poxvirus and human interleukin-18-binding proteins." J Virol **75**(20): 9947-9954.
- Yilmaz, A., S. Shen, et al. (2005). "Identification and sequence analysis of chicken Toll-like receptors." Immunogenetics **56**(10): 743-753.
- Yoon, H. J., Z. Zhu, et al. (1999). "Rhinovirus regulation of IL-1 receptor antagonist in vivo and in vitro: a potential mechanism of symptom resolution." J Immunol **162**(12): 7461-7469.
- Zipfel, P. F. and C. Skerka (2009). "Complement regulators and inhibitory proteins." Nat Rev Immunol **9**(10): 729-740.
- Zou, J., S. Bird, et al. (2000). "Molecular cloning of the gene for interleukin-1beta from *Xenopus laevis* and analysis of expression in vivo and in vitro." Immunogenetics **51**(4-5): 332-338.
- Zou, J., S. Bird, et al. (2004). "Identification and expression analysis of an IL-18 homologue and its alternatively spliced form in rainbow trout (*Oncorhynchus mykiss*)." Eur J Biochem **271**(10): 1913-1923.

Appendices

Appendix I: BLAST results

TBLASTN searches were performed in Chapter 4, section 4.3.1 and Chapter 6, section 6.3.1 against all 39 eukaryotic genomes present in ENSEMBL release 50 (July 2008).

These 39 species are: *Primates*: Bushbaby, Chimpanzee, Human, Macaque, Mouse Lemur, Orangutan; *Rodents*: Guinea pig, Mouse, Pika, Rabbit, Rat, Squirrel, Tree shrew; *Laurasiatheria*: Cat, Cow, Dog, Hedgehog, Horse, Microbat, Shrew; *Afrotheria*: Elephant, Lesser hedgehog tenrec; *Xenarthra*: Armadillo; *Marsupials and Monotremes*: Opossum, Platypus; *Birds*: Chicken; *Reptiles and Amphibians*: *X. tropicalis*; *Fish*: *Fugu*, *Medaka*, Stickleback, *Tetraodon*, Zebrafish; *Other chordates*: *C. intestinalis*, *C. savignyi*; *Other eukaryotes*: *Aedes*, *Anopheles*, *C. elegans*, Fruitfly, *S. cerevisiae*.

BLAST results are in Tables I and III.

Table I

Species	Genomic location	Statistics score	E-value	% amino acid identity	Length	Gene
Megabat	GeneScaffold_1674	274	4.0e-21	41.59	113	IL-1RN
Kangaroo Rat	GeneScaffold_3082	223	1.1e-23	42.67	75	IL-1RN
Horse	Chr:15	231	5.1e-16	34.82	112	IL-1RN
Hedgehog	GeneScaffold_4042	239	8.3e-22	44.59	74	IL-1RN
Lesser hedgehog tenrec	GeneScaffold_3935	255	1.4e-26	37.65	85	IL-1RN
Cat	GeneScaffold_4437	262	9.2e-17	46.74	92	IL-1RN
Human	Chr:2	228	9.9e-19	41.67	84	IL-1RN
Elephant	scaffold_21082	278	4.5e-17	48.89	90	IL-1F5
Macaque	Chr:13	229	5.8e-20	43.42	76	IL-1RN
Opossum	Chr:1	254	6.2e-21	45.45	77	IL-1RN
Mouse	Chr:2	283	1.0e-14	48.45	97	IL-1F5
Microbat	GeneScaffold_2623	263	6.5e-30	40.62	96	IL-1RN
Pika	GeneScaffold_4797	247	1.1e-25	40.66	91	IL-1RN
Platypus	Contig1254	253	5.2e-27	41.67	84	IL-1RN
Bushbaby	GeneScaffold_2376	251	6.8e-20	48.68	76	IL-1RN
Rabbit	GeneScaffold_3038	248	1.0e-27	43.37	83	IL-1RN
Chimpanzee	Chr:2a	236	1.5e-22	42.86	84	IL-1RN
Orangutan	Chr:2a	235	1.0e-21	40.24	82	IL-1RN
Hyrax ^a	scaffold_40202	243	2.8e-13	41.57	89	IL-1RN
Rat	Chr:3	228	1.7e-17	40.22	92	IL-1RN

Appendices

Shrew	scaffold_223412	274	1.7e-16	43.00	100	IL-1RN
Squirrel	scaffold_127907	251	5.9e-27	40.71	113	IL-1RN
Tarsier	scaffold_22964	232	2.3e-25	41.58	101	IL-1RN
Tree shrew	scaffold_109510	318	5.3e-21	48.91	92	IL-1RN
Dolphin	scaffold_102460	257	1.3e-17	38.89	126	IL-1F5
Dog	Chr:17	271	1.3e-21	49.45	91	IL-1F5
Cow	Chr:11	280	8.6e-15	46.67	90	IL-1F5

Table II

Chicken IL-1 family ESTs identified by reciprocal BLASTP analysis.

NCBI I.D.	Length (bp)	Aa identity (%)	BLAST result e-value	Gene identity
CK615408.1	432	98	8e-77	IL-1RN
BU214831.1	669	82	2e-70	IL-1RN
CK607391.1	364	100	4e-63	IL-1RN
BX257556.3	526	100	2e-36	IL-1RN
CN778914.1	709	33	3e-13	IL-1 β
BU432992.1	612	36	2e-10	IL-1 β
CK615181.1	291	39	1e-08	IL-1 β
CN231756.1	781	62	4e-07	IL-1RN*
CK615098.1	459	47	3e-06	IL-1 β
CK613911.1	426	47	3e-06	IL-1 β
BU455380.1	880	34	0.001	IL-1 β
CK615049.1	416	43	0.002	IL-1 β

*This EST is a composite of the 5' end of sIL-1RN joined to Tmed4 with *NotI* linkers, which explains the apparent contradiction between the relatively high % aa identity with a high e-value from the BLAST analysis.

Table III

Species	Genomic location	Statistics score	E-value	% amino acid identity	Length	Gene
Cow	Chr:11	186	3.5e-05	55.81	43	IL-1F5
Dog	Chr:17	197	1.3e-05	58.14	43	IL-1F5
Kangaroo Rat	scaffold_29650	182	1.0e-06	55.81	43	IL-1F5
Horse	Chr:15	202	7.8e-07	42.22	90	IL-1F5
Hedgehog	scaffold_296053	159	1.3e-05	42.86	63	IL-1F5
Human	Chr:2	186	0.0013	55.32	47	IL-1F5
Elephant	scaffold_21082	209	1.9e-09	50.85	59	IL-1F5
Macaque	Chr:13	181	0.00034	43.33	90	IL-1F5
Opossum ^a	Chr:1	148	0.17	47.62	42	IL-1F5
Mouse ^b	Chr:2	172	0.017	42.11	76	IL-1F5
Pika	GeneScaffold_4797	184	6.2e-06	55.81	43	IL-1F5
Platypus ^c	Contig1254	156	0.0012	45.45	44	IL-1F5
Rabbit	GeneScaffold_6992	189	1.6e-07	39.82	113	IL-1F5
Bushbaby	GeneScaffold_2376	183	1.7e-06	50.00	54	IL-1F5
Orangutan ^d	Chr:2a	197	0.068	40.35	114	IL-1F5
Hyrax ^e	GeneScaffold_3408	161	1.6e-06	32.97	91	IL-1F10
Rat	Chr:3	186	6.8e-05	51.67	60	IL-1F5
Dolphin ^f	scaffold_102460	188	6.0e-06	41.67	84	IL-1F5
Shrew	GeneScaffold_3283	211	9.5e-10	35.77	137	IL-1F5
Tarsier	scaffold_119097	204	8.2e-09	52.46	61	IL-1F5

Appendix II: Primers

Table I: Primers used in RT-PCR and PCR amplification of chIL-1 cytokines

Primer name	Target for amplification	Sequence (5'-3')
sIL-1RN F	sIL-1RN cDNA	ATGGCGCTCACCATCGCCCT
IL-1RN R	sIL-1RN/icIL-1RN cDNAs	GCTCAGCACAGCTGGAAGTA
sIL-1RNpHL F	Mature sIL-1RN. Includes <i>AgeI</i> restriction site.	GAGAGAaccggtGTGCCGTGCCGCGCGCCCGC
sIL-1RNpHL R	Includes <i>KpnI</i> restriction site.	GAGAGAggtaccGCACAGCTGGAAGTAGAAAT
icIL-1RN F	icIL-1RN cDNA	GGCATCTCATGGGTGAGG
icIL-1RNpHL F	icIL-1RN cDNA. Includes <i>AgeI</i> restriction site.	GAGAGAaccggtGGTGAGGCTGCCGGATCGGT
icIL-1RNpHL R	Includes <i>KpnI</i> restriction site.	GAGAGAggtaccGCACAGCTGGAAGTAGAAAT
IL-1RN ex5 F	IL-1RN. Used with IL-1RN R to amplify TAM32-21N6 DNA.	TCACCTTCTCCGCACCTAT
IL-1 β /1	IL-1 β . Used with IL-1 β /2 to amplify TAM32-21N6 DNA	CTTCACCTCAGCTTTCACG
IL-1 β /2	IL-1 β . Used with IL-1 β /1 to amplify TAM32-21N6 DNA	GCACGTCCACTGTGGTGTGC
IL-1RN Int2-3 F	IL-1RN intron 2	GCTGCAAACCAAAGTCTTCA
IL-1RN Int2-3 R	IL-1RN intron 2	GCGACTGCTGGTTCATATCC
IL-1Ra Int3-4 F	IL-1RN intron 3	AACCAGCAGTCGCTGTACCT
IL-1Ra Int3-4 R	IL-1RN intron 3	GCAGCTCGTGCTTGAAGAAG

Appendices

IL-1Ra Int1-2 F	IL-1RN intron 4	CTCCATTGGGGCATCTCAT
IL-1Ra 130bp R	IL-1RN intron 4	GGGCAGCTCCGTGATGTC
IL-1RN 5' RACE R	5' end of IL-1RN cDNA	ACAGCCCGTCCTTATAGGTGCGGAAGA
IL-1F5 pHL F	IL-1F5 cDNA. Includes <i>AgeI</i> restriction site.	GAGAGAaccggtGTGGCGCTGTTTCGATGAGTT
IL-1F5 pHL R	Includes <i>KpnI</i> restriction site.	GAGAGAggtaccCCGGCGCCGCAGGTAGAAGG
IL-1F5 fl F	IL-1F5 cDNA	ATGGTGGCGCTGTTTCGAT
IL-1F5 fl R22	IL-1F5 cDNA	TCACCGGCGCCGCAGGTAGAAG
IL-1F5 Int1 F	IL-1F5 intron 1	CCCACATCCCCTCACCTC
IL-1F5 Int1 R	IL-1F5 intron 1	GTCCGGACACGAAGGACAT
IL-1F5 332bp L	IL-1F5 intron 4, and to amplify TAM32-21N6 DNA	GAGAGCTCAGCCGTACCACTA
IL-1F5 437bp R	IL-1F5 intron 4, and to amplify TAM32-21N6 DNA	GCACGACAGCGCCTTATT
IL-1F5 Int5 F	IL-1F5 intron 5	GCAATAAGGCGCTGTCGT
IL-1F5 Int5 R	IL-1F5 intron 5	TCTTATAGAACGTGTAGGGAACG

Table II: Primers and probes used for real-time qRT-PCR (TaqMan®) quantification of chicken mRNA

Target	Sequence (5'-3')	Standard	Primer conc. (μM)
IL-1RN	F: CGCTGGAGGAGAAGGTGTTTT R: GATGTCGGCGTCCTGGAG P: CCCAACCGCTTCTTCAAGCACGA	ex-COS IL-1RN mRNA	0.4
IL-1RN SV1	F: ACCAAAGTCTTCAAATACCAGAAGGT R: GCGGATGCCCATGATGAC P: CGCTTCTTCAAGCACGAG	ex-COS IL-1RN SV1 mRNA	0.4
IL-1RN SV2	F: CCCACAGCCCACCCT R: GGAGGTGCAGAGGAACCAT P ^a : CCGTCCTGGAGCTGC	ex-COS IL-1RN SV2 mRNA	0.9
IL-1F5	F: GCCCCGAAGGTCTTATAGAA R: GCTGGAGGAGGTGAAGCTGTT P ^a : AACGGCCGCGTCC	ex-COS IL-1F5 mRNA	0.6
IL-1β	F: GCTCTACATGTCGTGTGTGATGAG R: TGTCGATGTCCCGCATGA P: CCACACTGCAGCTGGAGGAAGCC	ex-COS IL-1β mRNA	0.4
iNOS	F: TTGAAACCAAAGTGTGTAATATCTTG R: CCCTGGCCATGCGTACAT P: TCCACAGACATACAGATGCCCTTCCTCTTT	LPS-stimulated HD11 mRNA	0.2
28S	F: GGCGAAGCCAGAGGAAACT R: GACGACCGATTGACAGTC P: AGGACCGCTACGGACCTCCACCA	LPS-stimulated HD11 mRNA	0.6

^a Indicates MGB probe.

F = forward primer; R = reverse primer; P = probe.

Table III: Primers used for sequencing vector DNA inserts

Primer name	Plasmid	Sequence (5'-3')
T3	pCI-neo	ATTAACCCTCACTAAAGGGA
T7	pTargeT™ or pGEM®-T Easy	TAATACGACTCACTATAGGG
T7 (reverse)	pTargeT™	TTACGCCAAGTTATTTAGGTGACA
SP6	pGEM®-T Easy	TATTTAGGTGACACTATAG
pHLSec F	pHLSec	GCTGGTTGTTGTGCTGTCTCATC
pHLSec R	pHLSec	CACCAGCCACCACCTTCTGATAG
M13 forward (-40)	pBluescript II KS(+)	GTTTTCCCAGTCACGAC
M13 reverse	pBluescript II KS(+)	CAGGAAACAGCTATGAC

Appendix III: Buffers

Restriction enzyme buffers

Buffers from Invitrogen unless stated otherwise.

1X REact® 2: 50 mM Tris-HCl (pH 8.0)
 10 mM MgCl₂
 50 mM NaCl

1X REact® 3: 50 mM Tris-HCl (pH 8.0)
 10 mM MgCl₂
 100 mM NaCl

1X REact® 4: 20 mM Tris-HCl (pH 7.4)
 5 mM MgCl₂
 50 mM KCl

1X REact® 10: 100 mM Tris-HCl (pH 7.6)

Appendices

	10 mM MgCl ₂
	150 mM NaCl
1X NEBuffer 1: (NEB)	10 mM Bis-Tris-Propane-HCl
	10 mM MgCl ₂
	1 mM Dithiothreitol
	pH 7.0 @ 25°C

Buffer H: (Roche)	50 mM Tris-HCl (pH 7.5)
	10 mM MgCl ₂
	100 mM NaCl
	1 mM Dithioerythritol
	pH 7.5 @ 37°C

Qiagen molecular biology kit buffers

Details of most buffers supplied in nucleotide purification kits are not provided by Qiagen.

RNAlater®	Details not supplied
-----------	----------------------

RNeasy Mini Kit

Buffer RLT	contains guanidine thiocyanate
Buffer RW1	contains guanidine thiocyanate and ethanol
Buffer RPE	contains ethanol

DNeasy Blood & Tissue Kit

Buffer AL	contains guanidine hydrochloride
Buffer AW1	contains guanidine hydrochloride and ethanol
Buffer AW2	contains sodium azide and ethanol

QIAquick PCR Purification Kit

Buffer PB	contains guanidine hydrochloride and isopropanol
Buffer PE	contains ethanol
Buffer EB	10 mM Tris-Cl, pH 8.5

QIAquick Gel Extraction Kit

Buffer QG	contains guanidine thiocyanate
-----------	--------------------------------

Appendices

Buffer PE contains ethanol
Buffer EB as above

QIAprep Spin Miniprep Kit

Buffer P1 50 mM Tris-Cl (pH 8.0)
10 mM EDTA
100 µg/ml RNase A

Buffer P2 200 mM NaOH
1% SDS (w/v)

Buffer N3 contains guanidine hydrochloride
Buffer PB as above
Buffer PE as above

EndoFree® Plasmid Purification Kits (Maxi/Mega)

Buffer P1 as above
Buffer P2 as above
Buffer P3 3 M potassium acetate (CH₃CO₂K), pH 5.5
Buffer FWB2 1 M CH₃CO₂K, pH 5.0
Buffer QBT 750 mM NaCl
50 mM MOPS, pH 7.0
15% isopropanol (v/v)
0.15% Triton® X-100

Buffer QC 1 M NaCl
50 mM MOPS, pH 7.0
15% isopropanol (v/v)

Buffer QN 1.6 M NaCl
50 mM MOPS, pH 7.0
15% isopropanol (v/v)

Buffer ER contains isopropanol and polyethylene glycol octylphenyl ether
Buffer TE 10 mM Tris-Cl (pH 8.0)
1 mM EDTA

Macherey-Nagel molecular biology kit buffers

NucleoBond® BAC 100 kit

Buffer S1 50 mM Tris-HCl
10 mM EDTA
100 µg/mL RNase A, pH 8.0

Appendices

Buffer S2	200 mM NaOH 1% SDS
Buffer S3	2.8 M CH ₃ CO ₂ K, pH 5.1
Buffer N2	100 mM Tris 15% Ethanol 900 mM KCl 0.15% Triton® X-100 adjusted to pH 6.3 with H ₃ PO ₄
Buffer N3	100 mM Tris 15% Ethanol 1.15 M KCl adjusted to pH 6.3 with H ₃ PO ₄
Buffer N5	100 mM Tris 15% Ethanol 1 M KCl adjusted to pH 8.5 with H ₃ PO ₄

General buffers

Pre-hybridisation solution	200 µg per ml DNA in 10X SSC (1.5 M NaCl, 150 mM Na ₃ C ₆ H ₅ O ₇) 10X Denhardt's solution (20 g Ficoll, 20 g Polyvinylpyrrolidone, 20 g BSA)
TBS buffer	10 mM Tris·Cl, pH 7.5 150 mM NaCl
TBS-Tween/Triton buffer	20 mM Tris·Cl, pH 7.5 500 mM NaCl 0.05% (v/v) Tween 20
10X TBE	890mM Tris-borate 890mM boric acid 20mM EDTA pH 8.3
PBSa	10.0g NaCl 0.25g KCl 1.437g Na ₂ HPO ₄ 0.25g KH ₂ PO ₄ H ₂ O to 1 l pH 7.2

Appendices

Versene	0.25g KCl
	1.437g Na ₂ HPO ₄
	0.25g KH ₂ PO ₄
	0.2g EDTA
	H ₂ O to 1 l
	pH 7.2

Appendix IV: Cell culture reagents

HD11 cell growth media

10x RPMI 1640	50 ml
tryptose phosphate broth (TPB)	50 ml
FCS (2.5%)	12.5 ml
Chick serum (2.5%)	12.5 ml
7.5% NaHCO ₃	15 ml
200 mM L-glutamine	5 ml
1000X Penicillin/streptomycin	500 µl
5 M NaOH	~1 ml
H ₂ O	to 500 ml

COS-7 cell growth media

DMEM
10% Foetal calf serum (FCS) (10%)
1% 200 mM L-glutamine
400 µl 1000X Penicillin/streptomycin
4.0 ml 100X Non-essential amino acids

Serum-free COS-7 cell growth media as above minus FCS.

HEK293T growth media

The same as COS-7 cell growth media. Both serum-free and 2% serum-containing HEK293T media are also the same as above, minus FCS and with 2% FCS, respectively.